

**SEDIMENT DYNAMICS AND PROVENANCE OF HYDROLOGIC AND
VEGETATION SIGNALS OF THE MZIMVUBU CATCHMENT, EASTERN CAPE,
SOUTH AFRICA**



by

Tarryn Frankland

Submitted in Fulfilment of the academic requirements for the degree of Master of Science in
the Discipline of Geography

School of Agricultural, Earth and Environmental Sciences

University of KwaZulu-Natal

Pietermaritzburg

January 2020

ABSTRACT

Southern Africa has a high vulnerability to future climate change, therefore reliable and comprehensive information on local hydrological, vegetation and sediment processes are crucial for future mitigation and management practices. Marine sediments can provide valuable, continuous and long-term data about climatic, vegetation and sediment dynamics of the adjacent continent. To accurately interpret these records, the question of terrestrial organic and inorganic material provenance and their contribution to marine archives is essential. Provenance studies however, have mostly been conducted along the western shoreline, very few studies exist along the eastern shoreline. This study presents an investigation of inorganic and organic signals transported within the Mzimvubu Catchment, Eastern Cape. To investigate proxy provenance, plant leaf-wax derived long-chain *n*-alkanes, pollen grains and element compositions of 32 River Bed Sediment (RBS) and Suspended Particulate Matter (SPM) samples of the five major tributaries were compared over three different seasons. The $\delta^{13}\text{C}$ composition of river sediment yielded depleted values indicating input from predominantly C_3 vegetation. δD of RBS changed with increasing altitude and distance from the ocean and rainfall amount. Enriched $\delta^{13}\text{C}$ values, depleted δD values, reduced norm_{31} and low CPI values indicate input from arboreal vegetation with elevated sediment erosion rates originating from the northern tributaries. Depleted $\delta^{13}\text{C}$ values, enriched δD values, elevated norm_{31} and high CPI values indicate reduced sediment erosion rates and input from adjacent grasslands in the southern tributaries. XRF Fe/K, Ti/Al and Al/Si ratios revealed areas of high erosion of fine grained particles due to anthropogenic pressures and aeolian dust input from south easterly trade winds in the northern tributaries, compared to the fluvial input of coarse grained particles in the southern tributaries and river mouth. Proxy signals were influenced by various environmental, physiological and taphonomic processes. These findings present the first comprehensive multiproxy overview of vegetation, sediment and hydrologic provenance based on palynomorph abundance, *n*-alkane isotopic distributions and elemental compound dynamics within the Mzimvubu Catchment, which can aid the interpretation of marine cores extracted from the Indian Ocean for future palaeoclimatological and palaeoenvironmental research.

PREFACE

The experimental work described in this dissertation was carried out in the School of Agricultural, Earth and Environmental Sciences, University of KwaZulu-Natal, Pietermaritzburg, from January 2017 to January 2020, under the supervision of Dr J.M. Finch and Dr E. Schefuß.

These studies represent original work by the author and have not otherwise been submitted in any form of degree or diploma to any University. Where use has been made of the work of others it is duly acknowledged in the text.



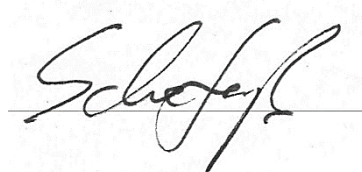
T. Frankland (candidate)

Date: 13 January 2020



Dr. J.M. Finch

Date: 13 January 2020



Dr. E. Schefuß

Date: 13 January 2020

ACKNOWLEDGMENTS

Thank you to **National Research Fund (NRF)** for providing the financial assistance which made this research possible.

Thank you to **RAiN** (Regional Archives for integrated Investigations) which falls under the **SPACES** (Scientific Partnership for the Assessment of Complex Earth System Processes) programme to conduct this palaeoclimatic research in South Africa, and for the skill set and capacity building opportunities.

To my supervisor **Dr Jemma Finch**, a heartfelt thanks to you for your time, continued support and guidance at every step of the journey, it is truly appreciated.

To **Dr. Enno Schefuß** and **Dr. Matthias Zabel**, thank you for your guidance and support, and for a warm welcome into University of Bremen, Germany.

Thank you to **Charlotte Miller** and **Annette Hahn** for being the greatest support and friends and for showing me the ropes in Germany. A big thank you to **Ralph Kreutz** for the continued guidance in the laboratory (University of Bremen, Germany).

A special thank you to **DAAD** for a fully financed exchange to the University of Bremen, Germany.

To **Dylind Kleynhans** and **Craig Cordier** for assisting me on my field trips and bring so much laughter and fun on those very long drives, you are both stars, without which these field trips would not have been possible. A very special thank you to Craig, for always being available to help and provide support and wisdom and for keeping me company on those long pollen counting days.

A very big thank you to **Brice Gijsbertsen** for your continued support on GIS and any technical difficulties, and for the many words of wisdom and tips you have shared with me over the last few years.

Thank you to my dear friend **Gugulethu Tshabalala**, for all your help, advice and support, you are amazing.

And to my incredible family and dearest Keith, thank you for your unconditional support, love and guidance, without you this thesis would not have been possible.

TABLE OF CONTENTS

PREFACE.....	ii
ACKNOWLEDGMENTS	iii
CHAPTER ONE	1
INTRODUCTION.....	1
1.1 INTRODUCTION.....	1
1.2 AIM AND OBJECTIVES	4
1.3 DISSERTATION OUTLINE.....	4
CHAPTER TWO	6
LITERATURE REVIEW	6
2.1 INTRODUCTION.....	6
2.2 PROXIES AS INDICATORS OF CLIMATE AND ENVIRONMENTAL CHANGE..	7
2.2.1 Introduction	7
2.2.2 Pollen.....	7
2.2.3 Organic geochemistry.....	17
2.2.4 Inorganic geochemistry (XRF).....	30
2.3 MODERN CALIBRATION CASE STUDIES FROM SOUTHERN AFRICA	36
2.3.1 Introduction	36
2.3.2 Existing modern provenance studies in southern Africa	37
2.3.3 Site suitability	40
2.3.4 The research gap in provenance research for southern Africa	41
2.4 CONCLUSION	41
CHAPTER THREE	42
METHODS.....	42
3.1 SITE DESCRIPTION	42
3.2 FIELD SAMPLING	43
3.2.1 Sample extraction	43
3.3 LABORATORY TECHNIQUES	49
3.3.1 Pollen.....	49
3.3 ORGANIC GEOCHEMISTRY	53
3.3.1 <i>n</i> -Alkane plant wax biomarker extraction	53
3.4 INORGANIC GEOCHEMISTRY	54
3.4.1 XRF element composition analysis	54

3.4.2 Element Ratios.....	54
3.5 DATA ANALYSIS	55
CHAPTER FOUR.....	56
RESULTS	56
4.1 INTRODUCTION.....	56
4.2 POLLEN ANALYSIS	56
4.2.1 Pollen counts.....	56
4.2.3 Pollen seasonality	56
4.2.4 Pollen biome comparison	62
4.2.5 Pollen Tributary Comparison	64
4.3 ORGANIC GEOCHEMISTRY	66
4.3.1 <i>n</i> -Alkane µg/g abundance.....	66
4.3.2. <i>n</i> -Alkane homologue composition.....	66
4.3.3 Norm31	70
4.3.4 Carbon Preference Index (CPI)	72
4.3.5 $\delta^{13}\text{C}_{29-31}$	74
4.3.6 δD_{29-31}	76
4.4 INORGANIC GEOCHEMISTRY	80
4.4.1 XRF element composition	80
4.4.3 Element ratios	81
4.5 ALL PROXY CORRELATION	89
4.6 CONCLUSION	91
CHAPTER FIVE	92
DISCUSSION.....	92
5.1 INTRODUCTION.....	92
5.2 THE DISCHARGED PROXY SIGNAL	92
5.2.1 Pollen.....	93
5.2.2 Leaf-wax derived long chain <i>n</i> -alkane	100
5.2.3 Element Ratios.....	107
5.3 THE RBS SIGNAL VERSUS THE SPM SIGNAL	110
5.3.1 <i>n</i> -Alkane homologue distribution.....	110
5.3.2 XRF elemental ratios	111
5.4 SIGNAL PROVENANCE	111
5.4.1 Pollen.....	112

5.4.2 Stable $\delta^{13}\text{C}_{29-31}$ and δD_{29-31} isotope compositions of <i>n</i> -alkane plant waxes	113
5.4.3 Element Ratios.....	115
5.5 IMPLICATIONS FOR FUTURE PALAEOENVIRONMENTAL RESEARCH	116
5.5.1 Palaeo-considerations	117
5.6 LIMITATIONS OF THE STUDY	119
5.6.1 Sample Design.....	119
5.6.2 Pollen.....	120
5.6.3 Stable isotopes	120
5.7 CONCLUSION	120
CHAPTER SIX	122
CONCLUSION	122
6.1 INTRODUCTION.....	122
6.2 SYNTHESIS OF PERTINENT FINDINGS	122
6.2.1 Pollen.....	122
6.2.2 <i>n</i> -Alkane distribution and isotope compositions	124
6.2.3 XRF elemental ratios	125
6.3 FUTURE RESEARCH RECOMMENDATIONS.....	126
6.4 REVIEW OF AIM AND OBJECTIVES	127
6.5 CONCLUDING REMARKS	129
REFERENCES.....	130
APPENDICES	i

LIST OF APPENDICES

Appendix A Procedure for preparing pollen samples.....	i
Appendix B <i>n</i> -Alkane separation of samples.....	iii
Appendix C Sample collection data sheet.....	viii
Appendix D Pollen raw count sheets.....	x
Appendix E Additional environmental, climatic and vegetation information for the Mzimvubu Catchment.....	xiii
Appendix F Additional pollen data.....	xv
Appendix G Proxy seasonal data maps.....	xvii
Appendix H All proxy correlations for each season.....	xxix

LIST OF FIGURES

Figure 2.1: Histogram showing the $\delta^{13}\text{C}$ values of C_3 (-29.6 ‰) and C_4 (-12.7 ‰) for modern C_3 and C_4 plants from the Gangetic Plain, India (Basu <i>et al.</i> , 2015).....	20
Figure 2.2: A schematic diagram showing the fractionation of hydrogen (deuterium δD) and depletion with increasing distance inland (continental effect), elevation (altitude effect), and rainfall (rainfall effect) (Bruckner, n.d. available on: https://serc.carleton.edu/microbelife/research_methods/enviro_n_sampling/stableisotopes.html).....	25
Figure 3.1: Topographical site map of the eleven sample sites chosen for the Mzimvubu Catchment.....	45
Figure 3.2: Topographical site map showing the upper (orange), middle (green), and lower (blue) catchment sections.....	46
Figure 3.3: Study area and sample sites projected over (a) MAP (mm), (b) MAT ($^{\circ}\text{C}$), and (c) major vegetation biomes for the Mzimvubu Catchment.....	47
Figure 4.1: Palynomorph abundance and diversity for the three sampling campaigns (dry, intermediate and wet) for the Mzimvubu Catchment.....	58
Figure 4.2: Palynomorph abundance and distribution across the sampling sites for the Mzimvubu Catchment.....	59
Figure 4.3: Pie charts showing the ecological groupings of pollen taxa within the catchment's three major biomes, (a) catchment average, (b) IOCB, (c), Savanna, and (d) Grassland.....	63
Figure 4.4: Pie charts showing the major ecological groupings for each major tributary of the Mzimvubu Catchment namely, (a) River mouth, (b) iTsitsa River, (c) Kinira River, (d) upper Mzimvubu River, and (e) the Mzimvubu River.....	65
Figure 4.5: Histogram showing norm31 ratios for RBS (blue) and SPM (orange) samples of each tributary, for the dry (a), intermediate (b) and wet (c) seasons.....	70
Figure 4.6: Histograms showing CPI ₂₅₋₃₃ for the RBS (blue) and SPM (orange) samples of each tributary for the dry (a), intermediate (b) and wet (c) seasons.....	73

Figure 4.7: Histograms showing $\delta^{13}\text{C}_{29-31}$ for RBS and SPM samples for each site, during the dry (a), intermediate (b) and wet (c) seasons.....	77
Figure 4.8: Histograms showing δD_{29} and δD_{31} for RBS (blue) and SPM (orange) and δD_{29-31} for the dry (a), intermediate (b) and wet (c) seasons.....	79
Figure 4.9: Histograms showing the element composition concentrations for the River mouth (a), iTsitsa River (b), Thina River (c), Kinira River (d) upper Mzimvubu River (e), Mzintlava River (f) and the total catchment average (g).....	82
Figure 4.10: Histograms showing Fe/K ratios for RBS (blue) and SPM (orange) samples for the dry (a), intermediate (b) and wet (c) seasons.....	84
Figure 4.11: Histograms showing the Al/Si ratios for RBS (blue) and SPM (orange) samples for the dry (a), intermediate (b) and wet (c) seasons.....	86
Figure 4.12: Histograms showing Ti/Al ratios of RBS (blue) and SPM (orange) samples for the dry (a), intermediate (b) and wet (c) seasons.....	88
Figure 5.1: δD_{29-31} of RBS and SPM samples averaged together for the three seasons.....	106
Figure 5.2: Fe/K of RBS and SPM samples averaged together for the three seasons.....	108
Figure 5.3: Al/Si ratios for RBS and SPM samples averaged together for the three seasons...	109
Figure 5.4: Ti/Al of RBS and SPM averaged together for the three seasons.....	109
Figure 5.5: Averaged norm31 RBS and SPM values for the three seasons.....	113

LIST OF TABLES

Table 4.1: Table showing the ecological classifications, number of pollen taxa per sample, climate indicator values and the general habitat of each pollen taxa within the Mzimvubu Catchment.....	57
Table 4.2: Table showing the $\mu\text{g/g}$ sediment, dominant homologue, ACL_{25-33} , CPI_{25-33} , $\delta^{13}\text{C}_{29}$, $\delta^{13}\text{C}_{31}$, δ^{13}_{29-31} , δD_{29} , δD_{31} , δD_{29-31} and Norm31 for RBS samples of the Mzimvubu Catchment.....	68
Table 4.3: Table showing the $\mu\text{g/g}$ sediment, dominant homologue, ACL_{25-33} , CPI_{25-33} , $\delta^{13}\text{C}_{29}$, $\delta^{13}\text{C}_{31}$, δ^{13}_{29-31} , δD_{29} , δD_{31} , δD_{29-31} and Norm31 for SPM samples of the Mzimvubu Catchment.....	69
Table 4.4: Correlation matrices for norm31 RBS and SPM samples to precipitation, elevation and temperature for the dry, intermediate and wet season. Significant correlations are bolded and highlighted in yellow, moderate correlations are highlighted in orange and inverse correlations are highlighted in blue. Level of significant for all calculation is 0.05 ($p=0.05$).....	71
Table 4.5: Correlation matrix of CPI RBS and SPM samples for the dry, intermediate and wet seasons.....	74
Table 4.6: Correlation matrices of $\delta^{13}\text{C}$ for RBS and SPM material for the dry, intermediate and we seasons.....	78
Table 4.7: Correlation matrices of δD_{29} , δD_{31} and δD_{29-31} to MAP, elevation and MAT of RBS samples for the dry, intermediate and wet seasons.....	80
Table 4.8: Table showing elemental Ti/Al, Al/Si, and Fe/K ratios of RBS and SPM samples for the dry, intermediate and wet seasons.....	83
Table 4.9: Correlation matrices of RBS and SPM Fe/K ratios to precipitation, elevation and temperature for the dry, intermediate and wet seasons.....	85
Table 4.10: Correlation matrices for RBS and SPM Al/Si ratios to precipitation, elevation for the dry, intermediate and wet seasons.....	87
Table 4.11: Correlation matrices for RBS and SPM Ti/Al samples to precipitation, elevation and temperature for the dry, intermediate and wet seasons.....	89

Table 4.12: Correlation matrices for all proxies: Fe/K, Al/Si, Ti/Al, norm31, δD_{29-31} , $\delta^{13}C_{29-31}$ and CPI, for the dry, intermediate and wet season.....	90
Table 5.1: Pollen climate indicator values and general habitat preferences.....	95

LIST OF PLATES

Plate 3.1: Sample extraction of SPM sediment using a battery powered bore-hole water sediment sampler. (c) Pilot study SPM extraction (Umkomaas), (d) SPM extraction (MZ10), (e) SPM being decanted into 5 L and 25 L jerry cans (MZ11), (f) SPM sample extraction (MZ5).....	50
Plate 3.2: Examples of modern pollen grains extracted from the RBS samples of the Mzimvubu Catchment: (a) Asteraceae <i>Tubuliflorae</i> , (b) Mimosaceae <i>Acacia</i> type I, (c) Pinaceae <i>Pinus</i> , (d) Aquifoliaceae <i>Ilex mitis</i> , (e) Cyperaceae, (f) Poaceae undiff.....	52

LIST OF ABBREVIATIONS

‰	Parts Per Thousand
$\delta^{13}\text{C}$	A measure of the ratio of stable isotopes ^{13}C : ^{12}C
δD	Deuterium isotope
ASE	Accelerated Solvent Extraction
XRF	X-Ray Fluorescence
RBS	River Bed Sediment
SPM	Suspended Particulate Matter
DPS	Dried Puddle Sample
MAP	Mean Annual Precipitation
MAT	Mean Annual Temperature
m.a.s.l	Meters above sea level
River mouth	MZ1 and MZ2
iTsitsa River	MZ3 and MZ7
Thina River	MZ4 and MZ8
Kinira River	MZ5 and MZ9
Mzimvubu River	MZ5 and MZ10
Mzintlava River	MZ6 and MZ11

CHAPTER ONE

INTRODUCTION

1.1 INTRODUCTION

Global climate change is occurring on shorter timescales and at greater magnitudes compared to prehistoric climatic variations. Although climate change is a natural phenomenon that occurs as a continual process over long geological time scales, there still remains large uncertainty surrounding how these changes will affect current and future global and local environments (Marchant, 2010; IPCC, 2014). Certain approaches and tools exist that can aid the investigation and prediction of changing climates. One such tool is to model climate systems which can then be compared with environmental (proxy) data. Obtaining information to predict for climate changes are essential at both a regional and global scale (Anderson *et al.*, 2007), however, the instrumental climatic data required to build and validate these models are limited as they have only been recorded over the last fifty to one hundred years (Hulme and Jones, 1994). Since global climate system change occurs over geological timescales, longer time records are needed to inform climatic modelling (Hulme and Jones, 1994; MacKellar *et al.*, 2014).

Long term climate records can be obtained from investigating and reconstructing past climate and environmental conditions and vegetation dynamics. These palaeoreconstruction studies utilise specific organic and inorganic signals imprinted in various palaeorecords over geological timescales such as foraminiferal assemblages, charcoal concentrations, pollen grains and organic and inorganic isotope signals called biomarkers (Lockheart, 1997; Garcin *et al.*, 2012). Such proxies can record both past and present environmental changes and conditions (Anderson *et al.*, 2007), and inform about climatic variability by recording organic, physical and chemical characteristics of the prevailing environment and climate and thus are used to interpret palaeoclimates (Lockheart, 1997). Organic and inorganic records exist within different environmental archives for instance speleothems (Cherisch and Wright, 2019, Braun *et al.*, 2018); hyrax middens (Chase *et al.*, 2010), ice cores (Lorius *et al.*, 1992) and marine and lake sediment cores (Niedermeyer *et al.*, 2016; Vogts *et al.*, 2016; Chase *et al.*, 2015). The environmental and climate data recorded by these archives can then be integrated into modern climate data and modelled to predict future climate changes locally and globally (Anderson *et al.*, 2007).

Due to its geographical location between different atmospheric circulation systems as well as two major ocean currents namely the Benguela and Agulhas current, South Africa is highly sensitive to both regional and global climate change (Dupont *et al.*, 2013). Over the last fifty years, a trend of increased aridity and dryness have been shown, as well as an increase in flooding events and storm events of more than 1.5 times the global average, with significant social, economic and environmental impacts (Ziervogel *et al.*, 2014). Palaeoclimate research can enhance the general understanding of prevailing climate systems, regional climate adaptation potential and planning and aid future climate studies (Norström *et al.*, 2014). However, palaeoclimate studies are severely lacking in South Africa due to poor proxy preservation resulting from a generally arid environment, instrumental limitations, scarcity of ideal study sites and analytical limitations (Coetzee and van Zinderen Bakker, 1970). Palaeoclimate records have been obtained from various sites around South Africa, however, long continuous high-resolution data are poorly preserved (Chase and Meadows, 2007). Thus, high resolution palaeoclimate research is much needed to enhance our current understanding of climate change and to forecast the effects of these changes.

Marine sediments can provide valuable, continuous and long-term data about climatic, vegetation and sediment dynamics from a neighbouring continent (Shi *et al.*, 2001; Neumann *et al.*, 2011). A method for comprehensively interpreting these records, is to determine terrestrial organic and inorganic provenance. Provenance research involves investigating the origin and transport routes of organic and inorganic signals transported within a specific environment or system (Galy *et al.*, 2011; Garcin *et al.*, 2012; Rommerskirchen *et al.*, 2003). Interpretation of these signals is obtained by developing a modern picture of a particular environment (Brewer *et al.*, 2013). This data can then be correlated with marine sediment cores to infer palaeoclimate conditions which can be used to validate climate models. Provenance studies can be based on analysis of fluvial modern surface sediments, either in the form of river bed sediments or the suspension load (Galy *et al.*, 2011; Manjoro *et al.*, 2016). The distribution of these organic (pollen, leaf-wax derived long chain *n*-alkanes) and inorganic (XRF) proxies within sediments can elucidate information about the surrounding and prevailing climate-vegetation relationship (Vogts *et al.*, 2009, 2012). Thus, the problem of a lack of suitable palaeoreconstruction sites can be addressed by incorporating the analyses of modern organic and inorganic proxies contained within terrestrial fluvial sediments (Lockheart, 1997; Vogel, 1978). These signals are ultimately transported and deposited into marine sediments offshore.

Provenance of organic matter can be established through various quantitative analytical methods which extract specific vegetation and hydrological signatures from the sediment. The most common methods are to identify the stable $\delta^{13}\text{C}$ and δD isotope signatures of *n*-alkane homologues found within sediments (Lockheart, 1997; Tipple *et al.*, 2013; Poynter and Eglinton, 1990). $\delta^{13}\text{C}$ and ultimately C_3/C_4 variability changes within the sediment source, and if the sediment source (provenance) changes, then so does the $\delta^{13}\text{C}$ signal within. These vegetation groups originate from particular plant types, and are driven by certain climatic and environmental conditions (Vogts *et al.*, 2009).

Historically, studies utilising these proxies in southern Africa have been performed in isolation and over small spatial geographic extents (Herrmann *et al.*, 2017). There is a great need for the enhancement of these studies in southern Africa to enhance our understanding of current and changing environmental and climatic conditions. A multiproxy approach can greatly enhance provenance-based research for marine sediments and modern terrigenous sediments. No single proxy is sufficient to comprehensively describe complex environmental and climatic systems. Therefore, by investigating and analysing a combination of proxies, a more comprehensive and robust picture of modern vegetation, hydrological and sediment fluxes can be established (Kiage and Liu, 2006).

With the high uncertainty of how changing climate will affect environments, future studies should focus on assessing local and regional scale impacts in the southern African context. An understanding of such environmental and climate data can provide palaeoresearchers and environmental and conservation strategists with key information to inform future management plans in southern Africa (Manjoro *et al.*, 2016; Madikizela and Dye, 2003). Some key issues facing many regions of southern Africa, especially poorer regions such as rural settlements in the former Transkei, are that there is high uncertainty around the impacts climate change will have on the hydrological processes within the Mzimvubu catchment. Municipal reports have reported a need to focus research on hydrological, vegetation and sediment dynamics and the interplay between them and climate within the Mzimvubu catchment, to properly plan for future climate change (DWS, 2017; Madikizela and Dye, 2003). Therefore a marine sediment core (GeoB20624-0-1) has been extracted from the Mzimvubu river mouth to investigate long term and short term climate conditions and dynamics within the Mzimvubu catchment and broader Eastern Cape. The interpretation of multiple records required an understanding of the key provenance signals transported within the Mzimvubu catchment, which is presented in this study. This research project aims to provide an understanding of general environmental and

climatic conditions such as elevation, vegetation, rainfall, temperature, and relative humidity on a local scale by investigating provenance of sedimentological, hydrologic and vegetation signals transported within a local catchment (the Mzimvubu catchment) in the Eastern Cape, South Africa.

1.2 AIM AND OBJECTIVES

This research aims to investigate contemporary vegetation and hydrologic provenance dynamics of fluvial sediment across the Mzimvubu Catchment, South Africa. The specific objectives are:

- 1) To characterise the sediment and organic matter signals transported in the Mzimvubu Catchment;
- 2) To determine sediment provenance and source areas across the Mzimvubu Catchment by relating proxy data to environmental characteristics (vegetation, climate, geomorphology);
- 3) To determine whether river sediments contain pollen and plant biomarkers representative of the dominant contemporary vegetation;
- 4) To determine whether element composition analysis and particle size are representative of the surrounding geomorphology and contemporary land-use practice; and
- 5) To discuss the implications for using terrestrial markers to interpret marine sediments offshore of the Mzimvubu Catchment.

1.3 DISSERTATION OUTLINE

The purpose of this chapter has been to introduce the broader theme of climate change under which palaeoclimatological research and provenance based research in southern Africa has occurred, as well as stating the aim and objectives for this study. Chapter two will review the current body of modern provenance based literature in southern Africa over the last few decades, how it has developed and where it is lacking. Chapter two will also describe the theory, applications, methodologies and limitations of pollen analysis, stable carbon and hydrogen analysis of *n*-alkane plant wax biomarkers and XRF elemental compound analysis of river sediment. Chapter three provides an outline of the methods and materials used to address

the research questions and objectives. Chapter four will present and describe the results of the study. Chapter five will investigate and evaluate the implications of the study results, the meaning of the proxy signal, proxy provenance, and the palaeoclimatological implications of the study results. The last chapter, chapter six, will synthesise the most significant findings of the study, and evaluate the extent to which the aim and objectives of the study were addressed, and lastly providing future recommendations.

CHAPTER TWO

LITERATURE REVIEW

2.1 INTRODUCTION

Terrestrial long term comprehensive records are lacking in southern Africa, as well as the modern calibration studies needed to interpret these records (Meadows *et al.*, 1996; Zhao *et al.*, 2015; Tabares *et al.*, 2018). One such method to overcome this knowledge gap is multiproxy provenance based approach on modern sediment samples, wherein the characteristics of modern terrestrial organic and inorganic source regions is established within a system. These signals can provide valuable modern climatological, sedimentological, hydrological and ecological information which can ultimately be used to reconstruct past climatic and environmental conditions.

A multiproxy approach can be used to accurately interpret and verify modern proxy provenance data (Daniau *et al.*, 2013). The need for multiproxy analysis is based on the fact that proxies can be widely distributed over large areas, originate from diverse source areas, and be the result of complex environmental and physiological processes which can often complicate results (ZhaAo *et al.*, 2015; Hahn *et al.*, 2018). The most commonly utilised proxies in provenance and palaeoreconstruction research are pollen grains, plant wax *n*-alkane lipid biomarkers and inorganic element compositions stored in lacustrine or marine sedimentary archives (Lockheart, 1997; Dupont *et al.*, 2013; Bliedtner *et al.*, 2018). Where organic compounds in sediment archives may be damaged or disaggregated due to chemical weathering and biological decay processes, inorganic compounds may prevail under these conditions and still provide information about the surrounding environment and climate (Collins *et al.*, 2013). Thereafter, multiple proxy data can be compared to fossil records to establish palaeovegetation and palaeoclimatic relationships (Tabares *et al.*, 2018).

This chapter will review, outline and describe how pollen *n*-alkanes and elemental compositions are indicators of climate and environmental change on a global scale, and how these proxies are utilised in provenance based research. Specific attention will be given to the applications and taphonomy of proxy transport. Thereafter, provenance research in southern Africa will be described and outlined with emphasis on how modern sedimentary archive analysis has been developed over the last four decades.

2.2 PROXIES AS INDICATORS OF CLIMATE AND ENVIRONMENTAL CHANGE

2.2.1 Introduction

To quantify and interpret changes in palaeoclimates and palaeoenvironmental conditions various components of the modern environment and climate need to be investigated. These include the establishment of organic and inorganic compounds stored within sedimentary archives. This section will provide a theoretical overview of pollen, *n*-alkane wax derived long-chain *n*-alkanes and inorganic element compositions, as well as the applications, limitations, methods and implications of and how they are used to establish source regions and climatic, vegetation and environmental conditions

2.2.2 Pollen

2.2.2.1 Background information

Pollen analysis, or palynology defined by Faegri and Iverson (1989) is a quantitative and qualitative tool to reconstruct both former and modern vegetation types, through the study of pollen grains. At the start of the twentieth century, Lennart von Post pioneered the use of pollen analysis to reconstruct vegetation from peat bogs. The technique has since been expanded and applied to a variety of sediment deposits around the world (Bunting, 2008), including modern fluvial sediments (Davis *et al.*, 2013; Moss *et al.*, 2005; Brown *et al.*, 2007; Hahn *et al.*, 2018; Chmura *et al.*, 1999), and marine sediments (Herrmann *et al.*, 2016; Yang *et al.*, 2016; Zhao *et al.*, 2015; Dupont *et al.*, 2013). Palynology enables researchers to describe how vegetation compositions respond to different climate conditions, which ultimately can help predict for future changes in climate and plant dynamics on regional and global scales scale (Anderson *et al.*, 2007; Watrin *et al.*, 2007; Bradshaw, 2008).

Pollen analysis are based on basic principles defined in Birks and Birks (1980) and state the various advantages of utilising pollen grains as recorders of environment and climate change. Pollen grains are abundantly produced by plants and thus can act as a representative of local vegetation compositions and dynamics (Birks, 1981). Another basic principle is that pollen grains can be counted resulting in a pollen spectrum that can be compared temporarily and spatially (Birks and Gordon, 1985). This spectrum of pollen rain should be an index of the vegetation at that point in space and time. Furthermore, pollen assemblages and concentrations are responsive to environmental factors such as soil type, acidity, water pH, water levels, water velocity and climates (Brewer *et al.*, 2013; Brown *et al.*, 2007; Delcourt and Delcourt, 1980). Therefore, by analysing pollen assemblages from various locations using a provenance based approach, vegetation similarities and differences can be determined. These modern records

may not be long term continuous records, however, they provide key data on prevailing conditions and within a specific system (Moss *et al.*, 2005; Tabares *et al.*, 2018).

Local climates drive and influence the distribution of vegetation compositions and plant types. Changes in these distributions in the past can be reconstructed by investigating a fossil pollen recorded in modern fluvial and marine sediments (Brewer *et al.*, 2013). However, it is difficult to quantify the processes and drivers of these changes, especially in the absence of long term vegetation composition datasets in South Africa (Tabares *et al.*, 2018). There remains a general reliance on marine sediment cores as well as lake sediment cores as records for providing environmental and climate information (Chase and Meadows, 2007), and a general lack of terrestrial records which analyse the provenance of sediment organic matter signals from fluvial environments. Whilst sediment core data provide long temporal data, issues around taphonomy, preservation and provenance have been raised (Lim *et al.*, 2016).

Long term comprehensive studies on environment and climate change are lacking in southern Africa. This is as a result of a lack of suitable study sites and poor preservation due to a generally arid climate (Fitchett *et al.*, 2017; Chase and Meadows, 2007). Historical palynological studies have focussed primarily on lakes and peat bogs, however these sites are widely spaced and concentrated in wetter environments. Site selection for palaeoclimatological research in southern Africa has previously been determined by site accessibility, and sites with highly sensitive ecological systems are often neglected (Fitchett *et al.*, 2016). This has resulted in discontinuous spatial and temporal environmental and climate data for many regions of southern Africa. Recent studies have highlighted the variability of moisture records derived from palaeoclimatological records. To overcome the paucity of suitable sites and to fill the gap in discontinuous records, researchers have explored the use of pollen grains preserved in modern fluvial surface sediments for arid and semi-arid regions (Moss *et al.*, 2005; Brown *et al.*, 2007; Clement *et al.*, 2017). These terrestrial modern records can provide an additional data source for studies investigating both contemporary and past environmental and climate conditions.

Some limitations of terrestrial records, however, include discontinuity due to being distributed over large areas of the continent (Neumann *et al.*, 2014), low temporal and spatial resolutions (Neumann *et al.*, 2011), low taxonomic resolution (Tabares *et al.*, 2018), and contradictory results produced by different proxies (Baker *et al.*, 1998). Record discontinuity could be due to the variable dispersal and preservation capabilities of pollen assemblages in fluvial sediment,

as well as the susceptibility of different taxa to different conditions and taphonomic processes which affect pollen preservation (de Villiers and Cadman, 1997). In some cases, pollen taxon groups contain a wide variety of species that can grow in climatically diverse habitats and studying pollen provenance in fragmented environments is complex (Tabares *et al.*, 2018). Therefore, a non-linear relationship exists between pollen assemblages and surrounding vegetation composition (Brewer *et al.*, 2013). Despite this, modern pollen samples have been found to reflect local environment and vegetation conditions (Herbert and Harrison, 2016). Pollen records have provided the necessary spatial information about vegetation distributions and ultimately climate conditions (de Villiers and Cadman, 1997; Mudie *et al.*, 1994; Scott, 1984). Pollen assemblages preserved in marine sediments record terrestrial vegetation and thus may reflect climate variations and can provide accurate information for palaeoreconstructions (Dupont *et al.*, 2013; Liu, 1989).

2.2.2.2 Applications

Pollen data are widely applied in palaeoclimatology, palaeoecology, stratigraphic correlations, archaeology and modern pollen studies. The modern pollen approach has been widely utilised in recent studies to better understand modern pollen-vegetation-climate conditions to forecast and predict for climate changes (Xu *et al.*, 2016). Specific vegetation compositions, environmental and climate conditions can be established through modern pollen assemblages, as these assemblages are driven by the nature of these conditions (Brewer *et al.*, 2013). A recent method for determining these conditions and changes is to extract pollen data from sediment in fluvial systems as these record information about prevailing sediment, hydrologic and vegetation systems (Chmura *et al.*, 1999; Parker *et al.*, 2004). A commonly used technique for determining modern pollen climate relationships is the modern analogue technique (Howe and Webb, 1983). The basic underlying principle is uniformitarianism, which means that the information needed to understand past conditions can be obtained by analysing the relationship between modern pollen assemblages, the plant types they represent and their related climates (Birks and Birks, 1980). This can be achieved by analysing the presence/absence of various palynomorphs in sediments (Brewer *et al.*, 2013). Ideally, pollen source regions and vegetation compositions can be determined using specific pollen assemblage changes, however various factors complicate these interpretations (Zhao *et al.*, 2015; Dupont *et al.*, 2013). One disadvantage of the modern analogue technique is that vegetation can represent varying climatic characteristics, and modern analogues may not exist for some fossil pollen assemblages (Herbert and Harrison, 2016; Chen *et al.*, 2004). Despite these limitations, these

data can potentially provide key information about hydrologic dynamics and vegetation compositions and changes (Brewer *et al.*, 2013). Not only can the modern provenance technique provide key data for local management strategies, these data are an essential first step for better understand past conditions through palaeoreconstruction studies and climate modelling (Clement *et al.*, 2017; Carrion, 2002; Delcourt and Delcourt, 1980).

The success of utilising a modern analogue approach is shown by (Groot, 1966; Peck, 1973; Chmura *et al.*, 1990, 1999). These studies investigated pollen in river sediments to determine whether pollen assemblages represent vegetation compositions and dynamics. However, some studies analysing pollen assemblages in small (Peck, 1973) and large (Traverse, 1988) river systems and catchments, have shown a seasonal effect on pollen assemblages from changing parent vegetation sources. Yang *et al.*, (2016) who extracted pollen data from 72 surface sediments (RBS) in the Liaodong Bay (China) including samples from the inflowing rivers found that pollen assemblages accurately represent forest compositions and transitions from grasslands to forests under different climate gradients. Therefore, to accurately interpret fossil records, understanding sediment provenance and ultimately the processes driving pollen provenance are important. Chmura *et al.*, (1999) found that pollen transported in fluvial systems is a better representation of vegetation compared to aeolian pollen. However, they also found that analysis and interpretation of pollen samples from fluvial systems is complicated by taphonomic processes such as mixing and reworking (Shi *et al.*, 2001; Chmura *et al.*, 1999; Zhao *et al.*, 2015), and therefore it is important to consider taphonomic processes and effects in provenance pollen research.

2.2.2.3 *Effects on the pollen signal*

Quantifying the pollen-vegetation relationship from pollen assemblages is a complicated process (Andersen, 1973; Bradshaw, 2008; Sugita, 1993). This is because pollen assemblages can be altered by pollen production mechanisms, pollen production, dispersal route into the depositional environment, reworking of pollen assemblages in fluvial systems (mixing), and pollen preservation in aerobic versus anaerobic environments (Delcourt and Delcourt, 1980; Yang *et al.*, 2016; Xu *et al.*, 2012; Campbell and Chmura, 1994; Li *et al.*, 2005; Birks and Birks, 1980). These processes and effects have been investigated and reviewed by various authors over the last six decades.

One of the first investigations into pollen taphonomy and preservation in fluvial systems was by Groot (1966). Groot (1966) analysed pollen assemblage transported in the estuary of the Delaware River, by correlating the concentrations of pollen to sediment compositions, and

found that most of the pollen grains were sourced from fluvial systems rather than aeolian mechanisms. A year later, Cushing (1967) analysed pollen assemblages in Quaternary sediments to determine different rates and categories of pollen preservations. Similarly, Havinga (1963, 1967, 1984) studied the sensitivity of different pollen types in different sediments to varying levels of corrosion and found that fluvial transport can have significant effects on pollen preservation and morphology. Similar to Groot (1966), Traverse (1988) stated that the importance of aeolian versus fluvial pollen pathways varies depending on the distance travelled, river discharge patterns and velocity and depositional environments. They found that aeolian depositions of pollen grains of the NW coast of Africa are far more significant compared to fluvial depositions of pollen grains on the eastern coast (Traverse, 1988). Conversely, Chmura *et al.*, (1999) found that pollen transported in fluvial systems is a better representative of vegetation than aeolian pollen. A study by Campbell and Chmura (1994) on fossil pollen assemblages found that preservation and deposition were a result of their depositional environments and transport routes and processes and therefore, fluvial sediments were accurate representatives of the surrounding environment but that taphonomic and environmental effect needed to be taken into consideration.

Barreto *et al.*, (2012) successfully analysed the process and dynamics controlling pollen transport and deposition in the Guanabara Bay, by analysing 27 surface sediment samples and sediment cores. They found that overall palynomorph diversity and abundance was low in river systems, especially the SPM fraction. However, the pollen assemblages in the surface sediments still represented the local vegetation of the Mzimvubu catchment basin. Any irregular pollen assemblage and damaged pollen grains and spores were as a result of tide velocity, abrasion during fluvial transport, human perturbations and reworking in the depositions environments. Similar results were found by Luz *et al.* (2005), however, they also found palynomorph morphology to be an important factor in determining pollen transport, deposition and preservation.

Origin, taphonomy and deposition

The nature of the pollen grain and assemblages itself can affect pollen reconstructions. For example, pollen records sampled from peat, lake and core sediments are a reliable record of regional pollen data and ultimately local vegetation and climate (Herbert and Harrison, 2016). Pollen grains found in wet sediment samples such as lakes and peat bogs are often less prone to preservation problems (Herbert and Harrison, 2016). However, accessing these sites is not always feasible or possible either due to logistical issues such as access restrictions, or limiting

climate factors such as arid conditions. Pollen grains damaged by erosional processes are as a result of periods of exposure to the atmosphere during dry periods and therefore can complicate interpretations. Similarly, pollen samples extracted from closed canopies are likely to be a better reflection of local vegetation rather than open environments which are affected by wind and rain erosion (Herbert and Harrison, 2016). A study by Holloway (1989) found that when pollen samples were wetted and dried at varying intervals and after a number of repetitions, most of the pollen taxa were found to have suffered damage. A similar study was performed by Campbell (1991) on *Pinus* pollen and their results showed that the rate of damage has a linear relationship to wet and dry cycles. The overall results of Campbell (1991) is that pollen grains are damaged by repeated wet-dry cycles. Therefore a river that experiences high sedimentation and resulting periods of exposure during low flow periods will contain less or damaged pollen grains (Campbell and Chmura, 1994). Other palynological studies in arid areas also show that pollen assemblages may be prone to overrepresentation of certain taxa (Carrion, 2002). For example, local taxa such as Poaceae and Cyperaceae produce large amounts of pollen grains during flowering seasons, whereas some trees and shrubs (e.g., *Combretum* and *Acacia*) produce little amounts of pollen into the air (Carrion, 2002).

In the past, pollen assemblages were assumed to have a linear relationship with vegetation and plant abundance (Birks, 1981). Previous studies were aware of the various taphonomical processes that affect fossil and modern pollen assemblages, however, these factors were often not considered when interpreting pollen data due to the complexities that arose (Xu *et al.*, 2016). An explanation for this is that variations in pollen assemblages and preservation in modern surface samples due to diversity processes in depositional environments and pollen production and pollen morphology, complicate the interpretation process (Xu *et al.*, 2016). In more recent years, this has changed and many studies have focussed on understanding pollen production and dispersal processes in fluvial sediments in determining pollen-vegetation-climate relationships (Li *et al.*, 2013).

When investigating pollen assemblages in fluvial systems, Smirnov *et al.*, (1996) found that pollen assemblages are less homogenised in fast flowing rivers, and thus produce an overall mixed signal. Chmura and Liu (1990) found that pollen can enter rivers from river bank erosion which is detected in the suspended sediment load of rivers, however these sediment yields are difficult to quantify. Therefore, the source region of local palynomorphs is dependent on river geomorphology. For example, pollen grains may preferentially fall in straight and fast flowing rivers compared to meandering rivers. Meandering rivers are accompanied by levees and sand

banks which results in deposition and aggradation of the alluvium on the floodplain (Chmura *et al.*, 1999). Therefore, fluvial sources and processes determine pollen assemblages (Baker *et al.*, (1998).

In addition, Fall (1987) investigated the taphonomy of pollen concentrations in a stream of the Arizona River and found that pollen concentrations differed depending on the nature of the sediment they travelled in. She found that coarse alluvium contained less pollen grains compared to fine alluvium, and this was as a result of sorting and mixing during pollen transport. Fall (1987) concluded that intensive mixing and sorting of alluvial sediments and pollen grains in rivers made them unsuited for palaeoreconstruction research. Similarly, Chmura and Liu (1989) found that pollen concentrations have a strong correlation to the suspended sediment load in a river and that increased sediment loads damaged pollen grains compared to reduced sediment loads. Pollen grains in fluvial systems are as much as a result of the sediment load as the vegetation it is supposed to represent (Campbell and Chmura (1994). Therefore, utilising surface samples alone should be done with caution since pollen concentrations are considerably lower, and river bed samples could potentially result in an overrepresentation of pollen grains. In addition, caution must be taken when interpreting pollen assemblages in sediment samples that could have experienced periods of wet-dry cycles. It has therefore been recommend that future pollen work in river sediments should extract both suspended particulate matter and river bed sediment samples to compare and contrast (Campbell and Chmura, 1994).

Dispersal mechanisms

Pollen dispersal distance varies between taxa as some pollen taxa can be dispersed over long distances (*Pinus*) whilst others do not disperse far (Scott, 1982). Firstly, wind borne pollen is determined by wind speed and pollen morphology (size, shape, presence or absence of air sacks) (Xu *et al.*, 2016). Secondly, river borne pollen accumulate after flowering seasons, where pollen grains are carried by wind and can become embedded in top soils, which can be then transported by sheet erosion to adjacent rivers. Pollen assemblages transported by rivers are different to wind borne pollen assemblages due to the sorting effect of rivers. Some studies argue that pollen which is transported as sedimentary particles in rivers and experience sorting are not a reflection of vegetation compositions near the sample site (Fall, 1987). It was suggested by Fall (1987) that reconstructing past climate changes using alluvial pollen is not suitable, as pollen assemblages and distributions are often are reflection of sediment and hydrologic processes rather than vegetation. Conversely, Hall (1989) stated that alluvial pollen

can be used if certain factors are taken into consideration such as that pollen grains are located in the suspension load of a river, and therefore sorting and mixing effects are small. Thirdly and lastly, pollen distribution by insects (entomophily) is also a significant dispersal mechanism for pollen grains (Scott, 1982). A study of alluvial pollen disposition in lakes of Daihai (China) found that 63 palynomorphs were present in the lake sediment core, however, only 42 of those palynomorphs were present in the inflowing rivers, therefore indicating an additional source such as insects. Quantifying the diverse range of pollen transport mechanisms and taphonomic processes can be complex and information can be lost due to over and under-representations of pollen assemblages. To overcome the issues of representivity a multiproxy approach should be considered, wherein additional organic and inorganic proxy data are analysed with and compared to pollen assemblage data. Despite the fact that palynology is based on sound principles and quantitative analyses, there are several limitations associated with the technique, which are discussed below.

2.2.2.3 Limitations of Palynology

Faegri (1966) and Scott (1984) outline several problems associated with pollen analysis for instance, taxonomic resolution, preservation issues and representivity. Pollen identification is achieved through comparison of existing pollen references and records. Identification, however, can be difficult and can only sometimes be achieved to the family taxonomic level. Pollen grain preservation is an important pre-requisite to ensure accurate identification, and studies have found that modern sediment samples are generally poorly preserved compared to peat bogs and lake sediments. When pollen grains are deposited into anaerobic, waterlogged environments, decomposition is reduced and the pollen grain exine is preserved. However, in modern sediments, pollen grains rapidly decay in the presence of oxygen and modern sites, such as river sediment, and are continuously re-oxygenated through water mixing and remobilisation of soil particles. This being said, it has been found that the pollen spectra preserved in modern samples are adequate to represent the surrounding vegetation composition and climate dynamic (Davis *et al.*, 2013). Lastly, modern pollen samples compared to fossil pollen records provide the most accurate representation of prevailing vegetation biomes, agricultural activity and climatic conditions (Davis *et al.*, 2013).

Representivity of the local environment is another problem associated with pollen grain analysis and interpretation. Jacobson and Bradshaw (1981) showed that local pollen is a combination of pollen originating from plants no more than 20 m away from the sample sites, and regional pollen which is transported from larger distances. Pollen source area and

representivity are an important consideration for modern and palaeoecological studies, and pollen dispersal mechanisms must be carefully considered as they can affect the local pollen record. Plants can be zoophilous (animal-pollinated), anemophilous (wind-pollinated), or entomophilous (insect-pollinated), with pollen productivity to accommodate a particular mode of pollination. Wind pollinated taxa will naturally be more widely dispersed compared to animal and insect pollinated taxa and thus represent a large source area. Whereas, animal and insect pollination may represent a smaller source area.

Pollen data are not presented as discrete numbers but rather as proportions of a total pollen sum. This can lead to problems of representivity between different taxa as pollen grain production varies from taxon to taxon. Some taxa are more cosmopolitan compared to rarer endemic species which have reduced environmental distributions. Furthermore, it is important to establish the start and end of growing season for the prevailing taxa in the study site, as pollen grain production is highest in the growing season, which can lead to issues of overprinting or underprinting during different seasons.

2.2.2.4 Methodological considerations for palynology

Site selection and field sampling

Although peat deposits contain the best pollen records (Jacobson and Bradshaw, 1981), modern pollen grains in modern river sediments are better indicators of the prevailing vegetation composition and ultimately climate (Davis *et al.*, 2013). Issues of pollen taphonomy should be considered as these directly affect pollen transport, preservation and deposition in different environments (Delcourt and Delcourt, 1980). To determine pollen provenance dynamics in fluvial environments, surface sediments should be extracted and analysed rather than sediment core samples. Provenance dynamics refer to the various origins, movements, deposition environments and transport pathways of the proxy signals within and throughout the catchment. The most common method for extracting surface sediment is a grab-sampling method, wherein a portion of sediment substrate is extracted from a river or lake bed (Coggan *et al.*, 2007). Consideration should be given to finding a suitable site for grab-sampling, as issues of water velocity, sedimentation due to deposition and water level are reported to affect pollen assemblage and distribution (Delcourt and Delcourt, 1980).

Laboratory procedures

Laboratory pollen processes comprises of three stages for instance: sediment subsampling, chemical and physical processing, mounting of samples onto slides, counting and microscopy. Subsampling should be conducted in a controlled and sterile laboratory environment, where

there is little chance for contamination of the samples. Contamination can be prevented by ensuring the surface of the subsample is removed with a clean knife or scalpel (Birks and Gordon, 1985). The sample resolution for modern studies are similar to that of fossil pollen sample resolution, wherein sample resolution is dependent on the resolution specified by the parameters of the study (Faegri and Iverson, 1989). Sediment samples are physically and chemically processed. Pollen chemical processing, defined by Faegri and Iverson (1989) is an effective and relatively fast method for processing pollen grains. The method utilises Hydrochloric acid, which removes the carbonate fraction from the samples, Potassium hydroxide which breaks down the sediment and removes the humic acids, Hydrofluoric acid which removes the silicate fractions and Acetolysis which removes the cellulose fraction. The safranin stain is used to stain the pollen grains red or pink which is useful for counting and identification. Traditionally 1cm^3 is volumetrically measured as suitable subsample for pollen analysis (Birks and Gordon, 1985), however, pollen analysis on fluvial river bed sediment has been shown to contain considerably lower pollen grains compared to sediment cores (Brown *et al.*, 2007; Davis *et al.*, 2013; Clement *et al.*, 2017). A typical sample amount for fluvial sediment containing pollen has not been established however, it is recommended by various modern pollen studies that more than 1cm^3 will be required for accurate pollen analysis (Hunt, 1987; Zhu *et al.*, 2002).

Mounting

When mounting the pollen samples, it is important to consider the use of the slides before deciding the method of mounting. For example, if the slides are to be used on a temporary basis or if permanent mounting is required (Faegri and Iverson, 1989). When choosing a mounting solution or method, the refractive index should be taken into consideration as this could affect the counting process (Faegri and Iverson, 1989). Various mounting agents exist that can be used, for example, silicon oil, glycerol, glycerine jelly and Aquatex mounting agent. The reason for mounting allows for identification of pollen grains at a later stage, as individual pollen grains or clusters of specific pollen grains can be photographed.

Counting

Pollen grains are counted and identified using a light microscope across an evenly spaced transect along the microscope slide. It is recommended that a full slide be counted for each sample to ensure the pollen grains are well represented. To ensure a reliable estimate of pollen abundance, a sufficient pollen grain count should be established (Birks and Gordon, 1985). Various studies report on different minimum counts, the most commonly utilised are 250, 500

and 1000 pollen grains. Clusters of pollen grains are considered rare in modern sediment samples as overall abundance is low compared to peat and lake sediments. Therefore a minimum of 50 is suited to modern pollen sediments (Moss *et al.*, 2005; Herbert and Harrison, 2016). It is also recommended that unidentified pollen grains be labelled as unidentified or unknown.

Data representation

Visually representing the pollen data is imperative for later interpretations (De Vries and Wijmstra, 1986). This can be achieved by using a series of diagrams known as pollen diagrams. Specialised programme software such as Psimpoll and Tilia, is used to create these diagrams. These diagrams accurately represent fluctuations in the pollen data and are plotted in the form of relative proportions of the pollen count (Bennett, 1988). Pollen diagrams are a representation of local and regional pollen abundances, as well as ecological groupings that are the result of major changes in climatic conditions (De Vries and Wijmstra, 1986).

Interpretation

Pollen data are a direct representation of the prevailing vegetation composition and climate conditions. Changes in pollen assemblages can be used to infer transitions between major ecological groupings (biomes) within an environment and the processes that drive these transitions (Birks, 1981). Pollen data can thus infer the vegetation-climate relationship, by investigating specific pollen assemblages and parent plant types under specific climate conditions, and ultimately to reconstruct palaeoclimates and palaeoenvironments (Birks, 1981).

2.2.3 Organic geochemistry

2.2.3.1 Background information

Recent changes in atmospheric CO₂ and greenhouse gasses have likely affected plant-atmosphere interactions. This change is described as a negative impact on plant distribution and functionality under increasing atmospheric CO₂ and greenhouse gas concentrations. Some plants respond negatively to elevated greenhouse gasses and CO₂ concentrations by decreasing stomatal openings (Cassia *et al.*, 2018). Large impacts of elevated CO₂ are seen in erratic and variable rainfall distributions and the occurrence of more intense weather conditions such as droughts and flooding (IPCC, 2014). These severe changes in weather may bring plants to beyond their capacity of adaption (Cassia *et al.*, 2018).

Obtaining information on how these plants respond to these changes would enable researchers to determine and model future responses and dynamics (Vogts *et al.*, 2012). To accurately interpret these climatic conditions, the analysis of a specific plant component such as leaf-wax

derived *n*-alkanes can be performed. Leaf-wax *n*-alkane analysis can yield valuable information on plant types, distributions and ultimately prevailing climatic conditions (Li *et al.*, 2018). By establishing leaf-wax derived *n*-alkane distributions and concentrations from sediment samples, a modern analogue of the surrounding vegetation and climate can be determined. This approach is based on the principle that all higher plant types are covered by an epicuticular wax which is exposed to external climate conditions. These waxes contain long chain *n*-alkanes, which can persist in sediments, are transported by fluvial or aeolian processes, are well distributed in different environments and represent specific hydrological and climate systems for example, increased aridity and solar irradiance, variations in rainfall amount and distribution. (Badewien *et al.*, 2015; Carr *et al.*, 2015; Vogts *et al.*, 2012). Moreover, they can be traced to specific locations or represent specific taxa and environmental and climatic conditions (Collins *et al.*, 2013; Rommerskirchen *et al.*, 2003; Schefuß *et al.*, 2003, 2005). A majority of these studies though report on the issues of resolving spatial heterogeneity and diverse source region complexities (Chase *et al.* 2013). In order to enhance these interpretations, and in an attempt to overcome spatial complexity issues, specific carbon ($\delta^{13}\text{C}$) and hydrogen (δD) isotope values from plant waxes have been analysed (Wang *et al.*, 2010; Chase *et al.*, 2013; Haggi *et al.* 2016). Both stable carbon ($\delta^{13}\text{C}$) and hydrogen (δD) isotope compositions found in plant leaf-wax derived *n*-alkanes are driven by temperature, precipitation, evaporation and moisture content, and can thus act as proxies of climatic and environmental conditions (Scott and Vogel, 2000). The main principles driving the investigation of *n*-alkanes as proxies for environmental and climate change are discussed below.

Chibnall *et al.*, (1934) performed one of the first analyses on plant waxes and found that terrestrial higher plant *n*-alkanes maximise at the nC_{25} to nC_{35} chain lengths with an odd-over-even chain length predominance. Plant types in arid, subtropical and tropical environments would synthesise longer *n*-alkane chain lengths (nC_{31} , nC_{33} , nC_{35}) compared to temperate regions, which would synthesise moderate to shorter chain lengths (nC_{25} , nC_{27} , nC_{29}). Longer *n*-alkane chain lengths have been associated with grasses and herbs (nC_{31} , nC_{33}), whereas shorter chain lengths represent trees and shrubs (Diefendorf and Freimuth, 2017; Diefendorf *et al.*, 2010; Vogts *et al.*, 2009, 2012). Contrary to this, some research from the 1960s and 1970s has shown that microbes (e.g. fungi, algae and bacteria) can also produce long chain *n*-alkanes (for example: Oró *et al.*, 1966; Jones, 1969). Oró *et al.*, (1966) reported on chlamydospores of *Sphacelotheca reiliana*, *Ustilago mydis*, *U. nuda* from higher plant tissues and found that the

n-alkane carbon chain length ranged from nC_{14} to nC_{37} Jones (1969) reported on some fungal species such as *Penicillium species* and *Aspergillus species* and found the *n*-alkane carbon chain lengths to range from nC_{15} to nC_{36} . It is also possible that microbes ingest other long chain *n*-alkanes and therefore can confound results (Jones, 1969). Despite these potential contributions to *n*-alkane chain lengths, there are significant uncertainties in this research whether the long-chain *n*-alkanes are produced by these microbes (Li *et al.*, 2018). Therefore, *n*-alkane distributions can potentially act as indicators of climate and vegetation change (Eglinton and Hamilton, 1963, 1967).

Plant wax *n*-alkanes can be transported by rivers and aeolian wind dynamics and deposited offshore in the adjacent ocean and are well preserved in lacustrine and marine sediments over geological timescales (Haggi *et al.*, 2016). Various environmental and climate conditions can be stored as specific isotope values within plant wax *n*-alkanes. For example, compound specific carbon ($\delta^{13}C$) and hydrogen (δD) isotopes can be used to infer vegetation forms and hydrologic processes. The stable $\delta^{13}C$ and δD isotope composition of plants differs with different photosynthetic pathways (C_3 , C_4 CAM). Since modern biomes follow climate gradients, if the predominant vegetation can be established through $\delta^{13}C$ analysis, climate therefore can be inferred (Vogts *et al.*, 2016). Plant wax leaf-wax derived long chain *n*-alkanes are also found in fossil records (Eglinton and Logan, 1991); modern leaves (Huang *et al.*, 1995); and fluvial and marine sediments (Sachse *et al.*, 2012; Schefuss *et al.*, 2011). The interpretation and application of sediment *n*-alkanes, especially for palaeoecological studies, requires a sound understanding of the prevailing modern environment from which they originate (Diefendorf *et al.*, 2011; Wang *et al.*, 2015). Thereafter, *n*-alkane data can be effectively utilised in palaeoreconstruction studies.

2.2.3.2 Applying $\delta^{13}C$ and δD analyses to modern sediments

Stable Carbon ($\delta^{13}C$) Isotopes

The analysis of carbon ($\delta^{13}C$) and hydrogen (δD) isotopes of plant wax is a useful tool for reconstructing modern and past climates and vegetation (Haggi *et al.*, 2016). Plants utilise three different photosynthetic pathways such as: C_3 , C_4 and Crassulacean Acid Metabolism (CAM) to fractionate atmospheric carbon. This results in distinct isotopic compositions of plant tissues for each plant type. CAM uses a combination of C_3 and C_4 and thus has an isotopic compositions between C_3 and C_4 . Analysing $\delta^{13}C$ values of plants has become an important tool for reconstructing C_3/C_4 vegetation compositions and transitions and their associated environmental conditions such sediment processes, hydrology and precipitation (climate). $\delta^{13}C$

of C₃ vegetation is on average lower (depleted) than C₄ vegetation, and the distribution of C₃/C₄ vegetation is controlled by temperature and precipitation during the growing season (Figure 2.1). C₃ vegetation comprises predominantly of trees and woody shrubs and some grasses that prefer cold growing seasons in temperate environments and shaded areas (Schefuß *et al.*, 2005, 2011). C₃ vegetation $\delta^{13}\text{C}$ values range from -23 ‰ to -35 ‰ (Vogts *et al.*, 2012; Wang *et al.*, 2015) (Figure 2.1).

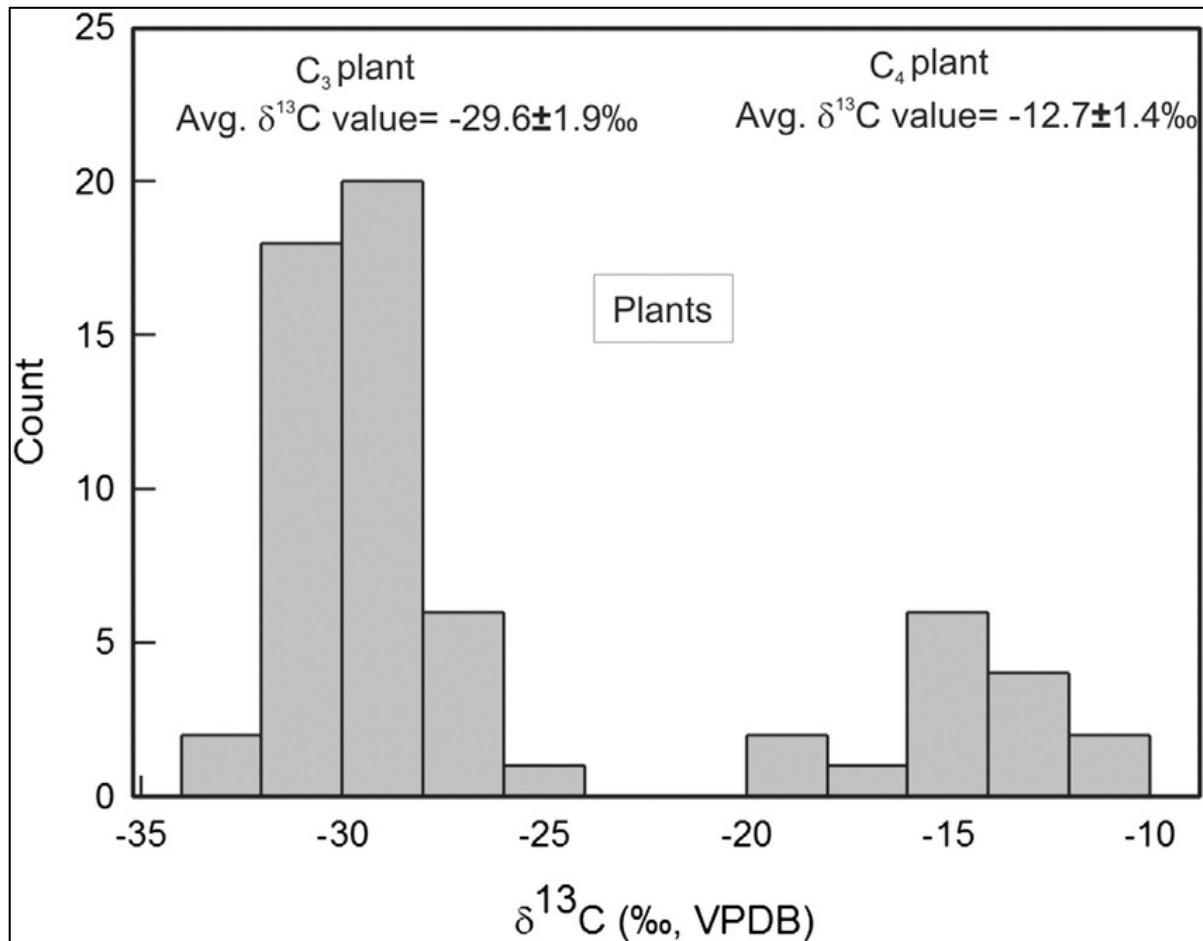


Figure 2.1: Histogram showing the $\delta^{13}\text{C}$ values of C₃ (-29.6 ‰) and C₄ (-12.7 ‰) for modern C₃ and C₄ plants from the Gangetic Plain, India (Basu *et al.*, 2015).

On the other hand C₄ vegetation comprises predominantly of cereal crops and grasses that are adapted to warm growing seasons, high temperatures, seasonality of rainfall and high radiation. C₄ vegetation $\delta^{13}\text{C}$ values on average range from -20 ‰ to -9 ‰ (Schefuß *et al.*, 2005; Vogts *et al.*, 2009) (Figure 2.1). In South Africa, C₃ vegetation prefers winter rainfall areas and cool summer rainfalls regions, whereas C₄ is found in warm, dry areas (Schefuß *et al.*, 2005; Haggi

et al., 2016). CAM plants have the ability to conserve their metabolic processes during dry periods which allows them to survive arid conditions. The stable carbon and hydrogen isotope technique is most suited for detecting changes in the composition of C₃/C₄ vegetation as well as prevailing climate and hydrological processes (Dupont *et al.*, 2013).

It has been suggested that the sourcing of plant lipid biomarkers may not be uniform within and across catchments, especially if the catchment is characterised by variable topography, vegetation zones, environmental variability and climates (Ponton *et al.*, 2014). Taphonomy is an important part of provenance studies as erosional and transport processes can lead to the loss of some organic matter compounds, whereas others may be preserved (Walling *et al.*, 1999; Wakeham *et al.*, 1997). The transport routes and depositional environments of terrigenous biomarkers are likely to be a function of the size, shape and density of the sediment particle as much as they represent the vegetation they pass through (Govin *et al.*, 2012). Variable erosional processes and reworking in fluvial and marine sediments has also been shown to alter the isotopic composition of plant biomarkers (Schefuß *et al.*, 2005, Bouchez *et al.*, 2014; Herrmann *et al.*, 2016). Various additional *n*-alkane indices have been developed in order to aid the establishment of sediment organic matter source regions and provenance.

Geochemical analyses of sediment *n*-alkane records apply various techniques and methods to better explain *n*-alkane distributions such as variations in *n*-alkane chain length ratios. For example, the ratio of long chain lengths (nC₃₁) to shorter chain lengths (nC₁₇) is used to determine terrestrial plant matter versus aquatic algae input into sediment archives (Ficken *et al.*, 2000; Cranwell *et al.*, 1987). For example, moderate chain lengths such as nC₂₃ and nC₂₅ have been used to represent *Sphagnum* moss (Ficken *et al.*, 2000). Other ratio indices include Average Chain Length (ACL) which calculate a weighted average of the carbon chain lengths, and Carbon Preference Index (CPI) (Eglinton and Hamilton, 1967). Most studies report that long chain *n*-alkanes (nC₃₁) in sediments represent input from grasses, whereas nC₂₇ and nC₂₉ indicate input from woody shrubs and trees (Meyers, 2003; Zhang *et al.*, 2006). However, the ability of a single *n*-alkane homologue to represent broad plant groups such as woody shrubs, trees and grasses has been questioned by many authors (Cranwell, 1984). Therefore, correlating *n*-alkane distributions with pollen grain assemblages and sedimentary elemental data, palaeoecological data can be accurately interpreted (Galy *et al.*, 2011; Herrmann *et al.*, 2017).

A confounding factor when analysing terrigenous organic fractions in sediments is that as *n*-alkane plant waxes, pollen and sediment particles likely represent different transport pathways

and source regions (Hahn *et al.*, 2018). For example, terrestrial leaf wax biomarkers from river sediment represent a wide range of diverse inputs or source regions (Galy *et al.*, 2011). Similarly, Rommerskirchen *et al.*, (2003) found that profiling biomarker distributions on continental margins were difficult due to the variability in transport mechanisms (aeolian and fluvial), sediment type, and sediment provenance, played an important role in biomarkers compositions and distribution. Therefore, it has been suggested that the study of fluvially transported biomarkers should also investigate whether or not the river is capable of transporting sediment organic matter with isotope signals that represent the surrounding vegetation, as well as the hydrological processes driving provenance (Ponton *et al.*, 2014).

Despite numerous effects on *n*-alkane plant wax biomarkers during transport and deposition, numerous studies have still found the isotope composition of *n*-alkane distributions, to be a good indicator of prevailing vegetation compositions and ultimately climate conditions (Vogts *et al.*, 2009, 2012; Rieley *et al.*, 1991). *n*-Alkane carbon isotope values are specifically related to plant photosynthetic pathway, and therefore, since each pathway produces its own unique isotope value, the differentiation between C₃, C₄ or CAM plants can be established (Cerling *et al.* 1993; Collister *et al.* 1994; Bassham *et al.*, 1954). Carbon isotope values from C₃ plants are more depleted in ¹³C than C₄ plants (Meyers 1997) and CAM plant carbon isotope values reside between C₃ and C₄ ¹³C isotope values. C₃ and C₄ plants respond differently to different climatic and hydrologic systems and conditions which gives them their unique distributions (Carr *et al.* 2006; Kuechler *et al.* 2013).

The issue of stable carbon isotope provenance

It has been suggested that photosynthetic pathway is not the only factor influencing the isotopic composition of plant leaf waxes. Some earlier studies proposed that plant wax *n*-alkane concentrations are higher in the growing season (Lockheart *et al.*, (1997; Eglinton and Hamilton, 1967). Similarly, Sachse *et al.*, (2009) found that plant leaf wax isotope composition changes throughout the growing season, inferring that leaf wax *n*-alkane concentrations are influenced by environmental conditions and plant type. Leaf physiology within a single tree will vary from shaded canopy to sun-exposed, which has been shown to effect overall *n*-alkane abundance and production (Lockheart *et al.*, 1997). Similarly, Bush and McInerney (2013) state that comparisons between modern leaf *n*-alkane concentrations and sedimentary *n*-alkane distributions from river sediments may be undermined if modern leaf samples were extracted during the growing season. Therefore, understanding *n*-alkane production within plant species

and intra-plant variations is essential for interpreting palaeoecological research (Bush and McInerney, 2013).

Furthermore, variations in $\delta^{13}\text{C}$ values also infer variations in the water use efficiency of different plants (Hou *et al.* 2007; Ehleringer & Dawson 1992; Seibt *et al.* 2008). These survival mechanisms have often been associated to semi-arid and arid regions in Africa, specifically West Africa (Tieszen *et al.*, 1997). Water loss and Stomatal closure under arid conditions leads to $\delta^{13}\text{C}$ isotope enrichment in plant wax lipids, whereas increased moisture and reduced water use efficiency leads to depleted $\delta^{13}\text{C}$ values (Leaney *et al.* 1985; Vogts *et al.*, 2016). Therefore, it can be proposed that precipitation is a driver of plant isotope composition (Dansgaard, 1964; Herrmann *et al.*, 2017; Niedermeyer *et al.*, 2016; Feakins and Sessions, 2010).

The fractionation of leaf wax $\delta^{13}\text{C}$ values for C_3 plants ranges from -29 ‰ to -39 ‰ based on the Vienna Pee Dee Belemnite Standard (VPDB) (Vogts *et al.*, 2009). When $\delta^{13}\text{C}$ isotope compositions display values within this range, it is likely associated with cooler and more humid conditions (Diefendorf *et al.*, 2010; Castaneda *et al.* 2011). C_4 plants however, are $\delta^{13}\text{C}$ enriched and range from -14 ‰ to -26 ‰ VPDB (Dupont *et al.*, 2013; Vogts *et al.*, 2009). CAM plants have been found to fall between the C_3 and C_4 isotope ranges (Dupont *et al.*, 2013). Most higher plants maximise at the nC_{29} and nC_{31} *n*-alkane homologue. A study by Castaneda *et al.*, (2011) found that the average $\delta^{13}\text{C}$ for nC_{29} homologue for C_3 vegetation to be -34.7 ‰ and for C_4 vegetation of -21.7 ‰. Similar results were found by Schefuß *et al.*, (2005) in marine sediment core extracted from the Congo river showed $\delta^{13}\text{C}$ values of C_3 plants range from -32 ‰ to -34.6 ‰, and $\delta^{13}\text{C}$ for C_4 values averaged at -20 ‰. Vogts *et al.*, (2012) conducted a study on elucidating the isotope characteristics of modern Atlantic Ocean sediments to determine the contribution of C_3 and C_4 plants into adjacent marine sediments. They also investigated whether C_4 plant types can be correlated to climate conditions (aridity and precipitation). Vogts *et al.*, (2012) found that the most negative $\delta^{13}\text{C}$ values were found at the river mouth due to more C_3 vegetation at the mouth or the presence of forest canopy. Rivers tend to transport more negative signal when near a forest Vogts *et al.*, (2012).

Stable Hydrogen (δD) Isotopes

The stable hydrogen (δD) isotope composition of plant waxes can be directly linked to hydrological and precipitation changes in the prevailing environment and climate. The epicuticular wax layer covering higher plant records changes in the isotopic composition of rainfall (Sachse *et al.*, 2012) (Figure 2.2). Hydrogen atoms enter plant tissue during photosynthesis, and since the water contained within the plant is controlled by soil water, which

is in turn controlled by precipitation, δD of plant tissues can be used as a proxy for determining hydrological dynamics (Sachse *et al.*, 2012). δD enrichment can infer warming and cooling on a temporal and spatial scale. Schefuss *et al.*, (2011) demonstrated that δD can be used to determine changes in dry and wet periods in South Africa. For example, δD of *n*-alkane plant wax will show enrichment in areas or periods of aridity and depleted rainfall, whereas δD depletion will occur in areas and periods of cooling and increased rainfall (Schefuss *et al.*, 2005).

Hydrogen deuterium (δD) fluctuations are also controlled by larger processes such as: ice effect, continental effect, temperature effect, the amount effect and altitude effects (Figure 2.2). It has been found that in subtropical and tropical areas, the hydrogen isotopic composition of precipitation (δD) reflects precipitation amount (amount effect) (Dansgaard, 1964). Similarly, Collins *et al.*, (2013) found that plant wax hydrogen composition is driven by the amount effect, wherein depleted (lower) δD values indicate increased rainfall and reduced evaporation of rain drops, and enriched (higher) δD values indicate reduced rainfall. The amount effect is active on both spatial and temporal scale, for example, depleted δD values have been reported during the summer (wet) months in South Africa, and enriched values occurred during the winter (dry) months (Collins *et al.*, 2013). Areas of high rainfall within a given environment, experience different amounts of precipitation year round. Therefore, gradients of δD enrichment and depletion can be found on a smaller scale between different rivers and catchments within a water system (Hahn *et al.*, 2018). The altitude and continental effect have also been shown to influence local δD amount. Both effects are based on the premise of the heavier isotope rainout during the movement of moisture inland from the ocean and with increasing elevation (Hahn *et al.*, 2018).

The issue of stable hydrogen isotope provenance

Hydrogen isotope (δD) of plant lipid waxes recorded sediment archives are good indicators of catchment precipitation and hydrology (Dupont *et al.*, 2013). Changes in δD isotope compositions are driven by changes in precipitation intensity, humidity and aridity (Sachse *et al.*, 2012) (Figure 2.2). Higher terrestrial plant matter tissue record changes in the isotopic composition of water sources such as precipitation. Terrestrial plant tissue is stored and therefore can be used as an indicator for continental precipitation and hydrological processes (Flanagan and Ehleringer, 1991; Sachse *et al.*, 2012; Dupont *et al.*, 2013).

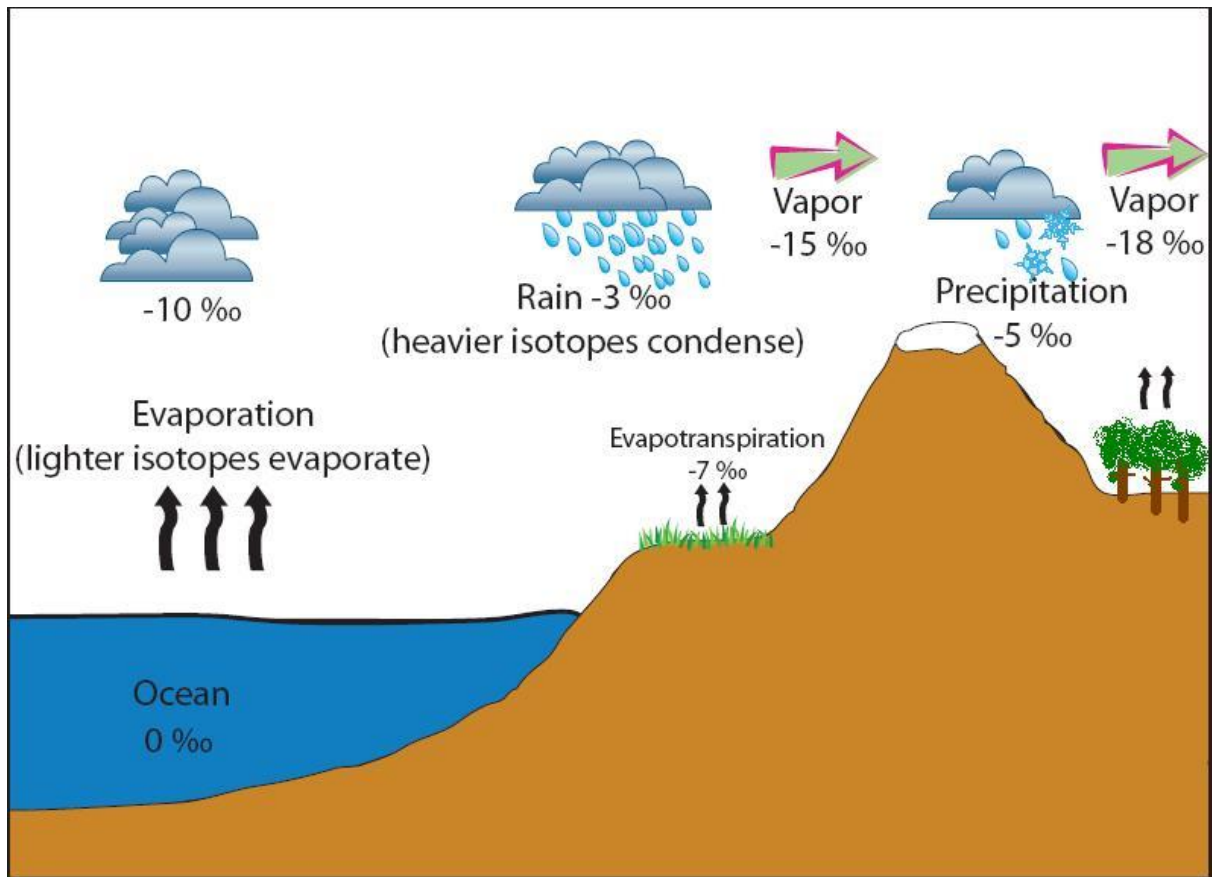


Figure 2.2: A schematic diagram showing the fraction of hydrogen (deuterium δD) and depletion with increasing distance inland (continental effect), elevation (altitude effect), and rainfall (rainfall effect) (Bruckner, n.d.: available on:

https://serc.carleton.edu/microbelife/research_methods/enviro_n_sampling/stableisotopes.html

which result in either subsequent enrichment or depletion of the δD isotope composition of precipitation. These processes have been defined by Dansgaard (1964) and Gat (1996) are listed below.

- 1) Changes in precipitation intensity (amount effect) wherein elevated rainfall amount and intensity leads to decreasing δD values, and reduced rainfall amount and intensity leads to increasing δD values (Niedermeyer *et al.*, 2016; Sachse *et al.*, 2012);
- 2) When δD of precipitation becomes more depleted as the system moves from the ocean inland, this is called the continental effect (Niedermeyer *et al.*, 2016);
- 3) Variations in altitude in the area of rainout (altitude effect). This occurs when δD becomes depleted with increasing rainout and increasing altitude.

- 4) An additional effect is that the δD isotope value is affected by the plant type and environmental conditions such as:
- a. The carbon fixation pathway (C_3 , C_4 , CAM) and plant type. For example, different plant types have been found to fractionate δD at different rates (Diefendorf and Freimuth, 2017; Diefendorf *et al.*, 2010)
 - b. Aridity, wherein increasingly arid conditions result in more enriched $\delta^{13}C$ values as there is higher fractionation of the heavy isotopes (Feakins and Sessions, 2010).
 - c. Evapotranspiration, wherein higher evapotranspiration rates results in δD enrichment (Feakins and Sessions, 2010; Ziegler *et al.*, 1976).

2.2.3.3 Limitations of *n*-alkane analyses

Limitations to *n*-alkane analyses have been outlined by various authors, including *n*-alkane plant wax overrepresentation and underrepresentation, the transport dynamics of *n*-alkane material downstream, sampling resolutions, and contemporary anthropogenic issues (Dupont *et al.*, 2013; Collins *et al.*, 2013; Hahn *et al.*, 2018).

n-Alkane distributions

Although *n*-alkanes are widely distributed within environments and accurately represent large vegetation groups and conditions, *n*-alkane production and distributions are highly variable within and between plant types. Distinctions between woody plants, shrubs and grasses are not as effective when based on *n*-alkane distributions and alone (Bush and McInerney, 2013). Utilising nC_{27} , nC_{29} and nC_{31} chain lengths to separate grasses from woody plants is difficult as all three chain lengths are produced in significant amounts (Bush and McInerney, 2013). However, in South Africa studies have found that the nC_{33} and nC_{35} chain lengths distinguish grasses from some woody trees and shrubs sufficiently. Thus, utilising chain length as a proxy of vegetation composition, is sufficient for South African climates and environments (Bush and McInerney, 2013).

An important consideration to note when utilising this method is that *n*-alkane distribution and abundance may be reflecting the local environment rather than plant type. Sediment *n*-alkanes can also originate from both terrestrial and aquatic sources, which can make interpretation difficult. One way to overcome multiple source region complexities is to correct for vegetation types by investigating the specific *n*-alkane distribution and abundances of specific vegetation types (Neumann *et al.*, 2011). Various studies have shown that *n*-alkane distributions from sedimentary organic matter are not indicators of specific plant species, however, are good

proxies for general environmental and vegetation compositions such as transitions between C₃, C₄ and CAM plant types (Collins *et al.*, 2013; Neumann *et al.*, 2011).

Another important consideration when investigative *n*-alkane distribution in sediment records is the issue of representivity. Plant wax *n*-alkane concentrations are highest during the growing season. Therefore implying that *n*-alkanes isotopic composition will change throughout the growing season (Sachse *et al.*, 2012), which could complicate interpretations. Therefore it is important to consider external environmental factors other than plant type such as: wind, temperatures and aridity. Within specific plant types such as arboreal taxa, leaf physiologic varies from shaded canopies to sun exposed positions on branches which can result in different isotopic *n*-alkane compositions on a single tree. These are important considerations for the interpretation of *n*-alkane distributions and isotope studies as this implies that *n*-alkane values do not simply reflect plant functional types, but also environmental pressures.

Sample resolution

It is likely that due to the diversity of terrestrial systems and processes within the site, and the spatial extent of the study site, accurately determining the spatial and temporal dynamics of sediment organic matter, will be complicated. To capture the full spatial extent of the signals within the catchment and their transport routes, origin and dynamics, Suspended Particulate Matter (SPM), River Bed Sediment (RBS) and Deposited Puddle Sediment (DPS) samples were extracted from each major tributary of the Mzimvubu Catchment as well as the river mouth. SPM refers to the particulate matter transported in the upper fast flowing channel of water (30 cm below the water surface). RBS refers to a grab sample of sediment collected from the river bed, and DPS refers to a previous flood deposit of sediment that has dried along the flood plain or river bank. The river mouth is assumed to represent the culmination of all signals transported within and throughout the catchment. Hahn *et al.*, (2018) showed that the SPM is able to capture the hydrologic, sediment and vegetation dynamics within a river. However, it was later found that a limitation to this approach is that SPM samples will only reflect conditions at a given moment in time. Therefore to capture seasonal variability of catchment vegetation and hydrology, RBS samples are extracted from the associated river bed sediment. RBS samples have been shown to represent a fluvial signal integrated over longer period of time (Hahn *et al.*, 2018). Another issue arising from utilising RBS samples is that these samples represent local conditions in a limited part of the catchment. Thus RBS and SPM samples should be extracted at the same locations to reduce temporal and spatial resolution issues, and

also to correlate RBS and SPM signal compositions to match the signal transport routes and origin.

Contemporary anthropogenic issues

In light of accelerating anthropogenic pressures and drivers, it is important to consider the effect these pressures will have on existing natural environments and ecosystems and ultimately sample comparability (Hahn *et al.*, 2018). Anthropogenic land use changes and impoundments such as water impoundments (dams and weirs), irrigation, farming and development can have significant effects on these signals transported within rivers. The Mzimvubu River is one of the largest last free flowing rivers in South Africa as it is not impounded by larger dams. However, even the presence of small farm dams, extensive irrigation schemes, and weirs can affect the transport and movement of vegetation, hydrological and sediment signals within the catchment. It is important to consider the effect that a weir may have on the transport of signals downstream. The weir is located just below the confluence of the major tributaries, which could complicate proxy signal transport pathways and deposition sites, as a weir could potentially trap sediment during periods of low rainfall and low flow velocity.

Due to the nature of the agricultural activities and land uses in the Mzimvubu Catchment, it is likely that these practices have altered catchment hydrology and vegetation over time. For example, irrigation practices often rely on redirecting water onto land and thus can affect the hydrogen isotope composition of plant wax *n*-alkanes. Furthermore, natural grassland, woodland and thicket has been replaced with agricultural croplands (maize) and Pine plantations, which can affect leaf *n*-alkane wax carbon isotope signals and pollen concentrations and compositions in sediments. It is also important to consider the presence of major towns and industrial development as these are often sites of increased pollution, land use change and vegetation removal. For example, studies have shown that coastal areas are often sites of elevated pollution (Hahn *et al.*, 2018; Vetrimurugen *et al.*, 2016). The various sources of two of the major tributaries (upper Mzimvubu River and Mzintlava River) as well as the river mouth are located in or near major towns. The river mouth, located at Port St Johns, is situated in a high tourism area where land use transformation and environmental pressures are high.

2.2.3.4 Methodological considerations of *n*-alkane analyses

Sampling in the field

Leaf wax *n*-alkanes are extracted from modern plant tissue in lacustrine and marine sediments. It is important to ensure that sampling of these sediments are performed using clean equipment. Contamination from petroleum oils would negatively affect the overall *n*-alkane signature (Ardenghi *et al.*, 2017). To avoid contamination of lipids, skin contact with the sediment samples must be avoided during the procedural analysis (Vogts *et al.*, 2009). It is strongly recommended that equipment is cleaned with *n*-hexane and dichloromethane (Vogts *et al.*, 2009).

Laboratory

There are many studies that describe the various methods for effective *n*-alkane extraction from plant leaf waxes, however, a standardised method has not yet be devised (Doan *et al.*, 2019). The method employed will differ depending on the ultimate use of the *n*-alkane data. Regardless of the method being utilised, it is important to ensure that all laboratory equipment and glassware is cleaned with *n*-hexane and dichloromethane before use (Vogts *et al.*, 2009). The most commonly utilised method is to run sediment samples through Accelerated Solvent Extraction (ASE), followed by chemical processes which extricate the long chain *n*-alkane wax lipid from each sample. This method has been standardised for marine sediment plant wax lipid biomarker extraction, a standardised method for fluvial lacustrine sediment biomarker extraction has not been established (Vogts *et al.*, 2009). These methods include saponification (which breaks down plant wax ester bonds), separating the neutral lipid fraction, removal of the unsaturated components of the *n*-alkane fractions and methylation of the humic acid plant wax fractions. Thereafter, samples are prepared for Gas Chromatography (GC) analysis, which determined plant wax biomarkers by comparison to standard reference mixtures. One common issue for plant lipid extraction is to reduce unwanted polar compounds from samples, that is, if the polar fraction is not needed. Polar compounds can affect the overall signal of *n*-alkane distributions. Subsampling can also produce biases pertaining to the *n*-alkane concentrations, distribution and isotopic compositions due to variability in plant type.

n-Alkane interpretative indices

In addition to utilising individual *n*-alkane abundances and ratios, there are several other indices that can be used for characterising *n*-alkane distributions. The most commonly used indices are Average Change Length (ACL), Carbon Preference Index (CPI) and norm31 (see Methods Chapter 3, section 3.3, page 50). These *n*-alkane indices are used to determine organic matter provenance in fluvial and marine sediments (Blidnter *et al.*, 2018; Bush and

McInerney, 2013; Wang *et al.*, 2015; Sojinu and Shittu, 2018). For the purpose of this study, CPI and norm31 were utilised.

Norm31 is suitable for determining the general environmental and climatic conditions and vegetation types within a site. Norm31 ratio is used to show the difference in *n*-alkane chain length patterns (Haggi *et al.*, 2016). For example, lower ratios <0.5 are characteristic sites dominated by trees and shrubs in cooler climates, and higher ratios >0.5 are typical of grassland and herb dominated sites in warm climates (Chevalier *et al.*, 2015). CPI on the other hand shows which odd numbered *n*-alkanes dominate over the even carbon chain lengths (Sojinu and Shittu, 2018). For example, CPI values >3 are used to represent terrestrial higher plant sources, whereas CPI <1 are indications of petrogenic and petroleum sources. CPI is thus also applied to determine the quality of soil organic matter and the contribution of additional sources, such as petrogenic sources to the overall organic matter signal (Eglington and Hamilton, 1967).

2.2.4 Inorganic geochemistry (XRF)

2.2.4.1 Background information

The specific elemental compositions (Fe, K, Al, Si and Ti) of this terrigenous material have been correlated to various climate and hydrological changes and can be used to reconstruct source regions and ultimately climate conditions of the terrestrial inputs (Clift *et al.*, 2014; Liu *et al.*, 2017; Calvert and Pedersen, 2007). Organic proxy provenance extracted from fluvial sediments (Haggi *et al.*, 2016; Hahn *et al.*, 2018), and marine sediments (Schefuss *et al.*, 2011; Zhao *et al.*, 2017, Collins *et al.*, 2013) can be achieved through establishing the characteristics and ultimately source region of the sediment it stored within. Sediment provenance is based on the assumption that unless sediment source material has been disaggregated due to mechanical processes, it is likely that the eroded material either fluvial or wind transported to the ocean, reflects the parent rock and region from which it came (Nesbitt and Young, 1996). Inorganic matter interpretations are based on some core principles which drive and guide the investigation approach, these principles are discussed below.

Particle grain size distribution is an accurate representation of the energy required to move particle grains, as well as being an important factor in controlling erosion in water bodies, surface and atmospheric transport (Switzer, 2013). Particle grain size distribution is strongly related to various land use practices, especially agriculture. However, particle size distribution also represents morphological characteristics of the physical process of landform development (Switzer, 2013; Deng *et al.*, 2017). Therefore, it is difficult to identify accurately the source of

sediment particles in a system. XRF analysis enables the identification of specific elements which can be linked to different land use activities as well as geomorphological processes. XRF analyses can aid the differentiation between natural and anthropogenic (in this case agricultural) land use practices. These impacts are discussed further in the subsequent sections below.

Inorganic geochemistry biomarkers such as element compositions can be preserved in lacustrine and marine sediments (Govin *et al.*, 2012). If the sources of the sediment and inorganic compound can be determined, the source region of the organic matter can also be determined (de Souza *et al.*, 2017; Chevalier *et al.*, 2015). These sediment organic compounds can elucidate information about sediment delivery, deposition patterns and transport pathways within a fluvial systems on both spatial and temporal scales (Shi *et al.*, 2001). The provenance of sediment inorganic material is likely to be specific, due to the wide variability of vegetation cover, topography, hydrology and sedimentology (Herrmann *et al.*, 2006). Modern sediment organic matter and its transport dynamics, deposition and source regions can be used to interpret marine sediment cores in palaeoclimatological studies. Two additional important factors to consider in these interpretations are, firstly, that different sediment proxies may have different source regions and transport routes, which are ultimately determined by sediment and hydrologic processes (Govin *et al.*, 2012). Secondly, that the downstream transport of sediment organic matter could be affected by temporary deposition and storage areas (Haggi *et al.*, 2016), riverine sediment transport (Hahn *et al.*, 2018) and individual catchment sediment dynamics (Herrmann *et al.*, 2016, Zhao *et al.*, 2015).

2.2.4.2 Applications of XRF

Various approaches have been applied to marine and fluvial sediments, to reconstruct sediment provenance dynamics (Peterson *et al.*, 2000; Huang *et al.*, 2001; Zabel *et al.*, 2001). Some of these approaches included, grain size analysis, reflective, magnetic techniques, and the distribution of clay versus sand minerals (Govin *et al.*, 2012). A more common and recent method is the use of X-Ray Fluorescence (XRF) which utilises major element compositions of lacustrine and marine sediment to trace terrigenous input by measuring the intensities and concentrations of major elements of surface and core sediments. This method works under the premise that, element concentrations can be traced to their places of origin. For example, the use of aluminium (Al), iron (Fe), titanium (Ti), potassium (K), and silicon (Si) can indicate certain characteristics of the terrigenous sediment input. However, despite the robust application of single terrigenous elements, elemental ratios have become a more comprehensive method for

determining inorganic matter input, transport routes and provenance within a large scale system with a variety of interacting environmental, climatological and hydrological factors (de Souza *et al.*, 2017; Govin *et al.*, 2012; Lopez *et al.*, 2006; Weltje and Tjallingii, 2008; Liu *et al.*, 2017).

Among some existing ratios are the three most commonly used iron and potassium (Fe/K), titanium and aluminium (Ti/Al) and aluminium and silicon (Al/Si). Element ratio concentrations are indicators of fluvial discharge and climate conditions, sea-level changes and grain size (Meyer *et al.*, 2011; Bouchez *et al.*, 2011), weathering, and provenance (Garzantini *et al.*, 2014). Elemental ratios can elicit important environmental systems and interactions compared to single element compositions (Govin *et al.*, 2012). For example, coarse grained sediment fractions show an enrichment in Ti, compared to finer clay particles which are associated with a high concentration of Al (Chen *et al.*, 2013; Lopez *et al.*, 2006). Therefore the elemental ratio Ti/Al can be used as an indicator of grain size, which can ultimately be used to determine Aeolian versus fluvial fluctuations (Zabel *et al.*, 1999; Govin *et al.*, 2012).

Furthermore, in tropical and subtropical regions, it was found that high precipitation amounts promote the chemical and mechanical weathering of bedrock. The presence of highly weathered soils from humid areas within elevated precipitation is indicated by an enriched Fe signal. K on the other hand is usually associated with dry areas with reduced precipitation (Govin *et al.*, 2012). Therefore Fe/K can represent fluvial versus aeolian sediment input. Lastly, Si in sediment is usually derived from clay minerals such as quartz (Govin *et al.*, 2012). Al is commonly associated with fine grained clay particles when they enter into natural rivers and streams via intensive chemical weathering. Therefore, Al/Si can be used as a proxy for grain size and chemical weathering intensity.

2.2.4.3. Using XRF as sediment organic matter tracers

Elemental information obtained from terrestrial and marine sediments have been used to reconstruct source regions and ultimately climate conditions of the terrestrial inputs (Clift *et al.*, 2014). A study by Bramlette and Bradley (1940) found that the mineralogy and lithology of ocean sediments could represent the series of glacial-interglacial deposits on the ocean floor. This research helped shape the foundation of current geochemistry related research of marine sediment deposits, and how geochemistry can be used to study the marine system (Calvert and Pedersen, 2007). Around the 1950s, Goldberg and Arhenius (1958) discovered that elemental variability, distribution, depletion and enrichments in marine sediments can aid the interpretation of sedimentary records. The element composition of sediment represents a

mixture of organic and inorganic components from various sources (Calvert and Pedersen, 2007). Marine element data has been used to elucidate information about the adjacent continent, and whether sediments originated during times of arid, humid or ice covered periods, by identifying specific organic and inorganic components that have been transported to marine sediments by rivers, aeolian processes (Calvert and Pedersen, 2007). Provenance studies using elemental data have a long history, however, much progress has been made in utilising element data from sediments to identify component source regions (Nesbitt and Young, 1982, 1996).

The main mechanisms for element compositions transport into ocean sediments are fluvial and aeolian processes (Milliman and Meade, 1983). It is important to consider these mechanisms as environmental factors such as aridity, wind direction and strength affect aeolian input (Rea, 1994), and sea level changes and continental precipitation dynamics (Milliman and Meade, 1983) affect the fluvial pathway of sediments (Govin *et al.*, 2012). Elemental composition of terrestrial and marine sediments provides information on source areas, sediment transport, climate, ocean currents, organic matter fractions and depositional re-working (Calvert and Pedersen, 2007). Recent approaches have focussed on identifying major element composition of different type of sediments to establish sediment provenance and subsequent deposition in marine sediments (Huang *et al.*, 2001; Zabel *et al.*, 2001). X-Ray Fluorescence (XRF) scanners has enhanced the use of element based proxy research in reconstruction terrestrial palaeoenvironments and palaeoclimates (Govin *et al.*, 2012). This approach been utilised in organic matter provenance studies, wherein element compositions in sediment aid in the identification of organic matter source regions (Galy *et al.*, 2011).

XRF works by identifying the concentration of individual element compositions in terrigenous sediments which can indicate various environmental, sedimentological and climate conditions. For example specific element compositions such as iron (Fe), aluminium (Al), potassium (K) and titanium (Ti) have been used to represent the aeolian or fluvial input of terrigenous material in lacustrine and marine sediments (Goldberg and Arrhenius, 1958; Jansen *et al.*, 1998; Chen *et al.*, 2010) from different source regions (Peterson *et al.*, 2000). It was also found that absolute single elements concentrations were influenced by changes in grain size, mixing during transport, different source areas and different chemical weathering rates from different source areas (Govin *et al.*, 2012) which resulted in ambiguous element fluxes and affect single interpretations (Lopez *et al.*, 2006; Liu *et al.*, 2017).

Therefore, elemental ratios have been suggested as a more effective approach for analysing elemental signals in sediment as they are resistant to dilution effects (Weltje and Tjallingii, 2008; Liu *et al.*, 2017). Element ratio concentrations are not only indicators of fluvial discharge and climate conditions, but also of sea-level changes, grain size (Meyer *et al.*, 2011; Bouchez *et al.*, 2011); weathering, provenance and other source to sink processes (Garzantini *et al.*, 2014). For example Al/Si can indicate degrees of chemical weathering and grain size (Govin *et al.*, 2012). High values of Al/Si or Si/Al have been found to indicate the deposition of coarse grained sediment particles, which could ultimately indicate an input of aeolian transport, and reduced values indicate the input of finer grained particles (Lopez *et al.*, 2006). It has also been shown that Al/Si values increase in humid and tropical areas and decrease in drier areas (Biscaye, 1965; Driessen *et al.*, 2001).

The Ti/Al can represent grain size characteristics of sediments, which is based on the fact that coarser grained sediments are Ti enriched, whereas Al is associated with fine grained particles (Govin *et al.*, 2012). When Ti/AL ratios increase, it is associated with an increasing coarser grain sizes and decreasing Ti/AL ratio indicates finer particle grain sizes (Nesbitt and Markovics, 1997; Govin *et al.*, 2012). Ti/Al ratio values can also change due to variations in sediment source regions and the effects of aeolian transport mechanisms. The Fe/K ratio shows a negative correlation to grain size as with Ti/Al, which infers that Ti/Al and Fe/K ratios are relatively good reflections of the input of terrigenous material in sediments (Lopez *et al.*, 2006). In tropical and subtropical regions, high precipitation amounts promote weathering of bedrock resulting in high Fe concentrations being transported to rivers (Middleburg *et al.*, 1988). On the other and, K (potassium) is characteristic of dry areas and low chemical weathering (Zabel *et al.*, 2001). Therefore Fe/K can be used as a proxy for eolian versus fluvial input of sediment fractions into ocean sediment archives.

2.2.4.4 Limitations of XRF analyses

The characteristic and composition of organic matter stored in sediment is directly related to its source origin (de Souza, 2017). Various studies promote the idea of utilising geochemical markers preserved in the sediment as a method for elucidating these places of origin. However, there are various limitations associated with this approach that have been outlined by various authors (Hahn *et al.*, 2018; Lopez *et al.*, 2006; Waterson and Canuel, 2008). Issues of singular versus multiproxy approaches, single compound versus elemental ratios, source region variability, and riverine effects on these biomarkers will be discussed.

A wide variety of research has focussed on a single pathway of organic matter and geochemical biomarkers rather than multiple pathways. The reason for this is due to complexities in quantifying a diverse range of source regions (Xu *et al.*, 2016). However, a limitation of this approach is that the data cannot be verified with other proxy data. One way to overcome this issues is to employ a multiproxy approach in provenance based research, wherein multiple proxies are analysed and interpreted simultaneously (Hahn *et al.*, 2018). It is recommended that the most suited proxies are established first, and that a multiproxy approach, wherein $\delta^{13}\text{C}$, δD , *n*-alkane distribution (CPI, norm31) and elemental compositions are analysed, will be able to achieve the aim of investigating sediment, hydrologic and vegetation provenance within a confined fluvial system.

The use of single element concentrations for geochemical provenance research have been found to be limiting in their application and interpretation, as element compositions are often highly variable in their concentrations and can often lead to ambiguous interpretations and correlations (Lopez *et al.*, 2006). One way of overcoming this issue is to utilise element ratios, which have become the preferred method for determining organic matter provenance in defined environments. Elemental ratios are good indicators of environmental systems and processes such as sediment provenance, transport and deposition. A limitation of utilising element ratios though, is that they can be poor indicators of climatic conditions, however this can be overcome by utilising a multiproxy approach wherein proxy data can be correlated against other proxy data.. This is because factors controlling organic matter preservation and distribution in riverine environments are poorly understood (Waterson and Canual, 2008).

Another issue pertaining to geochemical sediment analysis is that sediment budgets are often difficult to establish due to variations in delivery rates and anthropogenic pressures (Waterson and Canuel, 2008). The transport processes of sediment in rivers are complex and interact with a variety of different factors and processes. This can often lead to the possibility of underrepresentation and overrepresentation of various proxies which can complicate interpretations. A possible way to overcome this issue, it is important to establish, as best as possible, the variety of riverine fluxes and processes that control and drive sedimentation processes. Since this approach and goal is difficult to achieve, it is often omitted from provenance based research despite the fact that it can contribute greatly to verifying and enhancing the geochemical data.

2.2.4.5 Methodological considerations for XRF analyses

Sampling and sample preparation

XRF analysis is one of the most commonly utilised methods due its non-destructive and multi-elemental character and speed (IAEA, 1997). XRF can be applied to both lacustrine and marine sediment samples. Sediment samples are often heterogeneous in nature due to varying structural types and different compositions at different depths and locations. Therefore, sample homogenisation is essential before XRF analysis (IAEA, 1997). Homogenisation can be achieved through removing vegetation and debris and manually homogenising or utilising a ball mill to ensure samples are effectively ground into the relevant sample portions (4 g) (IAEA, 1997). Sample heterogeneities could comprise the final element competitions signal.

Laboratory considerations

It is important to consider that XRF is not an air-tight analyses, although having many advantages it is limited by certain factors. These factors include: radiation exposure for the XRF scanner user as well as the inability to measure radiation from each of the elements in the sample. Thus, ensuring that the XRF scanner is not disrupted or opened whilst running the specified samples, is essential. XRF scanners are fitted with lock front and back doors as well as dosimeter badges that can detect potential radiation leaks. The XRF scanner should be frequency calibrated to industry-standard reference material. Ensuring that accuracy is maintained for repeated uses and scanning cycles.

2.3 MODERN CALIBRATION CASE STUDIES FROM SOUTHERN AFRICA

2.3.1 Introduction

It is important to understand the interplay between different drivers of climatic and environmental change on a global and regional scale. However, due to the scarcity of suitable sites in southern Africa, wherein continuous marine and lacustrine sediment cores can be extracted, little is known about local climate-vegetation relationships (Zhao *et al.*, 2015; Neumann *et al.*, 2011). Historically, palaeoresearch focussed on changing environmental and climatic conditions in specific sites, few studies exist on catchment-integrated signals in southern Africa (Ponton *et al.*, 2014). One such method to synthesise this relationship is a provenance approach, wherein modern analogues of systems are developed for comparison to fossil records (Tabares *et al.*, 2018). Various studies which have investigated provenance in modern rivers and catchments have shown that determining the origin of the signal source to be complex task due to the overprinting and underprinting of signals during transport (Bouchez

et al., 2014; Galy *et al.*, 2011), and the preferential loss of certain proxies over others. Conversely, other studies have found the provenance approach combined with multiproxy analyses able to capture complex environmental and climate interactions over large geographical regions (Ponton *et al.*, 2014). This section will provide a review of provenance studies that have utilised modern sediment samples and recent marine sediment deposits as the basis for source-region determination and environmental, vegetation and climate interpretations. This section will review the current body of literature on modern provenance studies, current research gaps and how southern Africa has served as a suitable and unsuitable study site.

2.3.2 Existing modern provenance studies in southern Africa

Provenance based research in southern Africa aims to synthesise the relationship between climate, sedimentology and vegetation in ecosystems (Carr *et al.*, 2014; de Villiers and Cadman, 1997). However, this relationship is nonlinear and confounded by the interplay of different complex variables. Original provenance based research in southern Africa sought to identify and describe individual proxy data in relatively confined areas over small spatial extents. Historical research either focussed on inorganic geochemical markers or organic geochemical markers, but rarely both simultaneously (Lim *et al.* (2016). This could be due to various analytical limitations that confined researcher at the pioneering stages of these methods and techniques, and the inability to accurately quantify such complex processes over large geographical areas.

For example, a study by Mooney *et al.*, (1972) analysed the $\delta^{13}\text{C}$ isotope composition ratios of CAM succulent plants in the Western Cape and compared these results with plant forms, distribution and climate. The study aimed to synthesise the relationship between climate regimes and plant distribution patterns. However, since southern African is climatically diverse in that temperatures and rainfall are either evenly distributed annually or concentrated in the summer (SRZ) or winter (WRZ) months (Tyson and Preston-Whyte, 2000), vegetation compositions and the environmental variables that affect them are highly complex and diverse (Mucina and Rutherford, 2006). The study found that analysing a single proxy can be limiting in terms of providing comprehensive information about these vegetation, environmental and climatic interactions. Similarly, a study by Rundel *et al.*, (1999) analysed the $\delta^{13}\text{C}$ composition of vascular plants and sediment dynamics in northern Namaqualand to test the relationship between water use efficiency and $\delta^{13}\text{C}$. They found that other environmental and physiological factors affected isotope concentration within and between plant types. They were, however,

able to compare an additional proxy such as sediment composition and provenance with terrigenous organic matter, and found that this multiproxy comparison provided a unique perspective on provenance interpretations (Rundel *et al.*, 1999).

Thereafter, provenance based research in Africa started to consider a more comprehensive approach. For example, Huang *et al.*, (2000) showed a more diverse method of analysing aeolian dust sediment organic matter samples from North West Africa and marine sediment samples off the coast of northwestern Africa. Since aeolian and fluvial transport mechanisms have been established through marine sediment analysis, and aeolian dust samples contain high terrigenous components (Collister *et al.*, 1994), Huang *et al.*, (2000) attempted to apply the same principle to terrestrial dust samples. They mapped $\delta^{13}\text{C}$ values of *n*-alkane nC_{29} homologue from dust sample and compared these with marine sediment core samples in the east Atlantic which provided information about C_3 and C_4 contributions and vegetation dynamics. They found that climate variability affects plant isotope compositions alongside plant physiology, particularly CO_2 and temperature and aridity also affect distribution of C_3 and C_4 . From the terrestrial/marine comparison, they were able to confirm the vegetation-climate relationship. Datasets and maps such as these provided by Huang *et al.*, (2000), provided researches in southern Africa with key geographical data for palaeoreconstruction investigations and interpretations.

Once it was shown that a vegetation-climate relationship could be confirmed through sediment organic matter provenance and multiproxy comparisons, provenance studies started to integrate organic and inorganic proxy analyses simultaneously. Kiage and Liu (2006) found that pollen analysis combined with inorganic compound analysis of sediments provided informative and comprehensive information about climate and vegetation. Pollen records provided detailed information on vegetation dynamics, transitions and compositions and inorganic compound analysis stabilised sedimentological patterns within east Africa. Kiage and Liu (2006) confirmed a previous statement by Boyd and Hall (1998), in that multiproxy approaches are essential for accurately interpreting palaeoenvironmental data. For example, Boyd and Hall (1998) found that some environmental, taphonomic and preservation processes can hinder proxy transport and deposition and preservation. Periodic drought conditions could compromise the preservation of biological proxies (pollen, *n*-alkane), however, inorganic geochemical information such as $\delta^{18}\text{O}$, $\delta^{13}\text{C}$ and organic carbon can still be established through inorganic compound analysis (Tierney *et al.*, 2010; Schwab *et al.*, 2015).

Almost a decade later, provenance research in southern Africa has become widely utilised as researchers rely on input from various different proxies and proxy analyses to inform both modern and palaeointerpretations. However, also around this time certain questions started to arise pertaining to the effect plant physiological factors played in determining isotope compositions in plant matter. These effects were seen as being more significant than previously thought (Dupont *et al.*, 2013; Sachse *et al.*, 2012). Boom *et al.*, (2014) analysed the $\delta^{13}\text{C}$ isotope composition and contribution of CAM and C_4 plants in the Succulent Karoo to sediment records, and they were able to establish the effects that plant physiology have on isotope composition, however they also found that $\delta^{13}\text{C}$ was not an accurate tool for determining CAM and C_4 plant distributions due to variable effects of different plant physiologies. A more comprehensive analysis of organic matter provenance and contribution to marine sediments was performed by Garzantini *et al.*, (2014). They were able to present an original dataset on sediment grain size alongside other geochemical (element composition) and isotope characteristics, as well as the various factors controlling sediment composition, weathering and mixing during transport. The integration of inorganic geochemical and sediment size analysis enabled the origin of different rock types and sediment sources to be traced. The element compositions (Sr, K, Mg and Rb) enabled researches to establish areas of weathering and erosion within the catchment.

Similarly, Schwab *et al.*, (2015) sought to analyse the isotope composition of specific alkane homologues (nC_{29} and nC_{31}) in topsoil samples from different sites with different climate and vegetation gradients in western central Africa. Schwab *et al.*, (2015) confirmed that C_3 and C_4 and their specific $\delta^{13}\text{C}$ isotope compositions are affected by temperature and aridity. They confirmed with previous studies that carbon isotope analysis of surface sediments represents C_3 and C_4 vegetation patterns and contributions, wherein nC_{29} and nC_{31} *n*-alkanes appeared to dominate environments characterised by a mix of savanna and grassland vegetation shown through $\delta^{13}\text{C}$ depletion in C_3 plants (trees and shrubs) and enrichment in C_4 plants (C_4 grasses) (Vogts *et al.*, 2009, 2012). In addition to specific *n*-alkane isotope analysis, they analysed the hydrogen (δD) of sediment *n*-alkanes (nC_{29} and nC_{31}), and found that δD accurately represents precipitation amount and intensity (Feakins and Sessions, 2010; Diefendorf and Freimuth, 2017). In conclusion, they confirmed with previous studies that plant source water and seasonality are drivers of vegetation change (Schouten *et al.*, 2007).

Similarly Zhao *et al.*, (2015); Hemingway *et al.*, (2016) and Herrmann *et al.*, (2016) were able to successfully reconstruct vegetation compositions, and that vegetation is largely driven by

precipitation and climate. For example, arid regions consistently maximised at the nC₂₉ and nC₃₁ homologues (Niedermeyer *et al* 2016) and nC₂₉ represents savanna and shrubland and C₃ vegetation and nC₃₁ and higher represents grassland (Vogts *et al.*, 2009; Chevalier *et al.*, 2015). These studies consistently reported $\delta^{13}\text{C}$ values which correlate to previous studies in that nC₂₉ and nC₃₁ $\delta^{13}\text{C}$ values average at -26.7 ‰ and -28.7 ‰ (Schwab *et al.*, 2015); -34 ‰ (nC₂₉₋₃₁) for C₃ (Hemingway *et al.*, 2016); -29.5‰ (nC₂₉) and -31.2 ‰ (nC₃₁) (Herrmann *et al.*, 2016); -27 ‰ (nC₂₉) (Hahn *et al.*, 2018).

Recent provenance based studies have incorporated multiproxy datasets to cross validate and verify environmental and vegetation data. Cross validation of proxy data is important for southern Africa as there are few suitable sites available to test long term, high resolution records (Carr *et al.*, 2014). This was found in a study by Zhao *et al.*, (2017) who investigated dinoflagellate cysts in modern sediments of SW Africa and discovered that climate and environed factors such as aridity and temperature were important drivers of proxy preservation and distribution. The dynamism of the site regarding wind velocities and sporadic rainfall events altered the proxy signal. They concluded that studying dinoflagellate cysts in isolation led to discrepancies in the data that could not be quantified, therefore reiterating the importance of cross validating modern proxy data from modern sediments in provenance based research (Zhao *et al.*, 2017). Cross validation through a multiproxy approach especially true for sites such as southern Africa, where climate conditions are generally arid and not conducive to proxy preservation (Herrmann *et al.*, 2016).

2.3.3 Site suitability

Evidence of environmental change has been limited in southern Africa by the lack of suitable sites (Huang *et al.*, 2000). Limited recovery of palaeoclimate information from these sites is due to: poor preservation due to arid conditions and strong seasonal rainfall and temperature regimes, discontinuous records (Neumann *et al.*, 2011), low temporal and spatial resolutions, sites that are widely distributed over large areas (de Villiers and Cadman, 1997), and site which are difficult to relate to each other stratigraphically (Zhao *et al.*, 2015). Despite a paucity of suitable sites and limitations of identifying suitable sites in southern Africa, surficial sediments from fluvial and marine environments have proven to be useful archives from vegetation and climate reconstruction studies (Tabares *et al.*, 2018; Dupont and Behling, 2006). Various authors (Carr *et al.*, 2014; Herrmann *et al.*, 2017; Zhao *et al.*, 2017) have demonstrated that river sediments are suitable proxies for provenance based research. Garzanti *et al.*, (2014) and Mooney *et al.*, (1972) state that, although proxy vegetation is not always adequate, southern

Africa is located in a climatically diverse region. Southern Africa also experiences pronounced seasonality of rainfall and temperature drive by large seasonal changes in atmospheric circulation systems such as shifts in the south westerlies, tropical easterlies and ocean circulation currents (Zhao *et al.*, 2017; Herrmann *et al.*, 2017; Chase *et al.*, 2015).

2.3.4 The research gap in provenance research for southern Africa

The Western Cape and north-western Cape have received much of the attention around palaeoenvironmental and provenance studies. There exist very few long term climate datasets in the Eastern Cape (de Villiers and Cadman, 1997; Tabares *et al.*, 2018), and little is known about the different water use strategies and photosynthetic pathways and resultant isotope compositions of eastern cape vegetation (Rundel *et al.*, 1999); also and information on the mineralogy and geochemistry of sediments carried in rivers are far from complete in southern Africa (Garzanti *et al.*, 2014). There is a need to characterise and identify the sources of organic and inorganic terrigenous material to interpret environmental reconstructions. Therefore to overcome this issue, researchers suggest that a multiproxy approach, while complex, may allow for better interpretations and reconstructions of sediments (Zhao *et al.*, 2015).

2.4 CONCLUSION

It is clear from the synthesis presented above that, due to the paucity of suitable palaeoclimatological for long term terrestrial records, provenance based research on modern surface samples has much potential for southern Africa. Conflicting information regarding the use of *n*-alkane distributions as representations of local vegetation and climate (Bush and McInerney, 2013) can be overcome by incorporating a multiproxy approach (Daniau *et al.*, 2013; Boyd and Hall, 1998). Fluvial palynomorph abundance and assemblages can verify plant wax sediment *n*-alkane distributions in surface sediment archives (Boom *et al.*, 2014). The provenance of sedimentary organic matter can be determined through stable carbon and hydrogen analysis alongside elemental compound distributions (Poynter *et al.*, 1989; Galy *et al.*, 2011). The synthesis presented above has provided both a modern, palaeoenvironmental and palaeoclimatological context within which to place the approach of this thesis, whilst also simultaneously allowing for the comparison and discussion of the results that will be obtained.

CHAPTER THREE

METHODS

3.1 SITE DESCRIPTION

The Mzimvubu Catchment is situated along the boundary of the northern Eastern Cape region, and extends for ~200km from the Maloti-Drakensberg watershed of the Lesotho escarpment to Port St. Johns where it flows out into the Indian Ocean. (Figure 3.1). The catchment spans 19,852 km² and has five major tributaries such as: the iTsitsa River, Thina River, Kinira River, Mzimvubu River and Mzintlava River, which have their headwaters in the Drakensberg Mountains (Figure 3.1). The main stem of the catchment is the Mzimvubu River which flows over ~400km through deep incised river valleys from the source into the coastal belt before it discharges into the Indian Ocean at Port St Johns. The Mzimvubu Catchment is one of the last rivers in South Africa not impinged by major dams or water impoundments, as well as a marine sediment core (GeoB20624-0-1) which has been extracted just off the river mouth for palaeoecological applications, thus making it suitable for modern provenance research.

The Mzimvubu Catchment experiences a warm temperate climate with a Mean Annual Temperature (MAT) of 20.3 °C (Figure 3.2 a). Mean Annual Precipitation (MAP) is 1096 mm, and since the whole catchment lies with the Summer Rainfall Zone (SRZ), most of the annual precipitation falls during austral summer months (22 December – 20 March) (Figure 3.2 b). There are eight recognised biomes in the catchment, however, the three major vegetation biomes are Grassland (69%), Savanna (21%) and the Indian Ocean Coastal Belt (IOCB) (8 %) (Mucina and Rutherford, 2006) (Figure 3.2 c). Forest thicket, bushveld and plantations occupy small patches in each biome, and represent 2% of the total vegetation. The northern and central plateau areas of the catchment are characterised by the Grassland biome. The plateau transitions into Savanna vegetation in the western area of the catchment, and then eventually to coastal valley thicket and dune forests of the IOCB at the river mouth in the south eastern boundary of the catchment (Mucina and Rutherford, 2006; DWS, 2017).

The upper catchment Grassland is characterised by Highland sourveld Grassland, southern tall Grassland and Dhone grassland sourveld (Acocks, 1988). Poor grazing and land use practices are widespread in this section of the catchment (Madikizela and Dye, 2003). The growth of trees are restricted in the upper catchment due to cooler temperatures and fires, however,

smaller trees and shrubs (*Helichrysum* and *Rhus*) persist along river banks (Mucina and Rutherford, 2006). Common grasses in the Grassland biome are *Themeda triandra*, *Eragrostis curvula* and *Cymbopogon plurinodis* (DWS, 2017). High altitude grasses near the Lesotho escarpment are known as Montane Grassland and support high diversity and endemism (Madikizela and Dye, 2003). The middle catchment Savanna is characterised by a mixture of trees and grasses. The forest belt and thicket consist of four forest types such as: Afro montane and mistbelt which transition into coastal scarp and Pondoland coastal forest near the estuary (Mucina and Rutherford, 2006).

Highly erodible sedimentary rocks namely mudstone, sandstone and shale are present in the catchment (Manjoro *et al.*, 2016). The catchment in general forms part of the Karoo supergroup, and is underlain by Beufort group formations in the southeast and southwest direction (Cloete *et al.*, 1991). The higher altitude areas in the upper catchment comprise of Drakensberg, Clarens, Elliot and Molteno formations. The middle catchment is underlain by the Adelaide formations and the Ecca and Dwyka formations. Extensive Karoo dolerite intrusions are common in the catchment, especially near Moutn Ayliff in the middle catchment. The dolerite intrusions contribute to the generally rugged nature of the terrain of the upper catchment, which then gradually reduced to rolling hills towards the middle catchment (Cloete *et al.*, 1991).

3.2 FIELD SAMPLING

3.2.1 Sample extraction

River Bed Samples (RBS) and Suspended Particulate Matter (SPM) samples were collected from the Mzimvubu Catchment in Port St Johns by the examinee (Tarryn Frankland) with assistance from Craing Cordier and Dylind Kleinhans, over two consecutive sampling campaigns. The third sampling campaign and subsequent sample collection was conducted by Craig Cordier and Dylind Kleinhans, as the examinee had travelled to the MARUM Institute (University of Bremen, Germany) to process the samples from the first two campaigns (please refer to Acknowledgements section).

In total, 11 sample sites were identified across the Mzimvubu Catchment capturing the five major tributaries namely, Mzintlava River, Mzimvubu River, Kinira River, Thina River and iTsitsa River comprising the full spatial extent of the catchment. To capture temporal sediment dynamics within the catchment, three sampling campaigns such as: the dry

(June); intermediate (September) and wet (November) were selected according to monthly rainfall for the region (please see appendix C for field data collection sheets 1, 2 and 3).

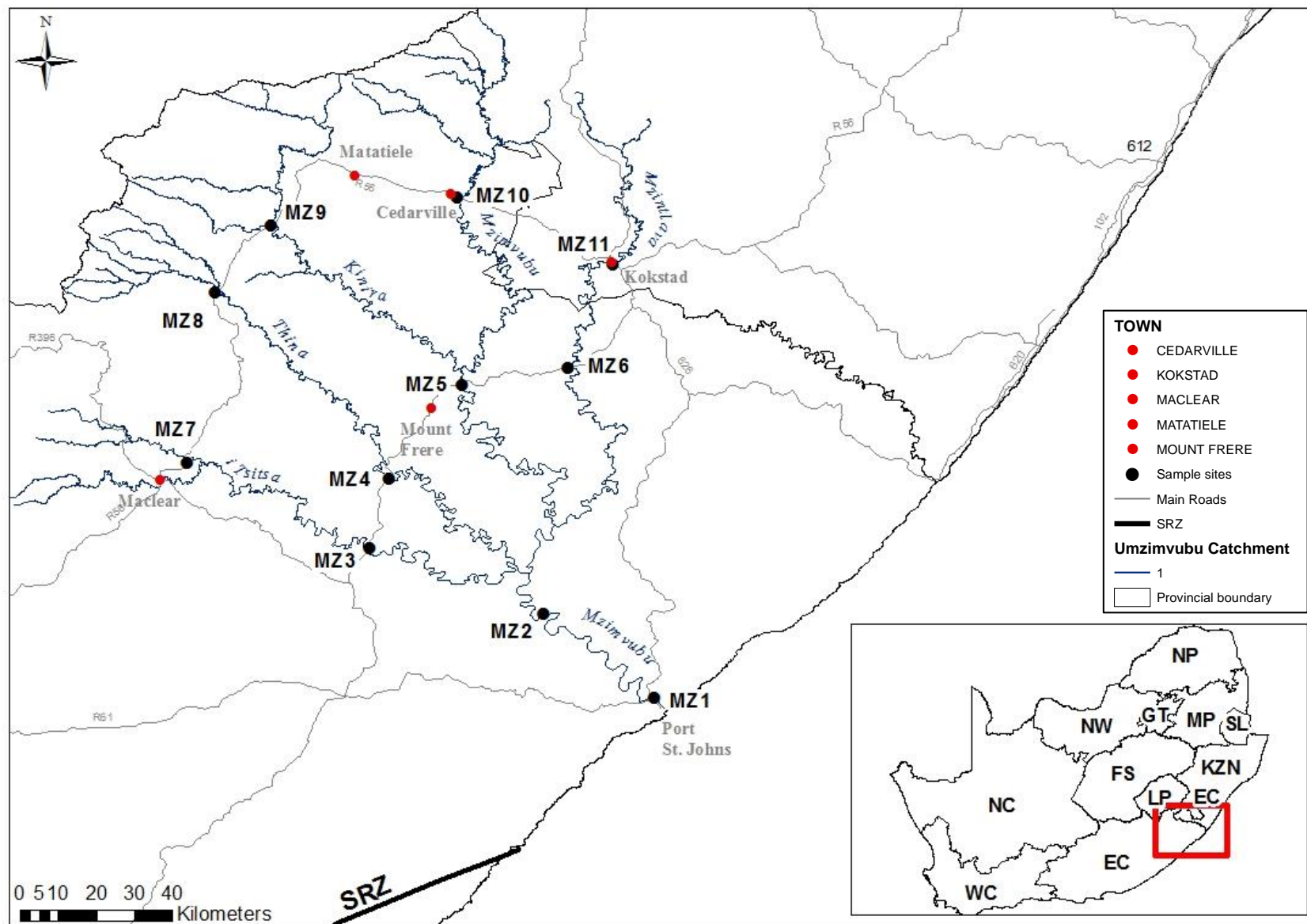


Figure 3.1: Topographical site map of eleven sample sites in the Mzimvubu catchment.

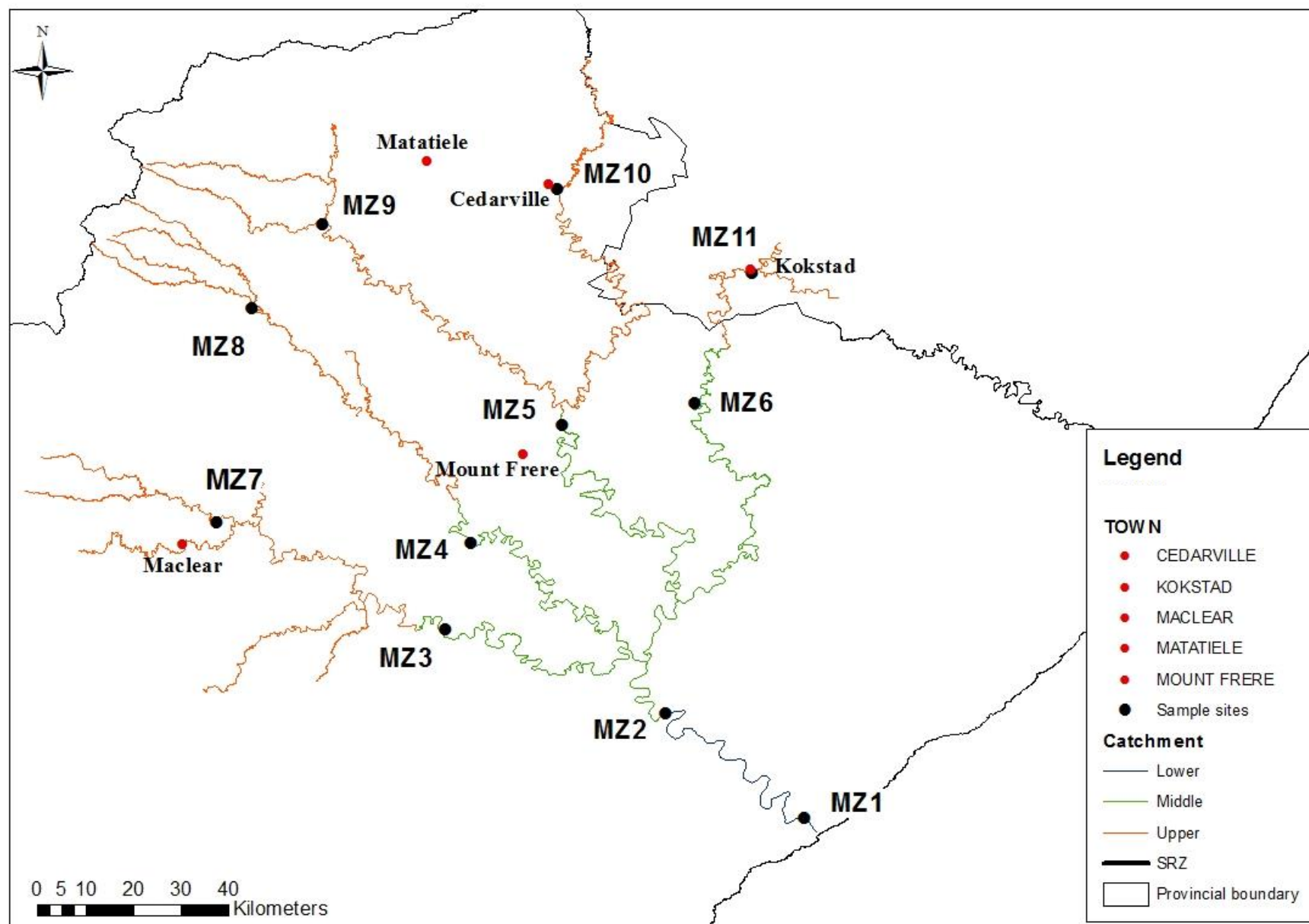
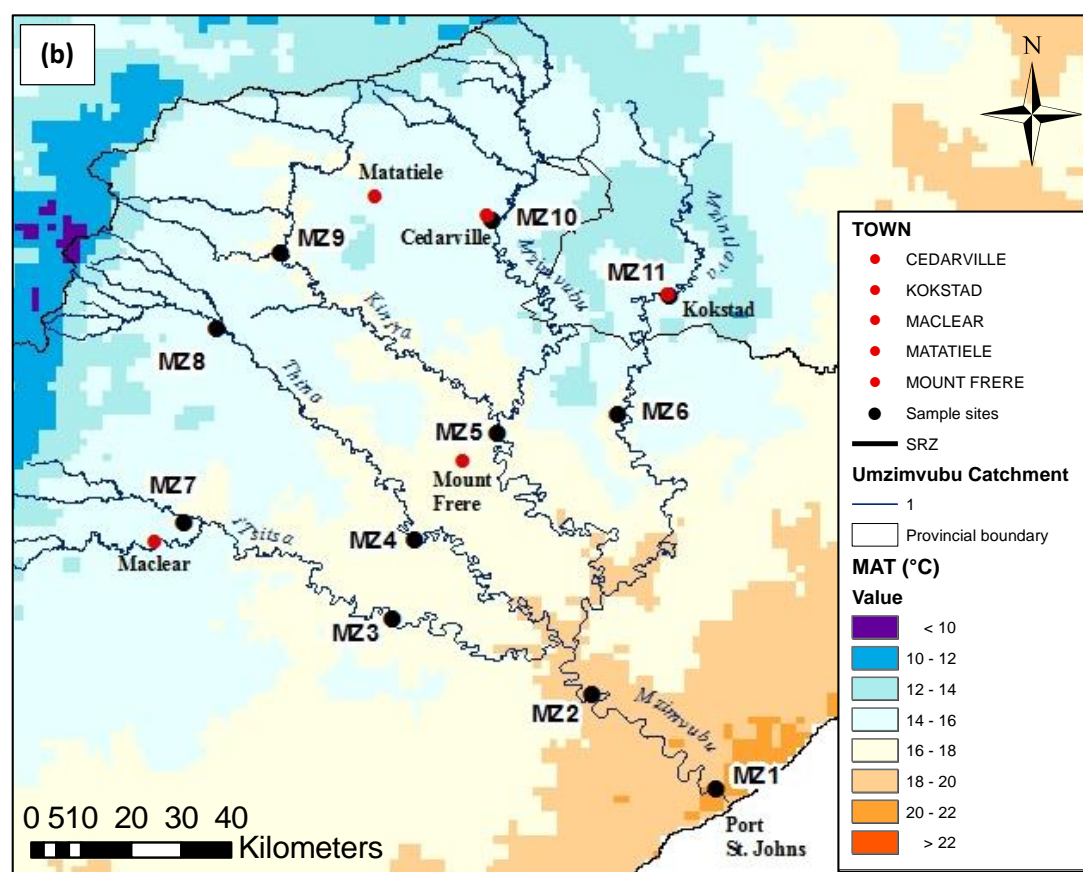
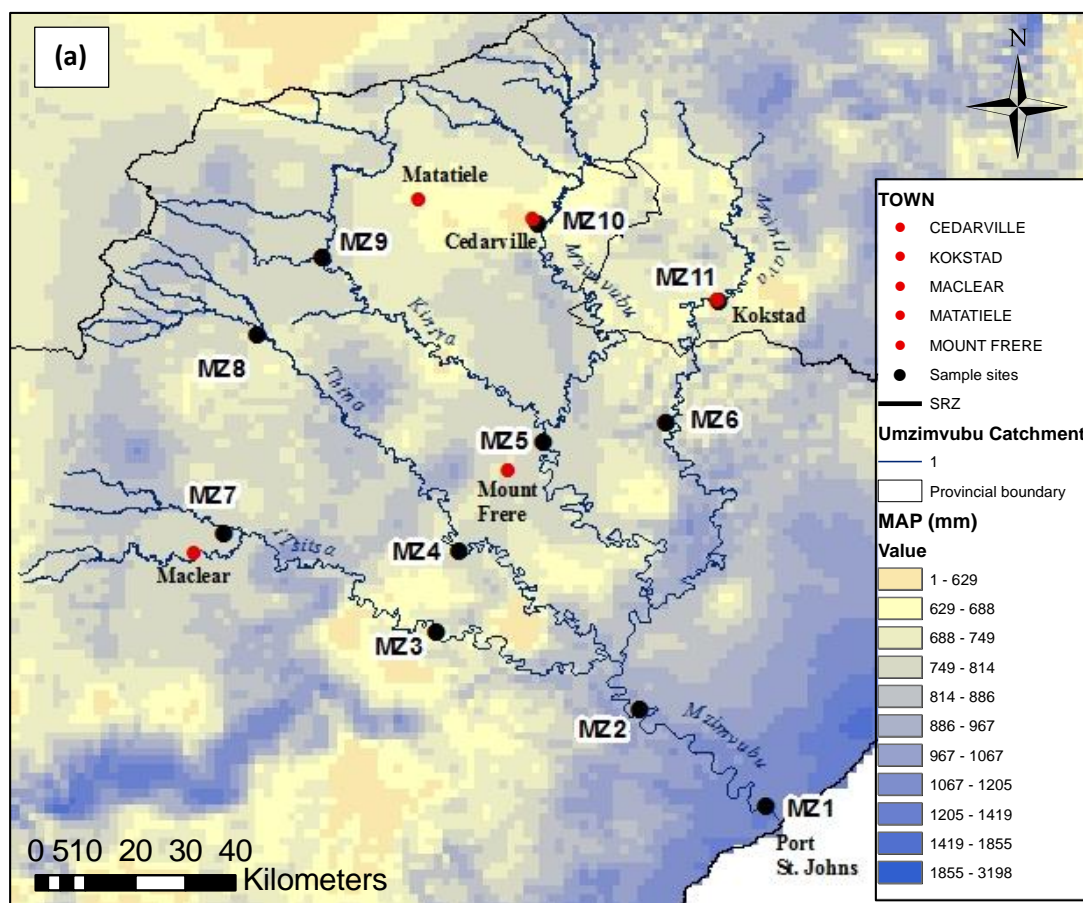


Figure 3.2: Topographical site map showing the upper (orange), middle (green) and lower (blue) catchment levels.



then likely to represent modern pollen compositions over a longer time period due to well established deposition times (Hahn *et al.*, 2018). SPM and RBS samples extracted along the river course of each major tributary within the catchment, thus provide an accurate method for determining the provenance, transport pathways and deposition processes of pollen assemblages.

SPM samples were collected and stored in 25 L plastic jerry cans, RBS samples were collected in 250 ml plastic containers, DPS samples in sealable plastic bags and water isotope samples in 45ml plastic vials (plate 3.1 a, b). In addition to the 25 L SPM sample, a 5 L additional SPM sample was collected. The RBS samples were collected using a scoop-sampling method from water depths from 10 to 30 cm (see appendix). The RBS samples represented deposition zones of organic and inorganic markers within. SPM samples were collected by deploying a portable water pump off of a bridge at the centre of the river to extract 25 L of river water from two thirds of the water column. DPS samples were taken from dried flood deposits where there was evidence of potential past flood events. Water isotope samples were collected at each site for $\delta^{18}\text{O}$ and $\delta^2\text{H}$ analysis, however, these data were excluded from the overall dataset as it did not show a major relation to the inorganic and organic signal provenance nor did it have a strong correlation to the other proxies.

3.3 LABORATORY TECHNIQUES

3.3.1 Pollen

Pollen subsampling

All pollen samples were processed and analysed by the examinee (Tarryn Frankland). Samples were stored for later analysis at University of KwaZulu-Natal (UKZN) in Pietermaritzburg, Geography department, Palaeo-lab. Pollen assemblages were originally going to be determined using SPM material, however, due to significantly low suspended sediment fractions which were unusable for pollen analysis, SPM sediment was not used. The SPM fractions were not enough to perform pollen, organic and inorganic analyses. Therefore, the RBS fractions were used as there was enough sediment for all three analyses and all proxies could be accurately compared. A portion of 3cm² of RBS were subsampled for pollen analysis. Remaining RBS and SPM samples were left to settle for three weeks and decanted, and were then oven dried at 40°C until dry for alkenone and XRF analysis. A total of 32 RBS samples were processed and analysed to determine pollen taxa abundance and diversity.

Pollen preparation procedures are based and adapted from Faegri and Iverson (1989) and Moore *et al.*, (1991). Pollen samples were chemically prepared using standard palynological



Plate 3.1: Sample extraction of SPM sediment using a battery powered bore-hole water sediment sampler. (a) Pilot study SPM extraction (Umkomaas), (b) SPM extraction (MZ10), (c) SPM being decanted into 5L and 25L jerry cans (MZ11), (d) SPM sample extraction (MZ5).

methods of Sodium hydroxide digestion, Hydrochloric acid (10%) for the elimination of carbonates, 40% HF for the elimination of silicates and clastic material and lastly acetolysis digestion to extricate organic detritus, which enable the concentration of pollen grains and assemblages to be established in a given amount of sediment (Faegri and Iverson, 1989).

The sediment fraction used were 3cm² of RBS and was sub-sampled volumetrically for pollen analysis. The 3cm² method was favoured instead of the standard 1cm² due to the sandy nature of the samples as well as being fluvial river sediment samples. This 3cm² RBS sample was then stored in a urine vial with 10ml distilled water at 4°C for later analysis. Thereafter samples were mounted onto glass microscope slides using Aquatex gel for counting and taxonomic identification. An Aquatex mounting agent was used as it is best suited for mounting of samples that have or currently contain traces of water. To avoid air bubbles and inclusions can occur under the coverslip of the slide, the volume of the mounting medium should be carefully considered and drying times for the slide should be observed. Despite this, the result of using Aquatex is that an airtight specimen slide is developed which can be used for microscopy at a later date. Since RBS samples were used for pollen analysis, it is advisable that the top 1 cm of sediment is removed from each grab sample. This ensures that the sediment sample is then representing the most modern material. The reason for subsampling more than the stipulated standard (Birks and Gordon, 1985) is that river bed sediments have been reported to contain low pollen grain counts (Davis *et al.*, 2013). Thus a minimum pollen count of 250 and an absolute minimum of 50 were employed for the purpose of this study.

Identification and counting of pollen grains were performed using a fixed traverse across the pollen slide at 400X magnification. 28 Palynomorphs were identified to the Family and genus level (Plate 3.2 a-f). The relative abundances were calculated for all palynomorphs for each site over the three sample campaigns. Palynomorphs were then grouped into their relevant ecological groupings, namely aquatics, fern spores, Fynbos elements, grasses, herbs and shrubs, trees and neophytes. A minimum count of 250 and an absolute minimum count of 50 was employed. Samples below the absolute minimum count were excluded from statistical analysis. Sample sites which consistently yielded high pollen concentrations were MZ1, MZ2, MZ4 and MZ10 for the dry (July), intermediate (September) and wet (November) seasons. Excluded samples due to not yielding pollen concentrations higher than the absolute minimum count (<50) were: MZ3, MZ5 and MZ9 for the dry season, MZ6 and MZ7 for the intermediate

season, and MZ5, MZ7, MZ8 and MZ9 for the wet season (please see appendix A for detailed pollen preparation and processing procedures).

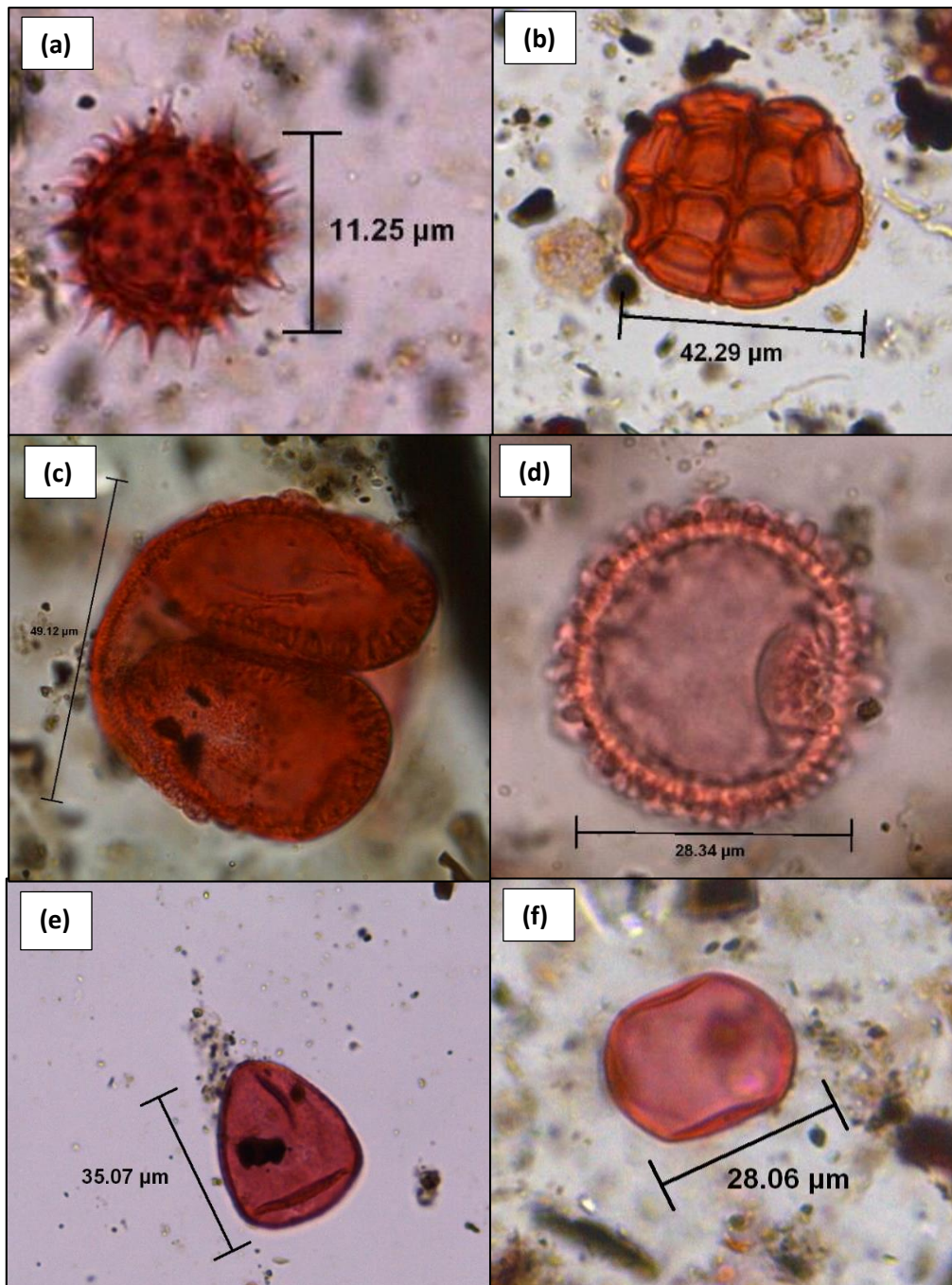


Plate 3.2: Examples of modern pollen grains extracted from the RBS samples of the Mzimvubu Catchment: (a) Asteraceae Tubuliflorae, (b) Mimosaceae Acacia type I, (c) Pinaceae Pinus, (d) Aquifoliaceae Ilex mitis, (e) Cyperaceae undiff., (f) Poaceae undiff.

3.3 ORGANIC GEOCHEMISTRY

3.3.1 *n*-Alkane plant wax biomarker extraction

n-Alkane lipid biomarker extraction from the July and September sampling campaigns were prepared and processed by the examinee (Tarryn Frankland) at the MARUM institute, University of Bremen. The November samples were processed by the MARUM institute due the duration of the examinees' exchange at the Institute ending before sampling processing of the third campaign could be completed (please refer to Acknowledgments).

Please see appendix B for detailed *n*-alkane separation procedure. nC_{19-35} concentrations were calculated for 32 RBS samples. Samples were ground using a pestle and mortar and then homogenised using a ball mill (650 rpm, thirty seconds per sample). The total sum of odd *n*-alkanes was calculated for each sample site for each sample campaign (Schefuss *et al.*, 2011; Hahn *et al.*, 2018). Total lipid extracts were extracted using a DIONEX Accelerated Solvent Extraction (ASE) with a 9:1 dichloromethane (DCM): methanol (MeOH) solvent mixture. Squalane was added to the samples as a standard prior to ASE extraction. A 5 % split was taken from each sample. Thereafter, lipid extracts were concentrated and solvent removed and saponification with 500µl of 0.1M KOH in MeOH solution to break down the wax ester bonds which could potentially interfere with alkenone quantification.

Column chromatography was used to separate the neutral lipid fraction using 10% deactivated silica gel and hexane (hydrocarbons). Subsequent elution with hexane, DCM and DCM:MeOH 1:1 yielded the ketone and polar fractions. Hydrocarbons containing *n*-alkanes were injected into a Thermo Scientific gas chromatograph. Comparison of peak areas to external and internal standards yielded the different *n*-Alkane chain lengths. Precision of compound quantification is about 5% based on the standard analyses. The CPI_{25-33} was calculated according to the following equation developed by Bray and Evans (1961):

$$CPI_{23-33} = 0.5 * (\sum C_{odd23-33} / \sum C_{even22-32} + \sum C_{odd23-33} / \sum C_{even24-34})$$

C_x represents the amount of each *n*-alkane homologue. *n*-Alkane Average Chain Length (ACL) was then determined using the following equation by Poynter and Eglinton (1990):

$$ACL_{25-35} = \frac{25 \times (nC_{25}) + 27 \times (nC_{27}) + 29 \times (nC_{29}) + 31 \times (nC_{31}) + 33 \times (nC_{33}) + 35 \times (nC_{35})}{(nC_{25} + nC_{27} + nC_{29} + nC_{31} + nC_{33} + nC_{35})}$$

The ratio between C_{29} and C_{31} *n*-alkanes (Norm31) was then calculated using the equation:

$$Norm31 = C_{31} / (C_{29} + C_{31})$$

For Norm31 and ACL calculations, nC_x represents the concentration of the n -alkane with x as the carbon number (please see appendix B for detailed n -alkane separation and processing procedures).

$\delta^{13}C$ and δD isotope extraction

Please see appendix B for detailed extraction procedure. Sample fractions containing n -alkanes were used for carbon and hydrogen isotope analyses. Stable hydrogen isotope analyses of C_{29} and C_{31} n -alkanes were carried out on a Trace GC (Thermo Fisher Scientific, Bremen, Germany). The $\delta^{13}C$ of the n -alkanes were analysed on a similar type of GC. Each sample was analysed twice except for a few samples where the n -alkane concentration was too low. The accuracy of the isotope measurements were assessed by analysing internal n -alkane laboratory standards of known isotopic composition every six measurements (please see appendix B for detailed $\delta^{13}C$ and δD processing and procedures).

3.4 INORGANIC GEOCHEMISTRY

3.4.1 XRF element composition analysis

XRF sample preparation and extraction for the July and September sampling campaigns were prepared and processed by the examinee (Tarryn Frankland) at the MARUM institute, University of Bremen. The November samples were processed by the MARUM institute due the duration of the examinees' exchange at the Institute ending before sampling processing of the third campaign could be completed (please refer to Acknowledgements).

Please see appendix B for detailed descriptions of sediment preparation and XRF processing procedures. The XRF element analysis of bulk RBS samples identified a total of 18 elemental compounds from the 32 RBS samples across for the three sampling campaigns. XRF spectrometer measurements were completed on 32 RBS using a PANalytical Epsilon3-XL XRF spectrometer. 20 g of dried RBS sediment were weighed and placed into a Ball Mill at 650rpm for 30 seconds. 4 g of the 20 g was then weighed and removed and utilised for XRF elemental analysis. A minimum of 12g were extracted from each sample for Alkenone analysis. Element composition profiles were performed using an Avaatech XRF Scanner.

3.4.2 Element Ratios

Element ratios were utilised to determine source area dynamics and sedimentological processes such as erosion, weathering and climate conditions (Chen *et al.*, 2013; Zabel *et al.*, 1999, 2001). Elemental ratios can be used to determine the ratio of clay versus coarse material, chemical

and mechanical weathering. The element ratios utilised for the purpose of this study were: Fe/K, Al/Si and Ti/Al. Fe/K can reflect the deposition of slightly weathered material from drier regions versus highly weathered material from humid regions. Al/Si indicates the fluvial input of highly weathered fine material from humid regions versus the fluvial input of less weathered material from drier regions. Lastly, Ti/Al reflects the relative contribution of coarse grain material versus fine grained material (Lopez *et al.*, 2006; Govin *et al.*, 2012; Hahn *et al.*, 2017).

3.5 DATA ANALYSIS

A sample data preparation for data analysis was performed using Microsoft Office Excel (2013) (Bricklin, 1978). Total pollen counts and ecological groupings for each season were plotted using Psimpoll 3.0 (Bennett, 2005), and the graphical output is displayed in GSview32 4.9 (Deutsch, 1986). Pollen diagrams were merged and edited using CorelDRAW X3 (Bouillon and Beirne, 1987). Correlations between RBS and SPM for each proxy were calculated on Excel 2013, using the Pearson Product-moment correlation coefficient for two values. ArcMap (Esri, 1999) was used to create locational maps of the sample area, including Mean Annual Precipitation (MAP) (mm), Mean Annual Temperature (MAT) (°C), and major vegetation biomes (Mucina and Rutherford, 2006) and veld types (Acocks, 1988).

CHAPTER FOUR

RESULTS

4.1 INTRODUCTION

The aim of this chapter is to present the results of pollen analysis, inorganic XRF analysis, inorganic stable isotope analysis, and organic plant wax lipid biomarker analysis. Provenance dynamics of each proxy is determined at a catchment and tributary scale. Furthermore, proxy data will be compared with environmental parameters (annual precipitation, elevation and annual temperature).

4.2 POLLEN ANALYSIS

4.2.1 Pollen counts

From the total of 32 pollen samples, nine were excluded from the dataset as they did not yield raw pollen counts ≥ 50 (see appendix D). Pollen grain preservation for the RBS samples of the Mzimvubu Catchment was generally poor with a percentage unknown ranging from ~4% (river confluence) to ~69% (Kinira River).

A total of 29 palynomorphs were identified from the RBS samples across each sample site for the three sampling campaigns (Table 4.1). On average, each site contained 21 of the total 29 palynomorphs identified, with the Mzintlava River and Mzimvubu River yielding the most variable palynomorph assemblages and the iTsitsa, Kinira River and river mouth yielding the least diverse palynomorph assemblages (please see appendix D for raw pollen counts).

4.2.3 Pollen seasonality

Dry season

Please see appendix F for additional pollen data and maps. Poaceae, Cyperaceae, *Tubuliflorae* and *Pinus* dominate the catchment during the dry season (Figure 4.1 and 5.2). Cyperaceae was present at every sample site, with MZ1 (river mouth), MZ4 (Thina River) and MZ10 (upper Mzimvubu River) yielding the highest frequencies. Liliaceae is present in low abundances compared to Cyperaceae except for site MZ7 (iTsitsa). MZ7 (iTsitsa) contains high frequencies of both Cyperaceae and Liliaceae. Fern spores are also present in high abundances during this season, specifically triletes

Table 4.1: Ecological classifications and number of pollen taxa per sample for each pollen taxa within the Mzimvubu Catchment.

Ecological classification	Family And genus	Number Of samples taxa was present
Aquatics	Cyperaceae undiff.	23
	Liliaceae undiff.	16
Fynbos Elements	Ericaceae undiff.	11
	Thymelaeaceae <i>Passerina</i>	5
Grasses	Poaceae undiff.	23
Herbs And Shrubs	Amaryllidaceae undiff.	7
	Anacardiaceae <i>Rhus</i>	21
	Asteraceae <i>Helichrysum</i>	13
	Asteraceae <i>Senecio</i>	16
	Asteraceae <i>Tubuliflorae</i>	20
	Asteraceae <i>Vernonia</i>	17
	Cheno-Am	16
	Euphorbiaceae <i>Acalypha</i>	8
	Euphorbiaceae <i>Euphorbia</i>	14
Neophytes (exotics)	Fabaceae <i>Sesbania</i>	1
	Pinaceae <i>Pinus</i>	21
	Poaceae <i>Zea mays</i>	8
	Salicaceae <i>Salix</i>	2
Trees	Aquifoliaceae <i>Ilex mitis</i>	12
	Cyatheaceae <i>Cyathea</i>	1
	Combretaceae <i>Combretum</i>	4
	Mimosaceae <i>Acacia</i> type I	20
	Myricaceae <i>Morella</i>	6
	Myrtaceae <i>Syzygium</i>	1
	Palmae <i>Borassus</i>	
	Podocarpaceae <i>Podocarpus</i>	7
Fern Spore	Pteridophytes <i>Monoletes</i>	16
	Pteridophytes <i>Triletes</i>	10

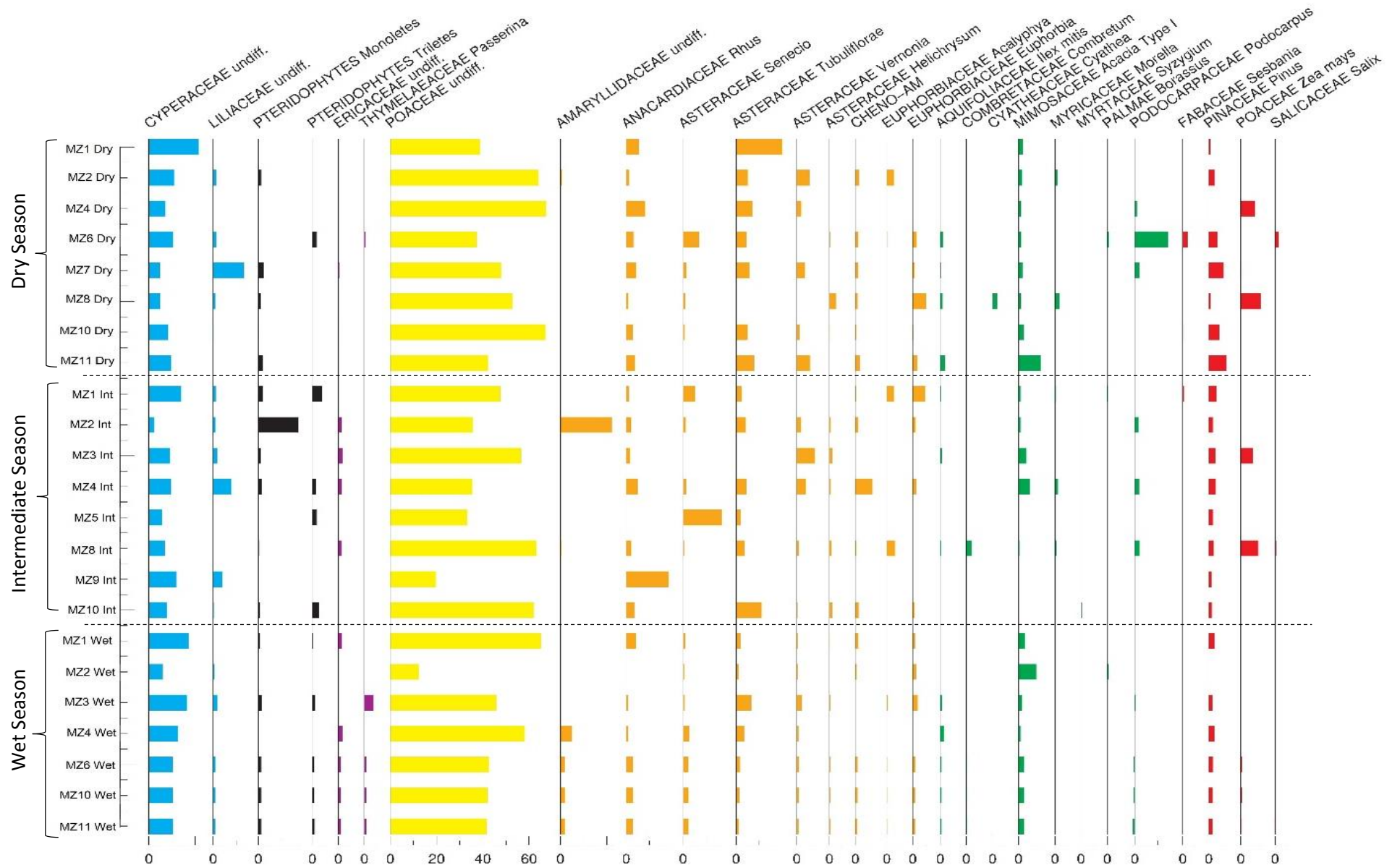


Figure 4.1 Palynomorph abundance and diversity for the three sampling campaigns (dry, intermediate and wet) for the Mzimvubu catchment.

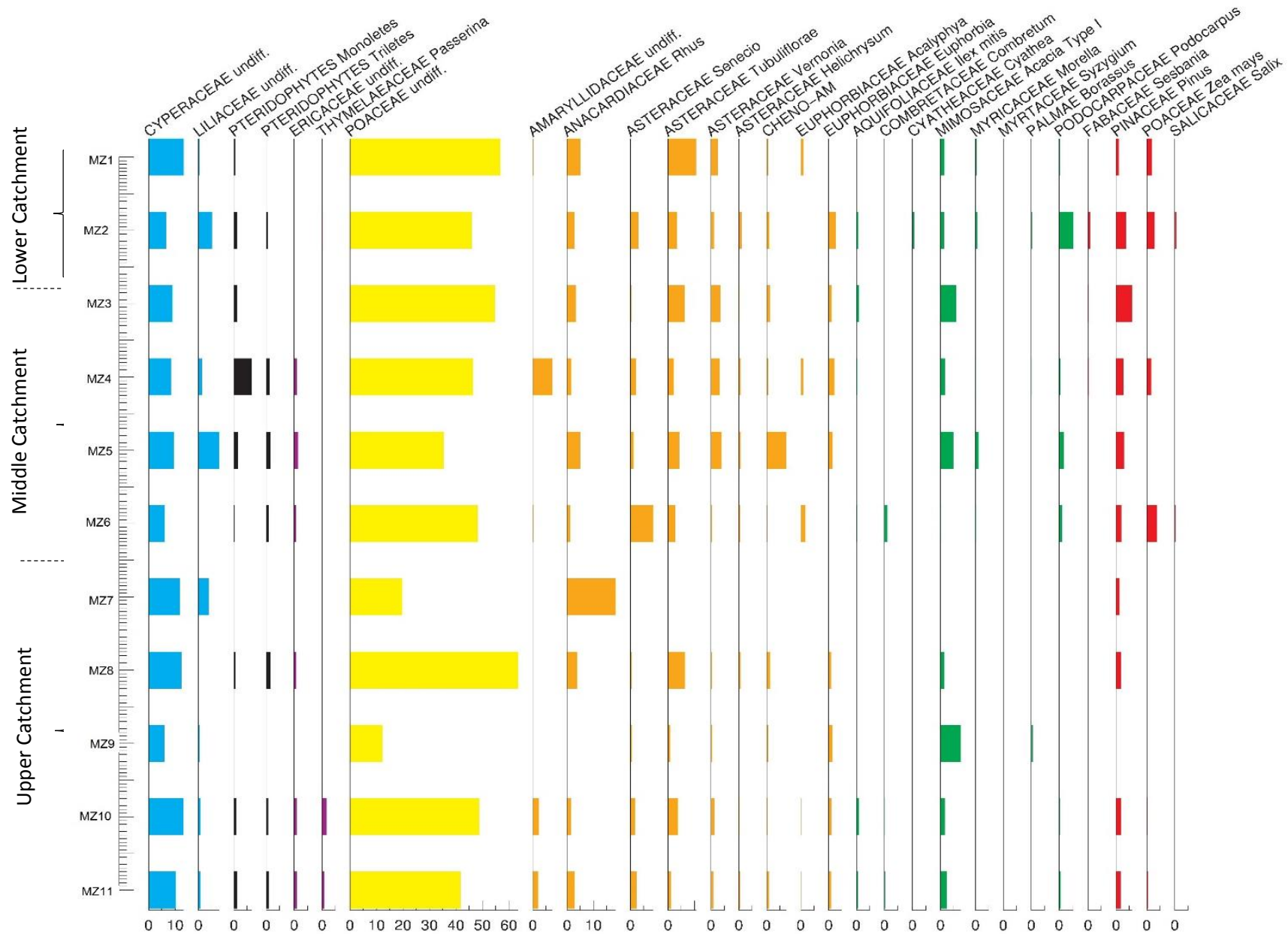


Figure 4.2: Palynomorph abundance and distributions across the sampling sites for the Mzimvubu Catchment.

which were present in almost all sample sites. Fynbos elements namely *Ericaceae* undiff. and *Passerina* showed relatively high frequencies at MZ2 (river confluence), MZ4 (Thina River), MZ10 (upper Mzimvubu River) and MZ11 (Mzintlava River) with MZ10 and MZ11 yielding the highest frequency.

Poaceae is the most abundant palynomorph in the dry season. MZ4 and MZ8 (Thina River) yielded the highest Poaceae abundance, whereas MZ7 (iTsitsa), MZ6 and MZ11 (Mzintlava River) yielded the lowest abundance. Herbs and shrubs are the most diverse vegetation group within the catchment, consisting of ten palynomorphs which dominate the lower to middle catchment. *Rhus* and *Tubuliflorae* are the most abundant taxa, occurring in almost all the samples sites. The least abundant herbs and shrubs are *Amaryllidaceae*, *Asteracea*, *Helichrysum*, *Vernonia*, *Cheno-Am*, *Acalypha* and *Sesbania*. Four tree palynomorphs namely, *Ilex mitis*, *Acacia* type I, *Borassus* and *Podocarpus* were identified during the dry season. *Acacia* type I are the most widespread and abundant tree in the catchment during the dry season followed by *Podocarpus*. However, *Podocarpus* is exclusively recorded at MZ2 (river mouth) during the dry season. Similarly, *Borassus* and *Ilex mitis* are also exclusively recorded at MZ2 (river mouth) but in lower frequencies compared to *Podocarpus*. Neophytic taxa such as *Pinus* and *Salix* were identified within the catchment. *Pinus* is the most abundant neophytic taxon, occurring at every sample site, with the highest frequencies occurring in the lower tributaries. *Salicaceae* *Salix* is not as widespread compared to the dry and wet seasons and is exclusive to MZ2 (river mouth). Poaceae *Zea mays* pollen is absent from the catchment during the dry season.

Intermediate season

Similar to the dry season, Cyperaceae, Poaceae, *Tubuliflorae* and *Pinus* dominate the Mzimvubu Catchment during the intermediate season (Figure 4.1 and 5.2). Cyperaceae is highest at sites MZ8 (Thina River) and MZ10 (upper Mzimvubu River), however, palynomorph diversity and abundance shows a general decline compared to the dry season. Liliaceae is present in fewer sites compared with the dry season, however, overall abundance rises significantly for the intermediate season. For example, Liliaceae more than doubles in abundance at MZ2 (river confluence) and is present at MZ5 (middle Mzimvubu River). Fern spores are also present in the intermediate season with pteridophyte monoletes increasing drastically in abundance and site diversity compared to the dry season. MZ4 (Thina River) contains the highest monoletes frequency compared to the frequency of the dry season. Triletes

fern spores show reduced abundance compared to the dry season and are restricted to sites MZ5 (lower Mzimvubu River) and MZ8 (Thina River).

Fynbos elements namely Ericaceae and *Passerina* were identified in the intermediate season in higher abundances compared with the dry season. Ericaceae are present at MZ5 (lower Mzimvubu River) and MZ8 (Thina River) and *Passerina* is present at MZ4 and MZ8 (Thina River), MZ5 and MZ10 (Mzimvubu River) with MZ 10 (upper Mzimvubu River) yielding the highest abundance. The intermediate season shows that Poaceae remains the most frequent taxon in the catchment during the intermediate season. Overall Poaceae abundance is higher compared to the dry season. MZ3 (iTsitsa), MZ8 (Thina River) and MZ1 (river mouth) contain the highest Poaceae frequencies whereas, MZ4 (Thina River), MZ5 and MZ9 (Kinira River) contain the lowest Poaceae frequency. Herbs and shrubs show a reduced frequency compared to the dry season, however, are higher in palynomorph diversity. *Rhus*, *Tubuliflorae*, *Vernonia* and Cheno-Am, are the most abundant taxa.

Euphorbia reduces in abundance but shows a higher site diversity compared to the dry season. *Sesbania* is absent in this season. A similar composition of tree types were present in the intermediate season as were present in the dry season. However, there is an increase in frequency of Myricaceae *Morella* at MZ1 (river mouth) and MZ5 (lower Mzimvubu River) for the intermediate season. *Acacia* type I remains the most abundant tree palynomorph followed by *Podocarpus*. *Ilex mitis* signal was only found at MZ10 (upper Mzimvubu River) in low abundance. *Pinus* was the only neophyte identified during the intermediate season. *Pinus* was present across the catchment with the exception of MZ9 (Kinira River). Overall MZ2 (river mouth) and MZ3 (iTsitsa) contain the highest abundances of *Pinus*, followed by MZ8 (Thina River). *Zea mays* and *Salix* pollen types were absent during the intermediate season.

Wet season

Cyperaceae, Poaceae, *Rhus*, *Tubuliflorae*, *Acacia* and *Pinus* represent the dominant wet season taxa within the catchment (Figure 4.1 and 5.2). Cyperaceae shows a moderately reduced abundance compared to the other seasons, which yielded highly variable frequencies. Cyperaceae is highest at MZ3 (iTsitsa), MZ10 (upper Mzimvubu River) and MZ11 (Mzintlava River) and lowest at MZ2 (river mouth) during the wet season. Similarly for Liliaceae, abundance is considerably lower compared to the other seasons. Monoletes and triletes fern spores yielded reduced frequency compared to the drier season. All seasons showed triletes preferring the upper tributaries, which is seen in the wet season as well.

Ericaceae and *Passerina* (fynbos elements) are present in low frequencies compared to the dry and intermediate season. These taxa consistently dominate the upper catchment at sites MZ10 (upper Mzimvubu River) and MZ11 (Mzintlava River) thus indicating a strong Fynbos signal originating from the upper catchment. Conversely to the general trend of lower Poaceae abundance for the dry and intermediate seasons, Poaceae reveals a consistently elevated signal for the wet season. MZ4 (Thina River), MZ1 (river mouth) and MZ6 (Mzintlava River) yielded the highest Poaceae frequency, with MZ3 (iTsitsa), MZ10 (upper Mzimvubu River) and MZ11 (Mzintlava River) yielding the lowest. Overall, a strong Poaceae signal originates from the Thina River and lower Mzintlava River tributaries during the wet season. Similarly, herb and shrub taxa reveal consistently high frequencies throughout the catchment, with the highest frequencies occurring the middle to lower catchment. *Rhus*, *Tubuliflorae* and *Vernonia* dominate the herb and shrub ecological group. These taxa are present at almost every site in high abundances compared to the intermediate season. *Sesbania* pollen was absent from the wet season campaign.

Tree palynomorphs are generally abundant and well distributed through the catchment during the wet season. *Acacia* type 1 and *Ilex mitis* are the most abundant tree taxa for the wet season. *Ilex mitis* yielded elevated abundances compared to previous seasons. *Acacia* type I is highest at MZ3 (iTsitsa) and MZ4 (Thina River) and lowest at MZ10 (upper Mzimvubu River) and MZ11 (Mzintlava River). Combretaceae *Combretum*, *Cyathea* and *Morella* are present in this season and tend to dominate the lower catchment sample sites. *Podocarpus* yields reduced abundances compared to previous seasons. Exotic *Pinus* is present at every site with the exception of MZ9 (Kinira River). The highest *Pinus* frequency occurs at MZ3 (iTsitsa) which gradually decreases towards the upper catchment. *Zea mays* is frequently present in this season at MZ1 (river mouth), MZ2 (river confluence), MZ4 (Thina River) and MZ6 (Mzintlava River).

4.2.4 Pollen biome comparison

Indian Ocean Coastal Belt (IOCB) - total catchment pollen abundance (Figure 4.3 a) shows a predominantly Poaceae (~52%) dominated environment. Herbs and shrubs account for ~25%, followed by aquatic types (~10%), trees (~5%), neophytes (~4%), pteridophytes (~3%) and Fynbos elements at (~1%). Poaceae (~56%) is the dominant palynomorph for the IOCB (Figure 4.3 b). Herbs and shrubs (~23%) account for the second largest ecological group followed by aquatics (~17%), neophytes (~2%) and trees (~2%). Fynbos elements and pteridophytes were not identified in this biome.

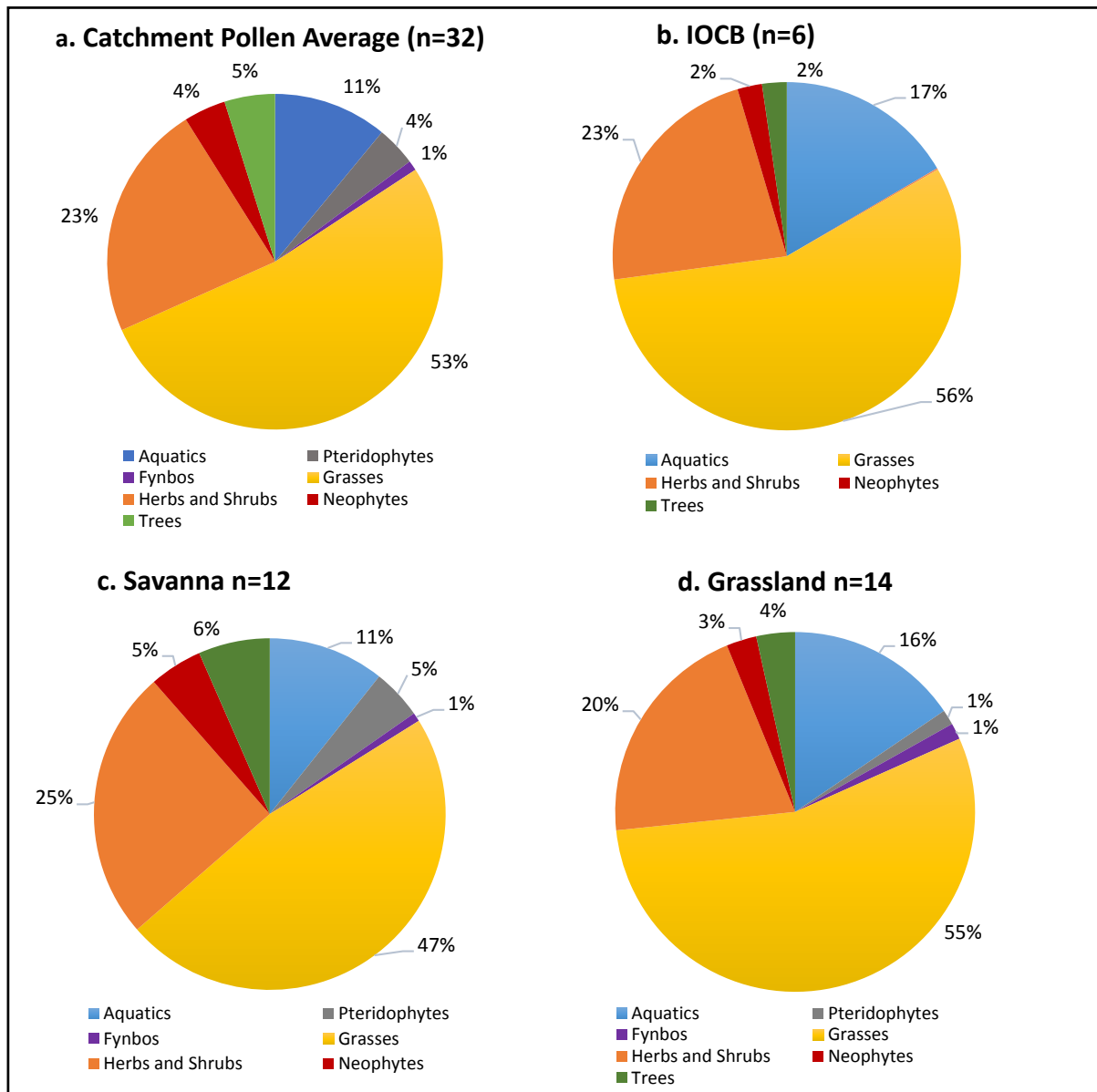


Figure 4.3: Pie charts showing the ecological groupings of pollen taxa within the catchment 's three major biomes namely, (a) catchment average, (b) IOCB (c), Savanna (d) and Grassland.

Savanna - the Savanna biome (Figure 4.3 c) yielded a more diverse pollen signal compared to the IOCB and Grassland biomes. Poaceae (~47%) remains the dominant palynomorph but contributes less to the total vegetation compared to herbs and shrubs and trees. Herbs and shrubs, trees, neophytes and pteridophytes show a higher abundance compared to the IOCB and Grassland biomes. Aquatics (~11%) account for smaller portion of the vegetation

composition compared to the IOCB and Grassland. Fynbos elements are introduced in this biome however, only account for a small percentage (~1%).

Grassland - the Grassland biome (Figure 4.3 d) yielded a typical Poaceae (~55%) dominated environment compared to the IOCB and Savanna biomes. Aquatics (~16%) comprise a large portion of the total vegetation compared to the Savanna biome but similar to the IOCB. Herbs and shrubs, trees and neophytes contribute a lower portion to the total Grassland vegetation compared to the IOCB and Savanna Biomes. Fynbos elements (~1%) and pteridophytes (~1%) account for a small percentage of the vegetation cover, similar to the Savanna Biome.

4.2.5 Pollen Tributary Comparison

The river mouth (Figure 4.4 a) represents the cumulative contribution of each tributary and thus, is used to represent the catchment vegetation. The iTsitsa River and Thina River display a strong grass signal, whereas the Kinira River, Mzimvubu River and Mzintlava River display a strong herbs and shrubs signal typical of Savanna type vegetation. The Mzintlava River shows a similar vegetation composition compared to the river mouth, except that Fynbos elements are introduced in this area. The Kinira River contains the highest herbs and shrub (~29%) and tree (~11%) composition and the lowest grass signal (~36%) compared to the other tributaries (Figure 4.4 a-f). Conversely, the iTsitsa River has the highest grass composition (~66%) and the lowest herb and shrub (~15%) and tree signal (~3%) compared to the other sites (Figure 4.4 a-f).

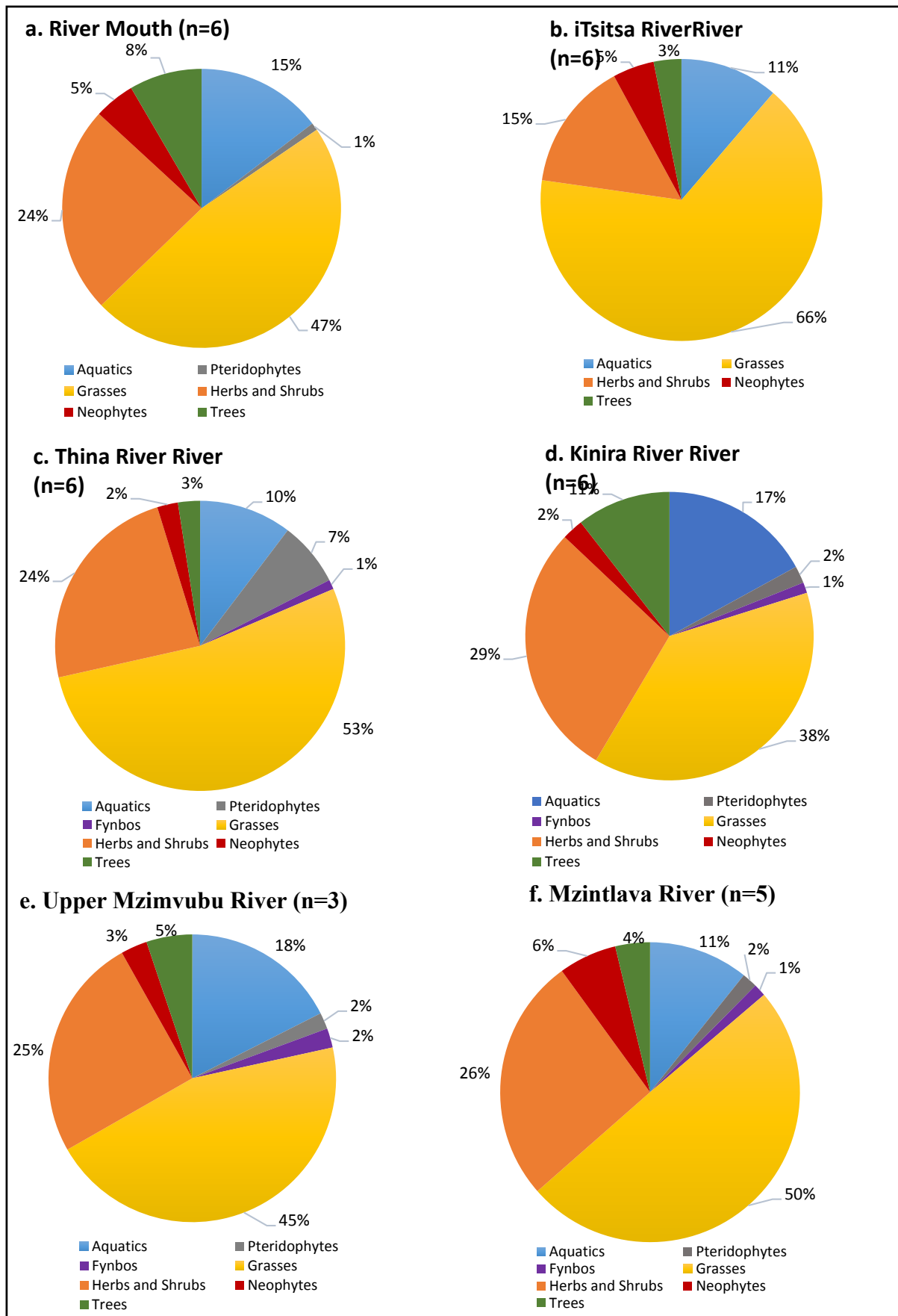


Figure 4.4: Pie charts showing the major ecological groupings for each major tributary of the Mzimvubu catchment, namely, River Mouth (a), iTsitsa River(b), Thina River (c), Kinria (d), upper Mzimvubu (e) and the Mzintlava (f).

4.3 ORGANIC GEOCHEMISTRY

4.3.1 *n*-Alkane $\mu\text{g/g}$ abundance

River Bed Sediment (RBS) Samples

Please see appendix G from a. to h. for additional seasonal *n*-alkane, ACL, CPI, Norm31, $\delta^{13}\text{C}$, δD and elemental ratio distributions.

n-Alkane concentrations within dry sediment for RBS samples ranged from 3.0×10^{-1} to $4.1 \times 10^2 \mu\text{g/g}$ (Table 4.2). The dry season yielded the highest *n*-alkane concentration, followed by the intermediate season, and lastly the wet season. RBS samples showed high *n*-alkane abundance originating from the Mzintlava River during the dry season ($2.1 \times 10^2 \mu\text{g/g}$) and wet season ($1.7 \times 10^2 \mu\text{g/g}$), and the Thina River River ($2.1 \times 10^2 \mu\text{g/g}$) for the intermediate season. The lowest *n*-alkane concentrations were recorded in the Kinira River for the dry ($4.4 \times 10^0 \mu\text{g/g}$) and intermediate ($1.8 \times 10^1 \mu\text{g/g}$) seasons, and the river mouth ($2.0 \times 10^0 \mu\text{g/g}$) for the wet season.

Suspended Particulate Matter (SPM) Samples

n-Alkane concentrations for SPM samples range from 2.8×10^0 to $2.1 \times 10^5 \mu\text{g/g}$ (Table 4.2). The intermediate season ($3.8 \times 10^4 \mu\text{g/g}$) yielded the highest $\mu\text{g/g}$ sediment, followed by the wet season ($2.2 \times 10^4 \mu\text{g/g}$), and lastly the dry season ($1.5 \times 10^3 \mu\text{g/g}$). The highest *n*-alkane concentration recorded in the SPM material occurred in the Mzintlava River ($6.7 \times 10^3 \mu\text{g/g}$) for the dry season, the Thina River ($1.5 \times 10^5 \mu\text{g/g}$) for the intermediate season and the iTsitsa River (2.9×10^4) for the wet season. Lowest $\mu\text{g/g}$ sediment occurred in the Kinira River for the dry ($7.1 \times 10^0 \mu\text{g/g}$) and wet ($7.4 \times 10^1 \mu\text{g/g}$) season, and the river mouth ($6.4 \times 10^2 \mu\text{g/g}$) for the intermediate season.

4.3.2. *n*-Alkane homologue composition

RBS Samples

The nC_{31} homologue characterises the river mouth during the dry season (Table 4.3). A strong nC_{31} signal can be traced to the iTsitsa, Thina River and Kinira River, and strong nC_{29} signal is present in the Mzimvubu River and Mzintlava River during the dry season. nC_{31} is the most abundant *n*-alkane homologue at the river mouth for the intermediate season. The iTsitsa, Thina River, Kinira River and Mzintlava River yielded a strong nC_{31} signal, and a strong nC_{27} signal was present in the Mzimvubu River. nC_{33} is the most common homologue at the river mouth for the wet season. A strong nC_{31} signal is present in the iTsitsa, Thina River, Kinira River and Mzimvubu River. nC_{27} is the most common homologue in the Mzintlava River River.

SPM Samples

The nC₃₁ homologue dominates the river mouth, iTsitsa, Thina River and Kinira River during the dry season (Table 4.2). A strong nC₃₃ signal originates from the Mzintlava River, whereas nC₂₉ is most

Table 4.2: Table showing *n*-alkane $\mu\text{g/g}$ sediment, the dominant homologue, ACL_{25-33} , CPI_{25-33} , $\delta^{13}\text{C}_{29}$, $\delta^{13}\text{C}_{31}$, $\delta^{13}\text{C}_{29-31}$, δD_{29} , δD_{31} , δD_{29-31} and Norm31 for RBS samples and marine sediment core top (GeoB20624-0-1) of the Mzimvubu Catchment.

Season	Site	$\mu\text{g/g}$ sediment <i>n</i> -alkanes	Dominant Homologue	CPI_{25-33}	$\delta^{13}\text{C}_{29}$	$\delta^{13}\text{C}_{31}$	$\delta^{13}\text{C}_{29-31}$	δD_{29}	δD_{31}	δD_{29-31} Weighted average	Norm31
GeoB20624-0-1		7.45×10^2	C ₃₁		-28.6	-28.5	-28.6	-142.1	-148.4	-145.3	
Dry	MZ 1	1.303×10^2	C ₃₁	7.1	-29.6	-29.9	-29.7	-125.8	-141.4	-133.6	0.63
	MZ 2	1.119×10^2	C ₃₁	7.2	-28.1	-29.2	-28.6	-133.9	-140.4	-137.2	0.63
	MZ 3	3.97×10^1	C ₃₁	6.5	-32.5	-31.7	-32.1	-112.6	-128.3	-120.5	0.62
	MZ 4	2.144×10^2	C ₃₁	8.0	-31.9	-30.2	-31.1	-121.9	-137.9	-129.9	0.63
	MZ 5	2.6×10^0	C ₃₁								0.70
	MZ 6	7.1×10^0	C ₃₁		-28.2	-29.0	-28.6	-131.8	-142.6	-137.2	0.76
	MZ 7	1.69×10^1	C ₃₁	5.1	-31.5	-28.4	-29.9	-132.7	-143.7	-138.2	0.56
	MZ 8	3.93×10^1	C ₃₁	9.0	-30.8	-28.1	-29.5	-126.1	-147.7	-136.9	0.67
	MZ 9	6.2×10^0	C ₃₁								0.56
	MZ 10	3.003×10^2	C ₂₉	7.9	-31.7	-28.9	-30.3	-155.5	-150.8	-153.1	0.46
	MZ 11	4.155×10^2	C ₂₉	2.1				-153.9	-145.2	-149.6	0.43
Intermediate	MZ 1	8.67×10^1	C ₃₁	8.1	-28.4	-30.1	-29.3	-132.4	-139.4	-135.9	0.58
	MZ 2	5.93×10^1	C ₃₁	7.9	-28.0	-29.1	-28.5	-133.7	-142.9	-138.3	0.70
	MZ 3	3.03×10^1	C ₃₁	4.7	-32.0	-30.8	-31.4	-116.1	-136.1	-126.1	0.63
	MZ 4	3.905×10^2	C ₃₁	2.4	-29.7	-29.1	-29.4	-125.5	-145.3	-135.4	0.62
	MZ 5	1.56×10^1	C ₃₁	3.9				-124.9	-142.7	-133.8	0.68
	MZ 6	1.09×10^1	C ₃₁	3.8	-28.0	-27.6	-27.8	-126.0	-150.2	-138.1	0.79
	MZ 7	1.55×10^1	C ₃₁	4.5	-30.0	-28.4	-29.2	-136.3	-143.7	-140.0	0.52
	MZ 8	3.07×10^1	C ₃₁	5.7	-30.9	-28.9	-29.9	-128.3	-151.9	-140.1	0.66
	MZ 9	1.95×10^1	C ₂₉	8.0	-32.0	-27.5	-29.8	-140.7	-147.9	-144.3	0.45
	MZ 10	1.568×2	C ₂₇	9.0	-32.1	-27.5	-29.8	-159.5	-150.	-154.8	0.29
Wet	MZ 1	2.9×10^0	C ₃₁	2.0	-29.9	-31.4	-30.6	-146.9	-150.6	-148.8	0.75
	MZ 2	1.1×10^0	C ₃₁	2.6							0.70
	MZ 3	7.1×10^0	C ₃₁	7.5	-29.4	-28.2	-28.8	-113.9	-139.3	-126.6	0.69
	MZ 4	5.0×10^0	C ₃₃	5.3	-32.8	-31.0	-31.9	-135.5	-148.8	-142.2	0.73
	MZ 5	1.35×10^1	C ₃₁	8.8							0.65
	MZ 6	1.129×10^2	C ₂₇	11.6	-29.5	-29.3	-29.4	-117.5	-139.2	-128.4	0.27
	MZ 7	8.6×10^0	C ₃₁	6.3	-32.3	-29.9	-31.1	-140.3	-145.7	-143.0	0.76
	MZ 8	1.07×10^1	C ₃₁	6.2	-31.8	-29.1	-30.4	-132.4	-157.2	-144.8	0.55
	MZ 9	2.22×10^1	C ₃₁	8.6	-28.6	-27.0	-27.8				0.61
	MZ 10	3.0×10^{-1}	-								0.63
	MZ 11	2.331×10^2	C ₂₉	4.5				-166.1	-160.6	-163.3	0.34

Equations: (i) $\text{CPI}_{23-33} = 0.5 * (\sum \text{C}_{\text{odd}23-33} / \sum \text{C}_{\text{even}22-32} + \sum \text{C}_{\text{odd}23-33} / \sum \text{C}_{\text{even}24-34})$. (ii) $\text{ACL}_{25-33}: 25 \times (\text{nC}_{25}) + 27 \times (\text{nC}_{27}) + 29 \times (\text{nC}_{29})$

+ $31 \times (\text{nC}_{31}) + 33 \times (\text{nC}_{33}) + 35 \times (\text{nC}_{35}) / (\text{nC}_{25} + \text{nC}_{27} + \text{nC}_{29} + \text{nC}_{31} + \text{nC}_{33} + \text{nC}_{35})$. (iii) Norm31: $\text{C}_{31}/(\text{C}_{29} + \text{C}_{31})$.

Table 4.3: Table showing the *n*-alkane concentration, dominant homologue, ACL_{25-33} , CPI_{25-33} , $\delta^{13}C_{29}$, $\delta^{13}C_{31}$, $\delta^{13}C_{29-31}$, δD_{29} , δD_{31} , δD_{29-31} and Norm31 for SPM samples of the Mzimvubu Catchment.

Season	Site	$\mu\text{g/g}$ sediment n-alkanes	Dominant Homologue	CPI_{25-33}	$\delta^{13}C_{29}$	$\delta^{13}C_{31}$	$\delta^{13}C_{29-31}$	Norm31
Dry	MZ 1	9.236×10^2	C ₃₁	2.6	-29.5	-28.8	-29.1	0.58
	MZ 2	1.20×10^1	C ₃₁			-29.3	-29.3	0.69
	MZ 3	8.74×10^1	C ₃₁		-30.1	-28.4	-29.3	0.70
	MZ 4	2.32×10^1	C ₃₁	4.4	-30.3	-29.0	-29.6	0.72
	MZ 5	1.14×10^1	C ₃₁	1.8	-29.0	-28.5	-28.7	0.71
	MZ 6	1.5911×10^3	C ₃₁	2.6	-29.5	-28.4	-28.9	0.78
	MZ 7	1.3838×10^3	C ₃₁			-27.7	-27.7	1.00
	MZ 8	5.33×10^1	C ₃₃	5.7	-29.3	-26.5	-27.9	0.73
	MZ 9	2.8×10^0	C ₂₉	5.5	-29.2	-27.7	-28.5	0.33
	MZ 10	6.16×10^1	C ₂₉	4.1	-31.6	-28.3	-29.9	0.41
	MZ 11	1.1895×10^4	C ₃₁	1.2				0.61
Intermediate	MZ 1	1.1847×10^3	C ₃₁	2.6	-28.8	-28.8	-28.8	0.58
	MZ 2	9.49×10^1	C ₃₁		-28.0	-30.9	-29.5	0.69
	MZ 3	1.4149×10^3	C ₃₁					0.70
	MZ 4	8.71559×10^4	C ₃₁	2.4	-29.5	-28.5	-29.0	0.70
	MZ 5	4.2239×10^3	C ₃₁		-30.7	-29.1	-29.9	1.00
	MZ 6	4.6131×10^3	C ₃₁	4.3	-29.1	-28.5	-28.8	0.72
	MZ 7	1.0757×10^3	C ₃₁		-31.2	-29.2	-30.2	0.74
	MZ 8	2.114236×10^5	C ₂₇	12.3	-29.1	-26.7	-27.9	0.27
	MZ 9	6.27057×10^4	C ₃₁	5.0	-30.0	-27.0	-28.5	0.71
	MZ 10	1.4470×10^3	C ₂₇	0.1				0.58
Wet	MZ 1	3.143×10^2	C ₃₁	1.4	-29.3	-28.7	-29.0	0.50
	MZ 2	5.63768×10^4	C ₂₇	1.0				0.52
	MZ 3	5.04041×10^4	C ₃₁	1.5		-30.0	-30.0	0.51
	MZ 5	7.44×10^1	C ₃₁	5.8	-28.5	-28.8	-28.7	0.72
	MZ 6	8.69909×10^4	C ₂₉	1.4	-29.7	-28.6	-29.1	0.49
	MZ 7	6.6329×10^3	C ₃₁	3.3	-29.0	-27.2	-28.1	0.61
	MZ 9	7.39×10^1	C ₃₁	2.9	-30.6	-28.7	-29.6	0.47
	MZ 10	1.1426×10^3	C ₂₉	4.6	-29.9	-27.9	-28.9	0.45
	MZ 11	3.583×10^2	C ₃₁	1.3	-30.2	-29.6	-29.9	0.52

Equations: (i) $CPI_{25-33} = 0.5 * (\sum C_{\text{odd}23-33} / \sum C_{\text{even}22-32} + \sum C_{\text{odd}23-33} / \sum C_{\text{even}24-34})$. (ii) $ACL_{25-33} = 25 \times (nC_{25}) + 27 \times (nC_{27}) + 29 \times (nC_{29}) + 31 \times (nC_{31}) + 33 \times (nC_{33}) + 35 \times (nC_{35}) / (nC_{25} + nC_{27} + nC_{29} + nC_{31} + nC_{33} + nC_{35})$. (iii) Norm31: $C_{31} / (C_{29} + C_{31})$.

abundant in the Mzimvubu River. The intermediate season is characterised by a predominance of the nC_{31} homologue at the river mouth, iTsitsa, Mzimvubu River and Mzintlava River. nC_{27} is most abundant in the Thina River River, and nC_{33} in the Kinira RiverRiver for the intermediate season. For the wet season, the river mouth yielded a strong nC_{27} n -alkane homologue signal. The Mzintlava River is characterised by the nC_{29} homologue. nC_{31} remains the most abundant homologue for the iTsitsa, Kinira River and Mzimvubu River for the wet season.

4.3.3 Norm31

RBS Samples

RBS Norm31 values fall between 0.27 to 0.79, avereagin at 0.61 across the three sampling campaigns (Table 4.3). The wet season yields the highest norm31 value of 0.61, followed by the dry season (0.60) and the intermediate season (0.59) (Figure 4.5 a-c). The highest norm31 ratios for the dry season occurred in the river mouth (0.63), and the lowest in the Mzimvubu River (0.58) (Figure 4.5 a). The Mzimvubu River (0.49) yielded the lowest norm31 ratio during the intermediate season (Figure 4.5 b), and the highest in the Mzintlava River (0.79) (Figure 4.5 c). Wet season norm31 ratios show the lowest value occurring at the Mzintlava River (0.30) and the highest values occurring at the iTsitsa River(0.71) (Figure 4.5 c).

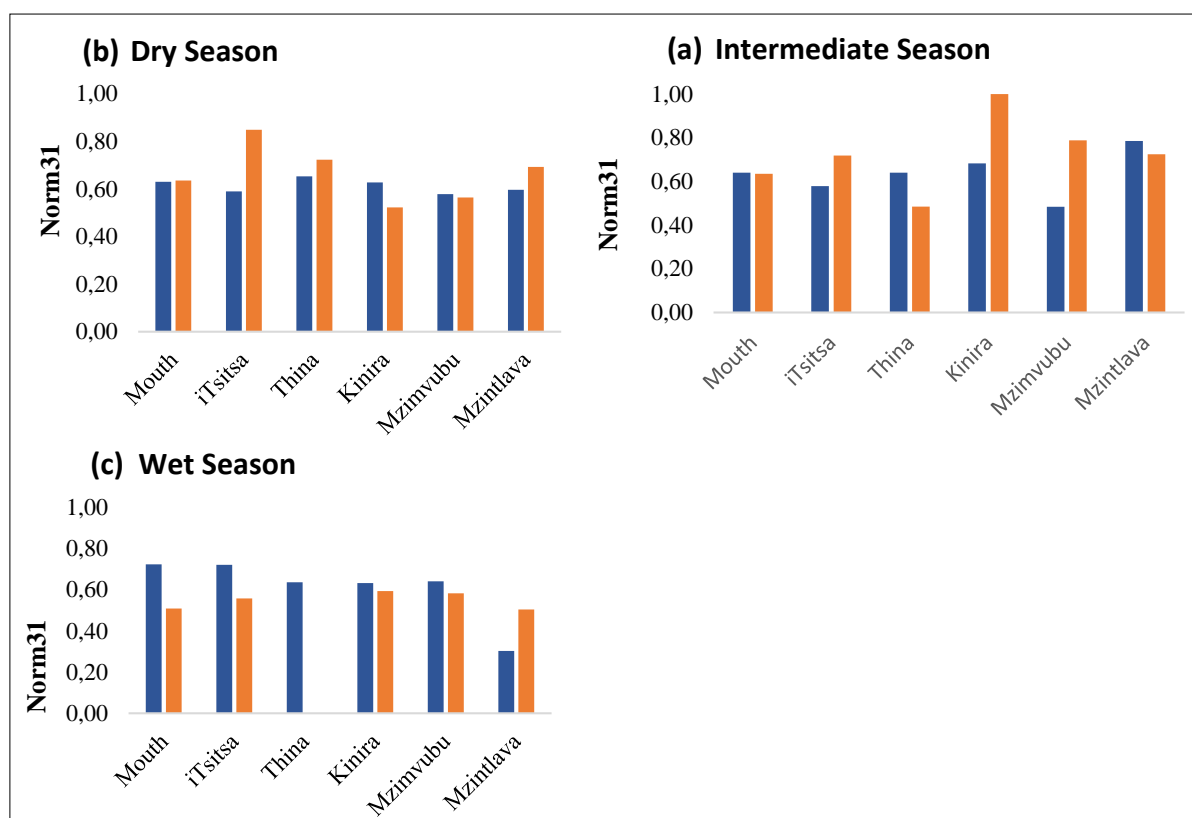


Figure 4.5: Histogram showing norm31 ratios for RBS (blue) and SPM (orange) samples of each tributary, for the dry (a), intermediate (b) and wet (c) seasons.

SPM Samples

SPM norm31 values fall between 0.27 and 1.00, averaging at 0.62 (Table 4.2). The intermediate season yields the highest norm31 average (0.67), followed by the dry season (0.66) and the wet season (0.53) (Table 4.2). The highest dry season ratio occurred in the iTsitsa River (0.85) and the lowest in the Kinira River (0.52) (Figure 4.5 a). The intermediate season shows the lowest value in the Thina River (0.48) and the highest value in Kinira River (0.85) (Figure 4.5 b). The wet season yielded the highest ratio in the Kinira River (0.59) and the lowest in the Mzintlava River (0.50).

Norm31 Correlation matrices

Please see appendix H for additional proxy correlations for each season.

Dry season RBS norm31 has a positive correlation to SPM norm31 ($r=0.426$), precipitation ($r=0.363$) and temperature ($r=0.309$), and is negatively correlated to elevation ($r=-0.414$) (Table 4.4). SPM norm31 shows no significant positive or negative correlations. SPM norm31 shows no significant positive or negative correlations for the intermediate season.

*Table 4.4: Correlation matrices for Norm31 RBS and SPM samples to precipitation, elevation and temperature for the dry, intermediate and wet season. Significant correlations are **bolded** and highlighted in yellow, moderate correlations are highlighted in orange and inverse correlations are highlighted in blue. Level of significance for all calculations is 0.95*

		RBS Norm31	SPM Norm31	Precipitation	Elevation	Temperature
Dry	RBS Norm31	1				
	SPM Norm31	0.426	1			
	Precipitation	0.363	0.198	1		
	Elevation	-0.414	-0.035	-0.617	1	
	Temperature	0.309	-0.036	0.772	-0.943	1
Intermediate	RBS Norm31	1				
	SPM Norm31	0.167	1			
	Precipitation	0.275	-0.141	1		
	Elevation	-0.488	-0.167	-0.595	1	
	Temperature	0.329	0.0517	0.752	-0.941	1
Wet	RBS Norm31	1				
	SPM Norm31	0.244	1			
	Precipitation	0.304	0.007	1		
	Elevation	-0.292	-0.006	-0.617	1	
	Temperature	0.394	-0.085	0.772	-0.943	1

SPM norm31 shows no significant positive or negative correlations for the wet season. Temperature and precipitation are strongly correlated ($r=0.772$). For the dry and wet seasons, precipitation and temperature are strongly correlated ($r=0.772$). Inverse correlations occur between precipitation and temperature ($r= -0.617$) and elevation and temperature ($r= -0.943$) (Table 4.4). Intermediate season precipitation and temperature are strongly correlated ($r=0.752$). Precipitation and elevation are inversely correlated ($r= -0.595$), and elevation and temperature are negatively correlated ($r= -0.941$) (Table 4.4).

4.3.4 Carbon Preference Index (CPI)

RBS Samples

n-Alkane analysis of RBS yielded predominantly odd numbered carbon chain lengths for each of the sampling seasons. RBS CPI values yielded a range between 2.0 and 11.6, averaging at 6.2 across the three seasons (Table 4.2). The dry season yielded the highest average CPI value (6.6) followed by the wet season (6.3) and intermediate season (5.8) (Figure 4.6 a-c). The Thina River yielded the highest CPI (8.5) during the dry season (Figure 4.6 a), whereas the river mouth showed the highest CPI (8.0) during the intermediate season (Figure 4.6 b), and the Mzimvubu River (8.8) during the wet season (Figure 4.6 c). The lowest CPI values occurred in the Mzintlava River during the dry (2.1) and intermediate seasons (3.8), and the river mouth yielded the lowest CPI value for the wet season (2.3).

SPM Samples

n-Alkane analysis of SPM samples yielded predominantly odd numbered carbon chain lengths for the three sampling campaigns (Table 4.2). SPM CPI values ranged from 0.1 to 12.3, averaging at 3.5 (Table 4.2). The highest CPI seasonal value is 4.4 for the intermediate season, followed by the dry season (3.5) and wet season (2.6) (Figure 4.6 a-c). The highest value for the dry season occurred in the Thina River (5.0), and the lowest value in the Mzintlava River (1.9). For the Intermediate season, the Thina River showed the highest CPI (7.3) and the Mzimvubu River yielded the lowest CPI (0.1). Wet season SPM samples were highest in the Mzimvubu River (5.2) and lowest at the river mouth (1.2).

CPI Correlation matrices

Dry season CPI RBS and CPI SPM samples are strongly positively correlated ($r= 0.900$) (Table 4.5). CPI SPM is moderately positively correlated to elevation ($r=0.412$). Dry season precipitation and temperature are strongly correlated ($r=0.772$) and elevation and MAT are inversely correlated ($r= -0.943$) (Table 4.5).

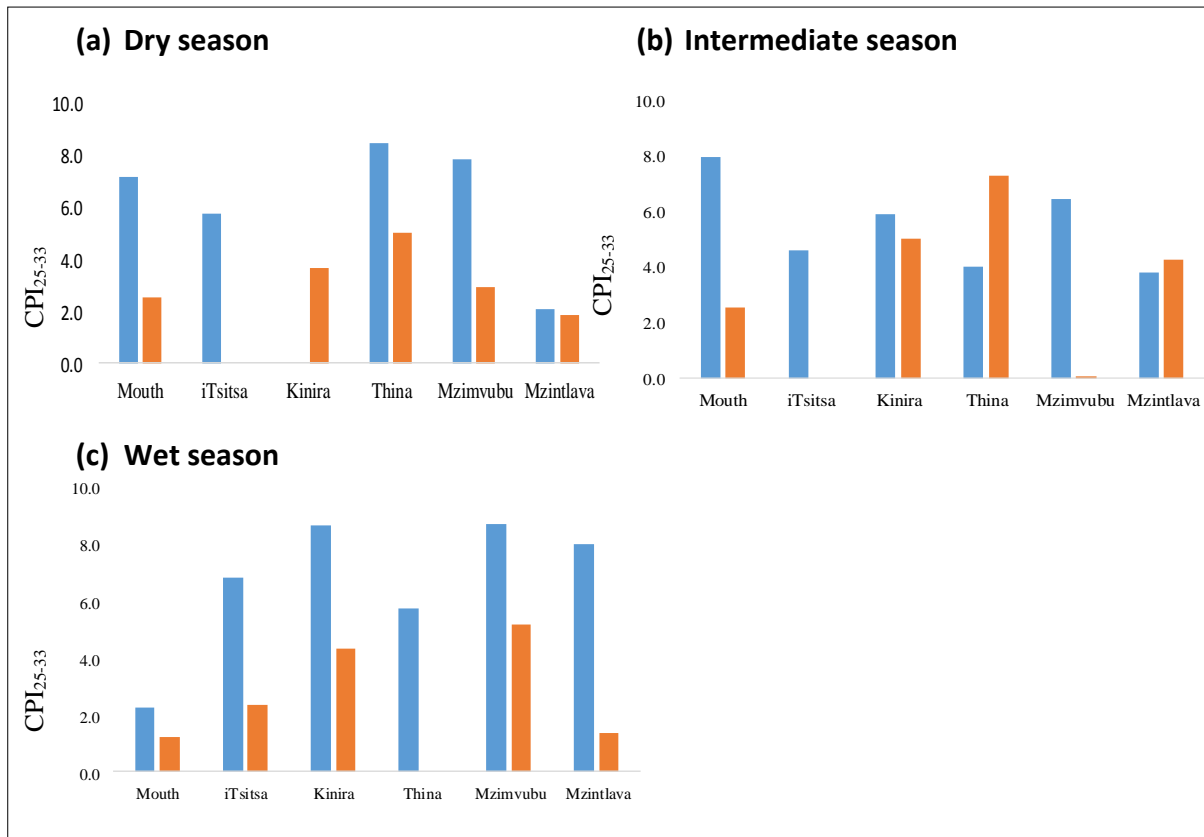


Figure 4.6: Histograms showing CPI_{25-33} for the RBS (blue) and SPM (orange) samples of each tributary, during the dry (a), intermediate (b) and wet (c) seasons.

Intermediate season CPI RBS is moderately correlated to temperature ($r= 0.339$) (Table 4.5). CPI SPM is moderately correlated to elevation ($r= 0.307$). Precipitation is strongly correlated to temperature ($r= -0.750$) and negatively correlated to elevation ($r= -0.595$). Elevation and temperature are inversely correlated ($r= -0.941$) (Table 4.5).

Wet season CPI RBS and SPM are weakly correlated ($r=0.382$) (Table 4.5). RBS and SPM samples are positively correlated to elevation ($r=0.512$ and $r=0.452$). RBS and SPM have a negative correlation to precipitation ($r= -0.492$ and $r= -0.373$), and temperature ($r= -0.619$ and $r= -0.455$). Precipitation and temperature have a negative correlation to elevation ($r= -0.617$) and ($r= -0.943$) respectively. Precipitation and temperature are positively correlated ($r=0.772$) (Table 4.5).

Table 4.5: Correlation matrix of CPI RBS and SPM samples for the dry, intermediate and wet seasons.

		CPI RBS	CPI SPM	Precipitation	Elevation	Temperature
Dry	CPI RBS	1				
	CPI SPM	0.900	1			
	Precipitation	0.181	-0.034	1		
	Elevation	-0.199	0.412	-0.617	1	
	Temperature	0.225	-0.209	0.772	-0.943	1
Intermediate	CPI RBS	1				
	CPI SPM	-0.196	1			
	Precipitation	0.263	0.0859	1		
	Elevation	-0.102	0.307	-0.595	1	
	Temperature	0.339	-0.254	0.750	-0.941	1
Wet	CPI RBS	1				
	CPI SPM	0.383	1			
	Precipitation	-0.492	-0.373	1		
	Elevation	0.512	0.452	-0.617	1	
	Temperature	-0.619	-0.455	0.772	-0.943	1

4.3.5 $\delta^{13}\text{C}_{29-31}$

RBS Samples

(i) $\delta^{13}\text{C}_{29}$

Compound specific $\delta^{13}\text{C}_{29}$ analysis of RBS samples yielded values from -28.0‰ to -32.8‰ across the three sampling seasons, and a total average of -30.4 (Table 4.2.). Wet season $\delta^{13}\text{C}_{29}$ values are the most depleted with an average of -30.6‰ , compared to the dry (-30.5‰) and intermediate (-30.1‰) seasons (Table 4.2). The Mzimvubu River showed the most enriched $\delta^{13}\text{C}_{29}$ signal for the dry (-28.2‰) and intermediate seasons (-28.0‰), and the Kinira River for the wet season (-28.6‰) (Table 4.2). The most depleted $\delta^{13}\text{C}_{29}$ signal originated from the iTsitsa River in the dry season (-32.0‰), the Mzimvubu River in the intermediate season (-32.1‰) and the Thina River in the wet season (-32.3‰) (Table 4.2).

(ii) $\delta^{13}\text{C}_{31}$

For the three sampling campaigns, $\delta^{13}\text{C}_{31}$ values of RBS samples yielded values between -27.0‰ to -31.7‰ , averaging at -29.4‰ (Table 4.2). The dry, intermediate and wet season seasons averages at -29.4‰ , -28.8‰ and -29.4‰ respectively (Table 4.2). The river mouth yielded an enriched $\delta^{13}\text{C}_{31}$ signal (-28.2‰) compared to the middle (-29.9‰) and upper

catchment (−31.2‰). The Mzimvubu River yielded the most enriched $\delta^{13}\text{C}_{31}$ signal for the dry season (−28.2‰), the Kinira River and Mzimvubu for intermediate season (−27.5‰), and the Kinira River for the wet season (−27.0‰). The most depleted $\delta^{13}\text{C}_{31}$ signals originated from the Mzimvubu River for the dry (−31.7‰) and intermediate season (−29.6‰) and the river mouth during the wet season (−31.4‰) (Table 4.3).

(iii) $\delta^{13}\text{C}_{29-31}$

$\delta^{13}\text{C}_{29}$ and $\delta^{13}\text{C}_{31}$ isotope values showed similar patterns across each sampling season, thus a combined weighted average ($\delta^{13}\text{C}_{29-31}$) was used for further analysis (Table 4.2). $\delta^{13}\text{C}_{29-31}$ analysis of RBS samples yielded values from −27.8‰ to −32.1‰ with a total average of −29.6‰ (Table 4.2). The intermediate season shows a slightly more enriched signal (−29.4‰) compared to the dry (−30.0‰) and wet (−30.0‰) seasons (Figure 4.7 a-c). $\delta^{13}\text{C}_{29-31}$ yielded enriched signals from the Mzintlava River (−28.6‰), Mzimvubu River (−27.5‰) for the dry, intermediate and wet seasons (Figure 4.7 a-c). Depleted $\delta^{13}\text{C}_{29-31}$ signals are traced to the iTsitsa River(−31‰), Kinira River (−29.8‰) and Thina River (−31.2‰) rivers during the dry, intermediate and wet seasons.

SPM Samples

(i) $\delta^{13}\text{C}_{29}$

Compound specific $\delta^{13}\text{C}_{29}$ analysis of SPM samples for the three sampling seasons yielded values from −28.0‰ to −31.6‰ with an average of −29.7‰ (Table 4.3). The intermediate and wet seasons show an average of −29.6‰ and the dry season yielded an average of −29.8‰ (Table 4.3). The river mouth (−29.0‰) yielded the most enriched SPM $\delta^{13}\text{C}_{29}$ signal for the three seasons compared to the middle catchment zone (−29.5‰) and the upper catchment (−30.0‰) (Table 4.3). The most enriched signals were present in the Kinira River (−29.1‰) during the dry season, the mouth (−28.4‰) during the intermediate season and the iTsitsa River(−29.0‰) during the wet season. The most depleted values occurred within Mzimvubu River (−30.3 ‰) for the dry season, the iTsitsa River(−31.2‰) for the intermediate season and the Mzintlava River (−29.9‰) during the wet season (Table 4.3).

(ii) $\delta^{13}\text{C}_{31}$

$\delta^{13}\text{C}_{31}$ analysis of SPM samples yielded values from −26.5 ‰ to −30.9‰ with an average of −28.5‰ (Table 4.3). The dry season is characterised by the most depleted average $\delta^{13}\text{C}_{31}$ signal (−29.8‰) compared to the intermediate (−28.6‰) and wet seasons (−28.7‰) (Table 4.3). $\delta^{13}\text{C}_{31}$ enrichment occurs in the upper tributary (−27.8‰) and depletion towards the middle of

the catchment (−28.8‰) and river mouth (−29.2 ‰) (Table 4.3). The iTsitsa River yielded the most enriched $\delta^{13}\text{C}_{31}$ signal during the dry season (−28.0‰) and intermediate (−27.6‰) seasons, however this signal moved to the Mzimvubu River during the wet season (−28.2‰) (Table 4.3). Depleted values occur at the river mouth for the dry season (−29.1‰), the iTsitsa River during the intermediate season (−29.2‰) and the Mzintlava River (−29.1‰) for the wet season (Table 4.3).

(iii) $\delta^{13}\text{C}_{29-31}$

$\delta^{13}\text{C}_{29}$ and $\delta^{13}\text{C}_{31}$ of SPM samples show similar trends of enrichment and depletion within the catchment, thus a weighted average $\delta^{13}\text{C}_{29-31}$ was used for further analysis. $\delta^{13}\text{C}_{29-31}$ of SPM samples show an average of −29.0‰ and range from −27.7‰ to −30.2‰ (Table 4.3). The dry season yields the most depleted signal (−28.9‰) compared to the intermediate (−29.1‰) and wet season (−29.2‰) (Figure 4.7 a-c). Overall, the iTsitsa River (−28.5 ‰), Mzintlava River (−28.8‰) and the Mzimvubu River (−28.8‰) are characterised by $\delta^{13}\text{C}$ enrichment for the dry, intermediate and wet seasons respectively (Figure 4.7 a-c). Depleted $\delta^{13}\text{C}_{29-31}$ signals occur in the Mzimvubu River (−29.3‰), iTsitsa River (−30.2‰) and the Mzintlava River (−29.5‰) for the dry, intermediate and wet seasons respectively (Figure 4.6 a-c).

$\delta^{13}\text{C}_{29-31}$ Correlation Matrices

For the dry season, RBS is correlated to precipitation ($r=0.5543$), and temperature ($r=0.3048$) (Table 4.6). SPM is positively correlated to elevation ($r=0.4431$), and is negatively correlated to temperature ($r= -0.3054$) (Table 4.6).

$\delta^{13}\text{C}_{29-31}$ Correlation matrices and environmental variables

Wet season RBS and SPM samples are negatively correlated to each other ($r= -0.8400$) (Table 4.6). SPM is correlated to precipitation ($r=0.4017$). For the dry, intermediate and wet seasons, precipitation and temperature are strongly correlated ($r=0.7718$; $r=0.7524$; and $r=0.7718$ respectively). (Table 4.6).

4.3.6 δD_{29-31}

δD_{29}

δD_{29} analysis of SPM could not be measured. Compound specific δD_{29} analysis of RBS samples yielded values from −113‰ to −166‰ and −128‰, with a total average of −133‰ (Table 4.2). δD_{29} enrichment occurs in the intermediate (−132 ‰) and dry season (−133‰), and depletion occurs towards the wet season (−136‰). The middle catchment (−122‰) yielded a more enriched δD_{29} signal compared to the river mouth (−137‰) and upper

catchment (-143‰). The iTsitsa River yielded the most enriched δD_{29} signal during the dry (-123‰), intermediate (-126‰) and wet (-127‰) seasons.

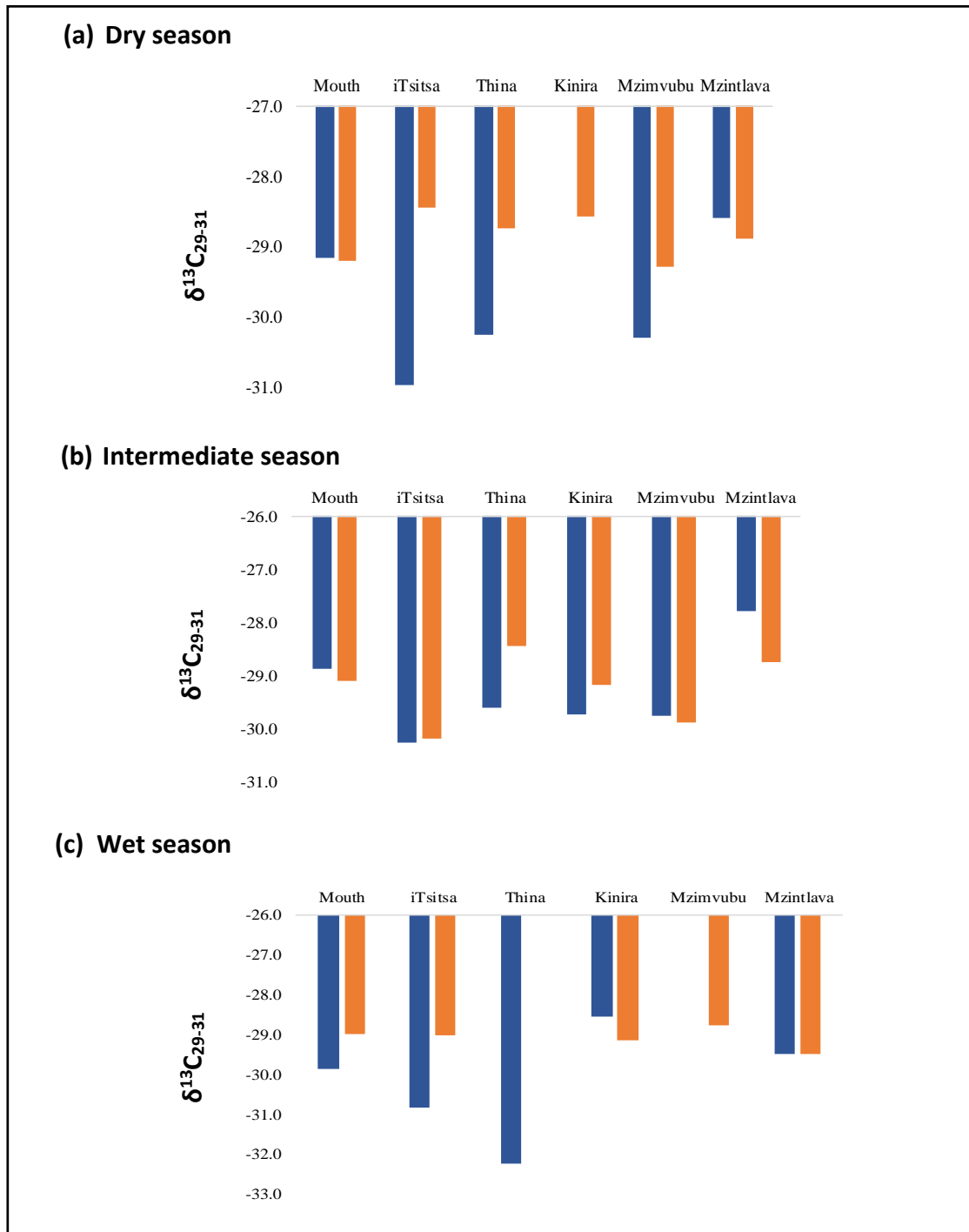


Figure 4.7: Histograms showing $\delta^{13}C_{29-31}$ for RBS and SPM samples for each site, during the dry (a), intermediate (b) and wet (c) seasons.

Table 4.6: Correlation matrices of $\delta^{13}\text{C}$ values for RBS and SPM material for the dry, intermediate and wet seasons.

		RBS $\delta^{13}\text{C}_{29-31}$	SPM $\delta^{13}\text{C}_{29-31}$	Precipitation	Elevation	Temperature
		31	31			
Dry	RBS $\delta^{13}\text{C}_{29-31}$	1				
	SPM $\delta^{13}\text{C}_{29-31}$		1			
	Precipitation	0.2879	0.2505	1		
	Elevation	-0.1646	0.4431	-0.6169	1	
	Temperature	0.3048	-0.3054	0.7718	-0.9428	1
Intermediate	RBS $\delta^{13}\text{C}_{29-31}$	1				
	SPM $\delta^{13}\text{C}_{29-31}$		1			
	Precipitation	-0.3433	-0.0047	1		
	Elevation	0.4908	0.0723	-0.5952	1	
	Temperature	-0.2298	-0.0541	0.7524	-0.9415	1
Wet	RBS $\delta^{13}\text{C}_{29-31}$	1				
	SPM $\delta^{13}\text{C}_{29-31}$		1			
	Precipitation	-0.8400	0.4017	1		
	Elevation	-0.2805	0.1130	-0.6169	1	
	Temperature	0.1744	0.0144	0.7718	-0.9428	1

The most depleted δD_{29} signals originate from the Mzimvubu River during the dry (-155‰) and intermediate (-142‰) seasons and the river mouth (-147‰) during the wet season (Table 4.2).

δD_{31}

δD_{31} analysis of SPM samples could not be measured. Compound specific δD_{31} analysis of RBS samples yielded values from -128‰ to -161‰ with a total average of -145‰ (Table 4.2). Dry, intermediate and wet season averages are -142‰ , -145‰ , and -149‰ respectively (Table 4.2). The most enriched δD_{31} signals originate from the iTsitsa River for the dry (-136‰), intermediate (-140‰) and wet (-143‰) seasons (Figure 4.8 a-c). The most depleted δD_{31} values occur in the Mzimvubu River (-151‰) for dry season, the Mzintlava River (-150‰) for the intermediate season, and the Thina River (-153‰) for the wet season (Table 4.3).

δD_{29-31}

δD_{29} and δD_{31} values show similar enrichment and depletion patterns throughout the catchment, and thus were weighted into mean δD_{29-31} average. Compound specific δD_{29-31} of RBS yielded values between -120‰ and -139‰ , averaging at -142‰ (Table 4.2).

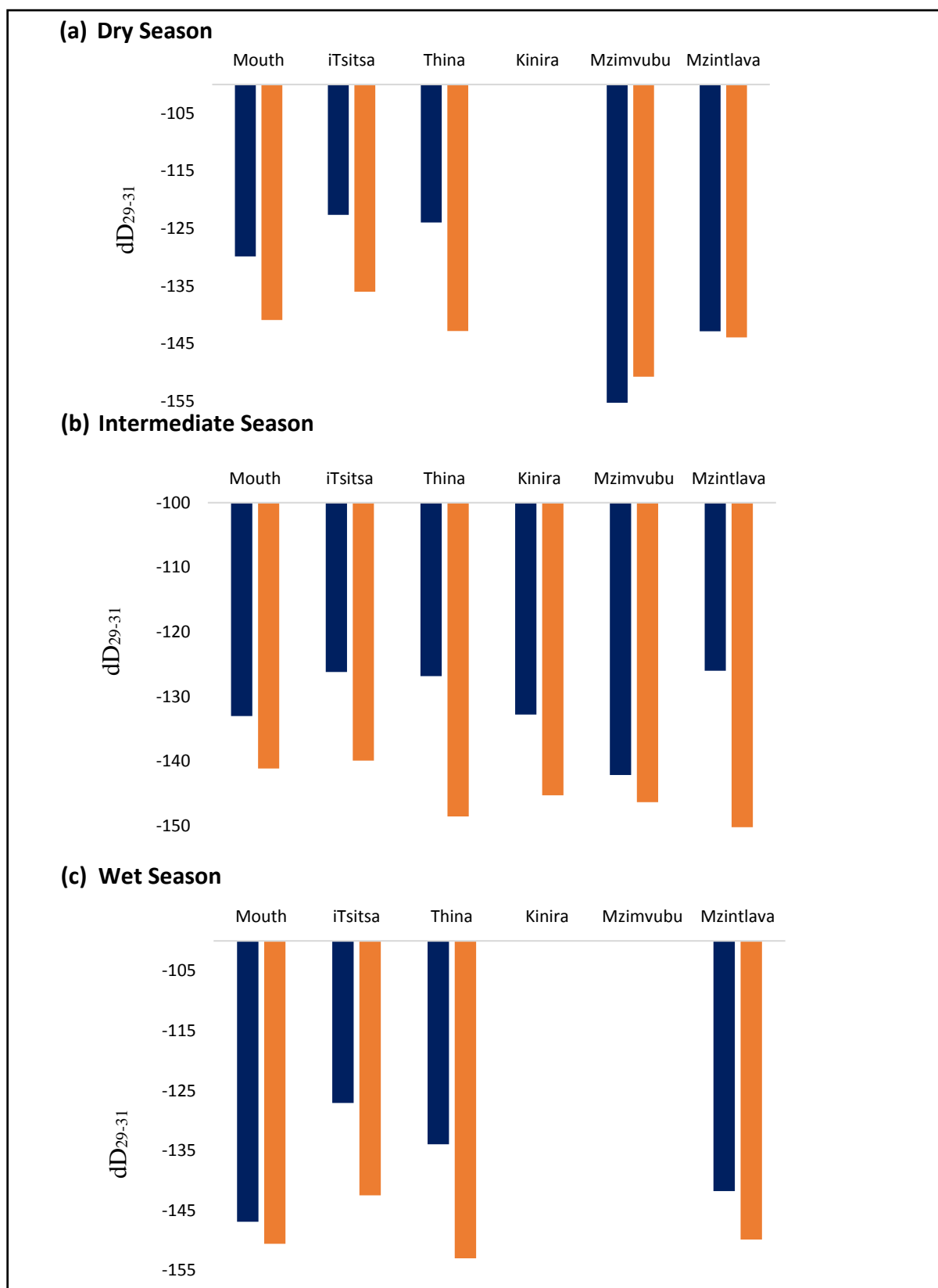


Figure 4.8: Histograms showing dD_{29} and dD_{31} for RBS (blue) and SPM (orange) for dD_{29-31} , for the dry season (a), intermediate (b) and wet (c) seasons.

An enriched δD_{29-31} signal originates from the iTsitsa River for the dry (-129‰), intermediate (-133‰) and wet (-135‰) seasons (Figure 4.8 a-c). A depleted δD_{29-31} signal originates from the Mzimvubu River during the dry (-153‰) and intermediate (-144‰) seasons and at the river mouth (-149‰) for the wet season (Figure 4.8 a-c).

δD Correlation Matrices

RBS δD_{29-31} is positively correlated to temperature ($r=0.3416$) for the dry season and negatively correlated with elevation ($r= -0.4595$) (Table 4.7). For the wet season δD_{29-31} is inversely correlated to elevation ($r= -0.5058$) (Table 4.7). For the dry, intermediate and wet season precipitation is inversely correlated to elevation ($r= -0.6160$; $r= -0.6169$; $r= -0.5952$ respectively), and positively correlated to temperature ($r=0.7718$, $r=0.7718$ and $r=0.7524$ respectively) (Table 4.7). Elevation and temperature are strongly inversely correlated for the dry ($r= -0.9428$), intermediate ($r= -0.9428$) and wet ($r= -0.9415$) season (Table 4.7).

Table 4.7: Correlation matrices of δD_{29} , δD_{31} and δD_{29-31} to MAP, elevation and MAT of RBS samples for the dry, intermediate and wet seasons.

		δD_{29-31}	Precipitation	Elevation	Temperature
Dry	δD_{29-31}	1			
	Precipitation	0.2199	1		
	Elevation	-0.4595	-0.6169	1	
	Temperature	0.3416	0.7718	-0.9428	1
Intermediate	δD_{29-31}	1			
	Precipitation	-0.0915	1		
	Elevation	-0.1439	-0.6169	1	
	Temperature	0.02835	0.7718	-0.9428	1
Wet	δD_{29-31}	1			
	Precipitation	0.1444	1		
	Elevation	-0.5058	-0.5952	1	
	Temperature	0.3173	0.7524	-0.9415	1

4.4 INORGANIC GEOCHEMISTRY

4.4.1 XRF element composition

XRF analyses identified several common elements of the RBS samples such as: Si (an average of 216.45 mg/kg); Al (36.77 mg/kg), Fe (17.21 mg/kg), K (7.21 mg/kg), Ca (4.82 mg/kg), Mg (4.16 mg/kg) and Ti (2.73 mg/kg) (Figure 4.9 a-g). The lower tributaries contain on average

higher abundances of common elements compared to the upper tributaries. The river mouth contains the highest Al (44.39 mg/kg) and K (8.95 mg/kg) concentrations (Figure 4.9 a-g). The iTsitsa River contains the highest Si concentration (250.33 mg/kg) (Figure 4.9, b). Fe (30.59 mg/kg); Ti (3.69 mg/kg), Ca (6.02 mg/kg) and Mg (6.61 mg/kg) are most abundant in the Mzintlava River (Figure 4.9, f). High Al, K and Ca concentrations occur in the Thina River and Mzintlava River rivers (Figure 4.9, c and f). Elevated Fe, Mg and Ti concentrations occur in the Mzimvubu River and Mzintlava River rivers and elevated Si concentrations occur in the iTsitsa River and Kinira River (Figure 4.9 a-g).

4.4.3 Element ratios

Fe/K RBS

RBS Fe/K values range from 1.31 to 4.03 with an average of 2.36 for all three sampling seasons (Table 4.8). The intermediate season (2.21) yielded the lowest Fe/K ratio compared to the dry (2.34) and wet season (2.51) (Table 4.8). The river mouth yielded an average of 2.14 for the dry season, which is similar to the Kinira River (2.28) (Figure 4.10 a). The lowest Fe/K ratio originates from the Thina River (1.86), and the highest ratio from the Mzintlava River (3.50). Fe/K for the river mouth during the intermediate season is 1.96, which is similar to the Thina River (1.53) and is the lowest ratio for this season (Figure 4.10 b). The Mzintlava River (3.77) yielded the highest Fe/K ratio (Figure 4.10 b). The Fe/K value for the river mouth during the wet season is 1.86, which is similar to the iTsitsa River (1.86) and Thina River (1.84) rivers (Figure 4.10 c). The Mzintlava River (3.49) and Kinira River (3.52) have the highest Fe/K ratios for the wet season (Figure 4.10 c). Fe/K SPM

Fe/K ratios for the SPM samples yielded values from 0.37 to 1.13 and average of 0.66 (Table 4.8). For the dry season, the river mouth (0.60) and Kinira River (0.64) share similar Fe/K ratios (Figure 4.11 a). The iTsitsa River (0.52) and Thina River (0.52) yielded the lowest Fe/K ratios, compared to the Mzimvubu River (0.72) and Mzintlava River (0.98) which yielded the highest values (Figure 4.10 a). The intermediate season Fe/K average at the river mouth is 0.55, which is similar to the Thina River (0.43) river and the lowest Fe/K ratio for this season (Figure 4.10 b). The Mzintlava River (1.06) produced the highest Fe/K ratio for the intermediate season (Figure 4.10 b). The wet season river mouth ratio is 0.62, which is similar to the iTsitsa (0.52) and Thina River (0.51) (Figure 4.10 c). The Mzintlava River (0.98) yielded the highest Fe/K ratios for the wet season (Figure 4.10 c).

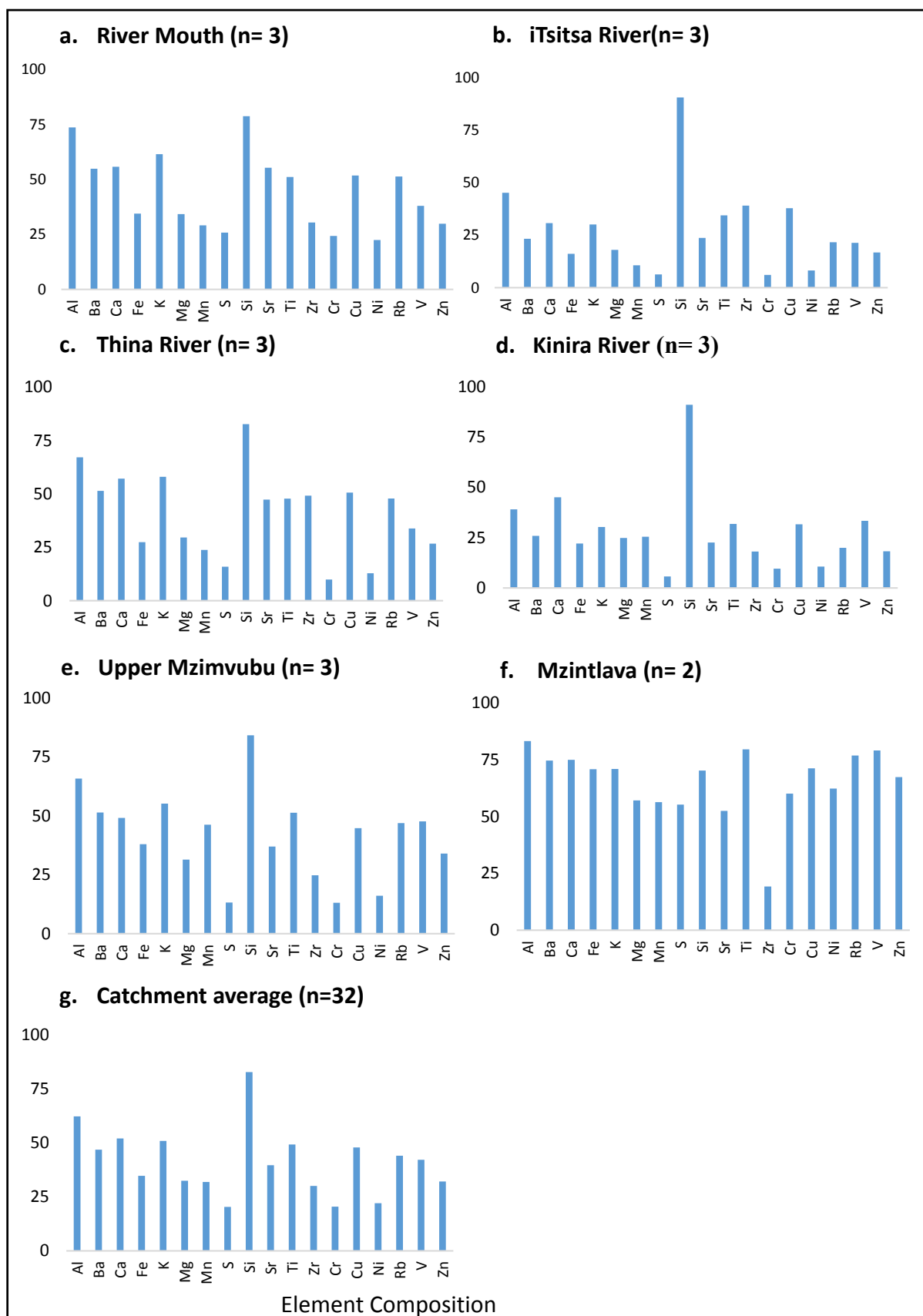


Figure 4.9: Histograms showing the element composition relative abundance for the River Mouth (a), iTsitsa River(b), Thina River (c), Kinira River (d), Mzimvubu (e), Mzintlava (f) and the total Catchment average (g).

Table 4.8: Table showing Fe/K, Al/Si and Ti/Al ratios of RBS and SPM samples for the dry, intermediate and wet seasons.

		Fe/K		Al/Si		Ti/Al	
Season	Site	RBS	SPM	RBS	SPM	RBS	SPM
Dry	MZ 1	2.01	0.56	0.26	1.17	0.05	0.54
	MZ 2	2.27	0.64	0.25	1.13	0.07	0.74
	MZ 3	1.77	0.50	0.16	0.70	0.06	0.57
	MZ 4	1.95	0.54	0.24	1.05	0.06	0.62
	MZ 5	2.69	0.75	0.12	0.52	0.13	1.35
	MZ 6	3.69	1.03	0.32	1.43	0.32	0.80
	MZ 7	1.98	0.55	0.07	0.33	0.07	0.70
	MZ 8	1.77	0.49	0.14	0.73	0.14	0.67
	MZ 9	1.87	0.52	0.08	0.34	0.08	0.64
	MZ 10	2.44	0.68	2.44	1.10	0.25	0.69
	MZ 11	3.32	0.93	0.25	1.11	0.25	0.95
Intermediate	MZ 1	1.94	0.54	0.21	0.95	0.05	0.97
	MZ 2	1.98	0.56	0.22	0.97	0.08	0.87
	MZ 3	1.78	0.50	0.19	0.84	0.05	0.53
	MZ 4	1.31	0.37	0.27	1.20	0.05	0.47
	MZ 5	2.08	0.58	0.14	0.61	0.05	0.55
	MZ 6	3.77	1.06	0.31	1.40	0.07	0.74
	MZ 7	2.70	0.75	0.06	0.28	0.13	1.34
	MZ 8	1.76	0.49	0.16	0.73	0.07	0.76
	MZ 9	2.49	0.70	0.08	0.36	0.05	0.55
	MZ 10	2.33	0.65	0.26	1.15	0.06	0.61
	MZ 11	-	-	-	-	-	-
Wet	MZ 1	1.92	0.54	0.17	0.74	0.05	0.54
	MZ 2	1.80	0.50	0.17	0.66	0.09	0.97
	MZ 3	2.02	0.57	0.11	0.47	0.12	1.25
	MZ 4	1.86	0.52	0.14	0.64	0.11	1.10
	MZ 5	3.01	0.84	0.09	0.39	0.12	1.25
	MZ 6	3.64	1.02	0.30	1.35	0.12	0.64
	MZ 7	1.69	0.47	0.10	0.45	0.10	0.56
	MZ 8	1.82	0.51	0.15	0.66	0.07	0.76
	MZ 9	4.03	1.13	0.08	0.37	0.05	0.47
	MZ 10	2.50	0.70	0.23	1.02	0.07	0.69
	MZ 11	3.35	0.94	0.19	0.85	0.17	1.71

Fe/K correlation matrices

Dry season Fe/K RBS and SPM ratios show no significant positive or negative correlations for the dry season (Figure 4.11 and Table 4.9). Intermediate season Fe/K RBS and SPM are perfectly correlated to one another ($r=1$) (Figure 4.11 and Table 4.9). Wet Season Fe/K RBS and SPM samples are perfectly correlated ($r=1$) and moderately correlated to elevation ($r=0.308$) and ($r=0.308$) respectively (Figure 4.11 and Table 4.9, wet season).

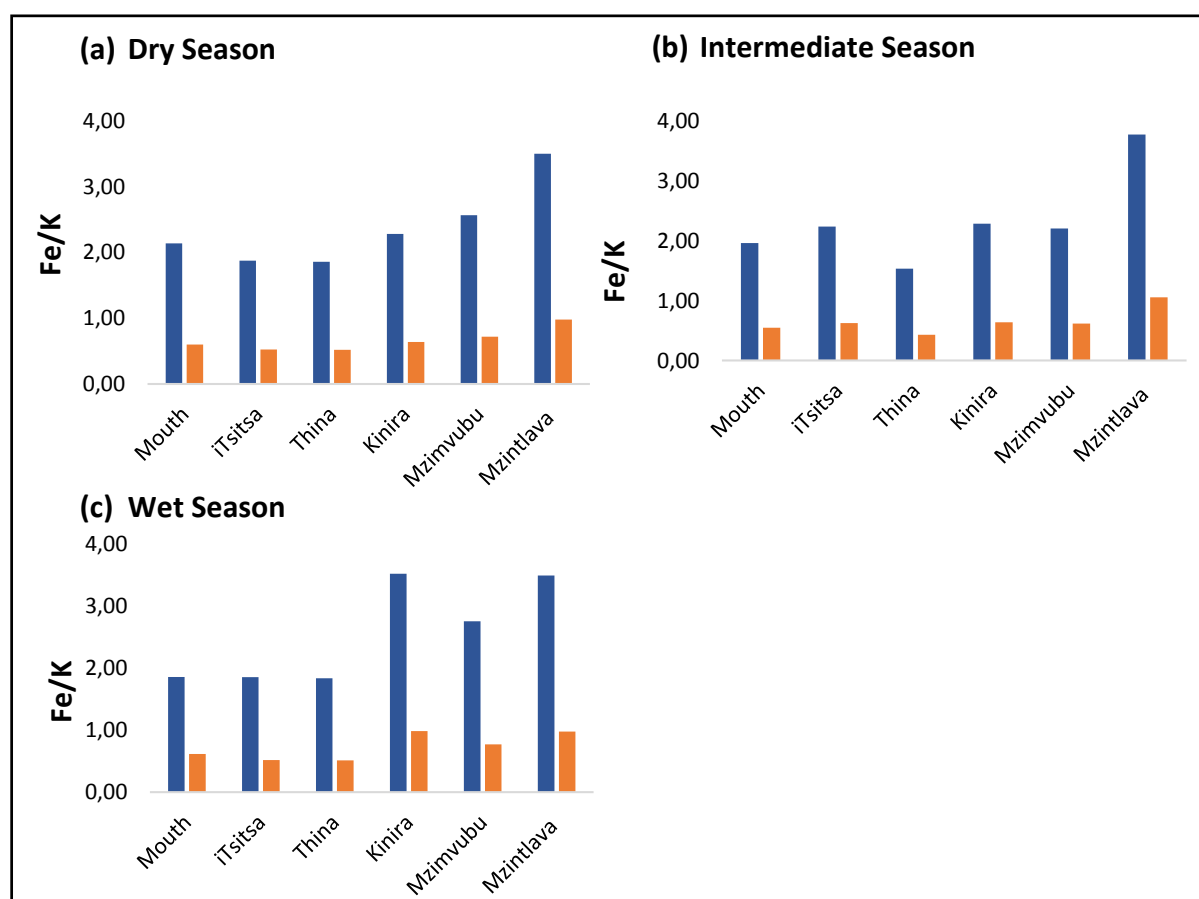


Figure 4.10: Histograms showing Fe/K ratio for RBS (blue) and SPM (orange) samples for the (a) dry, (b) intermediate and (c) wet seasons.

RBS and SPM Fe/K are inversely correlated to precipitation ($r= -0.314$) and ($r= -0.314$) respectively and temperature ($r= -0.339$) and ($r=0.339$) respectively (Figure 4.11, and Table 4.9). Overall, for the dry and wet season, precipitation and temperature are strongly correlated ($r=0.772$). Precipitation and elevation are negatively correlated ($r= -0.617$), and elevation and temperature ($r= -0.943$) (Figure 4.11, and Table 4.9).

Table 4.9: Correlation matrices of RBS and SPM Fe/K ratios to precipitation, elevation and temperature for the dry, intermediate and wet seasons.

		RBS Fe/K	SPM Fe/K	Precipitation	Elevation	Temperature
Dry	RBS Fe/K	1				
	SPM Fe/K	1	1			
	Precipitation	-0.189	-0.189	1		
	Elevation	0.040	0.040	-0.617	1	
	Temperature	-0.177	-0.177	0.772	-0.943	1
Intermediate	RBS Fe/K	1				
	SPM Fe/K	1	1			
	Precipitation	0.077	0.077	1		
	Elevation	0.265	0.265	-0.595	1	
	Temperature	-0.229	-0.229	0.752	-0.941	1
Wet	RBS Fe/K	1				
	SPM Fe/K	1	1			
	Precipitation	-0.314	-0.314	1		
	Elevation	0.308	0.308	-0.617	1	
	Temperature	-0.339	-0.339	0.772	-0.943	1

Al/Si RBS

Al/Si ratios for RBS samples yielded values from 0.06 to 0.32 with an average of 0.18 for the three sampling campaigns (Table 4.8). The dry and intermediate seasons yielded an average of 0.19 and the wet season an average of 0.15 (Table 4.8). Al/Si for the river mouth during the dry season is 0.26, which is similar to the Mzintlava River (0.28), and is the highest Al/Si ratio for the dry season (Figure 4.11 a). The lowest ratio Al/Si ratio occurred in the Kinira River (0.10) (Figure 4.11 a). The intermediate season Al/Si ratio for the river mouth is 0.21 which is similar to the Thian (0.22) and Mzimvubu River (0.20) (Figure 4.11 b). The highest Al/Si ratio occurred in the Mzintlava River (0.31) and the lowest ratio value in the Kinira River (0.11) (Figure 4.11 b). Al/Si ratios for the River mouth (0.16) and Mzimvubu River (0.16) are the same during the wet season (Figure 4.11 c). The Kinira River (0.08) yielded the lowest ratio whereas the Mzintlava River (0.25) yielded the highest ratio for the wet season (Figure 4.12 c).

Al/Si SPM

Al/Si ratios of SPM material yielded values from 0.28 to 1.43, with an overall average of 0.80 across the three sampling campaigns (Table 4.8). Dry season Al/Si values for the river mouth yields a ratio of 1.15 (Figure 4.11 a). The Kinira River (0.43) yielded the lowest ratio, whereas

the Thina River (0.85) yielded the moderately high ratio for the dry season (Figure 4.11 a). The river mouth (0.96) and Thina River (0.96) yielded the same Al/Si ratio values for the intermediate season (Figure 4.11 b). The lowest Al/Si ratio occurred in the iTsitsa River (0.56), and the highest ratios in the Mzintlava River (1.40) (Figure 4.11 b). Al/Si for the river mouth during the wet season is 0.79 (Figure 4.11 c). The Mzimvubu River (0.71) shares as similar Al/Si ratio to the mouth (Figure 4.11 c). The Kinira River (0.38) yielded the lowest Al/Si ratio, and the Mzintlava River (1.10) yielded the highest ratio for the wet season.

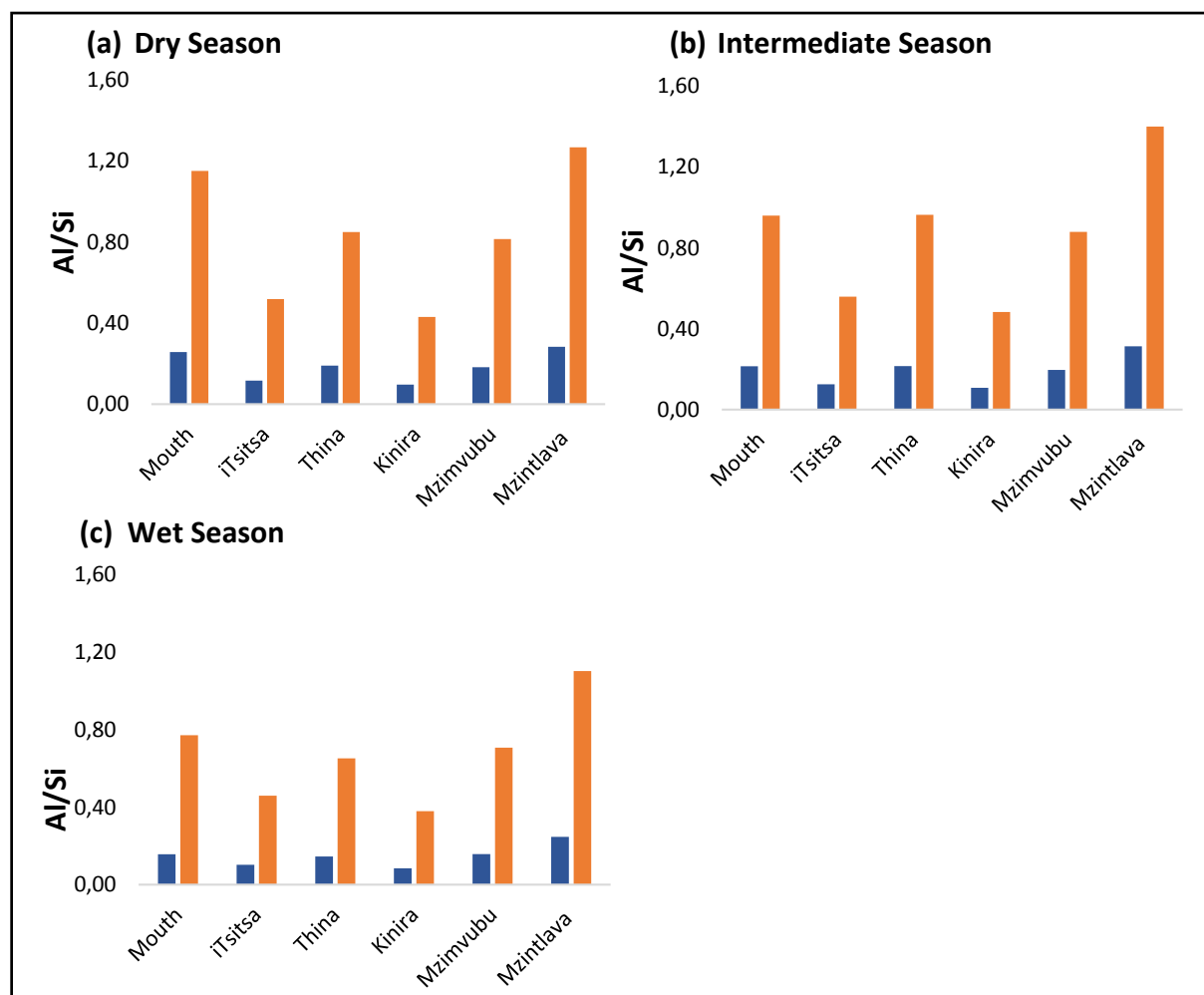


Figure 4.11: Histograms showing the Al/Si ratios for RBS (blue) and SPM (orange) samples for the dry (a), intermediate (b) and wet (c) seasons.

Al/Si correlation matrices

Dry season Al/Si RBS and SPM ratios are perfectly correlated ($r=1$). RBS and SPM Al/Si are inversely related to elevation ($r= -0.479$) and ($r= -0.479$) respectively. Intermediate season

RBS and SPM Al/Si values are perfectly correlated ($r=1$), and are inversely correlated to elevation ($r=0.392$) and ($r= -0.392$) respectively (Table 4.10). RBS and SPM Al/Si samples are perfectly correlated during the wet season ($r=1$). For the dry, intermediate and wet seasons, precipitation and temperature are strongly correlated ($r=0.772$). Elevation is negatively correlated to precipitation ($r= -0.617$), and elevation is negatively correlated to temperature ($r= -0.943$) (Table 4.10).

Table 4.10: Correlation matrices for RBS and SPM Al/Si ratios to precipitation, elevation, elevation for the dry, intermediate and wet seasons.

		RBS Al/Si	SPM Al/Si	Precipitation	Elevation	Temperature
Dry	RBS Al/Si	1				
	SPM Al/Si	1	1			
	Precipitation	0.130	0.130	1		
	Elevation	-0.479	-0.479	-0.617	1	
	Temperature	0.359	0.359	0.772	-0.943	1
Intermediate	RBS Al/Si	1				
	SPM Al/Si	1	1			
	Precipitation	-0.074	-0.074	1		
	Elevation	-0.392	-0.392	-0.617	1	
	Temperature	0.214	0.214	0.772	-0.943	1
Wet	RBS Al/Si	1				
	SPM Al/Si	1	1			
	Precipitation	-0.025	-0.0245	1		
	Elevation	-0.030	-0.030	-0.617	1	
	Temperature	-0.050	-0.050	0.772	-0.943	1

Ti/Al RBS

Ti/Al ratios of RBS samples yielded values from 0.05 to 0.17, with an average of 0.08 for the three seasons (Table 4.8). The dry and intermediate seasons yielded an average ratio of 0.07 and the wet season yielded a ratio of 0.09 (Table 4.8). Dry season Ti/Al ratio for the river mouth is 0.06, which is similar to the iTsitsa River(0.06) (Figure 4.12 a). The river mouth and iTsitsa River yielded the lowest Ti/Al values, and the Mzimvubu River (0.10) yielded the highest Ti/Al ratio (Figure 4.12 a). The river mouth (0.07) and Mzintlava River (0.07) share the same Ti/Al ratios for the intermediate season (Figure 4.12 b). The iTsitsa River(0.09) yielded the highest Ti/Al ratio, whereas the Kinria (0.05) yielded the lowest ratio for the intermediate season (Figure 4.12 b). Wet season Ti/Al for the river mouth is 0.07 (Figure 4.12 c). The

Mzintlava River (0.11) produced the highest Ti/Al, and the Kinira River (0.08) and river mouth produced the lowest Ti/Al values (Figure 4.12 c).

Ti/Al SPM

Ti/Al ratios of SPM samples yielded values from 0.47 to 1.71 with an average of 0.79 (Table 4.8). Ti/Al averages varied between the dry (0.77), intermediate (0.69) and the wet season (0.90) (Table 4.8). Dry season Ti/Al at the river mouth is 0.64, which is similar to the iTsitsa (0.63) (Figure 4.12 a). The Mzimvubu River (1.02) yielded the highest Ti/Al value. Low Ti/Al values occurred in the iTsitsa River(0.63) and river mouth (Figure 4.12 a). The average Ti/AL value for the river mouth during the intermediate season is 0.72, which is similar to the Mzintlava River (0.74) (Figure 4.12 b). The lowest Ti/AL ratios occurred in the Kinira River (0.55), and the highest ratio was recorded in the iTsitsa (0.93) (Figure 4.12 b). The wet season river mouth Ti/Al ratio is 0.80 which is similar to the Kinira River river (0.86) (Figure 4.12 c). The highest ratio occurred in the Mzintlava River (1.17), and the lowest values occurred in the Kinira River (0.55).

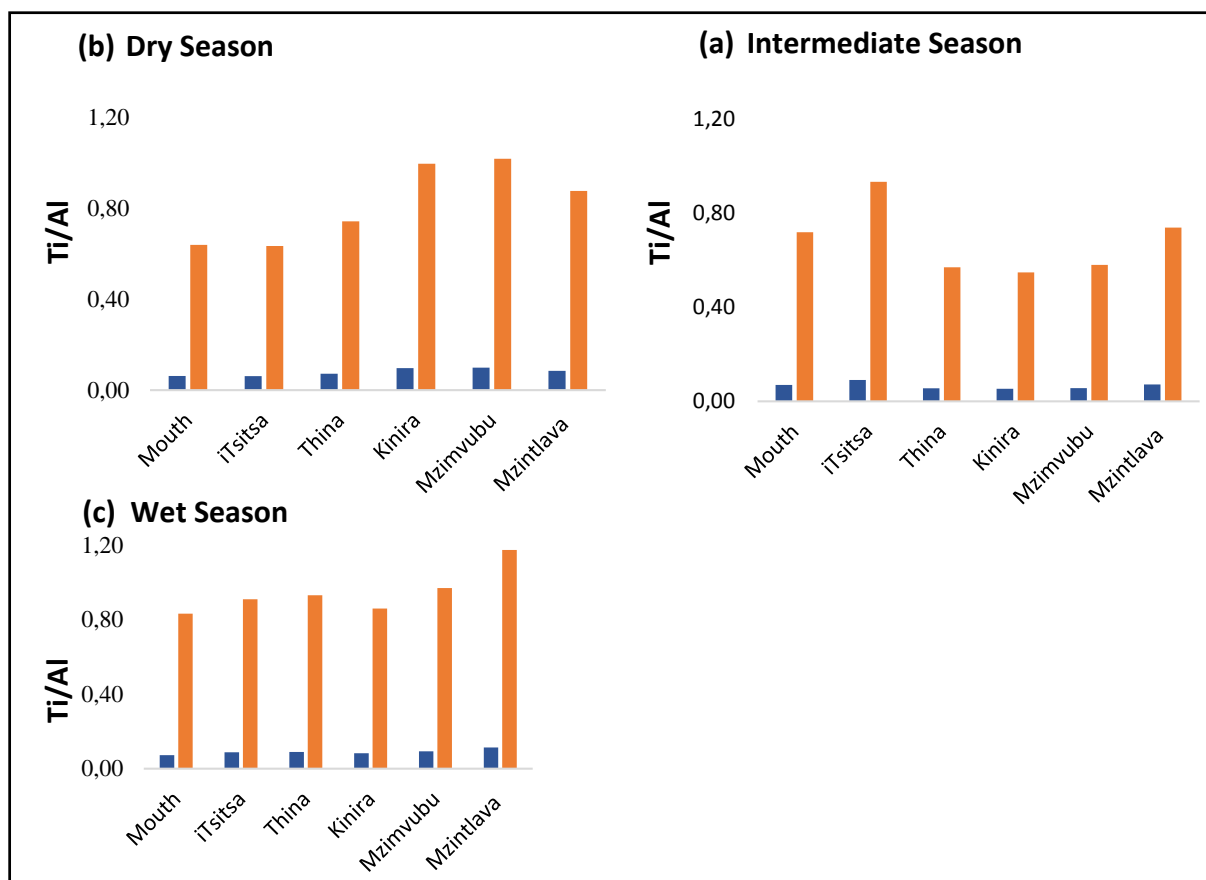


Figure 4.12: Histograms showing Ti/AL ratios of RBS (blue) and SPM (orange) samples for the dry (a), intermediate (b) and wet (c) seasons.

Ti/Al Correlation matrices

Ti/Al RBS and SPM are perfectly correlated during the dry season ($r=1$) (Table 4.11). Intermediate season Ti/Al RBS and SPM are perfectly correlated ($r=1$), and moderately correlated to precipitation ($r=0.309$; $r=0.309$ respectively)(Table 4.11). RBS and SPM Ti/Al show a very weak inverse correlation to temperature. Wet season RBS and SPM Ti/Al are perfectly correlated ($r=1$) (Table 4.11). Both RBS and SPM Ti/Al are inversely correlated to precipitation ($r=0.530$; $r=0.530$ respectively) (Table 4.11). For the dry and wet season, precipitation and temperature are strongly correlated ($r=0.772$). Precipitation and elevation are negatively correlated ($r=0.617$) as well as elevation and temperature ($r= -0.943$) (Table 4.11, dry and wet season).

Table 4.11: Correlation matrices for RBS and SPM Ti/Al samples to precipitation, elevation and temperature for the dry, intermediate and wet season.

		Ti/Al RBS	SPM Ti/Al	Precipitation	Elevation	Temperature
Dry	RBS Ti/Al	1				
	SPM Ti/Al	1	1			
	Precipitation	-0.286	-0.286	1		
	Elevation	0.172	0.172	-0.617	1	
	Temperature	-0.284	-0.284	0.772	-0.943	1
Intermediate	RBS Ti/Al	1				
	SPM Ti/Al	1	1			
	Precipitation	0.309	0.309	1		
	Elevation	0.246	0.246	-0.595	1	
	Temperature	-0.077	-0.077	0.752	-0.941	1
Wet	RBS Ti/Al	1				
	SPM Ti/Al	1	1			
	Precipitation	-0.530	-0.530	1		
	Elevation	-0.0627	-0.0627	-0.617	1	
	Temperature	-0.155	-0.155	0.772	-0.943	1

4.5 ALL PROXY CORRELATION

For the dry season, Fe/K is positively correlated to Al/Si ($r=0.565$) and Ti/Al ($r=0.472$). Fe/K is negatively correlated to CPI ($r= -0.603$) (Table 4.12). Al/Si is negatively correlated to δD_{29-31} ($r= -0.604$), whereas Ti/Al is positively correlated to δD_{29-31} ($r=0.436$) and $\delta^{13}C_{29-31}$ ($r=0.535$) (Table 4.12). Norm31 yielded no significant correlations to other proxies except for showing a marginal negative correlation to $\delta^{13}C_{29-31}$ ($r= -0.300$) (Table 4.12). δD_{29-31} is negatively

correlated to CPI ($r = -0.410$). Similarly, $\delta^{13}\text{C}_{29-31}$ has a negative correlation to CPI ($r = -0.602$) (Table 4.12).

The intermediate season shows that Fe/K has a positive correlations to Al/Si ($r=0.483$), Ti/Al ($r=0.680$) and norm31 ($r=0.689$) (Table 5.12). Al/Si and Ti/Al are also positively correlated to norm31 ($r=0.524$, $r=0.563$ respectively) (Table 4.12). Fe/K, Al/Si, Ti/Al and norm31 are negatively correlated to δD_{29-31} ($r = -0.743$, $r = -0.593$, $r = -0.657$, $r = -0.782$ respectively) and $\delta^{13}\text{C}_{29-31}$ ($r = -0.0.607$, $r = -0.420$, $r = -0.671$, $r = -0.616$ respectively) (Tale 4.12). δD_{29-31} retains a strong positive correlation to $\delta^{13}\text{C}_{29-31}$ ($r=0.755$) as with the dry season and negative correlation to CPI ($r = -0.566$). Similarly, $\delta^{13}\text{C}_{29-31}$ has a negative correlation to CPI ($r = -0.601$) as with the dry season (Table 4.12).

Table 4.12: Correlation matrices for all proxies and environmental variables for the dry, intermediate and wet season.

		Fe/K	AL/Si	Ti/Al	Norm31	δD_{29-31}	$\delta^{13}\text{C}_{29-31}$	CPI
Dry	Fe/K	1						
	AL/Si	0.565	1					
	Ti/Al	0.472	-0.175	1				
	Norm31	0.0689	-0.034	0.207	1			
	δD_{29-31}	-0.119	-0.604	0.436	-0.163	1		
	$\delta^{13}\text{C}_{29-31}$	0.397	-0.221	0.535	-0.300	0.353	1	
	CPI	-0.603	0.0989	-0.454	-0.165	-0.410	-0.602	1
Intermediate	Fe/K	1						
	AL/Si	0.483	1					
	Ti/Al	0.680	0.150	1				
	Norm31	0.689	0.524	0.563	1			
	δD_{29-31}	-0.743	-0.593	-0.657	-0.782	1		
	$\delta^{13}\text{C}_{29-31}$	-0.607	-0.420	-0.671	-0.616	0.755	1	
	CPI	0.364	0.256	0.220	0.134	-0.566	-0.601	1
Wet	Fe/K	1						
	AL/Si	0.231	1					
	Ti/Al	0.041	-0.088	1				
	Norm31	-0.123	-0.476	-0.089	1			
	δD_{29-31}	0.293	-0.206	-0.163	0.426	1		
	$\delta^{13}\text{C}_{29-31}$	-0.223	0.020	0.422	-0.121	0.416	1	
	CPI	0.594	-0.157	-0.048	0.170	0.201	-0.409	1

The wet season shows weak correlations between the Fe/K and Al/Si, Ti/Al and δD_{29-31} , however a positive correlation to CPI ($r=0.594$) (Table 4.12). Al/Si has a negative correlation to norm31 ($r= -0.476$), and Ti/Al shows a positive correlation to $\delta^{13}C_{29-31}$ ($r=0.422$). Norm31 and δD_{29-31} are positively correlated ($r=0.426$), as is δD_{29-31} with $\delta^{13}C_{29-31}$ ($r=0.416$) (Table 4.12). Consistent with the dry and intermediate seasons, $\delta^{13}C_{29-31}$ shows a negative correlation to CPI ($r= -0.409$) (Table 4.12).

4.6 CONCLUSION

The results presented and described in this chapter provided a short outline of the trends within pollen, stable carbon and deuterium isotopes, stable oxygen and hydrogen isotopes and XRF element data from Mzimvubu River. These results were described in terms of a modern provenance based approach in which the origin and transport pathways of each proxy were identified. Proxies were then correlated with environmental factors such as elevation, precipitation and temperature as well as to each other to establish relationships. These data identified significant environmental, physical and hydrological signals which can be applied to palaeoclimatic reconstruction investigations within the Mzimvubu Catchment, and to the broader Eastern Cape of South Africa.

CHAPTER FIVE

DISCUSSION

5.1 INTRODUCTION

A detailed assessment and comparison of the pollen results, stable $\delta^{13}\text{C}$ and $\text{d}\delta\text{D}$ isotope values, and XRF elemental results are presented in this chapter. These proxy data are evaluated in terms of their ability to accurately reflect surrounding vegetation and prevailing climate conditions within the Mzimvubu Catchment, with implications for proxy application and interpretation. Pollen data were used to develop a modern picture of the prevailing vegetation compositions and distributions within the catchment, as well as to verify *n*-alkane distribution data such as $\delta^{13}\text{C}_{29-31}$, $\text{d}\delta\text{D}_{29-31}$, CPI and norm31. $\delta^{13}\text{C}_{29-31}$ and norm31 signals are described in terms of the relative C_3 and C_4 plant type and broader vegetation groupings, and $\text{d}\delta\text{D}_{29-31}$ will be evaluated in terms of re-creating the hydrological processes and dynamics within the catchment. CPI and XRF element ratios are described in terms of the relative origins of organic matter within the catchment. The first section will describe the discharged proxy signal, detailing the nature and characteristics of the pollen, organic and inorganic signatures for the catchment. Secondly, a brief comparison between RBS and SPM samples and the similarities and discrepancies between the two sample types will be provided. This will be followed by a comparison of signals from RBS and SPM samples to see whether RBS samples could be taken as representative of the catchment, given that in many cases SPM yielded insufficient material for analysis. Thirdly, provenance dynamics of each major proxy within each tributary and the catchment as a whole will be discussed. Lastly, the results of this study will be compared to similar case studies. Throughout the chapter, the results of the research will be considered in terms of applications and implications for future palaeoclimate research in South Africa.

5.2 THE DISCHARGED PROXY SIGNAL

This section will provide a detailed interpretation of the specific pollen, organic lipid biomarker and inorganic XRF signals transported within each major tributary of the Mzimvubu Catchment. Similarities and differences in trends within and between proxy data will be discussed for pollen, *n*-alkane lipid biomarkers and XRF element compositions. Each proxy will be qualitatively assessed in relation to environmental parameters and the effect these conditions may have on the resultant signal transported by the five major tributaries.

5.2.1 Pollen

Seasonality of pollen data was not considered during interpretations as the influence of flowering seasons were too great. Therefore, a brief description of the most significant seasonal pollen findings is provided below, followed by a more detailed analysis of the pollen data and its relation to the surrounding vegetation and some environmental parameters.

Seasonality

Pollen signals for the dry, intermediate and wet seasons reflect transitions in flowering seasons for plant types in the surrounding catchment. Fluctuations in certain taxa are less affected by seasonality of pollen production and taphonomic processes, whereas others are significantly affected. Brewer *et al.*, (2013) found that pollen is not only a function of surrounding vegetation, but also pollen production which varies seasonally, making interpretations complex and nonlinear. Similarly, Brown *et al.*, (2007) established that there are strong seasonality effects on pollen percentages and taphonomic processes which can lead to issues of underrepresentation and overrepresentation of catchment vegetation. For the Mzimvubu River it was found that grasses, sedges, *Rhus*, *Tubuliflorae*, *Acacia*, *Podocarpus* and *Pinus* were ubiquitous throughout every season and sample site, with minimal seasonal variation. In contrast, strong seasonal effects were evident for *Sesbania*, *Combretum*, *Salix*, and *Zea mays*. Firstly, the presence of *Sesbania* pollen during the dry season could be due to some subspecies flowering throughout the year (Hoffmann and Moran, 1991) rather than being restricted to the the growing season. Secondly, *Combretum* flowers from August through to November which could explain its presence during the wet season (Jordaan *et al.*, 2011). *Combretum* also prefers low lying bushveld and thicket in dry and warm areas which are characteristic of the Mzintlava River River in the middle catchment during winter months. Thirdly, *Salix* pollen grains were recorded in the dry season at the river mouth exclusively, it is likely that RBS contained a signal stored and that a seasonal spike was picked up during counting and analysis. SPM samples would have been a beter representation compared to RBS, however, this was not possible due to SPM yielded consistently low concentrations compared to RBS. Lastly, *Zea mays* is present at the river mouth, confluence, Thina River and Mzintlava River during the wet season. This spike coincides with the planting of some maize crops as early as late September through to November in the former Transkei region soon after spring rainfall (DWS 2017). Some crops have been known to start flowering as soon as late November if planted in September which could explain the *Zea mays* palynomorph signal during the wet season only (Peterson, 2013). In addition, RBS samples could have preserved pollen signals over long time

periods, and the signal could have originated from a previous depositional event from previous flowering seasons.

Upper catchment

Pollen data in the upper Mzimvubu Catchment showed an environment characterised by grasses, sedges, fern spores, some herbs and shrubs and some trees (exotic and indigenous). The natural vegetation of the area is consists of treeless grassland and highland sourveld and southern tall grassland (Acocks, 1988; Madikizela and Dye, 2003). Compared to the middle and lower catchment, the most abundant palynomorphs in this section of the catchment are grasses. The grassland biome is affected by seasonality of rainfall and temperature (Acocks, 1988), therefore grasses in this area would have adapted better to the cooler temperatures and moist environments compared to some trees and shrubs (Scott, 1999) (Table 5.1). Therefore, it is likely that the grasses dominate the upper reaches of the catchment, and that these grasses are C₃ grasses (Scott, 1982; Vogts *et al.*, 2012). Sedges, Liliaceae, *Rhus* and *Tubuliflorae* are common herbs and shrubs found in the upper catchment area. The presence of the *Rhus* palynomorph as well as a high frequency of fern spores and sedges in this section of the catchment, represent the prevailing moist grassland under cool climate conditions (Table 5.1). Ericaceae and *Passerina* were also found in the Thina River, upper Mzimvubu River, and Mzintlava River tributaries which drain from the Drakensberg foothills. Ericaceae is more widespread compared to *Passerina*, despite *Passerina* having a wider distribution compared to Ericaceae in most environments (Coates Palgrave, 2002).

Similarly, *Acacia* type 1, *Ilex mitis* and *Pinus* are common arboreal palynomorphs recorded in the upper catchment. *Pinus* was present in the upper catchment, which could be due to the occurrence of commercial forestry plantations in the nearby towns and along the upper tributaries in Kokstad, Matatiele and Cedarville (DWS, 2017). *Ilex mitis* pollen grains were found in the upper Mzimvubu River and Mzintlava River, which is unexpected as *Ilex mitis* is a moisture dependent tree, and these sites are not characterised by high rainfall or moist conditions (Table 5.1). However, it is possible that microclimates along the banks of the upper Mzimvubu River and Mzintlava River tributaries can play a role in determining *Ilex Mitis* distributions (Coates Palgrave, 2002; Scott, 1999) (Table 5.1). A municipal report found *Podocarpus* to be a common tree present in the upper catchment (DWS, 2017). However, results of this study found no *Podocarpus* pollen grains in the RBS samples of the upper Mzimvubu River and Mzintlava River.

Table 5.1: Pollen climate indicator values and general habitat preferences

Family and Genus	Climatic Indicator Values	General habitat
Amaryllidaceae undiff.	Warm temperate, savanna environments, warm conditions (Scott, 1982).	Understory of forests, riverine environments (Scott, 1982).
Anacardiaceae <i>Rhus</i>	Tropical and subtropical environments (Scott, 1999).	Lowland Bushveld, coastal shrub and dune forest and forest edges (Scott, 1982).
Aquifoliaceae <i>Ilex mitis</i>	Wetter tropical and temperate conditions. Moisture dependant trees (Coates Palgrave, 2002).	Grassland, swamps, floodplains, river banks and moist woods and forests (Scott, 1999).
Asteraceae	Dry climatic indicator, tropical and subtropical climates (Scott, 1999).	Shrubland (Scott 1999).
Cheno-Am	Dry climatic indicator (Scott, 1999)	Halophytic plants, grassland, disturbed habitats (Scott 1999).
Combretaceae <i>Combretum</i>	Warmer, drier climates (Scott 1982).	Trees of woodlands, bushveld and riverine environments (Scott 1982).
Cyatheaceae <i>Cyathea</i>	Moisture dependant trees of the Tropics subtropics (Coates Palgrave, 2002).	High altitude streams banks, grasslands, forest margins (Coates Palgrave, 2002).
Cyperaceae undiff.	Wet climate indicator (Misha <i>et al.</i> , 2015).	Semi-aquatic, local swamps, deep soils, moist wetlands, forest and costal shrubs (Scott, 1999)
Ericaceae undiff.	Cool sub-humid conditions and WRZ (Scott 1999)	Mountain ranges, upland forests, local swamps of (Scott, 1982; Scott, 1999).
Euphorbiaceae	Warm conditions (Scott 1999)	Succulents, deep local soils. (Scott, 1982).
Fabaceae <i>Sesbania</i>	Warm conditions (Scott 1999).	Savanna, deep local soils (Scott 1999).
Liliaceae unfiff.	Wet climate indicator (Scott, 1999)	Semi-aquatic, local swamps, deep soils, moist wetlands, forest and costal shrubs (Scott, 1999)
Mimosaceae <i>Acacia type I</i>	Dry climate.	Bushveld, mistbelt, montane (Scott, 1982)
Myricaceae <i>Morella</i>	Sub-humid conditions (Scott 1999).	Mountain crests and valleys, escarpment, (Scott, 1982).
Myrtaceae <i>Syzygium</i>	No data found.	Swamp forest margins, stream-banks, riverine thicket, open grassy highlands (Scott 1982; Cock and Cheeseman, 2018).
Palmae <i>Borassus</i>	Warm, tropical and subtropical conditions (Coates Palgrave, 2002).	Savanna and wet lowland forests (Scott, 1982).

Pinaceae <i>Pinus</i>	High rainfall areas (Coates Palgrave, 2002).	Exotic Conifer used for timber plantations (Coates Palgrave, 2002).
Poaceae undiff.	High rainfall , warm tropical and temperate indicator (Fitchett and Bamford, 2017)	Grassland/Savanna (Scott 1999).
Poaceae <i>Zea mays</i>	Summer rainfall, tropical environments (Peterson, 2013).	Sunny environments, ubiquitous, ecosystem margins, moderately distributed sites (Peterson, 2013)
Podocarpaceae <i>Podocarpus</i>	Moist/wet conditions. Moisture dependant trees (Scott 1999a)	Large pollen grain production. Wind dispersal. Easily overrepresented in the pollen spectra. Montane forest. (Scott, 1982).
Pteridophyte	Wet, moist conditions (Scott, 1982).	Ferns (Scott, 1982).
Salicaceae <i>Salix</i>	High rainfall areas, moist to wet conditions, large water source (Kuzovkina and Quigley, 2005).	Introduced species planted along rivers, they have become naturalised and are invaders along water courses (Coates Palgrave, 2002).
Thymelaeaceae <i>Passerina</i>	Cool drier sub-humid conditions and WRZ (Scott, 1982; Scott 1999).	Highveld ericoid shrubs, mountain crests of the escarpment (Scott, 1982).

This is unexpected since *Podocarpus* is also found in the middle and lower catchment region, especially near the river mouth. It is possible though that the absence of *Podocarpus* in these sites is due to the extensive illegal collection and tree removal of yellowwoods by residents in nearby local villages and commercial loggers that occurs in this area (DWS, 2017). *Podocarpus* trees could have been subsequently removed for fuel wood harvesting, medicinal uses and commercial logging (Madikizela and Dye, 2003; Gess, 2012). It is also likely that the absence of *Podocarpus* could be due to the size of the pollen grain counts.

Middle Catchment

This middle catchment falls within a matrix of valley bushveld, southern tall grassland and Ngoni veld, which characterise the savanna biome (Acocks, 1988; Mucina and Rutherford, 2006). The warmer and drier conditions in this part of the catchment are characterised by a mixture of herbs and shrubs, grasses and trees (exotic and indigenous). Grasses remain the dominant palynomorph in the middle catchment, however, there is a substantial representation of tree and woody shrub vegetation compared to the grassland biome and IOCB. Grasses are most frequent in the Mzintlava River, Thina River, and iTsitsa which coincides with high norm31 ratios and long *n*-alkane chain lengths (nC_{31} to nC_{33}) (Carr *et al.*, 2014). A strong grass

signal originates from the upper Mzintlava River tributary which could be due to draining a grassland-rich environment characterised by highland sourveld, Dohne sourveld and Ngoni veld, compared to the other tributaries (Acocks, 1988). *n*-Alkane analysis of RBS samples from the Mzintlava River yielded chain lengths of nC_{33} , which is often associated with grasses and is the longest recorded chain length for the catchment (Vogts *et al.*, 2012).

Cyperaceae and Liliaceae are not as frequent in this section of the catchment compared to the grassland biome and IOCB. δD_{29-31} isotope analysis of RBS sediment organic matter showed that compared to the upper and lower catchment, the middle catchment likely experiences reduced rainfall and increased temperatures and higher evaporation rates indicated by enriched δD_{29-31} (Vogts *et al.*, 2016). Since Cyperaceae and Liliaceae prefer sunny moist to wet habitats as opposed to dry and warm environments (Scott, 1999), it is likely that the general increased dryness due to increased temperature and evaporation could account for the reduced frequency. The same general trend is evident in the pteridophyte vegetation, except for a sudden spike in monoletes frequency at in the Thina River. This spike could be due to the presence of *Pinus* forestry plantations in the Thina River, and the canopy cover the plantations provide could provide an ideal moist and shady environment for this plant type to persist (Della and Felkenberg, 2019). Herb and shrub palynomorphs are well represented in the savanna biome. Of particular interest, Amaryllidaceae, *Rhus*, *Senecio*, *Tubuliflorae*, *Vernonia*, Chenop., *Acalypha* and *Euphorbia* are significantly well represented compared to the upper catchment. The succession from grass to woody shrub and arboreal dominated vegetation, reflects the major vegetation change from upper catchment grassland to a warm and dry savanna in the middle catchment (Scott, 1982).

The arboreal signal is characterised by *Ilex mitis* and *Acacia* in the iTsitsa and Thina River, and *Combretum*, *Morella*, *Acacia* and *Podocarpus* in the Thina River, lower Mzimvubu River and Mzintlava River. There is a spike in frequency at MZ3 (iTsitsa) for *Acacia* type I which coincides with a high frequency of *Pinus* and *Ilex mitis* at the same site. It is interesting that a dry weather indicator tree such as *Acacia* and a moisture dependent, wet indicator tree such as *Ilex mitis* occupy the same area. It is possible that a generally wet climate and high rainfall at the river mouth provides a suitable environment for *Ilex mitis* to persist along the banks of the lower Mzimvubu River (Scott, 1982) (Table 5.1). In addition, the presence of *Pinus* at the river mouth which is also widely used for timber plantations, infers that small forestry timber plantations occur at the river mouth (DWS, 2017). Therefore, it is likely that the presence *Pinus*

palynomorph represent timber forestry plantations, and the presence of *Ilex mitis* could be due to the high rainfall and generally wet conditions at the river mouth (DWS, 2017).

Generally, the lower Mzimvubu River and Mzintlava River in the middle catchment yielded a higher frequency of arboreal taxa compared to the iTsitsa River and Thina River. This is to be expected since the iTsitsa and Thina River, despite being located in the savanna biome, drain predominantly grassland type vegetation in the upper catchment. The lower Mzimvubu River and Mzintlava River drain from indigenous forested areas as well as commercial forestry plantations in the upper catchment and typically represent a more savanna-type signal compared to a grassland signal in the iTsitsa and Thina River. *Pinus* is less common in the IOCB and upper catchment, but more common in the middle catchment. *Combretum*, *Acacia*, *Morella* and *Podocarpus*, which define the lower Mzimvubu River and Mzintlava River, are characteristically dry, warm sub-humid climate indicator taxa (Scott, 1982) (Table 5.1). $\delta^{13}\text{C}_{29-31}$ and δD_{29-31} RBS isotope data from the lower Mzimvubu River and Mzintlava River also indicate a trend of drying, warmer temperatures and increased evaporation. *Zea mays* pollen grains were recorded in the Thina River and Mzintlava River, indicating the presence of agricultural cereal crops, which coincide with commercially grown maize in sections of the Mzintlava River (Kokstad), Mzimvubu River (Cedarville), and the river mouth (Port St. Johns). These areas form the agricultural hub for maize production for the former Transkei region (DWS, 2017).

Lower catchment

Compared to the upper and middle catchment, the river mouth shows a well-mixed signal of grasses, sedges, herbs and trees (exotic and indigenous). Dune forest with sporadic patches of grasses and herbaceous shrub-like succulent vegetation characterise the IOCB (lower catchment) (Mucina and Rutherford, 2006). Grasses remain the dominant palynomorph, however, grasses were not as well represented in this section of the catchment compared to the upper and middle catchment. Aquatic taxa such as Cyperaceae and Liliaceae have a significant presence in the lower catchment compared to the middle and upper catchment, but fern spores decrease in abundance drastically in the lower catchment. This trend is different than expected as high sedge and Liliaceae frequencies coincide with high fern spore frequencies for both the middle and upper catchment. The lower fern spore frequency in the lower catchment could be due to brackish nature of the river mouth, as salt content increases, fern spore frequencies decrease (Della and Felkenberg, 2019).

Conversely to the aquatic and fern spores, herb and shrub vegetation are most frequent in the lower section of the catchment compared to the upper and middle catchment. *Rhus*, *Senecio*, *Tubuliflorae*, *Vernonia*, *Helichrysum*, *Cheno-Am*, *Acalypha*, *Euphorbia* and *Sesbania* define the herb and shrub signal for the lower catchment. *Cheno-Am* was found in higher frequencies at the river mouth compared to the river confluence, which could be explained by some *Cheno-Am* taxa being halophytic and accustomed to brackish water (Scott, 1999). The presence of *Euphorbia* and *Acalypha* are expected as succulent shrub like vegetation is commonly associated with IOCB vegetation (Mucina and Rutherford, 2006; Scott, 1999).

There is a marked lower frequency of *Ericaceae* and *Passerina* at the river confluence and the river mouth compared to the middle and upper catchment. Both palynomorphs prefer cool, dry sub-humid conditions (Scott, 1999) (Table 5.1), which are not characteristic of the lower catchment IOCB (Mucina and Rutherford, 2006). These palynomorphs, despite being widely distributed, prefer high altitude mountainous areas (Coates Palgrave, 2002) (Table 5.1). Therefore, it is likely that the presence of *Ericaceae* and *Passerina* at the river mouth, indicate that the pollen grains have been transported from the upper Mzimvubu River and Mzintlava River tributaries and deposited at the river mouth.

Arboreal palynomorphs show a similar diversity in the lower catchment compared to the savanna biome, however, there is a reduction in overall arboreal palynomorph abundance and an increase in grasses and herbs and shrubs. *Ilex mitis*, *Cyathea*, *Acacia*, *Morella*, *Borassus* and *Podocarpus* define the arboreal signal for the lower catchment. The sandy, well drained nature of the soil in the lower catchment could provide an ideal habitat for *Podocarpus*, *Cyathea* and *Morella* palynomorphs (Scott, 1999) (Table 5.1). Wet and moist conditions could enable moisture dependent trees such as *Ilex mitis* and *Borassus* to persist in the lower catchment region. *Pinus* and *Salix* are recorded in the river mouth and confluence, with the confluence yielding higher overall frequencies compared to the river mouth. *Salix* was not recorded in the upper and middle catchment, indicating that its source regions are located near the river confluence and the river mouth. However, personal observation during the sampling campaigns showed that some *Salix* trees grew along the upper Mzimvubu River stream banks (Jordaan, 2005). *Zea mays* pollen grains were recorded in the river mouth and confluence, with the confluence showing a higher frequency. This is unexpected as large scale commercial maize farms are not present in this section of the catchment. However, according to DWS (2017), maize production is present in the river confluence and Port St. Johns areas on a smaller subsistence based scale.

A discrepancy was found between palynomorph frequencies analysed at the river confluence and the river mouth, which could be due to the presence of a manmade weir at the river confluence. The weir could inhibit the transport of pollen grains, *n*-alkane lipid biomarkers and sedimentary elemental compounds downstream to the river mouth. Modern fossil pollen assemblages were analysed by Xu *et al.*, (2016), they found that anthropogenic pressures had a significant impact on pollen assemblages and distributions due to land use transitions and vegetation changes. Often the nature of these activities such as agriculture, land use change, water impoundments and vegetation removal have substantial impacts on vegetation composition of an area and ultimately the hydrologic, sediment and vegetation signature transported in the river (Xu *et al.*, 2016). This effect was seen at the confluence, wherein the pollen, *n*-alkane and inorganic XRF signals represented the diversity of source regions within the catchment compared to the river mouth. In light of this, the confluence would be a better representation of catchment vegetation composition compared to the mouth, which is likely representing the local signal.

5.2.2 Leaf-wax derived long chain *n*-alkane

n-Alkane homologue distribution

The Mzimvubu catchment maximises at the nC₃₁ *n*-alkane homologue for the three seasons, followed by nC₂₉ and nC₂₇. Short *n*-alkane chain lengths were not common in the Mzimvubu Catchment, indicating that terrestrial higher plants contributed the most to the sedimentary *n*-alkane signal (Vogts *et al.*, 2012). Both RBS and SPM consistently maximise at nC₂₇ and nC₃₁ for the three seasons which is to be expected for an environment characterised by grassland, savanna and IOCB vegetation (Poynter *et al.*, 1989). Typically, higher plants occur in the nC₂₅ to nC₃₅ *n*-alkane homologue range (Chibnall *et al.*, 1934; Eglinton and Hamilton, 1967). Within this range, chain lengths such as nC₂₇ and nC₂₉ have been proposed to originate from arboreal and shrub-like vegetation, compared to longer chain lengths (nC₃₁ and nC₃₃) originate from herbs and grasses (Shwark *et al.*, 2002). However, using *n*-alkane chain length distributions to discriminate between grass and woody vegetation should be done cautiously due to large variations within plant groups (Bush and McInerney, 2013). Despite this, other studies have confirmed it is still possible to utilise *n*-alkane chain length distributions as a semi-quantifiable proxy for vegetation groupings, especially when compared with other vegetation and climate proxies (Vogts *et al.*, 2012; Chavalier *et al.*, 2015).

Furthermore, when *n*-alkane chain length data were compared with pollen and norm31 data, occurrences of nC₂₇ and nC₃₁ coincided with the presence of arboreal/shrub vegetation and

grasses respectively at the same sites. High norm31 values coincided with longer *n*-alkane (nC₃₁ and nC₃₃) chain lengths in the upper Mzimvubu River and Mzintlava River tributaries, whereas lower norm31 ratios coincided with shorter *n*-alkane chain lengths (nC₂₇ and nC₂₉) (Chevalier *et al.*, 2015; Carr *et al.*, 2014; Zech *et al.*, 2012). There is a transition from grassland type vegetation in the upper catchment towards savanna vegetation in the middle catchment. Dry season RBS and SPM samples contribute a longer *n*-alkane chain length (nC₃₁ and nC₃₃), compared to the intermediate and wet season (nC₂₇). These results are in line with previous studies, for example, Vogts *et al.*, (2009) who stated that longer chain lengths are synthesised in warmer temperate regions and can represent a predominance of grasses (Rommerskirchen *et al.*, 2006; Schefuß *et al.*, 2004), whereas moderate to shorter chain lengths are indicative of trees and shrub-like vegetation (Vogts *et al.*, 2009; Carr *et al.*, 2014; Weijers *et al.*, 2009).

The range of short-to-long *n*-alkane changes for the dry season is less compared to that of the intermediate and wet season. For example, dry season homologue chain lengths ranged from nC₂₉ to nC₃₁, whereas wet season homologues ranged from nC₂₇ to nC₃₃ for RBS and SPM. This could be due to the wet season having more diverse organic matter signals as different plant types in the catchment experience their flowering season during November (wet season) (Brewer *et al.*, 2013). A reduced norm31 ratio is expected during the wetter months as this coincides with the start of the growing season (September – November) for arboreal taxa, agricultural crops and pine plantations (DWS, 2017). Although arboreal *n*-alkane contributions should ideally be low during the dry (non-growing) season, the signal would still be stored in RBS samples. Moreover, trees have a large spatial coverage and leaf biomass compared to grasses, and therefore would still contribute to the *n*-alkane signal (Diefendorf and Freimuth, 2017). However, due to the quantity and widespread distribution of grasses in the catchment during this season, it is likely that the grass signal overprinted the arboreal signal, thus resulting in a predominantly grass dominated *n*-alkane composition (Diefendorf and Freimuth, 2017).

CPI₂₅₋₃₃

CPI₂₅₋₃₃ values for RBS and SPM samples yielded predominantly odd-over-even chain lengths for the three seasons, which indicates that *n*-alkane organic matter in river sediment generally originated from terrestrial higher plants (Bray and Evans, 1961; Cranwell, 1984; Boot *et al.*, 2006). RBS and SPM yielded similar fluctuations in CPI values between the tributaries, however, SPM on average showed a consistently lower CPI compared to RBS. Reduced CPI values are common in areas of increased temperature and rainfall as these climatic factors enable high levels of erosion and organic matter degradation due to microbial activity in soils.

These findings corroborate with a finding by Richey *et al.*, (1990) wherein lower CPI values are likely as a result of biodegradation due to microbial processes in tropical soils. Therefore, low CPI values are unlikely to be representing the effects of precipitation induced erosion in the Mzimvubu Catchment as well as possibly anthropogenically induced soil erosion by agricultural activities and land use changes and biodegradation of organic compounds (Richey *et al.*, 1990).

Municipal reports state that sediment yielded are the highest in the Mzimvubu River compared to any other tributary, due to easily weathered parent rock material as well as improper land use practices (DWS, 2017). Reduced CPI values consistently originate from the Mzintlava River and river mouth samples which are underlain by easily weathered Ecca rock formations (Madikizela and Dye, 2003; Gess, 2012), located in areas of high anthropogenic activities (Madikizela and Dye, 2003). The high sediment yield entering the river from weathering and erosion processes can contribute to the reduced CPI values. Seasonally, the dry and intermediate seasons yield higher CPI values, which gradually decrease towards the wet season. Despite the fact that vegetation biomass is higher during the wet season, the lower CPI values could indicate soil erosion processes due to increased precipitation and easily weathered underlying parent rock material (Bouchez *et al.*, 2014; Haggi *et al.*, 2016; Sojinu and Shittu, 2018).

In contrast, high CPI values consistently originate from the Thina River and upper Mzimvubu. River These tributaries are surrounded by a high density of arboreal and shrub-like vegetation. RBS shows a weak positive correlation to temperature and precipitation which means that as temperatures and precipitation increase, so does CPI for RBS samples. Since this correlation occurred during the dry and intermediate season, which is not the growing season for majority of plant types in the catchment, it is likely that another factor is causing an elevated CPI value. It is possible that due to reduced rainfall during these seasons and lack of anthropogenic induced erosion, the vegetation signal, although low, could be the main contributor of the CPI sediment organic matter (Volkman *et al.*, 1992). Extensive pine plantations, verified by RBS *Pinus* pollen grains, are found on these river banks. These plantations persist during dry and intermediary seasons within the catchment (DWS, 2017) and could also contribute to elevated CPI values. Moreover, both rivers flow over the mudstones and shales of the Clarens and Elliot rock types which are less prone to weathering and erosion, which likely results in reduced sediment yields in the adjacent or overflowing rivers (Catuneanu *et al.*, 2005; Gess, 2012).

$$\delta^{13}C_{29-31}$$

RBS and SPM samples from the Mzimvubu Catchment featured a wide range of vegetation compositions inferred by pollen data and lipid biomarker data, and sediment particle sizes over each season. $\delta^{13}C_{29-31}$ values range from -27.8‰ to -32.1‰ which, according to various authors, is representative of an environment characterised by grasses, trees and shrubs (Lockheart *et al.*, 1997; Eglinton and Hamilton, 1967; Vogts *et al.*, 2009, 2012; Wang *et al.*, 2015; Boot *et al.*, 2006; Rieley *et al.*, 1991). The lowest $\delta^{13}C$ value for the catchment is -27.8‰ indicating that catchment vegetation is predominantly C_3 vegetation (Vogts *et al.*, 2009). C_4 vegetation typically yields $\delta^{13}C$ values from -14‰ to -20‰ , however, enriched $\delta^{13}C_{29-31}$ values like these were not recorded in the catchment (Vogts *et al.*, 2009). In addition, the dominance of the nC_{29} and nC_{31} n -alkanes infers that the vegetation is predominantly C_3 vegetation. It has been previously shown that a high abundance of nC_{31} and nC_{29} n -alkanes indicate C_3 plants rather than C_4 plants (Garcin *et al.*, 2012). Furthermore, the overall signal indicates a mixture of C_3 grassland and savanna type vegetation based on the dominance of the nC_{31} , nC_{29} and nC_{27} n -alkane homologues (Vogts *et al.* 2012; Lockheart *et al.*, 1997; Diefendorf *et al.*, 2010). Although specific taxon based n -alkane carbon stable isotope values were not established for the catchment vegetation, the sediment n -alkane $\delta^{13}C_{29-31}$ values corroborate with the general vegetation composition comprising of grassland, savanna and IOCB defined by Mucina and Rutherford (2006) and Acocks (1988). Depleted $\delta^{13}C$ values for RBS samples occur in the iTsista, upper Mzimvubu River and Thina River rivers, and it is likely that these $\delta^{13}C_{29-31}$ values are indicating C_3 grasses as they dominate the typical C_3 $\delta^{13}C_{29-31}$ range (O'leary, 1988; Vogts *et al.*, 2009; Bi *et al.*, 2005). We can assume that the depleted $\delta^{13}C_{29-31}$ signal should coincide with longer n -alkane chain length distributions and the presence of grass type vegetation over arboreal indicated by a high norm31 ratio (Chevalier *et al.*, 2015; Carr *et al.*, 2014).

There is a shift shorter chain lengths (nC_{27} and nC_{29}) during the wet and intermediate season could be due to pollen production of plants during the flowering season. *Podocarpus* for example, is known to produce large amounts of pollen during its flowering season (Scott, 1999), and some species of *Combretum* and *Sesbania* have been known to flower throughout the year (Jordaan, *et al.* 2011). The presence of these palynomorphs in the Mzimvubu River, Thina River and iTsitsia could account for the shorter n -alkane chain lengths. Despite this, the overall n -alkane chain length signal is dominated by the nC_{31} for these three tributaries. A predominantly grass environment is further shown through high norm31 ratios for the iTsitsia,

Thina River and Mzimvubu river. Pollen data (Figure 4.3) shows that Poaceae is the dominant taxa for the iTsisa and Thina River, however not for the Mzimvubu River. It is possible that the arboreal taxa signal which could originate from *Acacia* and *Pinus* timber plantations in the Mzimvubu River (DWS, 2017), could account for the marginally reduced grass signal and elevated arboreal signal.

$\delta^{13}\text{C}$ enrichment occurs in the Mzintlava River, Kinira River and river mouth, however these rivers are associated with increased levels of erosion, particularly the Kinira River which is characterised by sandy soil profiles. Therefore, the enrichment at these sites is likely due to an additional minor source. Some studies show petrogenic source to sediment organic matter as well as the presence of degraded and of *n*-alkane plant wax lipids can enrich the $\delta^{13}\text{C}$ signal (Bouchez *et al.*, 2014). A study conducted by Haggi *et al.*, (2016) found that petrogenic souring of *n*-alkane organic matter to be a likely cause of $\delta^{13}\text{C}_{29-31}$ enrichment in river bed sediments. It is also possible to infer that enrichment could be due to the contribution of some C_4 plants (Still and Powell, 2010; Chevalier *et al.*, 2015). A C_4 should be accompanied by an increase in *n*-alkane chain lengths, which is evident for the Mzintlava River (nC_{33}) and Kinira River (nC_{31} and nC_{33}), however not for the river mouth (nC_{27} and nC_{31}) (Rommerskirchen *et al.*, 2003; Hamilton *et al.*, 2004). Since no taxon-specific *n*-alkane chain length data exists for the catchment, pollen data was utilised in an attempt to verify this pattern. For example, aquatic pollen taxa such as Cyperaceae and Liliaceae are prevalent in Thina River, upper Mzimvubu River and Mzintlava River, and Cyperaceae is known to have both C_3 and C_4 plant types which could account for the marginal enrichment (Scott, 1999). In addition *Zea mays* pollen grains were identified in these tributaries, and maize is known to be a C_4 cereal crop, therefore indicating that the $\delta^{13}\text{C}_{29-31}$ enrichment could also be caused by C_4 maize crops.

However, since the most enriched $\delta^{13}\text{C}_{29-31}$ value for the catchment is -27.8‰ , this does not fall within the typical C_4 grass or cereal crop carbon isotope range (-14‰ to -20‰) (Vogts *et al.*, 2012). Therefore, the carbon isotope signal for these tributaries is also representing an additional petrogenic source of $\delta^{13}\text{C}_{29-31}$, or C_3 forest. A commercial pine timber plantations are present along the Mzintlava River and river mouth. *Combretum* and *Acacia* dominated the nC_{29} *n*-alkane chain length, and these two palynomorphs were recorded in the Mzintlava River and river mouth (Vogts *et al.*, 2009). Although the specific carbon isotope values of these arboreal taxa are unknown, it is likely that their presence in the tributaries are the cause of the marginal $\delta^{13}\text{C}_{29-31}$ enrichment (Vogts *et al.*, 2009, 2012, 2016; Scott and Vogel, 2000; McDuffee *et al.*, 2005; Badewien *et al.*, 2015)

δD_{29-31}

The Hydrogen that enters plant tissue during photosynthesis originates from soil water, which ultimately comes from precipitation (Session *et al.*, 1999; Sachse *et al.*, 2012). Therefore, changes in hydrogen isotope compositions of plant waxes can reflect isotopic shifts in precipitation. Generally, the upper catchment shows δD_{29-31} depletion (Figure 5.1 blue dots) and the river mouth show δD_{29-31} enrichment (Figure 5.1 yellow/red dots). However, the middle catchment yielded more enriched δD_{29-31} values compared to the river mouth (Figure 5.1 yellow/red dots). Throughout the tributary, depleted δD_{29-31} values occur in the northeast and northwest tributaries (Kinira River, upper Mzimvubu River, Mzintlava River), and δD_{29-31} enrichment towards the southeast tributaries (iTsitsa).

Variations within δD_{29-31} values of RBS sediments, indicate that depletion and enrichment change with increasing and decreasing elevation, distance from the sea and precipitation amount. These are known as isotopic “effects” (Herrmann *et al.*, 2017; Sachse *et al.*, 2012). The altitude effect is shown by how δD exhibits a strong inverse relationship to elevation for the dry, intermediate and wet season. The highest elevation sites within the catchment consistently correlate with the most depleted δD signals, and the lowest altitudes coincide with the most enriched δD signals (Herrmann *et al.* 2017; Dansgaard, 1964). As elevation changes, so does ambient temperature decrease. δD has a positive correlation to temperature, inferring that as temperatures and aridity rise, so do δD values become more positive (Gat, 1996). Linked to changes in altitude, is the change in the δD signal with distance from the sea (Continental effect) (Ponton *et al.* 2014; Herrmann *et al.*, 2017; Dansgaard, 1964). Sample sites and tributaries in close proximity to the ocean, namely the river mouth and iTsitsa, are δD enriched. Conversely, sample sites and tributaries which are furthest from the sea namely, the Mzimvubu River and Mzintlava River, are δD depleted. This trend occurs when a precipitating system moves inland from the coast, isotopically heavier rain water is preferentially “rained-out” closer to the coast (Sachse *et al.* 2012). The resulting precipitation will then be isotopically depleted the further inland the system moves, as there is less “heavy” isotope (Scheffuß *et al.* 2005). δD values of RBS samples also reveal changes in catchment hydrology, specifically precipitation intensity and amount (amount effect) (Dansgaard, 1964; Feakins *et al.*, 2016). Tributaries with depleted δD_{29-31} signals namely the Mzimvubu River, Mzintlava River and river mouth, are located in high rainfall areas (Hahn *et al.*, 2018), and tributaries with enriched δD_{29-31} signals such as the iTsitsa, coincide with areas of reduced rainfall.

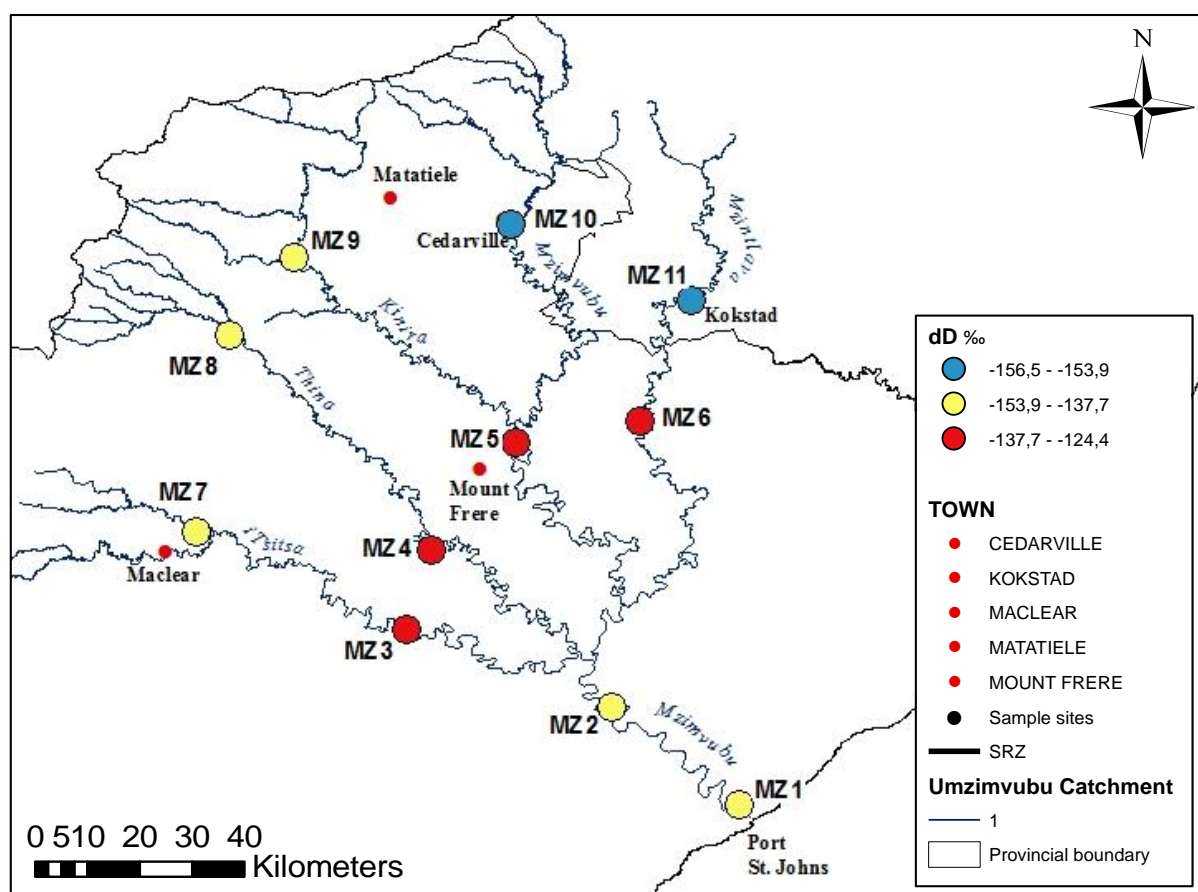


Figure 5.1: δD_{29-31} of RBS samples averaged together for the three seasons.

The δD_{29-31} composition of *n*-alkane in RBS sediment reflect catchment precipitation distribution. High precipitation is recorded at the river mouth which coincides with a moderate depleted δD_{29-31} signal (-137‰). The middle catchment sites show more enrichment to the river mouth, with an average δD_{29-31} of -129‰ . This is interesting as it is typical for precipitation to become more isotopically depleted with increasing distance from the seas (continental effect). However, this can be explained by recorded reduced rainfall and relative humidity as well as increased evaporation and temperatures compared to the lower and middle catchment (DWS, 2017). A study conducted by Herrmann *et al.*, (2017) showed δD_{29-31} isotopic compositions of plant waxes may become enriched in soil and leaf water during periods of low humidity and increased aridity (Krull *et al.*, 2006; Liu *et al.*, 2006). This indicates that plant physiology and plant types play an important role in determining δD_{29-31} enrichment and depletion (Kahmen *et al.*, 2013; Liu and Yang, 2008; Feakins and Sessions, 2010). In contrast, Niedermeyer *et al.*, (2016) put forward that this secondary enrichment should only have a minor influence on the δD_{29-31} signal of RBS sediments. Similarly, Hahn *et al.*, (2018) found that evapotranspiration has no major implication effects on the δD signal and that δD values of plant wax from arid areas cannot be clearly distinguished from humid areas. However, it was

found that secondary enrichment in the Mzimvubu Catchment could be attributed to vegetation composition, as the enrichment occurred in a savanna vegetation biome dominated by trees and shrubs rather than C₄ grasses and maize crops. Another possible explanation for δD_{29-31} enrichment, is that δD_{29-31} enrichment could also be attributed to reduced organic matter content as a result of higher contributions of petrogenic compounds (Haggi *et al.*, 2016). Petrogenic compounds have been found to be more δD enriched compared to organic material (Schimmelmann *et al.*, 2006). Enriched δD_{29-31} signals originated from the iTsitsa River and Kinira River, which have been characterised by high sediment yields due to increased soil erosion, therefore, making it likely that petrogenic contributions to RBS samples and δD_{29-31} enrichment (Li *et al.*, 2011).

5.2.3 Element Ratios

Three Elemental ratios namely, Ti/Al, Fe/K, and Al/Si represented important sedimentological and climatological dynamics within the Mzimvubu Catchment (Weltje and Tjallingii, 2008). Elevated Fe/K and Al/Si ratios indicate high levels of weathering in the northern tributaries (upper Mzimvubu River and Mzintlava River) (Govin *et al.*, 2012). Wilke *et al.*, (1984) showed that global patterns of Fe/K distributions along the Atlantic continent showed elevated values in surface sediments from tropical areas such as Africa and Brazil, and low Fe/K values from drier regions. Therefore, the results of this study are in line with Wilke *et al.*, (1984), as elevated Fe/K values were found in northern drier parts of the Mzimvubu Catchment and reduced Fe/K values in the southern wetter parts of the catchment (Figure 5.2). Moreover, high Fe/K ratios could also be attributed to the presence of intensive agricultural activities which often lead to surface sediment removal and erosion of sediment into adjacent rivers (DWS, 2017). It is also possible that iron phosphates from pesticides and fertilisers, which are commonly added to crop soils, enter into a river systems under high intensity rainfall events, therefore causing an increase in the Fe content of the river sediment (Ekstrom *et al.*, 2016).

Furthermore, high Al/Si values in the northern tributaries were indicative of high levels of erosion and sedimentation (Figure 5.3). These results align with Govin *et al.*, (2012), wherein high Al/Si ratios from Atlantic sediments represented the input of highly weathered fine material from humid areas in tropical Africa. Al/Si and Ti/Al were also good indicators of soil particle grain size, as high Al/Si and Ti/Al values indicate fine grained material, and low values indicate coarse grained material (Govin *et al.*, 2012; Haggi *et al.*, 2016).

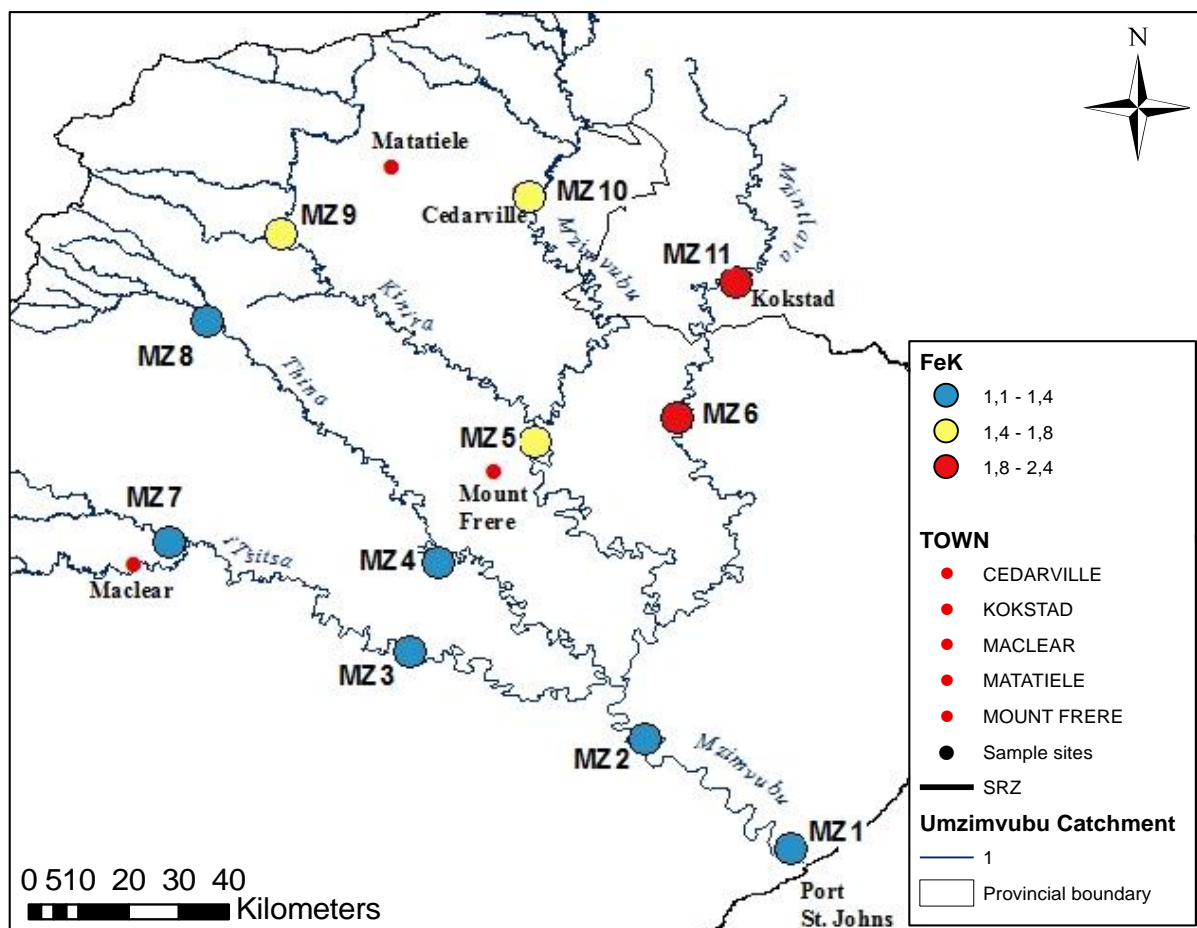


Figure 5.2: Fe/K RBS and SPM samples averaged together for the three seasons.

As with Al/Si ratios, Ti/Al ratio values represent particle grain size distributions within the upper Mzimvubu Catchment (Figure 5.4). Ti/Al values are lowest at the river mouth and highest at the Mzintlava River, which could imply that the river mouth is receiving fluvial input of large grained soil particles from the rest of the catchment and the Mzintlava River is receiving the fine grained particles transported via aeolian processes from the Indian Ocean. This study is different to previous studies which found a high correlation between high Fe/K and Al/Si ratios and humid climate conditions (Govin *et al.*, 2012). Fe/K and Al/Si ratios reflected the fluvial input of highly weathered material antropogenically induced soil erosion rather than precipitation.

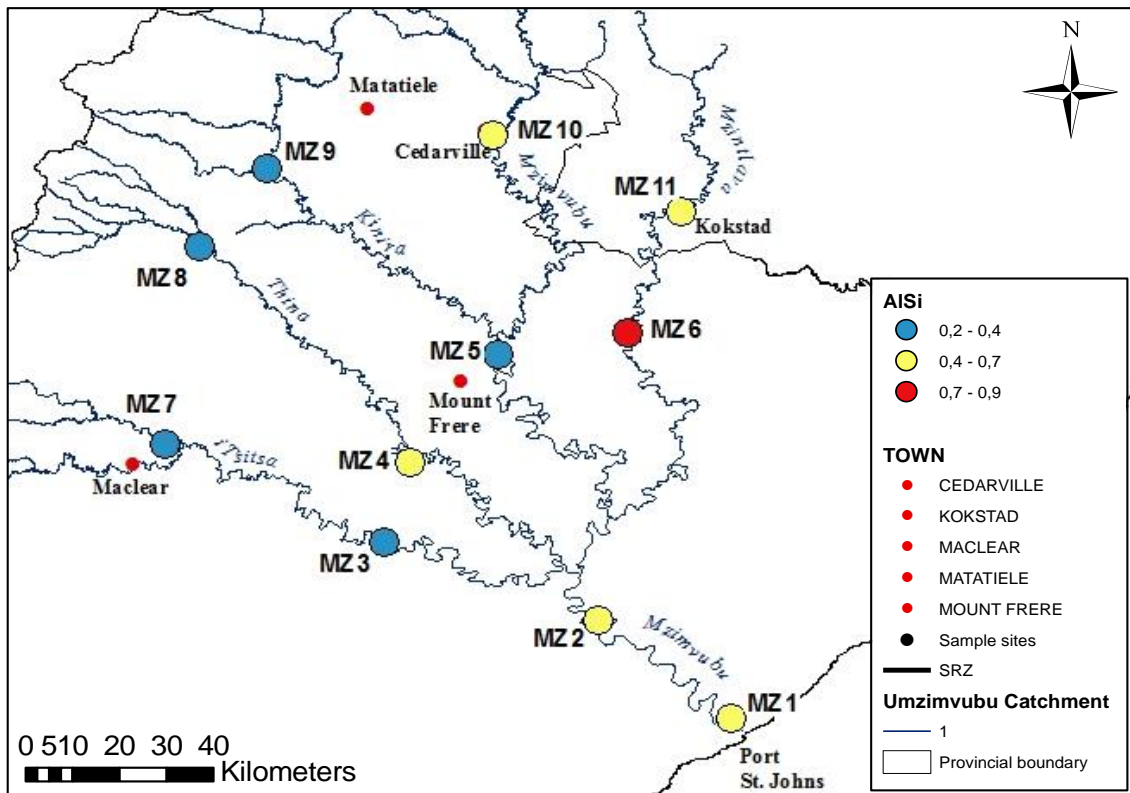


Figure 5.3: Al/Si ratios for RBS and SPM samples averaged together, for the three seasons.

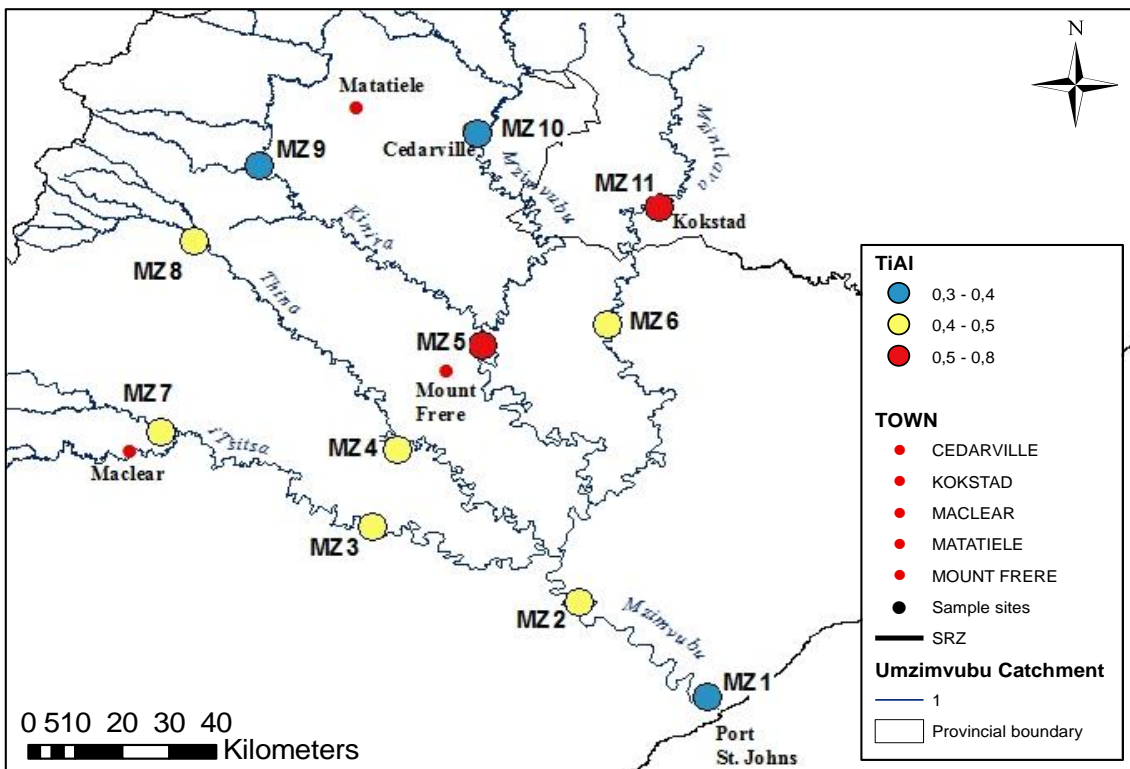


Figure 5.4: Ti/Al RBS and SPM averaged together for three months.

5.3 THE RBS SIGNAL VERSUS THE SPM SIGNAL

Both RBS and SPM samples were extracted from the Mzimvubu Catchment to compare and contrast the nature of the signals stored within. Due to the difference in the amount of sediment obtained from RBS samples compared to SPM samples, it was important to establish whether or not the two sample types reflect similar signal compositions and characteristics for future palaeoreconstruction studies, and potentially which one is better suited to these types of studies. RBS was chosen as the preferred sample type as there was enough sample sediment to perform multiproxy analyses, namely pollen, organic geochemistry and inorganic geochemistry analysis. SPM samples would be the preferred sample type for modern provenance studies, however, the overall sediment yield for SPM was very low and thus made it difficult to perform comparative multiproxy analyses. That being said, RBS and SPM data were obtained for *n*-alkane homologue distribution, CPI, $\delta^{13}\text{C}$, and norm31, however not for δD analysis, pollen and XRF. This section will investigate the similarities and discrepancies between RBS and SPM samples for *n*-alkane homologue distribution, CPI, norm31 and $\delta^{13}\text{C}$ data.

5.3.1 *n*-Alkane homologue distribution

For the most part, RBS samples reflect the SPM sample *n*-alkane homologue distribution dynamics, however some exceptions in the specific characteristics of the measured signal were found. RBS samples yielded on average much lower *n*-alkane sediment concentrations compared to SPM for the three seasons (Ponton *et al.*, 2014; Burdanowitz *et al.*, 2018; Bouchez *et al.*, 2014; Galy *et al.*, 2011). RBS and SPM samples differed slightly regarding specific homologue chain length signal characteristics. For example, Both RBS and SPM maximised at nC_{27} , nC_{29} and nC_{31} for each season. However, RBS revealed a more consistent longer chain (nC_{31}) signal compared to SPM which was dominated by moderately shorter chain lengths (nC_{27} and nC_{29}) over the three seasons (Galy *et al.*, 2011; Bouchez *et al.*, 2014). In addition norm31 RBS values did not show as much variation between the seasons compared to SPM norm31 values. RBS norm31 values show more variation between the sample sites compared to SPM norm31 values. Since high norm31 ratios are indicative of grasses and lower ratios trees and shrubs (Carr *et al.*, 2014, Vogel, 1978; Chevalier *et al.*, 2015), it is possible to infer that RBS is showing a stronger grass signal compared to SPM which is showing a mixture between grasses, trees and shrubs. RBS and SPM samples yielded similar fluctuations in CPI values across the sites and seasons, however, on average SPM shows much lower CPI values compared to RBS CPI values. Therefore, SPM is representing a more diverse range of source

regions of organic matter compared to RBS, as well as a more modern signal over shorter time periods (Hahn *et al.*, 2018; Haggi *et al.*, 2016). The lower CPI SPM values could also indicate that SPM is representing a more degraded CPI signal compared to RBS samples (Hahn *et al.*, 2018).

5.3.2 XRF elemental ratios

RBS and SPM Fe/K ratios reflect similar fluctuations within the tributaries. The SPM average shows a more reduced Fe/K signal compared to RBS for the three seasons (Figure 5.2 blue dots). This could imply that RBS samples are reflecting a signal that has accumulated over a time period, whereas SPM reflects the immediate prevailing climate and high sediment yield or pollution levels within the tributaries. An additional note to consider is that SPM could eventually form part of the RBS signal overtime, and RBS sediment could be re-worked back into the moving water column under turbulent episodes. RBS and SPM samples reflect similar fluctuations in Al/Si signals within the catchment. Overall, RBS yielded lower Al/Si ratios compared to SPM, which implies that RBS samples are revealing a coarser grained signal and drier climate compared to SPM samples could be representing finer grained particles, which are easily carried in the suspension load of a river, during humid climate conditions (Govin *et al.* 2012). This trend is seen in the change from high ratios during the dry and intermediate season, to lower ratios during the wet season. RBS and SPM samples reflect similar patterns of elevated and reduced signals within the catchment. RBS yielded much lower Ti/Al ratios compared to SPM samples, which implies that Ti/Al ratios are reflecting the fluvial deposition of larger coarse grained particles, and SPM samples reflect the aeolian deposition of finer grained soil particles. Finer grained particles are easily carried by wind currents as well as in the suspension load of a water course, whereas, larger soil particles would be readily deposited in the river sediments (Rommerskirchen *et al.*, 2003; Huang *et al.*, 2000; Govin *et al.* 2012).

5.4 SIGNAL PROVENANCE

This section will evaluate the source regions, transport pathways and deposition dynamics of pollen, *n*-alkane homologues and inorganic elemental compositions within the Mzimvubu Catchment. Each section will outline the possible origins of the specific organic and inorganic signals within each tributary of the catchment over the three seasons. The effect that various environmental parameters may have in determining proxy provenance will be investigated.

5.4.1 Pollen

The Mzimvubu Catchment is located in a high rainfall area which results in high sediment yields entering into the tributaries, and increased water flow velocities which pose significant threats to the deposition and preservation of pollen and other organic matter compounds such as leaf-wax derived long chain *n*-alkanes (Carrion, 2002; Collins *et al.*, 2013). The issue of taphonomy is an important effect to take into consideration when determining sediment organic matter provenance within fluvial systems (Delcourt and Delcourt, 1980; Clement *et al.*, 2017). Due to the dynamic and turbid nature of fluvial systems, it is likely that overall organic matter and subsequent pollen grain and *n*-alkane wax biomarkers preservation will be poor. Similar results were found by Brewer *et al.*, (2013) and Brown *et al.*, (2007) wherein modern pollen grain damage and degradation were linearly correlated to an increase in stream turbidity, velocity, re-oxygenation and mixing (Carrion, 2002). In addition, a study conducted by Delcourt and Delcourt (1980) found that pollen abundances and influx are as much as a result of the dispersal characteristics and depositional processes, as they are of the prevailing vegetation from which they originated.

Pollen data from RBS samples of major tributaries showed the results of some of these effects, wherein, sample sites with elevated levels of turbidity and sandy deposition environments produced overall lower *n*-alkane concentrations and pollen grains counts, and degraded pollen grains (Clement *et al.*, 2017; Delcourt and Delcourt, 1980). Sample sites with reduced stream turbidity, clay-rich and high vegetation biomass yielded high *n*-alkane concentrations and pollen grain counts which were well preserved (Delcourt and Delcourt, 1980). Norm31 ratios were correlated to pollen and it was found that elevated norm31 ratios, which broadly represent grass-dominated environments (Chevalier *et al.*, 2015; Yu *et al.*, 2016), also represented the southern tributaries (Thina River and iTsitsa). Elevated norm31 ratios coincide with elevated CPI and *n*-alkane concentrations, which are usually associated with increased vegetation biomass (Chevalier *et al.*, 2015; Boot *et al.* 2006). In comparison to the river mouth, pollen data showed that the grassland biome (upper catchment) contributed the highest long chain *n*-alkane homologues (nC₃₃) compared to the IOCB (river mouth) which represented a mixture of moderate chain lengths (nC₂₉), and the savanna biome (middle catchment) which is dominated by shorter chain lengths such as nC₂₇..

Cooler conditions characterise the Kinira River, upper Mzimvubu River and Mzintlava River rivers in the northern section of the catchment (Rowntree *et al.*, 2017; Mucina and Rutherford, 2006). Pollen data yielded Common taxa found in these tributaries are Cyperaceae, Liliaceae,

fern spores, *Passerina*, *Ericaceae* and moisture dependent trees such as *Ilex mitits*, *Combretum* and *Podocarpus*. Ultimately, pollen data combined with reduced norm31 ratios and low CPI values coincides with the presence of arboreal and shrub-like vegetation in the northern section of the catchment (Chevalier *et al.*, 2015; Carr *et al.*, 2014). A high norm31 ratio coincided with warmer climate conditions and a high frequency of grasses in the south and south west section of the catchment (Chevalier *et al.*, 2015).

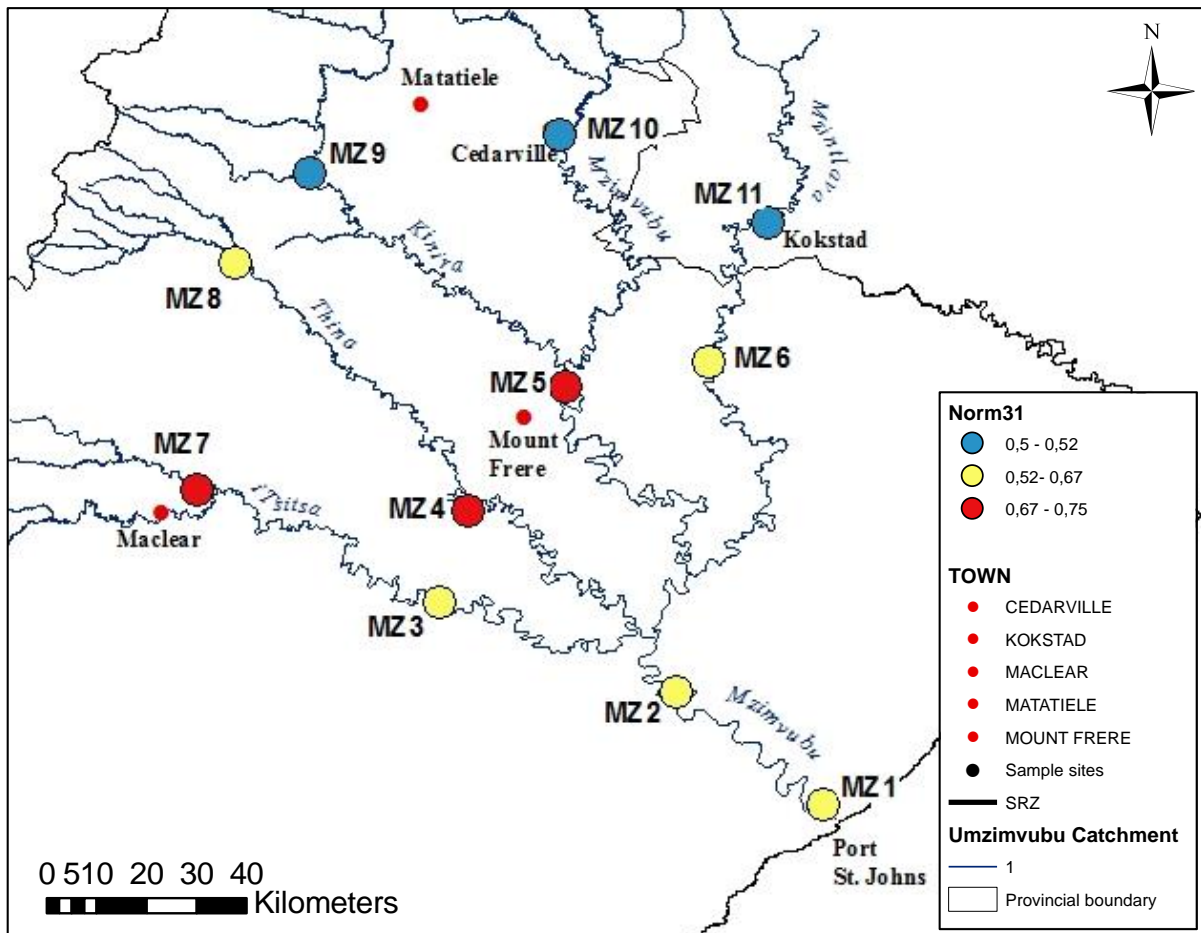


Figure 5.5: Average norm31 RBS and SPM values for the three seasons.

5.4.2 Stable $\delta^{13}\text{C}_{29-31}$ and δD_{29-31} isotope compositions of *n*-alkane plant waxes

Moderately enriched $\delta^{13}\text{C}_{29-31}$ signals can be traced to the northern tributaries (upper Mzimvubu River and Mzimvubu River) of the catchment. This enrichment could be due to the presence of agricultural C_4 cereal crops such as *Zea mays*, which is a C_4 plant (Peterson, 2013). Cyperaceae, whose pollen are present in high frequencies in the upper catchment, include both C_3 and C_4 plant types. Although it was not possible to identify Cyperaceae beyond the family level, it is likely that C_4 components do persists in this environment. Other studies also found

that local riverbank vegetation such as Cyperaceae, has an influence on the $\delta^{13}\text{C}_{29-31}$ isotope composition of river sediments (Hahn *et al.*, 2018). *Salix* has been reported to have on average $\delta^{13}\text{C}_{29-31}$ isotope value of -25.5‰ compared to other arboreal taxa (Wang *et al.*, 2015), and since *Salix* trees were observed along the banks of the upper Mzimvubu River and Mzintlava River, it is possible that a subsequent $\delta^{13}\text{C}_{29-31}$ secondary enrichment could occur in river bed sediments.

$\delta^{13}\text{C}_{29-31}$ data coincides with pollen and norm31 data, which shows that arboreal and shrub-like plants are dominant in the upper Mzimvubu River and Mzintlava River tributaries. The effect of climate gradients on $\delta^{13}\text{C}_{29-31}$ values should also be taken into consideration. For example, Herrmann *et al.*, (2016) found that vegetation biomes within southern Africa followed climate gradients and grasses were found to dominate warmer conditions, whereas woody vegetation dominated colder and moisture conditions (Rommerskirchen *et al.*, 2003). Vegetation of the Mzimvubu Catchment followed similar climate gradient trends wherein, woody vegetation (*Ilex mitis*, *Podocarpus*, *Acacia*, *Pinus*) tended to dominate the colder, moisture environments in the northern tributaries, and grasses (Poaceae) and shrubs (*Rhus*, *Cheno-Am*, *Acalypha*) dominated the warmer environments.

Similar to $\delta^{13}\text{C}_{29-31}$, δD_{29-31} showed that enrichment and depletion are specific to different tributaries within the catchment, and broadly reflects the prevailing hydrological and precipitation dynamics within the catchment (Feakins and Sessions, 2010; Vogts *et al.* 2016). Generally, δD_{29-31} depleted values occurred in tributaries characterised by cooler areas and enriched δD_{29-31} values occurred in warmer more arid tributaries. Similar trends were demonstrated by Schefuß *et al.*, (2005) where deuterium enriched soil water, occurs under more arid conditions. δD_{29-31} shows these isotopic effects, except for the sudden enrichment in the middle catchment compared to the river mouth and upper catchment. Generally, the river mouth should show an averaged value of the all the tributaries which flow, and should show a relatively enriched signal compared to the inland sample site in the upper tributaries. With increasing distance from the river mouth and increasing altitude, δD_{29-31} should become more isotopically depleted (Gofiantini *et al.*, 2001). However, the middle catchment sample sites show δD_{29-31} enrichment. This could be due to reduced precipitation in the middle catchment, resulting in drier and warmer conditions. Therefore, the increasing aridity, could result in an enriched δD_{29-31} signal in plant wax lipids (Schefuß *et al.*, 2005. 2011; Feakins and Sessions, 2010).

Other potential factors controlling δD_{29-31} of plant wax in river bed sediments are large scale climatic systems like precipitation amount (amount effect), the movement of a moisture system from the ocean inland (continental effect), attitude effect and the condensation with altitude effect (temperature effect) (Herrmann *et al.*, 2017; Niedermeyer *et al.*, 2016). Analysing δD_{29-31} within sediment samples over three seasons showed that the dry season on average was more enriched compared to the wet season. This could be due to the fact that the dry season receives on average less rainfall amount compared to the wet season, which receives more (rainfall amount). Similar findings occurred in a study conducted by Niedermeyer *et al.*, (2016), where δD_{29-31} depleted values were found in sediments in high rainfall seasons and δD enrichment in sediments occurred in areas of low rainfall seasons (Gofinatini *et al.*, 2001). δD_{29-31} values showed that despite the river mouth receiving the highest annual precipitation compared to the other sites, the δD_{29-31} signal is still relatively enriched compared to the other sites further inland. This could be due to the continental effect wherein there is preferential rainout of the heavier hydrogen isotopes at the river mouth leading to δD_{29-31} enrichment (Gofiantini *et al.*, 2001; Galy *et al.*, 2011). As is seen with δD_{29-31} enrichment occurring in tributaries closer to the coastline such as the iTsitsa, and δD_{29-31} depletion within the upper Mzimvubu River and Mzintlava River which are furthest from the coastline. Similar δD_{29-31} trends were found in Hahn *et al.* (2018) and Ponton *et al.*, (2014), wherein coastal areas with a lower altitude produced more enriched δD_{29-31} signals and inland areas at higher altitudes were more depleted δD_{29-31} signals.

5.4.3 Element Ratios

Three element ratios namely Fe/K, Al/Si and Ti/Al were used to investigate the movement of sediment, weathering and soil erosion processes and in turn the prevailing climatic conditions that drive these processes, within each major tributary (Bertrand *et al.* 2012; deSouza *et al.* 2017). These elevated signals indicative of high weathering processes, were found in the upper Mzimvubu River, Mzintlava River and Kinira River rivers for each season. It is likely that the erosion-prone underlying rock strata and intensive agricultural activities that lead to soil erosion, contributed to the elevated Fe/K values for these tributaries. These rivers flow over Ecca and Adelaide rock groups which comprise of easily weathered and eroded sandstones and mudstones which form coarse grained sand particles and are often eroded into the adjacent river(s) during rain events (Rowntree *et al.*, 2017). Reduced Fe/K ratios were found in the Thina River and iTsitsa River rivers which flow over Mudstones and Shales of the Clarens and Elliot rock formations and Basalts of the Suurberg rock group (Rowntree *et al.*, 2017;

Madikizela and Dye, 2003). These rock types are not as easily weathered and can result in less sediment being transported into rivers. Thus, variations in high and low Fe/K ratios can indicate the transition between high rainfall humid areas and low rainfall arid areas, underlying rock strata, as well as particle grains size, weather and erosion processes.

Compared to Fe/K, Al/Si is better at representing climatic conditions and soil particle size within the catchment. Elevated Al/Si ratios indicate highly weathered fine material originating from humid regions (Liu *et al.*, 2017). These elevated signals were located in the Mzintlava River and river mouth for both RBS and SPM samples. The Mzintlava River and river mouth receive high precipitation compared to the other tributaries. Al/Si does not accurately represent underlying rock strata compared to Fe/K ratios. Conversely, reduced Al/Si ratios indicate less weathered and larger coarse grained particles from drier regions such as the Kinira River and iTsitsa River. These tributaries are characterised by higher temperatures and reduced precipitation which could indicate a shift to a drier and warmer climate in the south section of the catchment.

Similarly, Ti/Al represents the prevailing sediment processes and the climate conditions that drive them. Generally, high Ti/Al ratios indicate the input of fine grained aeolian dust particles (Govin *et al.* 2012; Lopez *et al.*, 2006). The highest Ti/Al ratios occurred in the upper Mzimvubu River and iTsitsa River which are in close proximity to the ocean, and thus easily affected by the south easterly trade winds that blow inland from the Indian Ocean. These winds carry dust particles from various locations, which can be transported and deposited into rivers and lakes inland. Reduced Ti/Al ratios indicate the fluvial input of larger coarse grained particle sizes (Govin *et al.* 2012; Chen *et al.* 2013). During seasons of high rainfall, sediments are transported in abundance to ocean sediments (Niedermeyer *et al.*, 2016; Huang *et al.*, 2000). Therefore, the iTsitsa River could be representing the input of aeolian dust particles from south easterly trade winds (Liu *et al.*, 2017).

5.5 IMPLICATIONS FOR FUTURE PALAEOENVIRONMENTAL RESEARCH

This section will investigate whether the proxies measured in the Mzimvubu Catchment provide viable and reliable environmental and climatological data for future palaeoreconstruction studies. Pollen, leaf-wax derived long chain *n*-alkanes and inorganic XRF element analysis will be compared and contrasted in their ability to represent modern vegetation, sediment and hydrological conditions within each tributary of the Mzimvubu

Catchment. Proxies have been integrated and compared together to identify similarities in trends and patterns and the overall signal provenance and characteristic of the signal being transported.

5.5.1 Palaeo-considerations

Utilising leaf wax *n*-alkane distributions, pollen grains and inorganic elemental compounds from sediment archives for both modern analogue and palaeoreconstruction studies is an effective tool for establishing past and present vegetation, hydrologic and sediment dynamics within a system (Carr *et al.*, 2014). However, leaf wax *n*-alkane concentration production as well as distributios are non-linear which can affect interpretations (Diefendorf *et al.*, 2011). This should be taken into consideration for studies conducted in areas where potential source regions are poorly understood such as the Mzimvubu catchment (Boom *et al.*, 2014).

Modern studies which aim to estimate the changing presence, absence and distribution of plant types in terrestrial environments should consider that fluctuations in organic and inrognic proxies are affected by plant physiology, plant functional type, climate factors and seasonality (Carr *et al.*, 2014; Castaneda *et al.*, 2009; Bai *et al.*, 2008). It was found that *n*-alkane $\delta^{13}\text{C}_{29-31}$ and δD_{29-31} compositions in sedimentary records are also affected by soil erosion, which are driven by precipitation processes (Weijers *et al.*, 2000; Vogts *et al.* 2009; Herrmann *et al.*, 2017). These taphonomic processes are more common in fluvial systems and contribute to the degradation of organic and inorganic compounds in sediment records (Bliedtner *et al.*, 2018). This was found to be the case for the Mzimvubu Catchment, wherein degraded pollen grains were found in high velocity and turbid tributaries. In addition, some studies have promoted the incorporation of the effect of anthropogenically induced land use changes such as land cover transformation, development and agricultural land transformation as these affect the overall structure and composition of a proxy signal (Still and Powell, 2010). For example, changes in land use such as a transition from grassland to forestry plantations or the cutting down of C3 shrublands into C4 grasslands (Still and Powell, 2010). In the case of the Mzimvubu catchment, agricultural activities, which take the form of crops (maize for example) and timber plantations, can result in the overrepresentitivy and underrepresentivity of certain signals during different seasons.

The spatial integration of *n*-alkane plant waxes into sedimentary records represents a wide variety of potential source regions which can complicate interpretations (Ponton *et al.*, 2014; Galy, 2011). Therefore, when utilising $\delta^{13}\text{C}_{29-31}$ values as proxies of C₃ and C₄ vegetation, it is important to consider that C₄ plant types are mostly grasses (Vogts *et al.*, 2009). Since most

grasses use C₃ photosynthetic pathways, this can complicate the establishment of source regions (Cerling *et al.*, 1993; Diefendorf and Freimuth, 2017). Similar results were demonstrated by Bush and McInerney (2013) and Niedermeyer *et al.*, (2016) wherein plant functional types, *n*-alkane distributions, canopy position and distribution and the large variability in *n*-alkane concentration skewed the establishment of plant wax provenance. Therefore, utilising *n*-alkane plant wax data without the comparison of other proxy information to validate, is inadvisable.

Various authors have provided tools for overcoming these challenges, such as establishing ecosystem classifications of forest regions, woodlands and grassland within the study area and determine the appropriate ranges of δD_{29-31} , $\delta^{13}C_{29-31}$ for each classification (Cerling *et al.*, 1993). In addition, changes in *n*-alkane homologue distributions effects can be accounted for in end-member models (Zech *et al.*, 2012). These models use modern plant samples and sediment samples from sites with diverse, tree, shrub and grass compositions. Correcting for these factors in vegetation composition can be achieved by analysing *n*-alkane distributions in specific taxa (Collins *et al.*, 2013; Yang *et al.*, 2011). Such taxon-specific fractionation studies can provide the necessary information required for effective palaeoreconstruction studies in southern Africa.

Conversely, we found the multiproxy approach suitable for determining and comparing proxy provenance within the catchment. This study found a strong correlation between $\delta^{13}C_{29-31}$ and δD_{29-31} ($r=0.70749$) and between the three elemental ratios, therefore indicating that stable carbon and hydrogen isotope values can be used to reconstruct modern and past vegetation and hydrologic dynamics. In addition, elemental ratios are good indicators of grain size distributions and sedimentological processes within a fluvial system (Govin *et al.*, 2012). Norm31 values also showed positive correlations to $\delta^{13}C_{29-31}$ data throughout the season inferring that norm31 and $\delta^{13}C_{29-31}$ can be used comparatively when investigating vegetation compositions based on *n*-alkane distributions (Cheavlier *et al.*, 2015). Norm31, δD_{29-31} and Fe/K also showed strong correlations to CPI₂₅₋₃₃. This indicates that the hydrologic processes within the catchment drive sedimentological dynamics as well as vegetation composition which ultimately affect *n*-alkane degradation and concentration within sediment samples. With further investigation and comparison to other proxies, *n*-alkane data can become a valuable proxy for plant group types and vegetation composition (Bush and McInerney, 2013). The use of $\delta^{13}C_{29-31}$, δD_{29-31} , grain size and pollen samples enabled the effective reconstruction of past

vegetation compositions, hydrological dynamics and changes in aridity (Feakins *et al.*, 2016; Diefendorf and Freimuth, 2017).

5.6 LIMITATIONS OF THE STUDY

Results of pollen, *n*-alkane plant wax, and XRF analysis are quantitative, however, they are interpreted qualitatively and subjectively and thus require careful consideration. This section will discuss the potential limitations associated with the interpretation of the pollen and *n*-alkane data, while offering solutions to these problems. Problems of representivity, selective preservation, and interpretation of conflicting indicators will be discussed.

5.6.1 Sample Design

Time and spatial constraints

One of the most important considerations when investigating the characteristics and dynamics of hydrology, sediment and vegetation signals, are the issues of spatial and temporal representivity. This is difficult to quantify for study sites that span large geographic areas or unfavourable terrain. As a consequence, as much of the spatial extent of an environment should be sampled as well as consideration for the most appropriate sampling seasons. For the purpose of this study, samples were extracted from three parts of each tributary (upper middle and lower) including the river mouth, as well as being sampled over three consecutive seasons. One issue with sampling down course of a tributary is that, proxy data will almost always reflect signal transported from further upstream, and not necessarily represent the local vegetation. Despite this, this approach provided a fairly successful method for capturing the full spatial extent of the catchment, and the seasonal changes therein.

Sample design

Four types of samples were extracted at each site namely, RBS, SPM, DPS and water isotope samples. SPM samples remained too small to conduct a full range of proxy analyses, compared to RBS samples. One limitation of this, is that SPM samples are a better reflection of the modern vegetation composition, climate dynamics and other factors such as anthropogenic impacts. It was found that SPM consistently showed more variation in proxy signals over the three seasons, in the sense that more of the catchment vegetation was reflected in SPM compared to RBS. RBS samples, however, provide more bulk sample sediment to work with, and thus more proxy analyses can be utilised. A limitation of using RBS samples is that they are not representative of the modern catchment composition. One such method to overcome this issue is to allow for longer SPM sampling times, and to suspend the sampling equipment

10 to 40 cm below the surface of the water. Using filters attached to sampling equipment would also be ideal for collecting SPM material this could reduce processing times in the laboratory after sample collecting in the field. Or, alternatively to sample at subsequent depths from the water surface to the river bed to capture the full extent of the particulate matter being transported in the water column.

5.6.2 Pollen

Representivity

Pollen samples are a combination of both regional and local taxa, which can complicate interpretations. Pollen data were extracted to create a modern picture of the general vegetation compositions and climate conditions. It was found that RBS pollen data provided an accurate description of these conditions. Since stable $\delta^{13}\text{C}$ and δD_{29-31} analysis was conducted on river sediment, rather than specific plant types where C_3 or C_4 is known, pollen data was used to verify these isotope values and *n*-alkane indices such as CPI and norm31. It was found that the RBS pollen samples were sufficient enough to aid in the interpretation of stable isotope values for the Mzimvubu Catchment.

5.6.3 Stable isotopes

$\delta^{13}\text{C}_{29-31}$

$\delta^{13}\text{C}$ isotope values can often confound vegetation representivity, as it may only represent vegetation growing in a specific location. Interpretation of $\delta^{13}\text{C}$ in an environment with Cyperaceae is further complicated by the existence of C_3 and C_4 Cyperaceae. This limits the ability of the analyst to distinguish between arboreal and non- arboreal vegetation. *Zea mays* is also present in the catchment due to the presence of maize agriculture in the Mzintlava River, upper Mzimvubu River and Thina River rivers. Despite these limitations, pollen data was used to determine the presence of these conflicting taxa to interpret the $\delta^{13}\text{C}$ signal more accurately.

5.7 CONCLUSION

This study provided the first characterisation of the vegetation, sediment and hydrological signals transported within the sediment of the Mzimvubu Catchment. The catchment is characterised by a Catena of grassland, savanna and IOCB vegetation compositions which are driven by prevailing climatic conditions. Changes in vegetation and hydrological dynamics are confirmed by changes in pollen, $\delta^{13}\text{C}$ and δD_{29-31} isotope values for each tributary. δD_{29-31} represents precipitation dynamics but not isotope composition of precipitation. RBS and SPM

sediment are accurate representations of these changes. It was found that RBS should be considered when looking at long term regional changes of vegetation, hydrological and sediment changes. SPM should be the preferred sample type when analysing modern catchment dynamics and prevailing vegetation and climate systems.

CHAPTER SIX

CONCLUSION

6.1 INTRODUCTION

This chapter will synthesise the modern surface sediment characteristics of the Mzimvubu Catchment, thus highlighting the most pertinent results of the study. Through the application of a multiproxy approach, utilising pollen, organic and inorganic proxies, we were able to enhance the current understanding of the prevailing environmental and climatic data in the Eastern Cape region, therefore contributing to the paucity of data for this region. The aim and objectives of the research will be reviewed to establish whether these have been addressed and achieved, and lastly, based on the limitations and results of this research, to evaluate the success of the study and to make future recommendations.

6.2 SYNTHESIS OF PERTINENT FINDINGS

6.2.1 Pollen

Seasonality

A summary of modern pollen seasonal assemblages for the Mzimvubu Catchment in Figure 4.1. Figure 4.2 illustrates the spatial distribution of palynomorph assemblages across each sample site. It was found that pollen assemblages mirrored various taxa seasonal production trends and flowering seasons complicating interpretations. This study concludes that seasonality over a short time scale is not significant enough to show major trends in vegetation transitions and compositions (Brewer *et al.*, 2013). However, the effect of seasonality and flowering times of plant taxa should still be taken into consideration in modern pollen studies to account for potential over and underrepresentation of specific taxa (Brown *et al.*, 2007)..

Biomes

Palynomorph abundance represent the three major biomes of the Mzimvubu Catchment, defined by Mucina and Rutherford (2006) and Acocks (1988) namely, a grassland biome in the upper catchment, savanna vegetation in the middle catchment and the IOCB at the river mouth.

Upper – The upper catchment is defined by a mixture of grasses, sedges, fern spores, *Rhus*, *Tubuliflorae*, *Ericaceae*, *Themelaceae*, *Acacia*, *Pinus* and *Ilex mitis*. As is to be expected for the grassland, Poaceae is the dominant palynomorph which indicates the presence of open

grassland vegetation (Scott, 1999). Since the regions is characterised by cool wet conditions, grasses are likely to be C₃ grasses rather than C₄ grasses (Acocks, 1988; Scott, 1982, 1999; Vogts *et al.*, 2012). $\delta^{13}\text{C}$ values show depletion in the upper catchment and therefore could be representing C₃ grasses or forested areas (Schefuss *et al.*, 2011). $\delta^{13}\text{C}$ enrichment is present at MZ9 (Kinira River) and MZ8 (Thina River), which could indicate the presence of C₄ sedges, C₄ *Zea mays* or petrogenic sources of degraded *n*-alkane plant matter. .

Middle - This section of the catchment is defined by the savanna biome (Mucina and Rutherford, 2006) with transitions between valley bushveld, southern tall grassland and Ngoni veld (Acocks, 1988). Grasses remain the dominant palynomorph here, however, there is a substantial representation of tree and woody shrub vegetation. δD_{29-31} isotope analysis showed enrichment in the middle catchment which could indicate reduced rainfall and increased temperatures and higher evaporation rates, (Diefendorf *et al.*, 2010; Vogts *et al.*, 2016). Cyperaceae and Liliaceae are not as frequent in the middle catchment compared to the grassland biome and IOCB. Since Cyperaceae and Liliaceae prefer sunny moist to wet habitats (Scott, 1999), it is likely that the general increased dryness due to increased temperature and evaporation, demonstrated by enriched δD_{29-31} values, could account for the reduced frequency. The succession from grass dominated environment to woody shrub and arboreal dominated vegetation, reflects the major vegetation change from grassland to a warm and dry savanna in the middle catchment (Scott, 1982). Pollen assemblages also showed the effects of agricultural activities as *Zea mays* pollen grains were recorded in the Thina River and Mzintlava River tributaries. This finding corroborates with previous studies (Madikizela and Dye, 2003) and Municipal reports (DWS, 2017) which state that maize is commercially grown in lower sections of the Mzintlava River (Kokstad) and Mzimvu (Cedarville) river, and the river mouth (Port St. Johns). Maize is also grown on a smaller subsistence scale in the lower section of the Thina River river (Mount Fletcher) (Madikizela and Dye, 2003). These commercial and subsistence croplands were observed along these tributaries during sampling campaigns.

Lower - The IOCB is dominated by dune forest with sporadic patches of grasslands and herbaceous shrub-like succulent vegetation (Mucina and Rutherford, 2006). Pollen data coincides with this and revealed well-mixed signal of grasses, sedges, herbs and shrubs and some trees (exotic and indigenous). Aquatic taxa such as Cyperaceae and Liliaceae have a significant presence in the IOCB, however, fern spores are absent. This could be due to the brackish nature of the river mouth and estuary (Della and Felkenberg, 2019). The presence of

Euphorbia and *Acalypha* are expected as succulent shrub like vegetation is commonly associated with IOCB vegetation (Mucina and Rutherford, 2006; Scott, 1999).

6.2.2 *n*-Alkane distribution and isotope compositions

Fluvial sediment samples were used to reconstruct the local vegetation composition, sediment and hydrologic dynamics of the Mzimvubu River, using the following proxy methods: compound specific carbon ($\delta^{13}\text{C}$) and hydrogen (δD) isotope ratios and *n*-alkane abundance and distribution.

Stable carbon isotope ($\delta^{13}\text{C}_{29-31}$)

$\delta^{13}\text{C}$ provided insight into changing vegetation compositions and contributions of C_3 versus C_4 . RBS *n*-alkane sediment samples maximized at the nC_{31} nC_{29} and nC_{27} homologue which is to be expected for an environment characterised by grassland, savanna and IOCB vegetation (Poynter *et al.*, 1989). Shorter chain lengths were not common in the Mzimvubu Catchment, indicating that terrestrial higher plants contributed the most to the sedimentary *n*-alkane signal (Vogts *et al.*, 2012). When *n*-alkane chain length data were compared with pollen and norm31 data, it was found that occurrences of nC_{27} and nC_{31} coincided with the presence of arboreal/shrub vegetation and grasses respectively. Furthermore, high norm31 values coincided with longer (nC_{31} ad nC_{33}) chain lengths in the upper Mzimvubu River and Mzintlava River tributaries, whereas lower norm31 ratios coincided with shorter *n*-alkane chain lengths (nC_{27} and nC_{29}) (Chevalier *et al.*, 2015; Carr *et al.*, 2014). $\delta^{13}\text{C}$, *n*-alkane distributions and pollen data revealed a transition from grassland in the upper catchment towards savanna vegetation in the middle catchment, is also accompanied by an average $\delta^{13}\text{C}$ value of -29 ‰ indicating that the predominant vegetation is likely to be C_3 (Vogts *et al.*, 2009).

Conversely, $\delta^{13}\text{C}$ enrichment occurs in the Mzintlava River, Kinira River and river mouth. Fe/K, Al/Si ratios determined that these rivers are associated with increased levels of erosion. Therefore, the enrichment could be due a petrogenic source to sediment organic matter as well as the presence of degraded and of *n*-alkane plant wax lipids (Bouchez *et al.*, 2014). It is also possible to infer that the enrichment could be due to the contribution of C_4 Cyperaceae and *Zea mays* plant types (Still and Powell, 2010; Chevalier *et al.*, 2015; Hamilton *et al.*, 2004), which is evident for the Mzintlava River (nC_{33}) and Kinira River river (nC_{31} and nC_{33}) (Scott, 1999).

Stable hydrogen isotope (δD_{29-31})

This study concluded that hydrogen isotope values are driven by the continental effect and altitude effect rather than the amount effect (Sachse *et al.*, 2012; Gat, 1996; Collins *et al.*,

2013). Variations within δD_{29-31} values of RBS sediments, show the highest elevation sites within the catchment consistently correlate with the most depleted δD_{29-31} signals, and the lowest altitudes coincide with the most enriched δD signals (Herrmann *et al.* 2017; Dansgaard, 1964). (Sachse *et al.* 2012). This held true apart from one exception, which is that the middle catchment showed marginal δD_{29-31} enrichment compared to the river mouth. The enrichment could be due to increased aridity resulting from reduced rainfall and increased seasonality of rainfall indicative of a savanna biome (Mucina and Rutherford, 2006), as well as reduced organic matter content resulting from high concentrations of petrogenic compounds (Schimmelmann *et al.*, 2006).

CPI_{25-33} values yielded predominantly odd-over-even chain lengths, therefore, indicating that *n*-alkane organic matter in river sediment originated from terrestrial higher plants (Boot *et al.*, 2006) (Bray and Evans, 1961; Cranwell, 1984). Reduced CPI values for sediment are common in areas of increased temperature and rainfall as these climatic factors enable organic matter degradation in soils. These findings corroborate with a statement of Richey *et al.*, (1990) wherein lower CPI values are likely as a result of biodegradation due to microbial processes in tropical soils. Therefore, since the low CPI values for SPM samples are unlikely to be caused by microbial activity, SPM could be representing the effects of precipitation induced erosion in the Mzimvubu Catchment as well as anthropogenically induced soil erosion by agricultural activities and land use changes (Richey *et al.*, 1990).

6.2.3 XRF elemental ratios

Elemental ratios Ti/Al, Al/Si and Fe/K represented important sedimentological, erosional and climatological dynamics within the Mzimvubu Catchment (Weltje and Tjallingii, 2008; Zhao *et al.*, 2015). High levels weathering and the fluvial input of fine material were shown through elevated values of Fe/K and Al/Si. In the northern tributaries (Govin *et al.*, 2012). High Fe/K ratios were also attributed to the presence of intensive agricultural activities (iron phosphate in pesticides and fertilisers) and anthropogenic soil erosion (Ekstrom *et al.*, 2016; DWS, 2017). It was also concluded that underlying rock strata affects elemental ratios, wherein The Mzimvubu River and Mzintlava River are also characterised by Fe-rich sandstone, shale and mudstones of the Ecca formations, it is likely that the underlying rock, and subsequent weathering of these rock strata contributes to the elevated Fe/K ratio (Gess, 2012). Furthermore, Al/Si was found to be a good indicator of soil particle grain size. High Al/Si values indicated fine grained material, and low Al/Si values indicated coarse grained material (Govin *et al.*, 2012). As with Al/Si ratios, Ti/Al ratio values also represented particle grain size

distributions within the upper Mzimvubu Catchment. Elevated Ti/Al ratios are indicative of fine material or the aeolian input of dust particles. Reduced Ti/A ratios are an indication of the fluvial input of coarser large grains soil particles. Ti/Al values are lowest at the river mouth and highest at the Mzintlava River, which could imply that the river mouth is receiving fluvial input of large grained soil particles from the rest of the catchment and the Mzintlava River is receiving the fine grained particles transported via aeolian processes from the Indian Ocean.

6.3 FUTURE RESEARCH RECOMMENDATIONS

Taphonomy is a key concern in modern provenance studies as some organic data were lost and others preserved in river bed and suspended sediment samples (Walling *et al.*, 1999; Wakeham *et al.*, 1997). The dynamic transport routes and turbid the nature of depositional environment resulted in organic compounds often being a result of sediment fraction characteristics, as much as it represents the vegetation it passes through (Govin *et al.*, 2012). Erosional processes and reworking in lacustrine (Tierney *et al.*, 2008), marine (Schefuß *et al.*, 2005, 2011) sediments altered the isotope composition of plant biomarkers. This was seen when $\delta^{13}\text{C}$ and δD_{29-31} enrichment coincided with elevated levels of sediment and erosion, thus indicating the input of petrogenic sources and degraded *n*-alkane data over terrestrial plant matter (Bouchez *et al.*, 2014; Herrmann *et al.*, 2016).

When investigating provenance in modern systems, various anthropogenic effects such as water impoundments (dams) should be considered (Xu *et al.*, 2016). A discrepancy was found between palynomorph, *n*-alkane and inorganic frequencies analysed at the mouth compared to the river confluence where there is a man-made weir. An impoundment such as a weir could inhibit the transport of pollen grains, *n*-alkane lipid biomarkers and sedimentary elemental compounds downstream to the river mouth. In light of this, the confluence would be a better representation of catchment vegetation composition compared to the mouth. This is an important consideration for future palaeoreconstruction studies in the area, as the proxy trap could skew proxy provenance dynamics. Moreover, the effect of agricultural corp lands and land use change to anthropogenic pressures can significantly alter *n*-alkane isotope compositions and signatures. The effect of agricultural crops on carbon isotope signals was evident in the northern tributaries, wherein *C4 Zea mays* enriched the $\delta^{13}\text{C}$ signal, despite the general area yielding generally consistently depleted signals throughout the seasons. Land

transformation, erosion and degradation resulted in the addition of degraded organic plant wax lipids from petrogenic sources into river sediments (Vogts *et al.*, 2009).

6.4 REVIEW OF AIM AND OBJECTIVES

The aim of this research was to investigate contemporary fluvial sediment provenance dynamics of the Mzimvubu Catchment, Port St Johns, South Africa. This was achieved by addressing several specific objectives:

- i. To determine whether river sediments contain pollen and plant biomarkers representative of the dominant contemporary vegetation.**

Pollen data were interpreted by analysing the presence or absence of different taxa, whose modern environmental climate tolerances are known. Modern pollen sediment samples yielded pollen assemblages representative of grassland, savanna and IOCB as defined by Mucina and Rutherford (2006) and Acocks (1988). Variations in $n\text{-C}_{31}$ and $n\text{-alkane}$ distributions mirror transitions between grass dominated areas and forested areas. $\delta^{13}\text{C}$ variations indicate a mixture of C_3 grasses, C_3 arboreal vegetation and contributions of C_4 Cyperaceae and *Zea mays*.

- ii. To characterise the pollen, organic matter and sediment signal transported in the Mzimvubu Catchment.**

This objective involved the creation of pollen slides from fluvial river bed sediment to establish palynomorph abundance and assemblage and ultimately vegetation composition within each tributary. $n\text{-Alkane}$ concentrations and distributions and stable carbon and hydrogen isotopic compositions of $n\text{-alkane}$ homologue were established through geochemical analysis. Elemental data were established through XRF analysis and the dominant element compositions for each site were found.

- iii. To determine sediment provenance across the Mzimvubu Catchment by relating proxy data to environmental characteristics.**

Pollen assemblages seemed to follow general climate gradients for the catchment. Grasses and aquatics dominated cooler moister environments in the upper catchment, whereas hardier shrubs and trees dominated the middle catchment characterised by increased aridity, evapotranspiration and reduced rainfall. The lower catchment exhibited coastal dune forest and shrub like vegetation typical of the IOCB (Mucina and Rutherford, 2006).

The environmental and climate indicators derived from pollen data were compared and correlated to $\delta^{13}\text{C}_{29-31}$, δD_{29-31} and norm31 data so that a stronger modern analogue of the environment, vegetation and climate could be developed. $\delta^{13}\text{C}_{29-31}$ and δD_{29-31} were conducted on 32 fluvial river bed sediments. $\delta^{13}\text{C}$ provided data on the compositions of C_3 and C_4 vegetation from the upper catchment to the river mouth, which allowed for inferences to be made about climate conditions. Depleted values coincide with cooler and wetter conditions and enriched $\delta^{13}\text{C}$ values coincide within warmer and drier conditions in the southern tributaries (Ehleringer and Cooper 1988; Scott and Vogel 2000).

Elemental inorganic data provided the opportunity to establish regions of intense weathering, erosion and fluvial versus aeolian input. Element compositions were relatively good indicators of erosional processes, grain size and anthropogenic activities, and poor indicators of climate conditions. When inorganic elemental compositions were correlated to $\delta^{13}\text{C}$ and δD_{29-31} values, high sedimentation rates due to elevated petrogenic sources of organic material, coincided with enriched δD_{29-31} and $\delta^{13}\text{C}_{29-31}$ values (Bouchez *et al.*, 2014). δD_{29-31} enrichment coincided with low elevation areas in close proximity to the sea (Continental and altitude effect) and depleted values in high altitude areas. Therefore, δD_{29-31} represented rainout effect in the Mzimvubu catchment. δD_{29-31} showed a positive correlation to precipitation and temperature and a negative correlation to elevation.

A major advantage of multiproxy provenance studies is the unique contribution each proxy make towards environmental and climatic reconstruction (Lotter, 2005), as each proxy is subject to its own limitations and advantages, as evidenced by variations in $\delta^{13}\text{C}$, δD_{29-31} and pollen records.

iv. To determine whether element composition analysis are representative of the surrounding geomorphology and contemporary land-use practices.

Elemental compounds were analysed individually at first and the most abundant element compositions for each sample site. However, it was found that elemental ratios provided more compressive insight into climate-vegetation-sediment relationships in the catchment. In some instances in the northeastern tributaries, Fe/K and AL/Si ratios indicated high erosion rates due to anthropogenic causes and underlying rock strata. Ti/AL was found to be an accurate representation of grains size and aeolian versus fluvial input.

v. To discuss the implications for using terrestrial markers to interpret marine sediments offshore of the Mzimvubu Catchment.

We conclude that long chain *n*-alkanes from the Mzimvubu catchment represent a mixed signal from the upper, middle and lower tributaries. These findings should be considered in the interpretation of proxy records used in marine sediment palaeoclimatological studies. The results of this study have shown that $\delta^{13}\text{C}$, δD and XRF are accurate representations of the modern catchment environmental and climatological conditions, and therefore can provide a modern reference for marine sediment core interpretations. In order to expand and increase the understanding of vegetation, sediment and hydrological signals in the Mzimvubu catchment and marine sediment cores extracted from its river mouth, future studies should focus on the quantifying the contributions from different tributaries.

6.5 CONCLUDING REMARKS

This study has achieved its aims and has contributed to a more comprehensive understanding of the modern vegetation, sediment and hydrological conditions in the Mzimvubu catchment of the Eastern Cape region. Proxy signals were influenced by various environmental, physiological and taphonomic processes. These findings present the first comprehensive multiproxy overview of vegetation, sediment and hydrologic provenance based on palynomorph abundance, *n*-alkane isotopic distributions and elemental compound dynamics within the Mzimvubu Catchment, which can aid the interpretation of marine sediment cores for future palaeoclimatological and palaeoenvironmental research. Although δD_{29-31} and $\delta^{13}\text{C}_{29-31}$ produced reliable spatial and temporal datasets, it is important to consider the need for the multiproxy approach for this region. Without supplementing $\delta^{13}\text{C}_{29-31}$ and δD_{29-31} values with elemental compositions and pollen assemblages, it would have been difficult to account for and interpret $\delta^{13}\text{C}_{29-31}$ and δD_{29-31} variations. A cautionary measure should be taken when analysing modern sediment samples, which is the effects of taphonomy, transport processes and deposition environment and the effects these processes may have on terrestrial biomarker transport and preservation. Terrestrial sediment samples were successfully used to elucidate environmental and climate-vegetation relationships within the catchment to overcome the paucity of long term continuous temporal records. The multiproxy provenance approach presented here has shown that southern Africa is a suitable site for provenance based research and palaeoenvironmental research.

REFERENCES

- Acocks, J.P.H.(1988). Veld types of South Africa. *Memoirs of the Botanical Survey of South Africa*, 57, Botanical Research Institute, Pretoria.
- Andersen, S. (1973). The differential pollen productivity of trees and its significance for the interpretation of a pollen diagram from a forested region. In: Birks, H.J.H., West, R.G. (eds). *Quaternary Plant Ecology: 14th Symposium*, British Ecological Society, 109-115. Blackwell Scientific Publishers, Cambridge, London.
- Anderson, D.E., Goudie, A.S., Parker, A.G. (2007). *Global environments through the Quaternary: Exploring environmental change*. Oxford University Press, Oxford.
- Ardenghi, N., Mulch, A., Pross, J., Niedermeyer, E.M. (2017). Leaf wax *n*-alkane extraction: An optimised procedure. *Organic Geochemistry*, 113, 283-292.
- Badewien, T., Vogts, A., Rullkötter, J. (2015). *n*-Alkane distribution and carbon isotope composition in leaf waxes of C₃ and C₄ plants from Angola. *Organic Geochemistry*, 89-90, 71-79.
- Bai, Y., Fang, X., Nie, J., Wang, Y., Wu, F. (2008). A preliminary reconstruction of the paleoecological and paleoclimatic history of the Chinese Loess Plateau from the application of biomarkers. *Palaeogeography, Palaeoclimatology, Palaeoecology*, 271, 161-169.
- Baker, R.G., Gonzalez, L.A., Raymo, M., Bettis III, E.A., Reagan, M.K., Dorale, J.A. (1998). Comparison of multiple proxy records of Holocene environments in the Midwestern United States. *Geology*, 26(1), 1131-1134.

- Barreto, C., Vilela, C., Baptista-Neto, J.A., Barth, O.M. (2012). Spatial distribution of pollen grains and spores in surface sediments of Guanabara Bay, Rio de Janeiro, Brazil. *Anal. of the Brazilian Academy of Sciences*, 84(3), 627-643.
- Bassham, J.A., Benson, A.A., Kay, L.D., Harris, A.Z., Wilson, A.T., Calvin, M. (1954). The path of carbon dioxide in photosynthesis XXI. The cyclic regeneration of carbon dioxide acceptor. *Journal of the American Chemical Society*, 76, 1760-1770.
- Basu, S., Agrawal, S., Sanyal, P., Mahato, P. (2015). Carbon isotope ratios of modern C3-C4 plants from the Gangetic Plain, India and its implications to paleovegetational reconstruction. *Palaeogeography, Palaeoclimatology, Palaeoecology*, 440. Online: https://www.researchgate.net/figure/Histogram-of-d-13-C-values-of-C-3-and-C-4-plants-measured-in-this-study-The-average-d-13_fig2_281117418
- Bennet, K.D. (2005). C programs for plotting pollen diagrams and analysing pollen data. Quaternary Geology, Department of Earth Sciences, Sweden. Documentation manual for psimpoll 4.25 and pscomb 1.03.
- Bennett, K. D. (1988): Post-glacial vegetation history: ecological considerations. In: Huntley, B., and Thompson, W. (eds). *Vegetation History*, Springer Nature, Switzerland, 699-724.
- Bertrand, S., Huguenot, K.A., Sepúlveda, J., Pantoja, S. (2012). Geochemistry of surface sediments from the fjords of Northern Chilean Patagonia (44-47°S): Spatial variability and implications for palaeoclimate reconstructions. *Geochimica et Cosmochimica Acta*, 76, 125-146.
- Bi, X., Sheng, G., Liu, X., Li, C., Fu, J. (2005). Molecular and carbon hydrogen isotopic composition of *n*-alkanes in plant leaf waxes. *Organic Geochemistry*, 36, 1405-1417.
- Birks, H.J.B. (1981). The use of pollen analysis in the reconstruction of past climates: a review. In: Wigley, T.M.L., Ingram, M.J., Farmer, G. (eds). *Climate and History. Studies in past climate and their impact of man*, Cambridge University Press, Cambridge, 111-138.
- Birks, H.J.B., and Birks, H.H. (1980). *Quaternary Palaeoecology*, Edward Arnold, London.
- Birks, H.J.B., and Gordon, A.D. (1985). *Numerical methods in Quaternary pollen analysis*, Academic Press, London.
- Biscaye, P. E. (1965), Mineralogy and sedimentation of recent deep-sea clay in the Atlantic Ocean and adjacent seas and oceans. *Geological Society of America Bulletin*, 76(7), 803-832.

- Blaser, M., and Conrad, R. (2016). Stable isotope fractionation as tracer of carbon cycling in anoxic soil ecosystems. *Current Opinion in Biotechnology*, 41, 122-129.
- Bliedtner, M., Schäfer, I.K., Zech, R., von Suchodoletz, H. (2018). Leaf wax *n*-alkanes in modern plants and topsoils from eastern Georgia (Caucasus): implications for reconstructing regional paleovegetation. *Biogeosciences*, 15, 3927-3936.
- Boom, A., Carr, A.S., Chase, B.M., Grimes, H.L., Meadows, M.E. (2014). Organic Geochemistry Leaf wax *n*-alkanes and $\delta^{13}\text{C}$ values of CAM plants from arid southwest Africa. *Organic Geochemistry*, 67, 99-102.
- Boot, C.S., Ettwein, V.J., Maslin, M.A., Weyhenmeyer, C.E., Pancost, R.D. (2006). A 35,000 year record of terrigenous and marine lipids in Amazon Fan sediments. *Organic Geochemistry*, 37, 208–219.
- Bouchez J., Gaillardet J., France-Lanord C., Maurice L. and Dutra-Maia P. (2011). Grain size control of river suspended sediment geochemistry: clues from Amazon River depth profiles. *Geochemistry, Geophysics, Geosystems*, 12, 24.
- Bouchez, J., Galy, V., Hilton, R. G., Gaillardet, J., Moreira-Turcq, P., Pérez, M. A., et al. (2014). Source, transport and fluxes of Amazon River particulate organic carbon: Insights from river sediment depth-profiles. *Geochimica et Cosmochimica Acta*, 133, 280–298.
- Bouillon, M., and Beirne, P. (1987). CorelDRAW. Corel Corporation.
- Boyd, W.E. and Hall, V.A. (1998). New frontiers and applications in palynology. In: IX International Palynological Congress, Houston, Texas, USA. *Review of Palaeobotany and Palynology*, 103, 1-83.
- Bradshaw, R.H.W. (2008). Detecting human impact in the pollen record using data-modelled comparison. *Vegetation History and Archaeobotany*, 17, 597-603.
- Bramlet, M. N., and Bradley, W. H. (1940). Geology and biology of North Atlantic Deep sea cores between Newfoundland and Ireland Part 1: Lithology and geologic interpretation. *Geological Survey Professional*, Paper 196-A, 1-222.
- Braun, K., Nehme, C., Pickering, R., Rogerson, M., Scroxton, N. (2018). A window into Africa's past hydroclimates: the SISAL_V1 database contribution. *Quaternary Reviews*, 2(4), 1-28.

- Bray, E.E. and Evans, E.D. (1961). Distribution of *n*-paraffins as a clue to recognition of source beds. *Geochimica et Cosmochimica Acta*, 22, 2-15.
- Brewer, S., Guiot, J., Barboni, D. (2013). Pollen methods and studies: Use of pollen as climate proxies. University Paul Cezanne, Elsevier B.V.
- Bricklin, D., (1978). *Mircosoft Excel*.
- Brown, A.G., Carpenter, R.G., Walling, D.E. (2007). Monitoring fluvial pollen transport, its relationship to catchment vegetation and implications for palaeoenvironmental studies. *Review of Palaeobotany and Palynology*, 147, 60-76.
- Bruckner, M.Z., n.d. *A Primer on Stable Isotopes and Some Commone uses in Hydrology*. Montana State University, Bozeman. Available online: https://serc.carleton.edu/microbelife/research_methods/environ_sampling/stableisotopes.html
- Bunting, M.J. (2008). Pollen in Wetlands: using simulations of pollen dispersal and deposition to better interpret the pollen signal. *Biodiversity Conservation*, 17, 2076-2096.
- Burdanowitz, N., Dupont, L., Schefuß, E., Zabel, M. (2018). Holocene hydrologic and vegetation developments in the Orange River catchment (South Africa) and their controls. *The Holocene*, 1–13.
- Bush, R.T., and McInerney, F.A. (2013). Leaf wax *n*-alkane distributions in and across modern plants: Implications for paleoecology and chemotaxonomy. *Geochimica et Cosmochimica Acta*, 117, 161-179.
- Calvert, S., and Pedersen, T.F. (2007). Chapter fourteen Elemental proxies for palaeoclimatic and palaeoceanographic variability in marine sediments: Interpretation and Application. In: *Developments in Marine Geology*, Elsevier, B.V. doi: 10.1016/S1572-5480(07)01019-6
- Campbell, I.D. (1991). Experimental mechanical destruction of pollen grains. *Palynology* 15: 29-33.
- Campbell, I.D., and Chmura, G.L. (1994). Pollen distribution in the Atchafalaya River, U.S.A. *Palynology*, 18, 55–65.
- Carr, A.S., Boom, A., Chase, B.M., Meadows, M.E., Grimes, H.L., (2015). Holocene sea level and environmental change on the west coast of South Africa: evidence from plant biomarkers, stable isotopes and pollen. *Journal of Paleolimnology*, 53, 415–432.

- Carr, A.S., Boom, A., Grimes, H.L., Chase, B.M., Meadows, M.E., Harris, A., (2014). Leaf wax n-alkane distributions in arid zone South African flora: Environmental controls, chemotaxonomy and palaeoecological implications. *Organic Geochemistry*, 67, 72–84.
- Carr, A.S., Thomas, D.S.G., Bateman, M.D., Meadows, M.E., Chase, B.M., (2006). Late Quaternary palaeoenvironments of the winter-rainfall zone of southern Africa: Palynological and sedimentological evidence from the Agulhas Plain. *Palaeogeography, Palaeoclimatology, Palaeoecology*, 239, 147–165.
- Carrión, J.S. (2002). A taphonomic study of modern pollen assemblages from dung and surface sediments in arid environments of Spain. *Review of Palaeobotany and Palynology*, 120, 217–232.
- Cassia, R., Nociono, M., Correa-Aragunde, N., Lamattina, L. (2018). Climate change and the impact of greenhouse gasses: CO₂ and NO₂, friends and foes of plant oxidative stress. *Frontiers in Plant Science*, 9, 273 – 284.
- Castaneda, I.S., and Schouten, S. (2011). A review of molecular organic proxies for examining modern and ancient lacustrine environments. *Quaternary Science Reviews*, 30, 2851–2891.
- Castañeda, I.S., Werne, J.P. Johnson, T.C., Filley, T.R., (2009). Late Quaternary vegetation history of southeast Africa: The molecular isotopic record from Lake Malawi. *Paleogeography, Palaeoclimatology, Palaeoecology*, 275, 100–112.
- Catuneanu, O., Wopfner, H., Eriksson, P.G., Cairncross, B., Rubidge, B.S., Smith, R.M.H., Hancox, P.J. (2005). The Karoo basins of south-central Africa. *Journal of African Earth Sciences*, 43, 211–253.
- Cerling, T., Wang, Y., Quade, J. (1993). Expansion of C₄ ecosystems as an indicator of global ecological change in the late Miocene. *Letters to Nature*, 361, 344–345.
- Chase, B.M., and Meadows, M.E. (2007). Late Quaternary dynamics of southern Africa's winter rainfall zone. *Earth-Science Reviews*, 84, 103–138.
- Chase, B.M., Boom, A., Carr, A.S., Meadows, M.E., Reimer, P.J. (2013). Holocene climate change in southernmost South Africa: rock hyrax middens record shifts in the southern westerlies. *Quaternary Science Reviews*, 82, 199–205.

- Chase, B.M., Lim, S., Chevalier, M., Boom, A., Carr, A.S., Meadows, M.E., Reimer, P.J. (2015). Influence of tropical easterlies in southern Africa's winter rainfall zone during the Holocene. *Quaternary Science Reviews*, 107, 138-148.
- Chase, B.M., Meadows, M.M., Carr, A.S., Reimer, P.J. (2010). Evidence for progressive Holocene aridification in southern Africa recorded in Namibian hyrax middens: Implications for African Monsoon dynamics and the "African Humid Period". *Quaternary Research*, 74, 36-45.
- Chen H.F., Yeh, P.Y., Song, S.R., Hsu, S.C., Yang, T.N., Wang, Y., Chi, Z., Lee, T.Q., Chen, M.T., Cheng, C.L., Zou, J., Chang, Y.P. (2013). The Ti/Al molar ratio as a new proxy for tracing sediment transportation processes and its application in aeolian events and sea level change in East Africa. *Journal of Asian Earth Science*, 73, 31-38.
- Chen, C., Deng, Y., Zheng, Z., Zhang, H. (2004). Distribution characteristics of pollen and spores in surface sediments of near shore waters between Hong Kong and Daya Bay. *Journal of Tropical Oceanography*, 23, 75-81.
- Chen, H.F., Song, S.R., Lee, T.Q., Löwemark, L., Chi, Z.Q., Wang, Y., Hong, E. (2010). A multiproxy lake record from Inner Mongolia displays a late Holocene teleconnection between central Asian and North Atlantic climate. *Quaternary International*, 227, 170–183.
- Cherisch, M.F. and Wright, C.Y (2019). Climate change adaptation in South Africa: a case study on the role of the health sector. *Globalisation and Health*, 15(22), 1-16.
- Chevalier, M., and Chase, B.M. (2015). Southeast African records reveal a coherent shift from high- to low-latitude forcing mechanisms along the east African margin across last glacial–interglacial transition. *Quaternary Science Reviews*, 125, 117–130.
- Chibnall, A.C., Piper, S.H., Pollard, A., Williams, E.F., Sahai, P.N. (1934). The constitution of the primary alcohols, fatty acids and paraffins present in plant and insect waxes. *Biochemical Journal*, 28, 2189-2208.
- Chmura, G.L., and Liu, K.-B. (1990). Pollen in the lower Mississippi. *Reviews of Palaeobotany and Palynology*, 64, 252–261. Chmura, G.L., Smirnov, A., Campbell, I.D. (1999). Pollen transport through distributaries and depositional patterns in coastal waters. *Palaeogeography, Palaeoclimatology, Palaeoecology*, 149, 257-270.

- Clément, L., Muriel, V., Aurélie, P., Nathalie, C.-N., Vincent, L., Olivier, R., Gwendoline, G. (2017). Modern palynological record in the Bay of Brest (NW France): Signal calibration for palaeoreconstructions. *Review of Palaeobotany and Palynology*, 244, 13-25.
- Clift, P.D., Wan, S.M., Blusztajn, J. (2014). Reconstructing chemical weathering, physical erosion and monsoon intensity since 25 Ma in the northern South China Sea: a review of competing proxies. *Earth Science Reviews*, 130, 86–102.
- Cloete, A.J., Coetzee, F. (1991). *Geological Survey: [South Africa] 1:250 000 Umtata*. Pretorial (South Africa), Government Printer, series (3128).
- Coates Palgrave, K. (2002). *Trees of Southern Africa*. Coates Palgrave, M. (ed), 3rd edition. Struik Publishers (Pty) Ltd., Cape Town.
- Coetzee, J.A., and van Zinderen Bakker, E.M. (1970). Palaeoecological problems of the quaternary of Africa. *South Africa Journal of Science*, 66, 78-84.
- Coggan, R., Populus, J., White, J., Sheehan, K., Fitzpatrick, F., Piel, S. (eds.) (2007). *Review of Standards and Protocols for Seabed Habitat Mapping*. MESH.
- Collins, J.A., Schefuß, E., Mulitza, S., Prange, M., Werner, M., Tharammal, T., Paul, A., Wefer, G. (2013). Estimating the hydrogen isotopic composition of past precipitation using leaf-waxes from western Africa. *Quaternary Science Reviews*, 65, 88–101.
- Collister, J.W., Rieley, G., Stern, B., Eglinton, G., Fry, B. (1994). Compound-specific $\delta^{13}\text{C}$ analyses of leaf lipids from plants with differing carbon dioxide metabolisms. *Organic Geochemistry*, 21, 619–627.
- Cranwell P. A. (1984) Lipid geochemistry of sediments from Upton Broad, a small productive lake. *Organic Geochemistry*, 7, 25–37.
- Cranwell P. A., Eglinton G., Robinson N. (1987) Lipids of aquatic organisms as potential contributors to lacustrine sediments – II. *Organic Geochemistry*. 11, 513–527.
- Cushing, E. J. (1967). Evidence for differential pollen preservation in late Quaternary sediments in Minnesota. *Reviews of Palaeobotany and Palynology*, 4: 87 – 101.
- Daniau, A.-L., Sánchez Goni, M.F., Martinez, P., Urrego, D.H., Bout-Roumazeilles, V., Desprat, S., Marlon, J.R. (2013). Orbital-scale climate forcing of grassland burning in southern Africa. *Proceedings of the National Academy of Sciences*, 110-5069-5073.

Dansgaard, W. (1964). Stable isotopes in precipitation. *Tellus*, 16(4), 436–468. Available at: <https://doi.org/10.1111/j.2153-3490.1964.tb00181>.

Davis, B.A.S., Zanon, M., Collins, P., Mauri, A., Bakker, J., Barboni, D., Barthelmes, A., Beaudoin, C., Bjune, A.E., Bozilova, E. (2013) The European Modern Pollen Database (EMPD) project. *Vegetation History and Archaeobotany*, 22: 521–530

de Souza, J.R.B., Zucchi, M.R., Costa, A.B., de Azevedo, A.E.G., Spano, S. (2017). Geochemical markers of sedimentary organic matter in Todos os Santos Bay, Bahia-Brazil. Indicators of sources and preservation. *Marine pollution*. Available at: <http://dx.doi.org/10.1016/j.marpolbul.2017.04.020>.

de Villiers, S.E., and Cadman, A., (1997). Palynology of tertiary sediments from a palaeochannel in Namaqualand, South Africa. *Palaeontologica Africana*, 34, 69-99.

De Vries, B. J. and Wijmstra, T. A. (1986): Some aspects of plotting pollen diagrams. *Pollen et Spores*, 28, 457-468.

Delcourt, P.A., and Delcourt, H.R. (1980). Pollen preservation and Quaternary environmental history in the south-eastern United States. *Palynology*, 4, 215–231.

Della, A.P., and Falkenberg, D.B. (2019). Pteridophytes as ecological indicators: an overview. *Hoehnea*, 46(1), 1-25.

Deng, Y., Cai, C., Xia, D., Ding, S., Chen, J. (2017). Fractal features of soil particle size distribution under different land-use patterns in the alluvial fans of collapsing gullies in the hilly granitic region of southern china. *PLOS ONE*, 12 (3). Available on: <https://doi.org/10.1371/journal.pone.0173555>.

Department of Water and Sanitation (DWS), South Africa. (2017). *Determination of Water Resource Classes and Resource Quality Objectives for Water Resources in the Mzimvubu Catchment*. Status Quo and (RU and IUA) Delineation Report. Prepared by Rivers for Africa eFlows Consulting (Pty) Ltd. for Scherman Colloty and Associates cc. Report no.: WE/WMA7/00/CON/CLA/0316

Deutsch, L.P., (1986). Ghostscript. Alladin enterprises.

Diefendorf A. F., Freeman K. H., Wing S. L. and Graham H. V. (2011) Production of n-alkyl lipids in living plants and implications for the geologic past. *Geochimica et Cosmochimica Acta*, 75, 7472–7485.

- Diefendorf, A.F., and Freimuth, E.J. (2017). Extracting the most from terrestrial plant-derived *n*-alkyl lipids and their carbon isotopes from the sedimentary record: A review. *Organic Geochemistry*, 103, 1-21.
- Diefendorf, A.F., Mueller, K.E., Wing, S.L., Koch, P.L., Freeman, K.H. (2010). Global patterns in leaf $\delta^{13}\text{C}$ discrimination and implications for studies of past and future climate. *Proceedings of the National Academy of Sciences*, 107(13), 5738-5743.
- Doan, L.P., Nguyen, T.T., Pham, M.Q., Tran, Q.T., Pham, Q.L., Tran, D.Q., Than, V.T., Bach, L.G. (2019). Extraction process, identification of fatty acids, tocopherols, sterols and phenolic constituents and antioxidant evaluation of seed oils from five Fabaceae species. *Processes*, 7(456), 1-11.
- Driessen, P., Deckers, J., Spaargaren, O., Nachtergaele, F. (2001). *Lecture Notes on the Major Soils of the World*, Food and Agricultural Organisation, Rome.
- Dupont, L.M., Rommerskirchen, F., Mollenhauer, G., Schefuß, E. (2013). Miocene to Pliocene changes in South African hydrology and vegetation in relation to the expansion of C₄ plants. *Earth and Planetary Science Letters*, 375, 408–417.
- Eglinton G., and Logan G. A. (1991) Molecular preservation. *Transactions of the. Royal Society London Biological Science*, 333, 315–328.
- Eglinton, G., and Hamilton, R.J. (1967). Leaf epicuticular waxes. *Science*, 156, 1322-1335.
- Eglinton, G., Hamilton, R.J., 1963. The distribution of alkanes. In: Swain, T. (ed.), *Chemical Plant Taxonomy*. Academic Press, New York, 187–217.
- Eglinton, T.I., Eglinton, G., Dupont, L., Sholkovitz, E.R., Montluçon, D., Reddy, C.M. (2002). Composition, age, and provenance of organic matter in NW African dust over the Atlantic Ocean. *Geochemistry Geophysics Geosystems* 3, 1050.
- Ehleringer, J.R., and Cooper, T.A. (1988). Correlations between carbon isotope ratio and microhabitat in desert plants, *Oecologia*, 76, 562–566.
- Ehleringer, J.R., and Dawson, T.E. (1992). Water uptake by plants: perspectives from stable isotope composition. *Plant, Cell and Environment*, 15, 1073–1082.

- Ekstrom, S.M., Regnell, O., Reader, H.E., Nilsson, P.A., Löfgren, S., Kritzberg, E.S. (2016). Increasing concentrations of iron in surface waters as a consequence of reducing conditions in the catchment area. *Journal of Geophysical Research: Biogeosciences*, 121, 479-493.
- Environmental Systems Research Institute (ESRI). (1999). ArcMap Release 8.0. Redlands, CA.
- Faegri, K., (1966). Some problems of representativity in pollen analysis. *Palaeobotany*, 15, 135-140.
- Faegri, K., and Iverson, J. (1989). *Textbook of pollen analysis*, John Wiley and Sons, Chichester.
- Fall, P.L. (1987). Pollen taphonomy in a canyon stream. *Quaternary Research*, 28, 393-406.
- Feakins, S.J., and Sessions, A.L. (2010). Controls on the D/H ratios of plant leaf waxes in an arid ecosystem. *Geochimica et Cosmochimica Acta*, 74, 2128–2141.
- Ficken, K.J., Li, B., Swain, D.L., Eglinton, G. (2000). An *n*-alkane proxy for the sedimentary input of submerged/floating freshwater aquatic macrophytes. *Organic Geochemistry*, 31, 745–749.
- Fitchett, J.M., Grab, S.W. Bamford, M.K., Mackay, A.W. (2016). A multi-disciplinary review of late Quaternary palaeoclimates and environments for Lesotho. *South African Journal of Science*, 112 (7-8), 1-9.
- Fitchett, J.M., Grab, S.W. Bamford, M.K., Mackay, A.W. (2017). Late Quaternary research in southern Africa: progress, challenges and future trajectories. *Transactions of the Royal Society of South Africa*, doi: 10.1080/0035919X.2017.1297966.
- Flanagan, L.B., and Ehleringer, J.R. (1991). Stable isotope composition of stem and leaf water: applications to the study of plant water use. *Functional Ecology*, 5, 270–277.
- Galy, V., Eglinton, T., France-Lanord, C., Sylva, S. (2011). The provenance of vegetation and environmental signatures encoded in vascular plant biomarkers by the Ganges-Brahmaputra rivers. *Earth and Planetary Science Letters*, 304, 1-12.
- Garcin, Y., Schwab, V.F., Gleixner, G., Kahmen, A., Todou, G., Séné, O., Onana, J.M., Achoundong, G., Sachse, D. (2012). Hydrogen isotope ratios of lacustrine sedimentary *n*-

alkanes as proxies of tropical African hydrology: insights from a calibration transect across Cameroon. *Geochimica et Cosmochimica Acta*, 79, 106-126.

Garzanti, E., Vermeesch, P., Andò, S., Lustrino, M., Padoan, M., Vezzoli, G., (2014). Ultra-long distance littoral transport of Orange sand and provenance of the Skeleton Coast Erg (Namibia). *Marine Geology*, 357, 25–36.

Gat, J.R. (1996). Oxygen and hydrogen isotopes in the hydrologic cycle. *Annual Review of Earth and Planetary Sciences*, 24, 225-262.

Gess, R. 2012. *Proposed Tombo Mafini electrical transmission line in the Port St. Johns local municipality- palaeontological impact assessment*. Research Associate of the Albany Museum.

Goldberg, E.D., and Arrhenius, G.O.S. (1958). Chemistry of Pacific pelagic sediments. *Geochimica et Cosmochimica Acta*, 13, 152–212.

Gonfiantini, R., Roche, M.A., Olivry, J.C., Fontes, J.C., Zuppi, G.M. (2001). The altitude effect on the isotopic composition of tropical rains. *Chemical Geology*, 181, 147–167.

Govin, A., Holzwarth, U., Heslop, D., Ford Keeling, L., Zabel, M., Mulitza, S., Collins, J.A., Chiessi, C.M. (2012). Distribution of major elements in Atlantic surface sediments (36°N-49°S): Imprint of terrigenous input and continental weathering. *Geochemistry, Geophysics, Geosystems*, 13, 1–23.

Groot, J.J. (1966) Some observations on pollen grains in suspension in the estuary of the Delaware River. *Marine Geology*, 4: 409-416.

Haggi, C., Sawakuchi, A.O., Chiessi, C.M., Mulitza, S., Mollenhauer, G., Sawakuchi, H.O., Baker, P.A., Zabel, M., Schefuß, E. (2016). Origin, transport and deposition of leaf wax biomarkers in the Amazon Basin and the adjacent Atlantic. *Geochimica et Cosmochimica Acta*, 192, 149-165.

Hahn, A., Miller, C., Bouimetarhan, A.S., Cawthra, H.C., Garzanti, E., Green, A.N., Radeff, G., Schefuß, E., Zabel, M. (2018). The provenance of terrigenous components in marine sediments along the East coast of Southern Africa. *Geochemistry, Geophysics, Geosystems*, 19, 1-17.

Hall, S.A., (1989). Pollen analysis and palaeoecology of alluvium. *Quaternary Research*, 31, 435–438.

- Hamilton S. K., Sippel S. J. and Melack J. M. (2004) Seasonal inundation patterns in two large savanna floodplains of South America: the Llanos de Moxos (Bolivia) and the Llanos del Orinoco (Venezuela and Colombia). *Hydrological Processes*, 18, 2103–2116.
- Havinga, A. J. (1967). Palynology and pollen preservation. *Reviews of Palaeobotany and Palynology*, 2: 81-89.
- Havinga, A.J. (1963). A palynological investigation of soil profiles developed in cover sand. *Mededelingen Landbouwhogeschool Wageningen*, 63(1), 1-93.
- Havinga, A.J. (1984). A 20-year experimental investigation into the differential corrosion susceptibility of pollen and spores in various soil types. *Pollen et Spores*, 26: 541-558
- Hemingway, J.D., Schefuß, E., Dinga, B.J., Pryer, H. Galy, V.V. (2016). Multiple plant-wax compounds record differential sources and ecosystem structure in large river catchments. *Geochimica et Cosmochimica Acta*, 184, 20-40.
- Herbert, A.V., and Harrison, S.P. (2016). Evaluation of a modern-analogue methodology for reconstructing Australian palaeoclimate from pollen. *Review of Palaeobotany and Palynology*, 2(26), 65-77.
- Herrmann, N., Boom, A., Carr, A.S. Chase, B.M., West, A.G., Zabel, M., Schefuß, E. (2017). Hydrogen isotope fractionation of leaf wax *n*-alkanes in southern African soils. *Organic Geochemistry*, 109, 1-13.
- Herrmann, N., Boom, A., Carr, A.S., Chase, B.M., Granger, R., Hahn, A., Zabel, M., Schefuß, E. (2016). *Quaternary Science Reviews*, 149, 215-229.
- Hoffman, J.H., and Moran, V.C. (1991). Biological control of *Sesbania punicea* (Fabaceae) in South Africa. *Agriculture, Ecosystems and Environment*, 37, 157-173.
- Holloway, R.G. (1989). A 20-year experimental investigation into the differential corrosion susceptibility of pollen and spores in various soil types. *Pollen et Spores*, 26, 541-558.
- Hou, J.Z., D'Andre, W.J., MacDonald, D., Huang, Y. (2007). Hydrogen isotopic variability in leaf waxes among terrestrial and aquatic plants around Blood Pond, Massachusetts, USA. *Organic Geochemistry*, 38, 977-84.
- Howe, S., and Webb, T. (1983). Calibrating pollen data in climatic terms: improving the methods. *Quat. Sci. Rev.* 2, 17–51.

- Huang Y., Street-Perrott F. A., Metcalfe S. E., Brenner M., Moreland M. and Freeman K. H. (2001). Climate change as the dominant control on glacial-interglacial variations in C₃ and C₄ plant abundance. *Science*, 293, 1647–1651.
- Huang, Y., Dupont, L., Sarnthein, M., Hayes, J.M., Eglinton, G. (2000). Mapping of C₄ plant input from North West Africa into North East Atlantic sediments. *Geochimica et Cosmochimica Acta*, 64(20), 3505-3513.
- Huang, Y., Lockheart, M., Collister, J.W., Eglinton, G. (1995). Molecular and isotopic biogeochemistry of the Miocene Clarkia formation: Hydrocarbons and Alcohols. *Organic Geochemistry*, 23, 785-801.
- Hulme, M., and Jones, P.D. (1994). Global climate change in the instrumental period. *Environmental Pollutions*, 83, 23-36.
- Hunt, C.O. (1987). Comment: the palynology of fluvial sediments: with special reference to alluvium of historic age from the Upper Axe Valley, Mendip Hills, Somerset. *Transactions of the Institute of British Geographers*, 12(3), 364-367.
- Intergovernmental Panel on Climate change (IPCC). (2014). Summary for Policymakers: In: *Climate change 2014: Synthesis Report*. Contribution of Working Group I, II and III to the Fifth Assessment Report (AR5) of the Intergovernmental Panel on Climate Change [Core Writing Team: Pachauri, R.K., Meyers, L.A. (eds), IPCC, Geneva, Switzerland].
- International Atomic Energy Agency (IAEA). (1997). *Sampling, storage and sample preparation procedures for X-ray fluorescence analysis of environmental materials*, IAEA-TECDOC-950. IAEA, Austria.
- Jacobson, G.L and Bradshaw, R.H.W. (1981). The selection of sites for palaeovegetational studies. *Quaternary Research*, 16, 80-96.
- Jansen, J.H., Van Der Gaast, S.J., Koster, B., Vaars, A.J. (1998). CORTEX, a shipboard XRF-scanner for element analyses in split sediment cores. *Marine Geology*, 151, 143–153.
- Jones, J.G. (1969). Studies on lipids of soil micro-organisms with particular reference to hydrocarbons. *Microbiology*, 59, 145-152.
- Jordaan, M. (2005). FSA contributions 18: Salicaceae s. str. *Bothalia*, 35(1), 7-20.

- Jordaan, M., van Wyk, A.E., Maurin, O. (2011). A conspectus of *Combretum* (Combretaceae) in southern Africa, with taxonomic and nomenclature notes on species and sections. *Bothalia*, 41(1), 135-160.
- Kahmen, A., Hoffmann, B., Schefuß, E., Arndt, S. K., Cernusak, L. A., West, J. B., Sachse, D. (2013). Leaf water deuterium enrichment shapes leaf wax n-alkane δD values of angiosperm plants II: Observational evidence and global implications. *Geochimica et Cosmochimica Acta*, 111, 50–63.
- Kiage, L.M., and Liu, K.B. (2006). Late Quaternary paleoenvironmental changes in Easter Africa: a review of multiproxy evidence from palynology lake sediments, and associated records. *Progress in Physical Geography*, 30(5), 633-658.
- Krull, E., Sachse, D., Mügler, I., Thiele, A., Gleixner, G. (2006). Compound-specific $\delta^{13}C$ and δ^2H analyses of plant and soil organic matter: a preliminary assessment of the effects of vegetation change on ecosystem hydrology. *Soil Biology and Biochemistry*, 38, 3211–3221.
- Kuechler, R.R., Schefuß, E., Beckmann, B., Dupont, L., Wefer, G. (2013). NW African hydrology and vegetation during the Last Glacial cycle reflected in plant-wax-specific hydrogen and carbon isotopes. *Quaternary Science Reviews*, 82, 56-67.
- Leaney, F.W., Osmond, C.B., Allison, G.B., Ziegler, H. (1985). Hydrogen-isotope composition of leaf water in C3 and C4 plants - its relationship to the hydrogen isotope composition of dry matter. *Planta*, 164, 215–220.
- Li C., Sessions A. L., Valentine D. L. and Thiagarajan N. (2011). D/H variation in terrestrial lipids from Santa Barbara Basin over the past 1400 years: a preliminary assessment of paleoclimatic relevance. *Organic Geochemistry*, 42, 15–24.
- Li, L., Li, Q., Tian, J., Wang, H., Wang, P. (2013). Low latitude hydro-climatic changes during the Plio-Pleistocene: evidence from high resolution alkane records in the southern South China Sea. *Quaternary Science Reviews*, 78, 209–224.
- Li, Y.-C., Xu, Q.-H., Y, X.-L., Chen, H., Lu, X.-M. (2005). Pollen-vegetation relationship and pollen preservation on the Northeastern Qinghai-Tibetan Plateau. *Grana*, 44(3), 160-171.
- Lim, S., Chase, B.M., Chavalier, M., Reimer, P.J. (2016). 50,000 years of vegetation and climate change in the southern Namib Desert, Pella, South Africa. *Palaeogeography, Palaeoclimatology, Palaeoecology*, 451, 197-209.

- Liu, J.L. (1989). Vegetational and climatic changes at Gushantun bog in Jilin, NE China since 13000 Y.BP. *Acta Palaeontologica Sinica*, 28, 240-248.
- Liu, W., and Yang, H. (2008). Multiple controls for the variability of hydrogen isotopic compositions in higher plant n-alkanes from modern ecosystems. *Global Change Biology* 14, 2166–2177.
- Liu, W., Yang, H., Li, L. (2006). Hydrogen isotopic compositions of *n*-alkanes from terrestrial plants correlate with their ecological life forms. *Oecologia*, 150, 330-338.
- Liu, X.T., Rendle-Bühning, R., Kuhlmann, H., Li, A. (2017). Two phases of the Holocene East African Humid Period: inferred from a high-resolution geochemical record off Tanzania. *Earth and Planetary Science Letter*, 460, 123-134.
- Lockheart M. J., van Bergen P. F. and Evershed R. P. (1997) Variations in the stable carbon isotope composition of individual lipids from the leaves of modern angiosperms: implications for the study of higher land plant-derived sedimentary organic matter. *Organic Geochemistry*, 26, 137–153.
- Lopez, P., Navarro, E., Ordonez, J., Caputo, L., Armengol, J. (2006). Elemental ratios in sediments as indicators of ecological processes in Spanish reservoirs. *Limnetica*, 25(1-2). 499-512.
- Lotter, A.F. (2005): Multi-proxy climatic reconstructions. In: A. Mackay, R.W. Battarbee, H.J.B. Birks and F. Oldfield (eds), *Global change in the Holocene*, Hodder Arnold, London, 373-383.
- Lorius, C., Jouzel, J., Raynaud, G., Wllr., McCave, I.N., Moore, C. (1992). The ice core record: past archive of the climate and signpost to the future. *Antartica and Environmental Change*, 338 (1285), 227-234.
- Luz, C.F.P., Barth, O.M., Silva, C.G. (2005). Spatial distribution of palynomorphs in the surface sediments of the Lagoa do Campelo lake, North region of Rio de Janeiro State, Brasil. *Acta Botanica Brasilica*, 19(4): 741-752.
- MacKellar, N., New, M., Jack, C. (2014). Observed and modelled trends in rainfall and temperature for South Africa: 1960-2010. *South African Journal of Science*, 110(7/8), 1-13.

- Madikizela, B.R., and Dye, A.H. (2003). Community composition and distribution of macroinvertebrates in the Mzimvubu River, South Africa: a pre-impoundment study. *African Journal of Aquatic Sciences*, 28(2), 137-149.
- Manjoro, M., Rowntree, K., Kakembo, V., Foster, I., Collins, A.L. (2016). Use of sediment source fingerprinting to assess the role of subsurface erosion in the supply of fine sediment in a degraded catchment in the Eastern Cape, South Africa. *Journal of Environmental Management*, 1-15.
- Marchant, R. (2010). Understanding complexity in savannas: climate, biodiversity and people. *Current Opinion in Environmental Sustainability*, 2, 101-108.
- McDuffee, K.E., Eglinton, T.I., Sessions, A.L., Sylva, S., Wagner, T., Hayes, J.M. (2005). Rapid analysis of ^{13}C in plant-wax *n*-alkanes for reconstruction of terrestrial vegetation signals from aquatic sediments. *Geochemistry, Geophysics, Geosystems*, 5(10), 1525-2027.
- Meadows, M. E. and Asmal, O. (1996). Chronology, sedimentology and geochemistry of sediments at Verlorenvlei (Western Cape Province, South Africa) as evidence of anthropogenically-induced land degradation. *Zeitschrift für Geomorphologie Supplementband*, 107, 45-62.
- Meyer, I., Davies, G.R., Stuut, J.-B.W. (2011). Grain size control on Sr-Nd isotope provenance studies and impact on paleoclimate reconstructions: An example from deep-sea sediments offshore NW Africa. *Geochemistry, Geophysics, Geosystems*, 12(3), 1525-2027.
- Meyers, P. A. (2003) Applications of organic geochemistry to paleolimnological reconstructions: a summary of examples from the Laurentian Great Lakes. *Organic Geochemistry*, 34, 261–289.
- Meyers, P. (1997). Organic geochemical proxies of paleoceanographic, paleolimnologic and paleoclimate processes. *Organic Geochemistry*, 27, 213–250.
- Middelburg, J. J., van der Weijden, C.G., Woittiez, J.R.W. (1988), Chemical processes affecting the mobility of major, minor and trace elements during weathering of granitic rocks. *Chemical Geology*, 68(3–4), 253–273.
- Milliman, J. D., and R. H. Meade (1983), World-wide delivery of river sediment to the oceans. *Journal of Geology*, 91(1), 1–21.

- Mooney, H.A. (1972). The Carbon Balance of Plants. *Annual Review of Ecology and Systematics*, 3, 315–346.
- Moss, P.T., Kershaw, A.P., Grindrod, J. (2005). Pollen transport and deposition in riverine and marine environments within the humid tropics of northeastern Australia. *Review of Palaeobotany and Palynology*, 134, 55-69.
- Mucina, L. and Rutherford, M.C. (2006). *The Vegetation of South Africa, Lesotho and Swaziland*. Strelitzia, South African National Biodiversity Institute, Pretoria.
- Mudie, P.J., McCarthy, F.M.G. (1994). Pollen transport processes in the western North Atlantic: evidence from cross margin and north-south transects. *Marine Geology*, 118, 79-105.
- Nesbitt H. W. and Young G. M. (1996). Petrogenesis of sediments in the absence of chemical weathering: effects of abrasion and sorting on bulk composition and mineralogy. *Sedimentology*, 43, 341–358.
- Nesbitt, H.W., and Markovics, G. (1997). Weathering of granodioritic crust, long-term storage of elements in weathering profiles, and petrogenesis of siliciclastic sediments. *Geochimica et Cosmochimica Acta*, 61 (8), 1653–1670.
- Nesbitt, H.W., and Young, G.M. (1982). Early Proterozoic climates and plate motions inferred from major element chemistry of lutites. *Nature*, 299 (21), 715–717.
- Neumann F.H., Scott, L., Bamford, M.K. (2011). Climate change and human disturbance of fynbos vegetation during the late Holocene at Princess Vlei, Western Cape, South Africa. *The Holocene*, 21(7): 1137–1149
- Niedermeyer, E.M., Forrest, M., Beckmann, B., Sessions, A.L., Mulch, A., Schefuß, E. (2016). The stable hydrogen isotopic compositions of sedimentary plant waxes as quantitative proxy for rainfall in the West African Sahel. *Geochimica et Cosmochimica Acta*, 184, 55-70.
- Norström, E., Neumann, F.H., Scott, L., Smittenberg, R.H., Holmstrand, H., Lundqvist, S., Snowball, I., Sundqvist, H.S., Risberg, J., Bamford, M., (2014). Late Quaternary vegetation dynamics and hydro-climate in the Drakensberg, South Africa. *Quaternary Science Reviews*, 105, 48-65.
- Neumann, F.H., Botha, G.A., Scott, L. (2014). 18,000 years of grassland evolution in the summer rainfall region of South Africa: evidence from Mahwaqa Mountain, KwaZulu-Natal. *Vegetation History and Archaeobotany*, 23(6), 665-681.

- O'Leary, M.H. (1988). Carbon Isotopes in Photosynthesis. *BioScience*, 38, 328–336.
- Oró, J., Laseter, J.L., Wber, D. (1966). Alkanes in fungal spores. *Science*, 154, 399–400.
- Pancost R. D., and Boot C. S. (2004). The palaeoclimatic utility of terrestrial biomarkers in marine sediments. *Marine Chemistry*, 92, 239–261.
- Parker, A.G., Eckersley, L., Smith, M.M., Goudie, A.S., Stokes, S., Ward, S., White, K., Hodson, M.J. (2004). Holocene vegetation dynamics in the northeastern Rub' al-Khali desert, Arabian Peninsula: a phytolith, pollen and carbon isotope study. *Journal of Quaternary Science*, 19(7), 665–676.
- Peck, R.M. (1973). Pollen budget studies in a small Yorkshire catchment. In: Birks, H.J.B., West, R.G. (eds.), *Quaternary Plant Ecology*. The 14th Symposium of the British Ecological Society. Blackwell Scientific Publications, University of Cambridge, pp. 43–60.
- Peterson, L. C., Huang, G.H., Huguen, K.A., Rhol, U. (2000), Rapid changes in the hydrologic cycle of the tropical Atlantic during the last glacial, *Science*, 290(5498), 1947–1951,
- Peterson, P.M. (2013). *Poaceae (Graminaeae)*. In: eLS. John and Wiley and Sons, Ltd: Chichester, doi:10.1002.9780470015902.a0003689.pub2
- Ponton, C., West, A.J., Feakins, S.J., Galy, V. (2014). Leaf wax biomarkers in transit record river catchment composition. *Geophysical Research Letters*, 41, 6420–6427.
- Poynter, J.G., Eglinton, G. (1990). The molecular composition of three sediments from Hole 717c, The Bengal Fan. In: Cochran, J.R., Stow, D.A.V. (eds.), *Procedures of the Ocean Drilling Program Scientific Results Section*, 116, 155–161.
- Poynter, J.G., Farrimond, P., Brassell, S.C., Eglinton, G. (1989). Aeolian-derived higher plant lipids in the marine sedimentary record: links with paleoclimate. In: Leinen, M., Sarnthein, M. (eds.), *Palaeoclimatology and Palaeometeorology: Modern and Past Patterns of Global Atmosphere Transport*, NATO ASI Series, D. Kluwer, 435–462.
- Rea, D. K. (1994). The paleoclimatic record provided by aeolian deposition in the deep sea: The geologic history of wind. *Reviews of Geophysics*, 32(2), 159–195,
- Richey, J. E., Hedges, J. I., Devol, A. H., Quay, P. D., Victoria, R., Martinelli, L., Forsberg, B. R. (1990). Biogeochemistry of carbon in the Amazon River. *Limnology and Oceanography*, 35, 352–371.

- Rieley, G., Collier, R.J., Jones, D.M., Eglinton, G. (1991). The biogeochemistry of Ellesmere Lake, UK. 1. Source correlation of leaf wax inputs to the sedimentary lipid record. *Organic Geochemistry*, 17, 901–912.
- Rommerskirchen F., Eglinton G., Dupont L., Gunter U., Wenzel C. and Rullkötter J. (2003). A north to south transect of Holocene southeast Atlantic continental margin sediments: relationship between aerosol transport and compound-specific $\delta^{13}\text{C}$ land plant biomarker and pollen records. *Geochemistry, Geophysics, Geosystems*, 4, 1101–1128
- Rommerskirchen F., Plader A., Eglinton G., Chikaraishi Y. and Rullkötter J. (2006). Chemotaxonomic significance of distribution and stable carbon isotopic composition of long-chain alkanes and alkan-1-ols in C_4 grass waxes. *Organic Geochemistry*, 37, 1303–1332.
- Rowntree, K., Mzobe, P., van Der Waal, B. (2017). *Sediment source tracing in the Thina River catchment, Eastern Cape, South Africa*. CAS-Chengdu, China, 11-15 October. IAHS Publication, 356, 404-411.
- Rundel, P.W., Esler, K.J., Cowling, R.M. (1999). Ecology and phylogenetic patterns of carbon isotope discrimination in the winter-rainfall flora of the Richtersveld, South Africa. *Plant Ecology*, 142, 133–148.
- Sachse D., Kahmen A. and Gleixner G. (2009). Significant seasonal variation in the hydrogen isotopic composition of leaf-wax lipids for two deciduous tree ecosystems (*Fagus sylvatica* and *Acer pseudoplatanus*). *Organic Geochemistry*, 40, 732–742.
- Sachse, D., Billault, I., Bowen, G. J., Chikaraishi, Y., Dawson, T. E., Feakins, S. J., Freeman, K.H., Magill, C.R., McInerney, F.A., van der Meer, M.T.J., Polissar, P., Robins, R., Sachs, J.P., Schmidt, H.-L., Sessions, A.L., White, J.W.C., West, J.B., Kahmen, A. (2012). Molecular Paleohydrology: Interpreting the hydrogen-isotopic composition of lipid biomarkers from photosynthesizing organisms. *Annual Review of Earth and Planetary Sciences*, 40(1), 221–249.
- Schefuß E., Ratmeyer V., Stuut J.-B. W., Jansen J. H. F. and Damsté J. S. S. (2003). Carbon isotope analyses of n-alkanes in dust from the lower atmosphere over the central eastern Atlantic. *Geochimica et Cosmochimica Acta*, 67, 1757–1767.
- Schefuß, E., Kuhlmann, H., Mollenhauer, G., Prange, M., Pätzold, J. (2011). Forcing of wet phases in southeast Africa over the past 17,000 years. *Nature*, 480, 509-512.

- Schefuß, E., Versteegh, G.J., Jansen, J.H., Sinninghe Damsté, J. (2004). Lipid biomarkers as major source and preservation indicators in SE Atlantic surface sediments. *Deep Sea Research Part I. Oceanographic Research Papers*, 51, 1199–1228.
- Schefuß, E., S. Schouten, R. R. Schneider. (2005), Climatic controls on central African hydrology during the past 20,000 years. *Nature*, 437(7061), 1003–1006.
- Schimmelmann A., Sessions A. L. and Mastalerz M. (2006) Hydrogen isotopic (D/H) composition of organic matter during diagenesis and thermal maturation. *Annual Review of Earth and Planetary Science*, 34, 501–533.
- Schouten, S., Huguët, C., Hopmans, E.C., Kienhuis, M.V.M., Damsté, J.S.S. (2007). Analytical Methodology for TEX₈₆ Paleothermometry by High-Performance Liquid Chromatography/Atmospheric Pressure Chemical Ionization-Mass Spectrometry. *Analytical Chemistry*, 79, 2940–2944.
- Schwab, V.F., Garcin, Y., Sachse, D., Todou, G., Séné, O., Onana, J.M., Achoundong, G., Gleixner, G. (2015). Effect of aridity on $\delta^{13}\text{C}$ and δD values of C₃ plant- and C₄ graminoid-derived leaf wax lipids from soils along an environmental gradient in Cameroon (Western Central Africa). *Organic Geochemistry*, 78, 99–109.
- Scott, L. (1982). Late Quaternary fossil pollen grains from the Transvaal, South Africa. *Review of Palaeobotany and Palynology*, 36, 241–466.
- Scott, L. (1984). Palynological evidence for Quaternary palaeoenvironments in southern Africa. In: Klein, R.G. (ed). *Southern Africa prehistory and palaeoenvironments*, Balkema, Rotterdam, 65–80.
- Scott, L. (1999). Palynological analysis of the Pretoria Saltpan (Tswaing Crater) sediments and vegetation history in the bushveld savanna biome, South Africa. In: Partridge, T.C. (ed). *Tswaing- Investigations into the origin, age and palaeoenvironments of the Pretoria Saltpan*. Council for Geosciences, Pretoria, 143–166.
- Scott, L., and Vogel, J.C. (2000). Evidence for environmental conditions during the last 20 000 years in southern Africa from ^{14}C in fossil hyrax dung. *Global and Planetary Change*, 26, 207–215.

- Scott, L., Neumann, F.H., Brook, G.A., Bousman, C.B., Norström, E., Metwally, A.A. (2012). Terrestrial fossil-pollen evidence of climate change during the last 26 thousand years in southern Africa. *Quaternary Science Reviews*, 32, 100-118.
- Seibt, U., Rajabi, A., Griffiths, H., Berry, J. (2008). Carbon isotopes and water use efficiency: sense and sensitivity. *Oecologia*, 155, 441–454.
- Sessions, A.K., Burgoyne, T.W., Schimmelmann, A., Hayes, J.M. (1999). Fractionation of hydrogen isotopes in lipid biosynthesis. *Organic Geochemistry*, 30, 1193-200.
- Shi, N., Schneider, R., Beug, H.-J., Dupont, L.M. (2001). Southeast trade wind variations during the last 135 kyr: evidence from pollen spectra in eastern South Atlantic sediments. *Earth and Planetary Science Letters*, 187, 311-321
- Smirnov, A., Chmura, G.L., Lapointe, M.F. (1996). Spatial distribution of suspended pollen in the Mississippi River as an example of pollen transport in alluvial channels. *Review of Palaeobotany and Palynology*, 92, 69–81.
- Sojinu, O.S., and Shittu, A.O. (2018). Higher plants *n*-alkane profile as indicators of anthropogenic environmental pollution. *Journal of Chemical Society Nigeria*, 43(3), 387-399.
- Still, C. J., and Powell, R. L. (2010). Continental-scale distributions of vegetation stable carbon isotope ratios. In: J. B. West, G. J. Bowen, T. E. Dawson, K. P. TuIsoscapes (Eds.), *Understanding movement, pattern, and process on Earth through isotope mapping: Isoscapes*, 179–193.
- Sugita S. (1993). A Model of Pollen Source Area for an Entire Lake Surface. *Quaternary Research*, 39: 239-244.
- Switzer, A.D. (2013). Measuring and Analysing Particle Size in a Geomorphic Context. In: Shroder, J., (Editor in Chief), Switzer, A.D., Kennedy, D.M., (Eds). *Treatise on Geomorphology*, 14, 224 – 242, Academic Press, San Diego, CA
- Tabares, X., Mapani, B., Blaum, N., Herzsuh, U. (2018). Composition and diversity of vegetation and pollen spectra along gradients of grazing intensity and precipitation in southern Africa. *Review of Palaeobotany and Palynology*, doi:10.1016/j.revpalbo.2018.04.004
- Tierney J. E., Russell J. M., Huang Y., Sinninghe Damsté J. S., Hopmans E. C. and Cohen A. S. (2008). Northern hemisphere controls on tropical Southeast African climate during the past 60,000 years. *Science*, 322, 252–255.

- Tierney, J.E., Russell, J.M., Eggermont, H., Hopmans, E.C., Verschuren, D., Damsté, J.S.S. (2010). Environmental controls on branched tetraether lipid distributions in tropical Easter African lake sediments. *Geochimica et Cosmochimica Acta*, 74, 4902-4918.
- Tieszen, L.L., Reed, B.C., Bliss, N.B., Wylie, B.K., DeJong, D.D. (1997). NDVI, C₃ and C₄ production, and distributions in Great Plains grassland land cover classes. *Ecological Applications*, 7, 59–78.
- Tipple, B.J., Berke, M.A., Doman, C.E., Khachatryan, S., Ehleringer, J.R. (2013). Leaf wax *n*-alkanes record the plant–water environment at leaf flush. *Proceedings of the National Academy of Sciences*, 110, 2659– 2664.
- Traverse, A., 1988. Paleopalynology. Unwin Hyman, London.
- Tyson, P.D., and Preston-Whyte, R.A. (2000). The Weather and Climate of Southern Africa Second edi. A. Attwell, ed., South Africa: Oxford University Press. Tyson, 1995.
- Vetrimurugan, E., Jonathan, M. P., Roy, P. D., Shruti, V. C., Ndwandwe, O. M. (2016). Bioavailable metals in tourist beaches of Richards Bay, KwaZulu-Natal, South Africa. *Marine Pollution Bulletin*, 105(1), 430–436.
- Vogel, J. C. (1978): Isotopic assessment of dietary habits of ungulates. *South African Journal of Science*, 74, 298-301.
- Vogts, A., Badewien, T., Rullkötter, J., Schefuß, E. (2016). Near-constant apparent hydrogen isotope fractionation between leaf wax *n*-alkanes and precipitation in tropical regions: Evidence from a marine sediment transect off SE Africa. *Organic Geochemistry*, 96, 18-27.
- Vogts, A., Moossen, H., Rommerskirchen, F., Rullkötter, J. (2009). Distribution patterns and stable carbon isotopic composition of alkanes and alkan-1-ols from plant waxes of African rain forest and savanna C₃ species. *Organic Geochemistry*, 40, 1037–1054.
- Vogts, A., Schefuß, E., Badewien, T., Rullkötter, T. (2012). *n*-Alkane parameters from a deep sea sediment transect off southwest Africa reflect continental vegetation and climate conditions. *Organic Geochemistry*, 47, 109-119.
- Volkman, J.K., Holdsworth, D.G., Neill, G.P., Bracor Jr, H.J. (1992) identification of natural anthropogenic and petroleum hydrocarbons in aquatics sediments. *The Science of the Total Environment*, 112, 203-219.

- Wakeham, S.G., Hedges, J.I., Lee, C., Peterson, M.L., Hernes, P.J. (1997). Compositions and transport of lipid biomarkers through the water column and surficial sediments of the equatorial Pacific Ocean. *Deep-Sea Research II*, 44(9-10), 2131-2162.
- Walling, D.E., Owens, P.N., Leeks, G.J.L. (1999). Fingerprinting suspended sediment sources in the catchment of the River Ouse, Yorkshire, UK. *Hydrological Processes*, 13, 955-975.
- Wang, J.H., Shen, Y.M., Guo, Y.K. (2010). Seasonal circulation and influence factors of the Bohai Sea: a numerical study based on the Lagrangian particle tracking method. *Ocean Dynamics*, 60, 1581–1596.
- Wang, M., Zhang, W., Hou, J. (2015). Is average chain lengths of plant lipids a potential proxy for vegetation, environment and climate change. *Biogeosciences Discussions*, 12, 5477-5501.
- Waterson, E.J., and Canuel, E.A. (2008). Sources of sedimentary organic matter in the Mississippi River and adjacent Gulf of Mexico as revealed by lipid biomarkers and $\delta^{13}\text{C}_{\text{TOC}}$ analyses. *Organic Geochemistry*, 39, 422-439.
- Watrin, J., Lézine, A., Gajewski, K., Vincens, A. (2007) Pollen-plant-climate relationships in sub-Saharan Africa. *Journal of Biogeography*, 34, 489-499.
- Weijers, J.W.H., Schouten, S., Schefuß, E., Schneider, R., Sinninghe Damsté, J. (2009). Disentangling marine, soil and plant organic carbon contributions to continental margin sediments: A multi-proxy approach in a 20,000 year sediment record from the Congo deep-sea fan. *Geochimica et Cosmochimica Acta*, 73, 119–132.
- Weltje, G.J., and Tjallingii, R. (2008). Calibration of XRF core scanners for quantitative geochemical logging of sediment cores: theory and application. *Earth and Planetary Science Letters*, 274, 423–438.
- Wilke, B. M., B. J. Duke, and W. L. O. Jimoh. (1984). Mineralogy and chemistry of harmattan dust in Northern Nigeria, *Catena*, 11(1), 91–96,
- Xu, Q., Tian, F., Bunting, M.J., Li, Y., Ding, W., Cao, X., He, Z. (2012). Pollen source areas of lakes with inflowing rivers: modern pollen influx data from lake Baiyangdian, China. *Quaternary Science Reviews*, 37, 81-91.
- Xu, Q.-H., Zhang, S.-R., Gaillard, M.-J., Li, M.-Y., Cao, X.-Y., Tian, F. (2016). Studies of modern pollen assemblages for pollen dispersal- deposition- preservation process

understanding and for pollen-based reconstructions of past vegetation, climate, and human impact: a review based on case studies in China. *Quaternary Science Reviews*, 149, 151–166.

Yang, H., Liu, W., Leng, Q., Hren, M.T., Pagani, M. (2011). Variation in *n*-alkane δD values from terrestrial plants at high latitude: implications for palaeoclimatic reconstruction. *Organic Geochemistry*, 42, 283-288.

Yang, S., Liu, K.B., Yi, S., Ye, S., Li, J., Yuan, H., Zhao, G., Pei, S., He, L., Ding, X., Cho, T.S. (2016). Distributions and provenance of modern pollen and spores in the surface sediments of Liaodong Bay, China. *Marine Geology*, doi:10.1016/j.margeo.2016.03.004.

Yu, Y., Li, Y., Guo, Z., Zou, H. (2016). Distribution and sources of *n*-alkanes in surface sediments of Taihu Lake, China. *Archives of Environmental Protection*, 42(1), 49-55.

Zabel, M., Schneider, R.R., Wagner, T., Adegbe, A.T., de Vries, U., Kolonic, S. (2001). Late Quaternary climate changes in Central Africa has inferred from terrigenous input to the Niger Fan. *Quaternary Research*, 56, 207-2017.

Zabel, M., T. Bickert, L. Dittert, and R. R. Haese (1999), Significance of the sedimentary Al/Ti ratio as an indicator for variations in the circulation patterns of the equatorial North Atlantic, *Paleoceanography*, 14(6), 789–799,

Zech, M., Rass, S., Bugge, B., Löscher, M., Zöller, L. (2012). Reconstruction of the late Quaternary paleoenvironments of the Nussloch loess paleosol sequence, Germany, using *n*-alkane biomarkers. *Quaternary Research*, 78, 226–235.

Zhang, R. (2006). How cold were the tropics and subtropics at the Last Glacial Maximum? *Quaternary Science Reviews*, 25, 1150-1151.

Zhao, X., Dupont, L., Meadows, M.E., Wefer, G. (2015). Pollen distribution in the marine surface sediments of the mudbelt along the west coast of South Africa. *Quaternary International*, 1–13.

Zhao, X., Dupont, L., Schefuß, E., Bouimtarhan, I., Wefer, G. (2017). Palynological evidence for Holocene climatic and oceanographic changes off western South Africa. *Quaternary Science Reviews*, 165, 88-101.

Zhao, X., Dupont, L., Schefuß, E., Meadows, M.E., Hahn, A., Wefer, G. (2016). Holocene vegetation and climate variability in the winter and summer rainfall zones of South Africa. *The Holocene*, 26(6), 843-857.

Zhu, Y., Chen, F., Cheng, B., Zhang, J.-W., (2002). Pollen assemblage features of modern water samples from the Shiyang River drainage, arid region of China. *Acta Botanica Sinica*, 44(3), 367-372.

Ziegler, H., Osmond, C.B., Stichler, W., Trimborn, P. (1976). Hydrogen Isotope Discrimination in Higher Plants: Correlations with Photosynthetic Pathway and Environment. *Planta*, 128, 85–92.

Ziervogel, G., New, M., Archer can Garderen, E., Midgley, G., Taylor, A., Hamann, R., Stuart-Hill, S., Myers, J., Warburton, M. (2014). Climate change impacts and adaptation in South Africa, *WIREs Climate Change*, 5, 605-620.

APPENDICES

APPENDIX A

Procedure for preparing pollen samples

Source: adapted after Faegri and Iverson (1989), Moore *et al.*, (1991), Baxter (1996) and Finch (2005).

Notes:

- Centrifuge at 4000 rpm for 3 minutes, unless otherwise specified.
- Use 100 ml profiled, sealable polypropylene tubes in a swing-out centrifuge.
- The temperature of the water bath should be maintained between 50-60°C unless otherwise stated.
- Label all samples clearly.

A. Measurement of Sediment

Each sample should contain 3cm³ of wet sediment. Accurate sample volumes were obtained by measuring out 10cm³ of distilled water into a measuring cylinder and adding sediment until the total volume in the measuring cylinder reached 13cm³.

B. Addition of pollen spike

1. Place pollen spike solution on a magnetic stir plate for at least 1 hour prior to use.
2. Add 1 ml of spike to each sediment sample using a graduated plastic syringe or pipette.

C. Removal of humic acids and clay materials (Sodium hydroxide digestion)

1. Add 20ml 15% sodium hydroxide (NaOH) to each sample and stir.
2. Place samples in a heated water bath for 10 minutes and stir.
3. Wash and strain through a 180µm sieve using distilled water.
4. Centrifuge and decant.
5. Repeat step 3 until supernatant becomes clear.

D. Removal of clastic material (Hydrofluoric acid digestion)

1. Add 20ml 10% Hydrochloric acid (HCl) in each sample. Stir, centrifuge and decant.
2. In a fume cupboard, add 20 ml concentrated (40%) HF, place in polypropylene tubes in a heated water bath for three hours, stirring regularly.

3. Seal centrifuge tubes, centrifuge for five minutes and decant.
4. Add 20 ml 10% HCl. Place sample in a heated water bath for 20 minutes, stirring regularly.
5. Remove from water bath.
6. Stir, centrifuge and decant.

E. Acetolysis digestion of extraneous organic detritus

1. Add 20 ml glacial acetic acid. Stir, centrifuge and decant, making sure to discard as much as the supernatant as possible to avoid remaining acetic acid from reacting with the acetolysis mixture.
2. Add 20 ml acetolysis mixture (containing 9 parts acetic anhydride ($[\text{CH}_3\text{CO}]_2\text{O}$): 1 part concentrated sulphuric acid $[\text{H}_2\text{SO}_4]$). Place in a heated water bath for 10-15 minutes, stirring regularly.
3. To stop the reaction, remove from water bath and place in cold water for a few seconds. Stir, centrifuge and decant.
4. Add 20 ml glacial acetic acid. Stir, centrifuge and decant.
5. Add 9 ml distilled water and 1 ml 10% NaOH to neutralise sample.
6. Rinse three times with distilled water, add two drops of safranin stain to the last rinse and place into a labelled 30 ml storage vial.

F. Mounting

1. Allow the processed solution to settle overnight in a refrigerator. Using a glass pipette, remove the clear liquid so as to concentrate the pollen.
2. Place a single drop of Aquatex mounting solution on a sterile glass microscope slide.
3. Use a micropipette or a blunt toothpick to extract approximately three drops of the pollen solution. Add to the Aquatex, using a toothpick to mix the pollen suspension evenly within the Aquatex.
4. Place a coverslip over the Aquatex suspension and let the mixture spread to all edges. This may be aided by applying light pressure with a dissecting needle.
5. The slide should be allowed to stand for at least four hours prior to counting, to allow the pollen to disperse evenly across the slide.

APPENDIX B

***n*-Alkane separation of samples**

nC₁₉₋₃₅ concentrations were calculated for 32 RBS samples. The samples were ground and homogenised using a pestle and mortar first followed by a ball mill (650 rpm, 30 seconds per sample) for the dry, intermediate and wet sample campaigns. The total sum of odd n-alkanes was calculated for each sample site for each sample campaign (Schefuß *et al.*, 2005; Schefuß *et al.*, 2011; Hahn *et al.*, 2017).

A. Sample extraction with ASE

1. Dried and ground sediments are added into ASE cells, thereafter add 100µl of standard mixture.
2. DCM:MeOH = 9:1_[ES1] (1000 psi, 3 cycles, five minutes for each sample).
3. Concentrate extract by transferring into a round-bottom flask, then “roto-evaporate” until almost dry.
4. Transfer the samples into 4 ml vials and let dry overnight.

B. Take off 5 % split of TLE

1. Label GC vial (Sample name and depth and 5% TLE), put into a combusted spring and 100 µl insert.
2. Add 1000µl DCM to TLE using blue Eppendorf pipette, and vortex.
3. Take off 50µl with small Eppendorf pipette and put into labelled GV vial.
4. Let both vials dry overnight.

C. Saponification (breaks open the wax ester bonds)

1. Add 500µl of 0.1 M KOH-solution to the dry extract (“Hex”) in a 4 ml vial.
2. Close the lid (use Teflon tape to seal) and vortex.
3. Place onto a heater at 85°C for 2 hours and cover with Al-foil.
4. Prepare and label two new 4 ml vials (“neutral” and “acid”).
5. Add a bit of bidest water to samples to improve separation.
6. Add approximately 1 ml hexane to samples, close, vortex, and pipette hexane layer into new 4 ml vials (“neutral”), repeat until vial is full.
7. Add two drops of concentrated HCl to saponified solvent (“Hex”)_[ES3].
8. Add approximately 1 ml hexane/DCM = 4:1 to sample, close, vortex, pipette the upper layer into a new 4 ml vial (“acid”), repeat until vial is full.
9. Dry both extracts.

10. The rest of the saponification can be thrown out (preferably rinse before as it could be acidic).

D. Column separation of neutral fraction

1. Plug lower end of pipette with combusted glass wool, add 4-5 cm of combusted 10% deactivated Silica, and pat the tip gently.
2. Prepare and label 3 new 4 ml vials (“apo”, “keot”, and “polar”).
3. Rinse the column with hexane twice and throw out the rinse solvent.
4. Place “apo” vial under the column.
5. Add ca. 0.5 ml of hexane to dry extract (“neutral”), vortex and pipette into column.
6. Rinse vial (“neutral”) with more hexane and put onto column until vial is full (“apo”).
7. Place “keto” vial under column.
8. Add 1 ml DCM to “neutral” vial and transfer onto column.
9. Rinse vial (“neutral”) with more DCM and put onto column until vial is full (“keto”).
10. Place “polar” vial under column.
11. Add 1 ml DCM/MeOH = 1/1 and put onto column until vial is full (“polar”).
12. Dry all extracts, let column dry in waste container, dispose the solid phase in waste and throw pipette into glass waste.

E. Removal of unsaturated components in alkane fraction (“apo*”)

1. Plug lower end of pipette with combusted glass wool, add 4-5 cm of AgNO₃Si, and pat the tip gently.
2. Prepare and label new 4 ml vial (“apo*”).
3. Rinse column with hexane and throw out rinse solvent.
4. Place “apo*” vial under column.
5. Add ca. 0.5 ml of hexane to dry extract (“apo”), vortex and pipette onto column.
6. Rinse vial (“apo”) with more hexane and put onto column until vial is full (“apo*”).
7. Dry extract, let column dry in waste container, and dispose solid waste, through pipette into glass waste.

F. Methylation of acid fraction

1. Add ca. 2 ml MeOH(iso)/12N HCl = 95/5 to “acid” fraction (2mlMeOH(iso)) + two drops of (12n HCl).
2. Blow nitrogen into vial, quickly close cap and secure with Teflon tape.
3. Place onto heater at 50°C for ca. 12 hours (staying longer, e.g., overnight is no problem).
4. Evaporate under Nitrogen to 1 ml.

5. Add ca. 1 ml of milliQ water (bi-distilled water).
6. Add approximately 1 ml hexane to samples, close, vortex, pipette hexane layer into new 4 ml vial ("FA"), repeat until vial is full.
7. Dry extract ("FA"_[ES4]), throw out remaining phase ("acid").

G. Clean-up of FA fraction

1. Plug lower end of pipette with combusted glass wool, add 4 cm of combusted Silica, pat the tip gently, add ca. 0.5 cm of Na₂SO₄ (not combusted is ok).
2. Prepare and label new 4 ml vial ("FAME").
3. Rinse column with DCM and throw out rinse solvent.
4. Place "FAME" vial under column.
5. Add ca. 0.5 ml of DCM to dry extract ("FA"), vortex and pipette onto column.
6. Rinse vial ("FA") with more DCM and put onto column until vial is full ("FAME").
7. Dry extract ("FAME"), let column dry in waste container, dispose solid phase in waste, throw pipette into glass waste.

H. Preparation for GC analysis

1. Carefully transfer fraction of interest (apo*, keto or FAME) with hexane in GC vial with insert (repeat 2-3 times to be quantitative), blow down with N₂ (careful to not blow out the sample).
2. Fill with 100µl toluene.
3. Ready for GC analysis.

GC analysis

Saturated hydrocarbons containing n-alkanes were injected into a Thermo Scientific Focus gas chromatograph equipped with a DB-5ms column (30 m X 0.25 mm, 0.25µm) film thickness (Agilent Technologies, Palo, Alto, USA) coupled to a flame ionisation detector (GC-FID). The oven is held at 70°C for 2 min, then heated at a rate of 20°C min⁻¹ to 150°C, and after with a rate of 4° Cmin⁻¹ to 320°C, and remained at this temperature for 16.5 min. n-Alkanes of different chain lengths were quantified by comparing peak areas of the compounds to external standard solutions and to the internal squalane standard added prior to ASE extraction. Analyses of the external alkane standard with known concentrations of n-alkanes were performed every 6 samples. Precision of compound quantification is about 5% based on the standard analyses. The CPI₂₅₋₃₃ was calculated according to the following equation developed by Bray and Evans (1961):

$$\text{CPI}_{23-33} = 0.5 * (\sum \text{C}_{\text{odd}23-33} / \sum \text{C}_{\text{even}22-32} + \sum \text{C}_{\text{odd}23-33} / \sum \text{C}_{\text{even}24-34})$$

C_x represents the amount of each n-alkane homologue. n-Alkane Average Chain Length (ACL) was then determined using the following equation by Poynter and Eglinton (1990):

$$\text{ACL}_{25-35} = \frac{25 \times (nC_{25}) + 27 \times (nC_{27}) + 29 \times (nC_{29}) + 31 \times (nC_{31}) + 33 \times (nC_{33}) + 35 \times (nC_{35})}{(nC_{25} + nC_{27} + nC_{29} + nC_{31} + nC_{33} + nC_{35})}$$

The ratio between C_{29} and C_{31} n-alkanes (Norm31) was then calculated using the equation:

$$\text{Norm31} = C_{31} / (C_{29} + C_{31})$$

For Norm31 and ACL calculations, nC_x represents the concentration of the n-alkane with x as the carbon number.

$\delta^{13}C$ and δD isotope extraction

Sample fractions containing n-alkanes were used for compound-specific carbon and hydrogen isotope analyses. Compound specific stable hydrogen isotope analyses of C_{29} and C_{31} n-alkanes were carried out on a Trace GC (Thermo Fisher Scientific, Bremen, Germany) coupled to a MAT 253 IRMS (Finnigan MAT, Bremen, Germany) via a pyrolysis reactor which operates at 1420°C. The PTV injector is maintained at 45°C and then heated to 340°C after injection. This is done to transfer the sample on the GC column. The compounds are then separated on a Rxi-5ms silica column. The GC is maintained at 120°C for 3 minutes then heated to 200°C with 30°Cmin⁻¹, then at 4°C min⁻¹ to 320°C and held there for 24 minutes. Deuterium (δD) isotope were measured against a calibrated H₂ reference gas. The $\delta^{13}C$ of the n-alkanes were analysed on a similar type of GC coupled to a MAT 252 IRMS via a GC/C III combustion interface which operates at 1000°C. The GC and injector settings were similar to that used for isotope calibration. Each sample was analysed twice except for a few samples where the n-alkane concentration was too low (the concentration was determined on the GC machine remember). The accuracy of the isotope measurements were assessed by analysing internal n-alkane laboratory standards of known isotopic composition every six measurements.

XRF element composition analysis

The XRF element analysis of bulk RBS samples identified a total of 18 element compositions from the 32 RBS samples across for the three sampling campaigns. XRF spectrometer measurements were completed on 32 RBS using a PANalytical Epsolon3-XL XRF spectrometer using energy dispersive polarisation X-Ray Fluorescence (EDP-XRF) spectroscopy. 20 g of dried RBS sediment were weighed and placed into a Ball Mill at 650rpm for 30 seconds. 4 g of the 20 g was then weighed and removed and utilised for XRF elemental

analysis. A minimum of 12g were extracted from each sample for Alkenone analysis. Element composition profiles were performed using an Avaatech XRF Scanner at MARUM (University of Bremen). The scanner is equipped with an Oxford Instrument 50W XTF5011 rhodium X-ray tube, a Canberra X-PIPS silicon drift detector which runs at 50eV resolution and a Canberra digital spectrum analyser (DAS1000). To detect different elemental groups, the vertical resolution is set to 1cm with two generator settings.

APPENDIX C

Table 3.1 Three types of sediment samples and one water sample collected for the three sampling campaigns.

Season	Site	River	Latitude (S)	Longitude (E)	Location In Catchment	Elevation	RBS	SPM	DPS	δ^{2h} And δ^{18o} Water Samples	Height Of Bridge
DRY	MZJ-1	Mzimvubu	29.52756	-31.59468	Mouth	4	x	x		x	9 m
	MZJ-2	Mzimvubu	29.26517	-31.39581	Confluence	113	x	x		x	Weir
	MZJ-3	iTsitsa	28.84483	-31.23697	Middle	762	x	x	x	x	9 m
	MZJ-4	Thina River	28.89564	-31.07361	Middle	780	x	x		x	10 m
	MZJ-5	Mzimvubu	29.06989	-30.85067	Middle	826	x	x	x	x	10 m
	MZJ-6	Mzintlava River	29.32133	-30.80772	Middle	890	x	x	x	x	Sampled under bridge
	MZJ-7	iTsitsa	28.45392	-30.94903	Upper	1501	x	x	x	x	9 m
	MZJ-8	Tina	28.48103	-30.62989	Upper	1368	x	x	x	x	Sampled under bridge
	MZJ-9	Kinira River	28.61550	-30.47114	Upper	1357	x	x	x	x	12 m
	MZJ-10	Mzimvubu	29.05747	-30.40289	Upper	1434	x	x	x	x	9 m
	MZJ-11	Mzintlava River	29.42964	-30.56128	Upper	1249	x	x		x	6 m
INT	MZS-1	Mzimvubu	29.52756	-31.59468	Mouth	4	x	x		x	9 m
	MZS-2	Mzimvubu	29.26517	-31.39581	Confluence	113	x	x		x	Weir
	MZS-3	iTsitsa	28.84483	-31.23697	Middle	762	x	x	x	x	9 m
	MZS-4	Thina River	28.89564	-31.07361	Middle	780	x	x	x	x	10 m
	MZS-5	Mzimvubu	29.06989	-30.85067	Middle	826	x	x		x	10 m
	MZS-6	Mzintlava River	29.32133	-30.80772	Middle	890	x	x	x	x	Sampled under bridge
	MZS-7	iTsitsa	28.45392	-30.94903	Upper	1501	x	x	x	x	9 m
	MZS-8	Tina	28.48103	-30.62989	Upper	1368	x	x	x	x	Under bridge
	MZS-9	Kinira River	28.61550	-30.47114	Upper	1357	x	x	x	x	12 m

	MZS-10	Mzimvubu	29.05747	-30.40289	Upper	1434	x	x	x	x	9 m
	Site	River	Latitude (S)	Longitude (E)	Location In Catchment	Elevation	RBS	SPM	DPS	δ^{2h} And δ^{18o} Water Samples	Height Of Bridge
	MZS-11	Mzintlava River	29.42964	-30.56128	Upper	1249				x	Sampled downstream
WET	MZN-1	Mzimvubu	29.52756	-31.59468	Mouth	4	x	x		x	9 m
	MZN-2	Mzimvubu	29.26517	-31.39581	Confluence	113	x	x		x	Weir
	MZN-3	iTsitsa	28.84483	-31.23697	Middle	762	x	x	x	x	9 m
	MZN-4	Thina River	28.89564	-31.07361	Middle	780	x	x		x	10 m
	MZN-5	Mzimvubu	29.06989	-30.85067	Middle	826	x	x		x	10 m
	MZN-6	Mzintlava River	29.32133	-30.80772	Middle	890	x	x	x	x	Sampled under bridge
	MZN-7	iTsitsa	28.45392	-30.94903	Upper	1501	x	x		x	9 m
	MZN-8	Tina	28.48103	-30.62989	Upper	1368	x	x		x	Under bridge
	MZN-9	Kinira River	28.61550	-30.47114	Upper	1357	x	x	x	x	12 m
	MZN-10	Mzimvubu	29.05747	-30.40289	Upper	1434	x	x	x	x	9 m
	MZN-11	Mzintlava River	29.42964	-30.56128	Upper	1249	x	x		x	6 m

APPENDIX D

Pollen Raw Count Sheets

a. July sampling campaign (dry season)

PALYNOMORPH	MZ 1	MZ 2	MZ 3	MZ 4	MZ 5	MZ 6	MZ 7	MZ 8	MZ 9	MZ1 0	MZ1 1
Pollen Spike											
AMARYLLIDACEAE undiff.	0	0	0	0	0	0	0	0	0	0	0
ANACARDIACEAE Rhus	18	20	0	4	0	0	14	13	2	2	19
AQUIFOLIACEAE Ilex mitis	0	7	0	1	0	0	0	0	0	2	1
ASTERACEAE Senecio	0	45	0	18	0	9	0	0	0	2	14
ASTERACEAE Tubuliflorae	66	29	0	8	0	1	0	40	0	18	9
ASTERACEAE Vernonia	0	0	0	0	0	0	0	1	0	6	5
ASTERACEAE Helichrysum	0	2	0	0	0	0	0	4	0	1	0
CHENO-AM	0	7	0	1	0	0	0	5	0	0	0
COMBRETACEAE Combretum	0	0	0	0	0	0	0	0	0	0	0
CYATHEACEAE Cyathea	0	0	0	0	0	0	0	0	0	0	0
CYPERACEAE undiff.	71	68	0	49	0	3	9	28	0	45	25
ERICACEAE undiff.	0	0	0	0	0	0	0	0	0	0	0
EUPHORBIACEAE Acalypha	0	1	0	11	0	0	0	0	0	1	5
EUPHORBIACEAE Euphorbia	0	11	0	19	0	0	0	3	1	6	16
FABACEAE Sesbania	0	14	0	2	0	0	0	0	0	0	4
LILIACEAE undiff.	0	9	0	4	0	0	3	1	0	5	5
MIMOSACEAE Acacia Type I	6	8	0	3	0	0	0	0	0	4	1
MYRICACEAE Morella	0	0	0	1	0	0	0	0	0	0	1
MYRTACEAE Syzigium	0	0	0	0	0	0	0	1	0	0	0
PALMAE Borassus	0	5	0	1	0	0	0	0	0	0	0
PINACEAE Pinus	2	24	0	12	0	1	1	5	0	4	5
POACEAE undiff.	128	244	1	168	1	18	15	225	16	126	81
POACEAE Zea mays	0	0	0	0	0	0	0	0	0	0	0
PODOCARPACEAE Podocarpus	0	94	0	0	0	0	0	0	0	1	0
PTERIDOPHYTA Monoletes	0	0	0	7	0	0	0	2	0	1	1
PTERIDOPHYTA Triletes	0	12	0	14	0	1	0	10	0	6	1
SALICACEAE Salix	0	10	0	0	0	0	0	0	0	0	0
THYMELAEACEAE Passerina	0	4	0	0	0	0	0	0	0	11	1
ULMACEAE Celtis	0	10	0	0	0	0	0	3	0	0	7
UNDETERMINED	40	41	7	30	8	21	34	25	1	34	21
MAIN SUM	331	665	8	353	9	54	76	366	20	275	222

b. September sampling campaign (intermediate season)

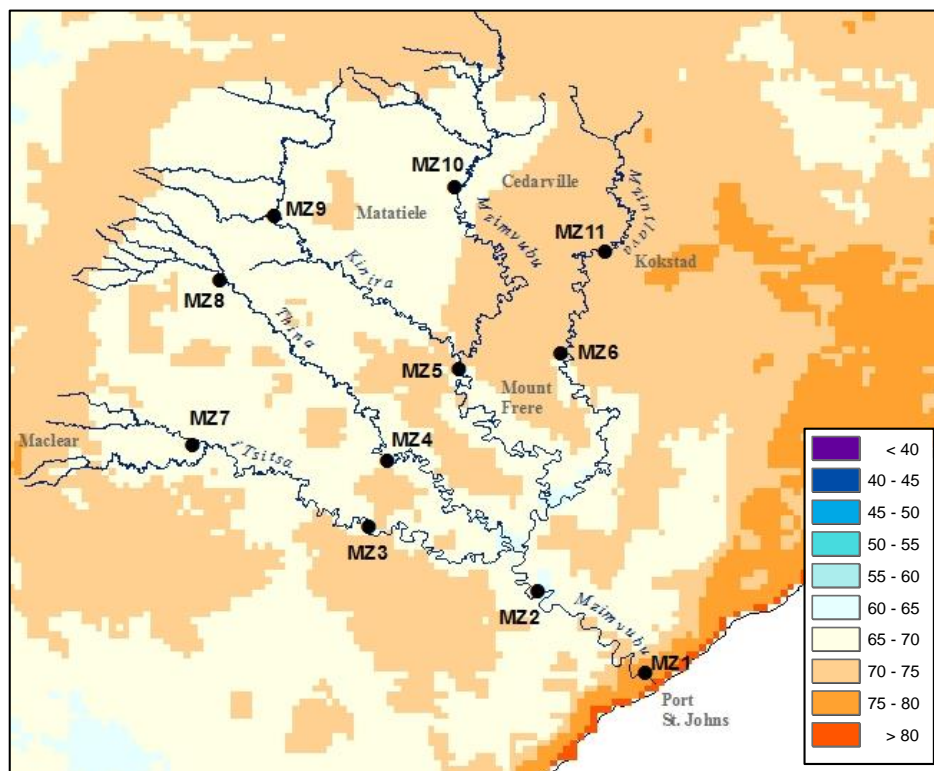
PALYNOMORPH	MZ1	MZ2	MZ3	MZ4	MZ5	MZ6	MZ7	MZ8	MZ9	MZ10
Pollen spike										
AMARYLLIDACEAE undiff.	2	0		175	0	0	0	0	0	6
ANACARDIACEAE Rhus	4	21	14	16	16	0	0	24	0	1
AQUIFOLIACEAE Ilex mitis	0	1		0	0	0	0	0	0	2
ASTERACEAE Helichrysum	0	6	3	9	4	0	0	5	1	3
ASTERACEAE Senecio	16	27	24	33	14	0	0	11	2	4
ASTERACEAE Tubuliflorae	17	17	6	14	13	1	0	3	1	1
ASTERACEAE Vernonia	0	0	1	5	2	0	0	1	0	0
CHENO-AM undiff.	5	5	2	9	24	0	0	7	1	0
COMBRETACEAE Combretum	0	0	0	0	0	0	0	0	0	0
CYATHEACEAE Cyathea	0	0	0	0	0	0	0	0	0	0
CYPERACEAE undiff.	34	22	41	17	31	0	5	97	13	15
ERICACEAE undiff.	0	2	1	11	5	0	0	9	0	2
EUPHORBIACEAE Acalypha	10	0	0	0	0	0	0	0	0	0
EUPHORBIACEAE Euphorbia	0	4	1	10	5	1	2	5	3	0
FABACEAE Sesbania	0	0	1	0	0	0	0	0	0	0
LILIACEAE undiff.	4	63	1	8	26	0	0	0	1	0
MIMOSACEAE Acacia Type 1	5	8	11	6	16	0	0	16	17	1
MYRICACEAE Morella	3	0	0	1	4	0	0	0	0	0
MYRTACEAE Syzigium	0	0	0	0	0	0	0	0	0	0
PALMAE Borassus	0	0	0	0	0	0	0	0	1	0
PINACEAE Pinus	8	31	22	15	10	0	0	14	0	3
POACEAE undiff.	199	227	330	280	116	15	6	369	27	69
POACEAE Zea mays	0	1	0	0	0	0	0	0	0	0
PODOCARPACEAE Podocarpus	0	9	0	28	9	0	0	0	0	0
PTERIDOPHYTA Monoletes	4	11	1	120	2	0	0	4	0	0
PTERIDOPHYTA Triletes	0	0	0	0	5	0	1	2	0	0
SALICACEAE Salix	0	0	0	0	0	0	0	0	0	0
THYMELAEAEAE Passerina	0	0	0	0	0	0	0	0	0	0
ULMACEAE Celtis	0	0	1	0	0	0	0	0	0	0
UNDETERMINED	0	19	33	31	26	25	0	0	153	12
Main sum	311	474	493	788	328	42	14	567	220	119

c. November sampling campaign (wet season)

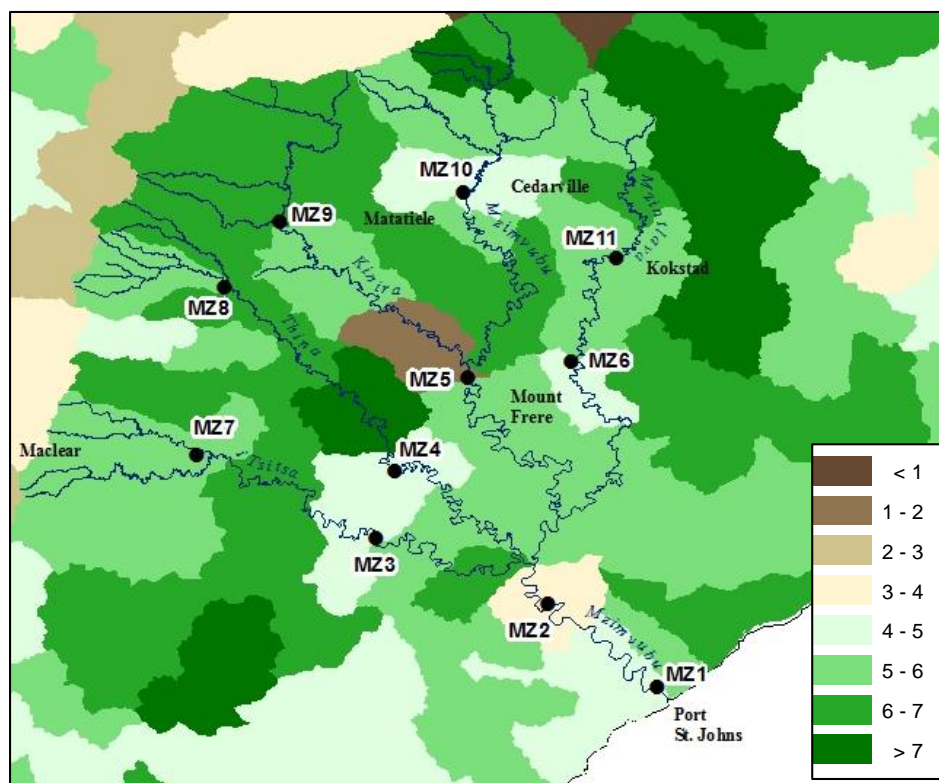
PALYNOMORPH	MZ 1	MZ 2	MZ 3	MZ 4	MZ 5	MZ 6	MZ 7	MZ 8	MZ 9	MZ1 0	MZ1 1
Pollen spike											
AMARYLLIDACEAE undiff.	0	0	0	0	0	1	0	0	0	2	0
ANACARDIACEAE Rhus	8	1	2	3	0	5	0	0	0	9	31
AQUIFOLIACEAE Ilex mitis	0	1	1	1	0	1	0	0	0	2	0
ASTERACEAE Helichrysum	0	1	0	0	0	1	0	0	0	0	1
ASTERACEAE Senecio	7	0	4	0	0	8	0	0	0	28	0
ASTERACEAE Tubuliflorae	2	0	3	14	0	2	0	0	0	0	16
ASTERACEAE Vernonia	0	3	0	2	0	2	0	0	0	4	0
CHENO-AM undiff.	0	1	1	0	0	1	0	0	0	2	3
COMBRETACEAE Combretum	0	0	0	0	0	5	0	0	0	0	0
CYATHEACEAE Cyathea	0	2	0	0	0	0	0	0	0	0	0
CYPERACEAE undiff.	7	5	5	16	0	15	0	0	0	25	24
ERICACEAE undiff.	0	0	0	3	0	3	0	0	0	0	5
EUPHORBIACEAE Acalypha	0	0	0	0	0	8	0	0	0	0	0
EUPHORBIACEAE Euphorbia	0	6	1	0	0	0	0	0	0	2	2
FABACEAE Sesbania	0	0	0	0	0	0	0	0	0	0	0
FABACEAE undiff.	0	0	0	0	0	0	0	0	0	0	0
LILIACEAE undiff.	0	1	0	3	0	0	0	0	0	6	1
MIMOSACEAE Acacia type 1	1	1	5	6	0	1	0	0	0	3	0
MYRICACEAE Morella	0	2	0	0	0	1	0	0	0	0	1
MYRTACEAE Syzigium	0	0	0	0	0	0	0	0	0	0	0
PALMAE Borassus	0	0	0	0	0	0	0	0	0	0	0
PINACEAE Pinus	0	1	4	5	0	5	0	0	0	4	9
POACEAE undiff.	66	56	22	100	0	142	0	0	0	82	77
POACEAE Zea mays	6	9	0	9	0	17	0	0	0	5	4
PODOCARPACEAE Podocarpus	1	0	0	0	0	5	0	0	0	4	1
PTERIDOPHYTA Monoletes	0	1	1	2	0	1	0	0	0	0	5
PTERIDOPHYTA Triletes	0	0	0	0	0	0	1	0	0	0	2
SALICACEAE Salix	0	0	0	0	0	1	0	0	0	0	0
THYMELEACEAE Passerina	0	0	0	0	0	0	0	0	0	1	0
ULMACEAE Celtis	0	0	0	0	0	0	0	0	0	0	0
Undetermined	0	15	3	13	22	0	19	0	0	0	14
Main sum	98	106	52	177	22	225	20	0	0	179	196

APPENDIX E

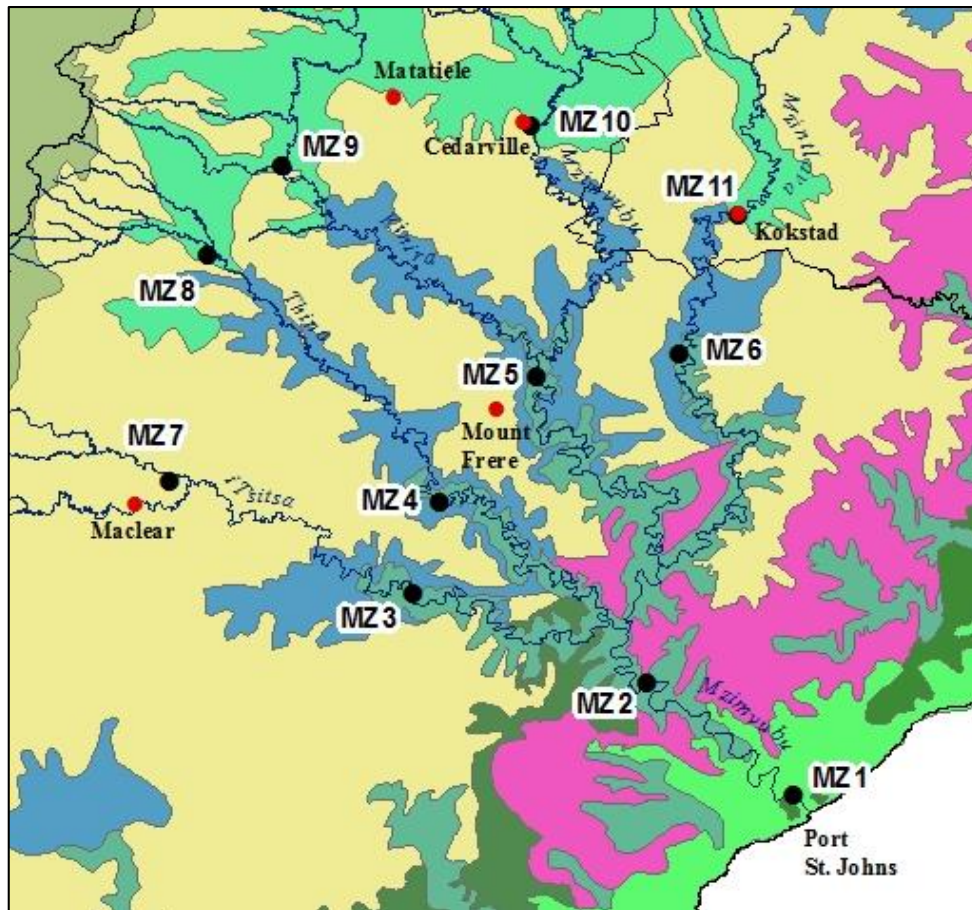
Additional climatic, environmental and vegetation information for the Mzimvubu Catchment



1. Relative humidity (%) for the Mzimvubu



2. Maize production (t/ha season) for the Mzimvubu Catchment.



Legend

VELD TYPES After Acocks (1988)

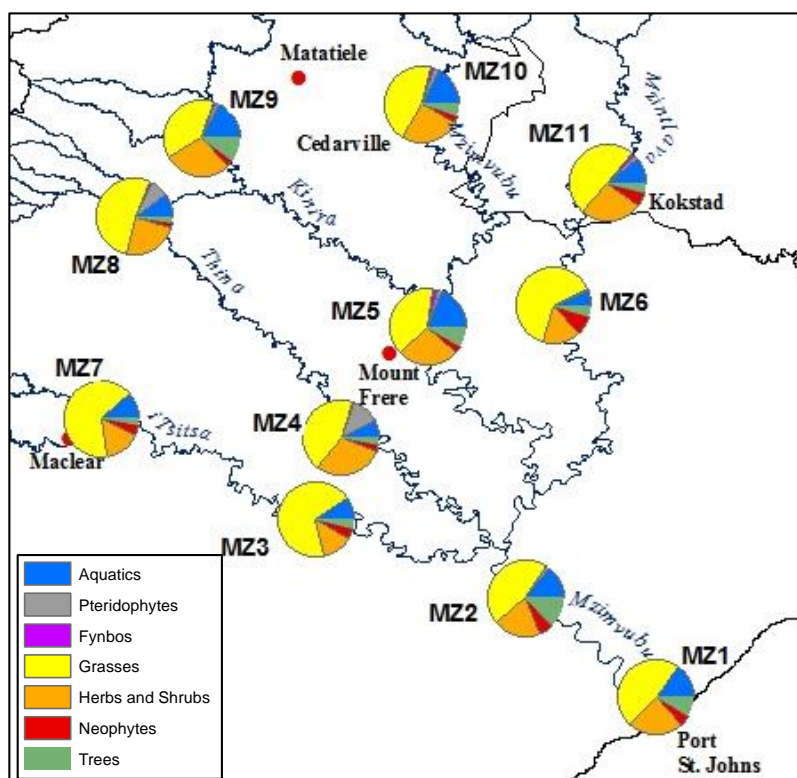
DESCRIPTION

■	COASTAL FOREST AND THORNVELD
■	EASTERN PROVINCE THORNVELD
■	HIGHLAND SOURVELD AND DOHNE SOURVELD
■	HIGHLAND SOURVELD TO CYMBOPOGON-THEMEDA VELD
■	NGONGONI VELD
■	NGONGONI VELD OF NATAL MIST-BELT
■	PONDOLAND COASTAL PLATEAU SOURVELD
■	SOUTHERN TALL GRASSVELD
■	THEMEDA VELD TO HIGHLAND SOURVELD TRANSITION
■	THEMEDA-FESTUCA ALPINE VELD
■	VALLEY BUSHVELD

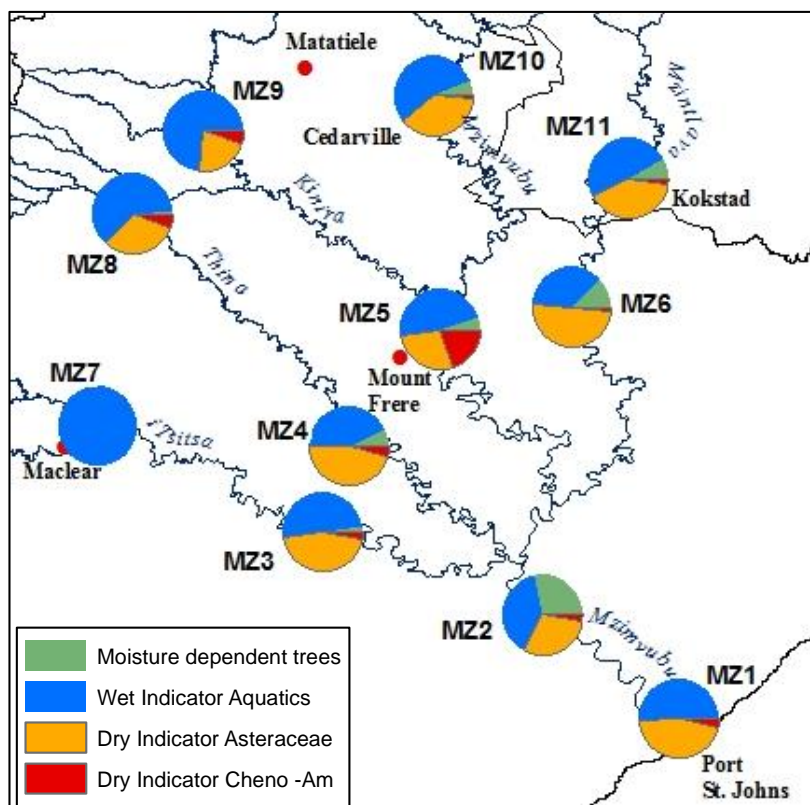
3. Veld types after Acocks (1988) of the Mzimvubu

APPENDIX F

Additional pollen data



1. Pollen biome pie charts for each sample



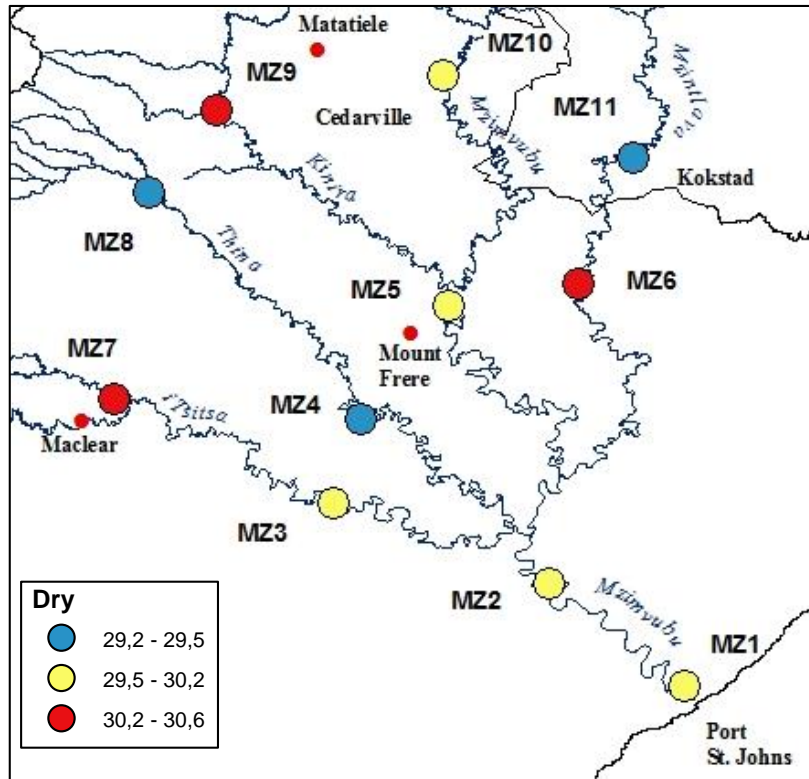
2. Wet versus dry indicator species pie charts for each sample

APPENDIX G

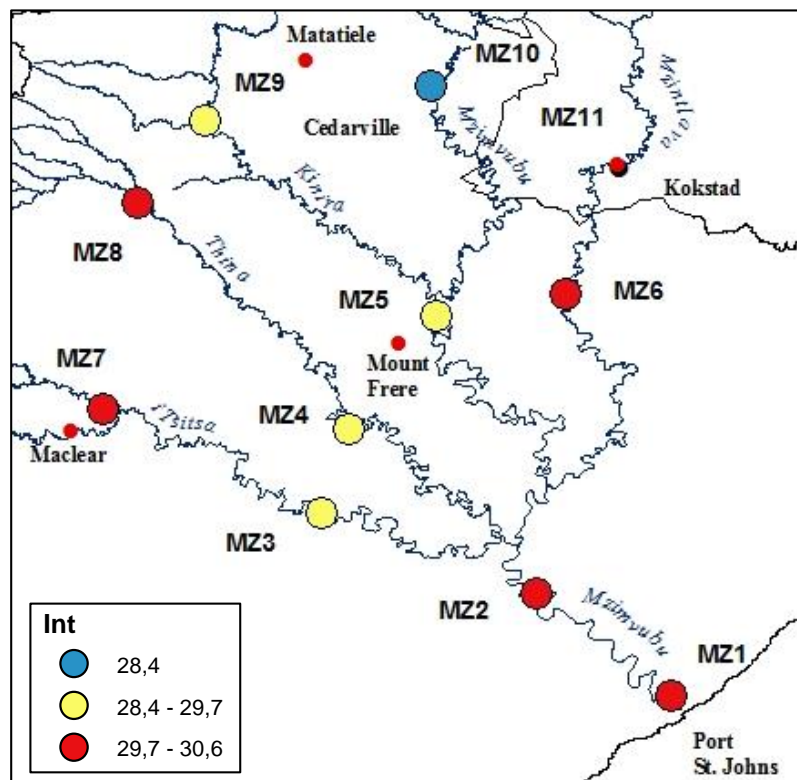
Proxy seasonal data

A. Average Chain Length (ACL) for the dry, intermediate and wet season.

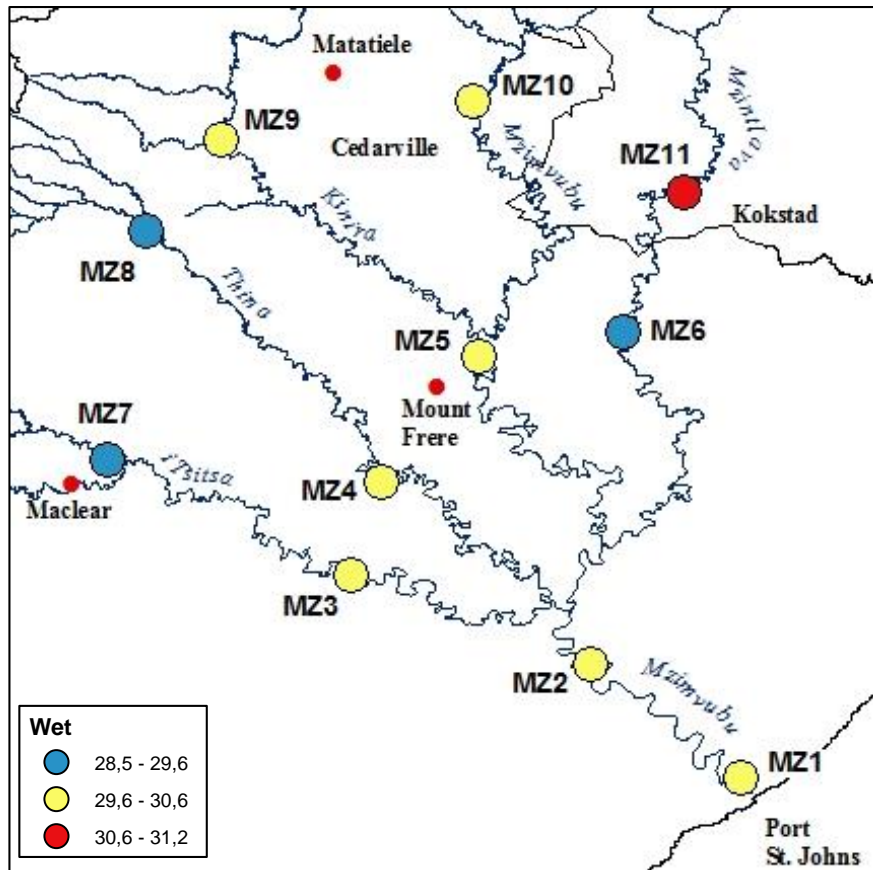
i.



ii.

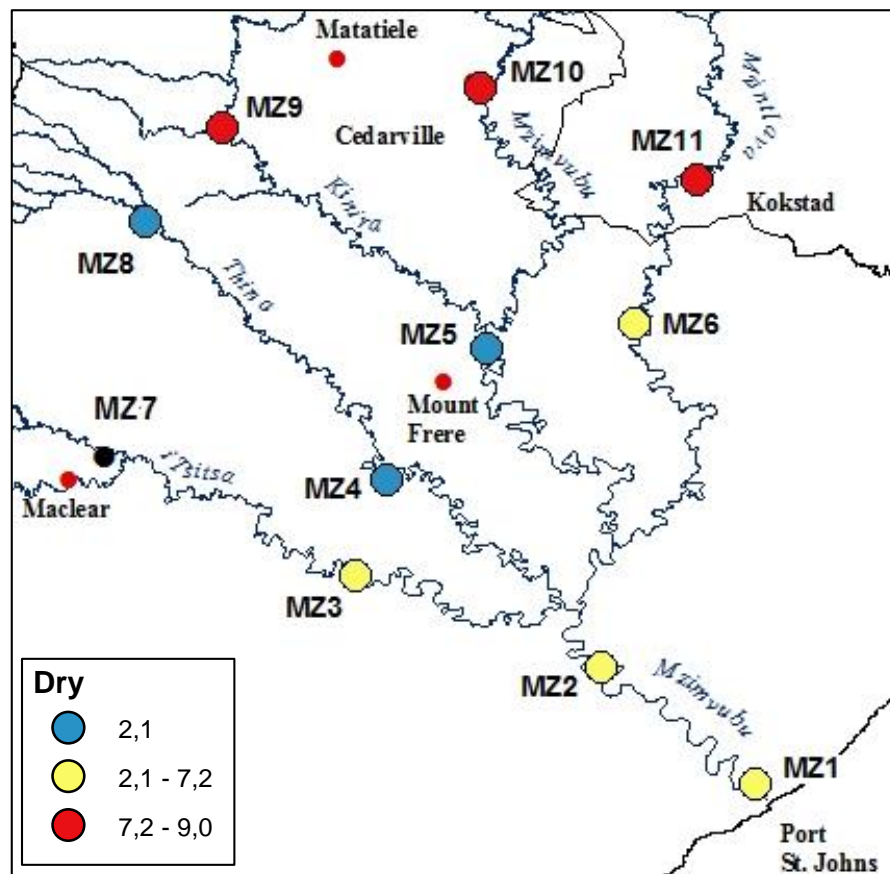


iii.



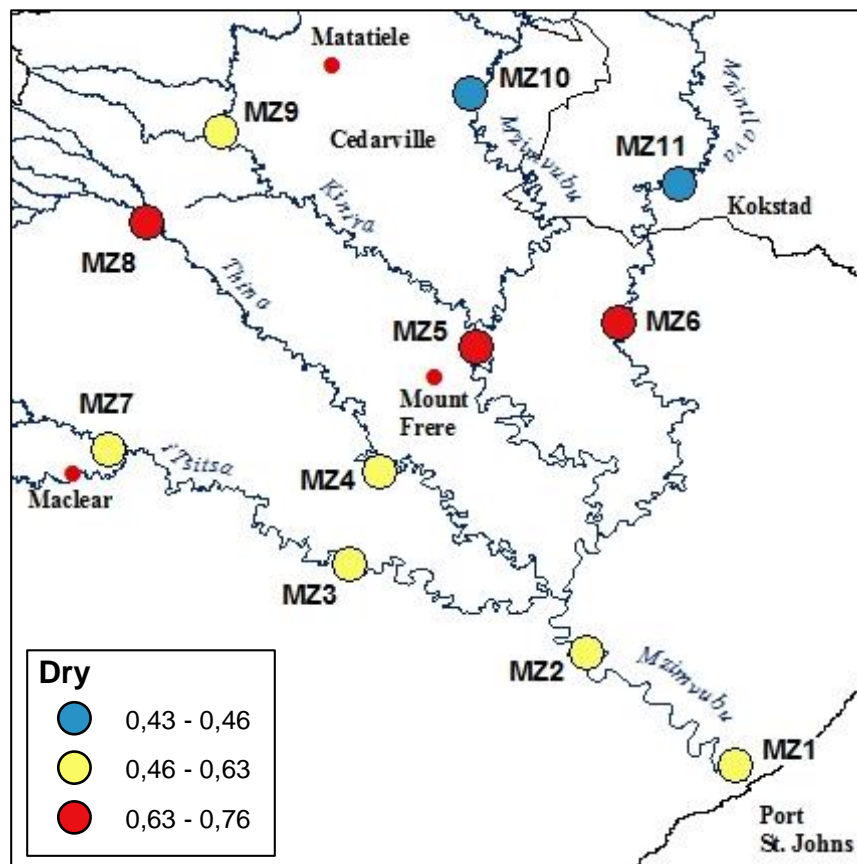
B. Carbon Preference Index (CPI_{25-33}) for the dry, intermediate and wet season.

i.

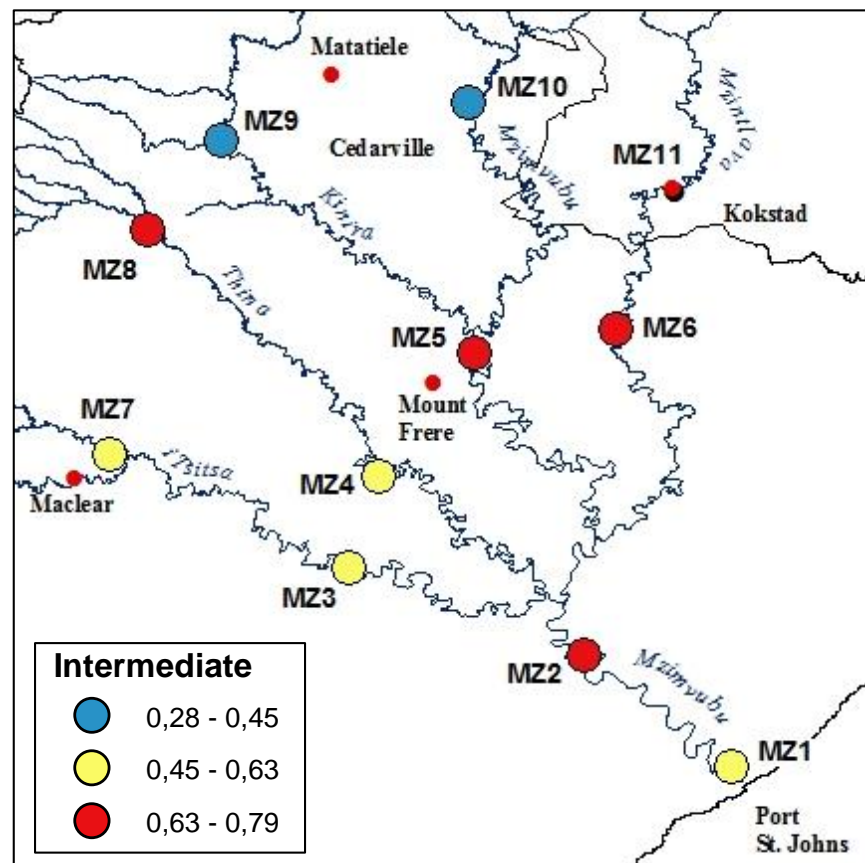


C. Norm31 for the dry, intermediate and wet season.

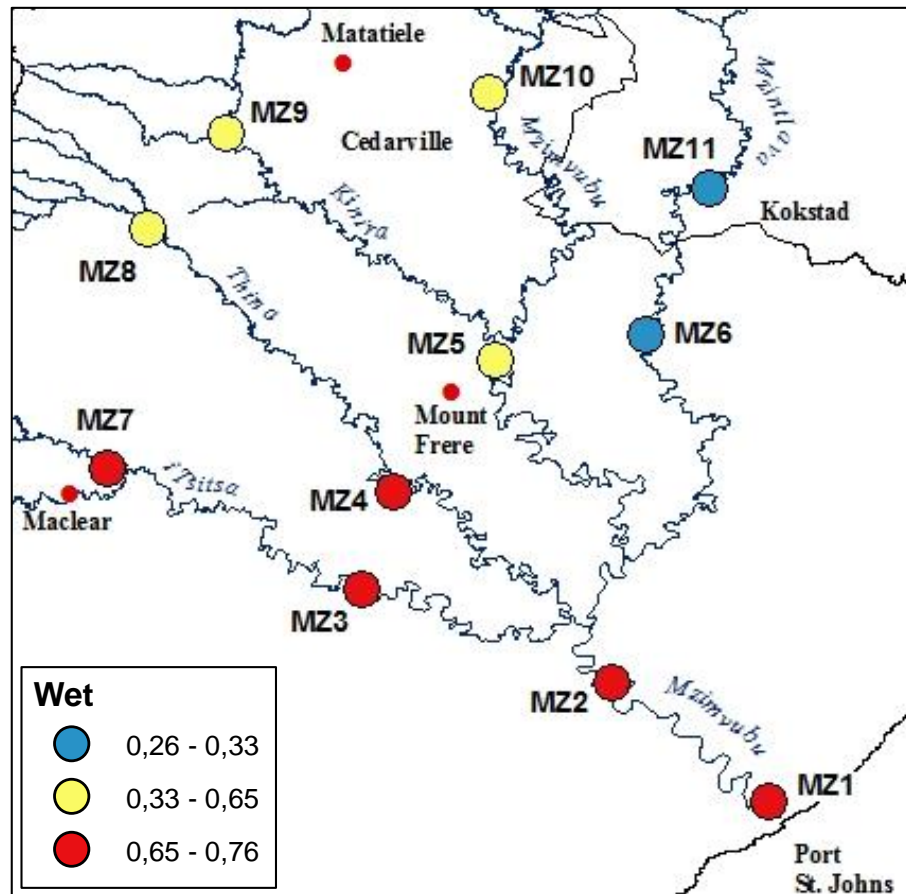
i.



ii.

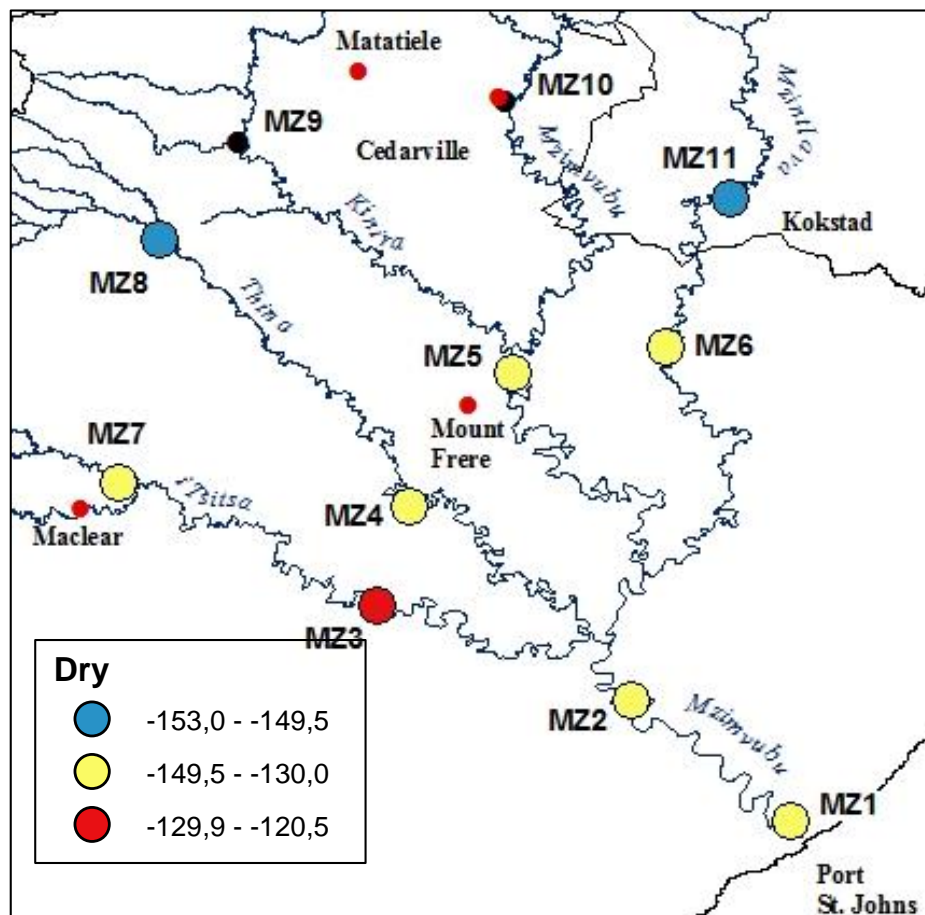


iii.

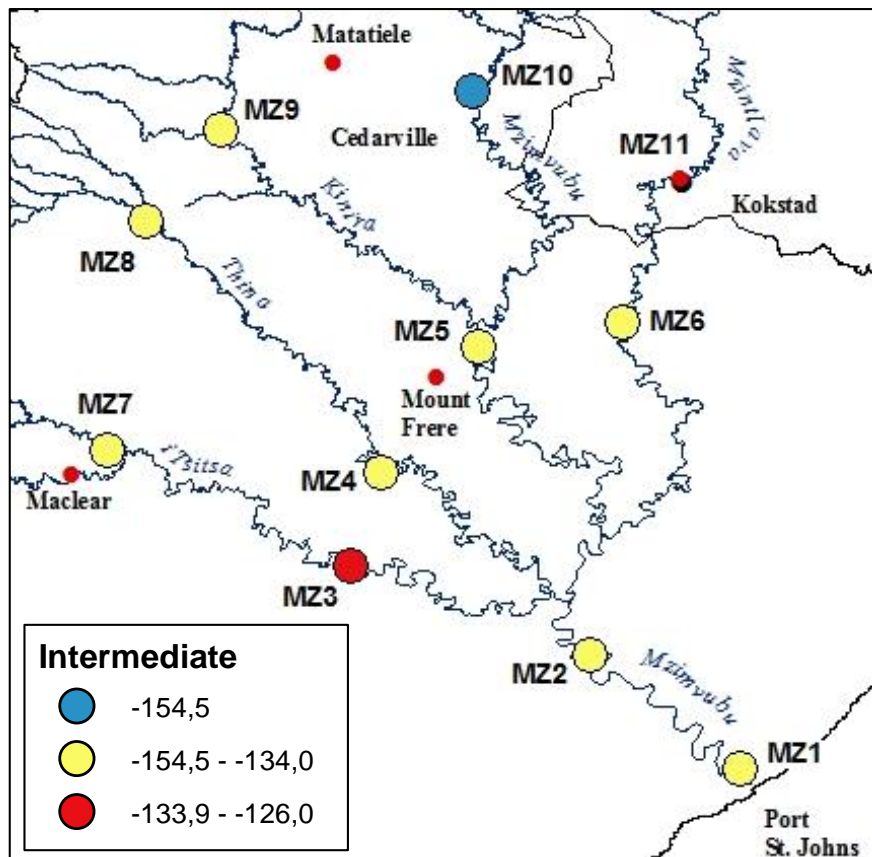


D. δD (Hydrogen isotope) for dry, intermediate and wet season.

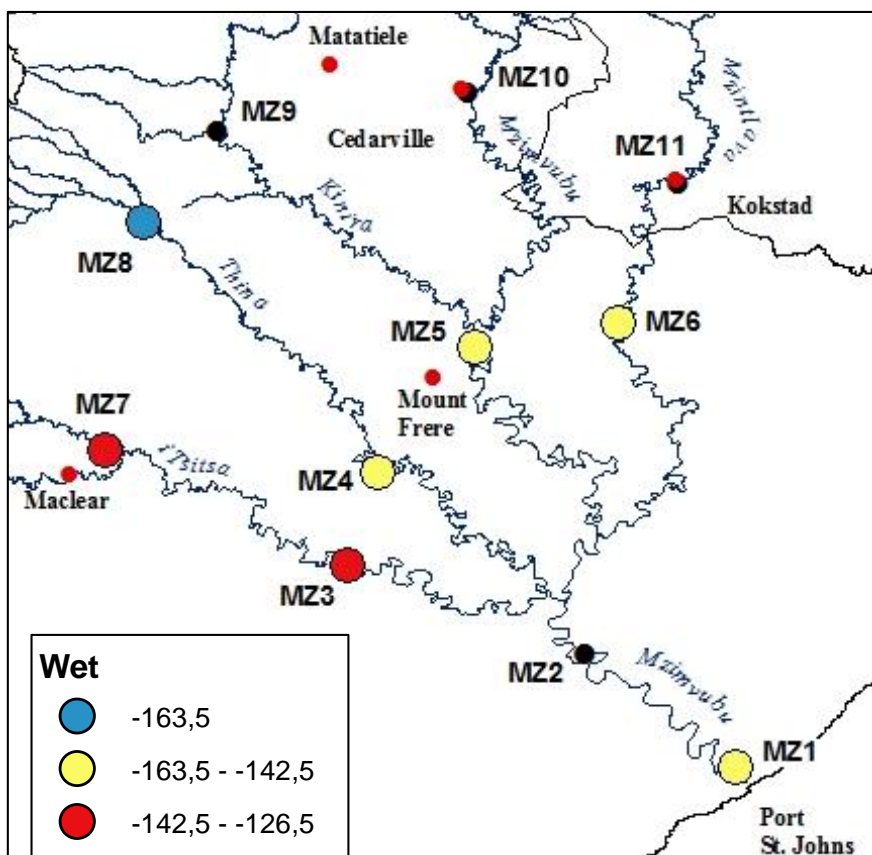
i.



ii.

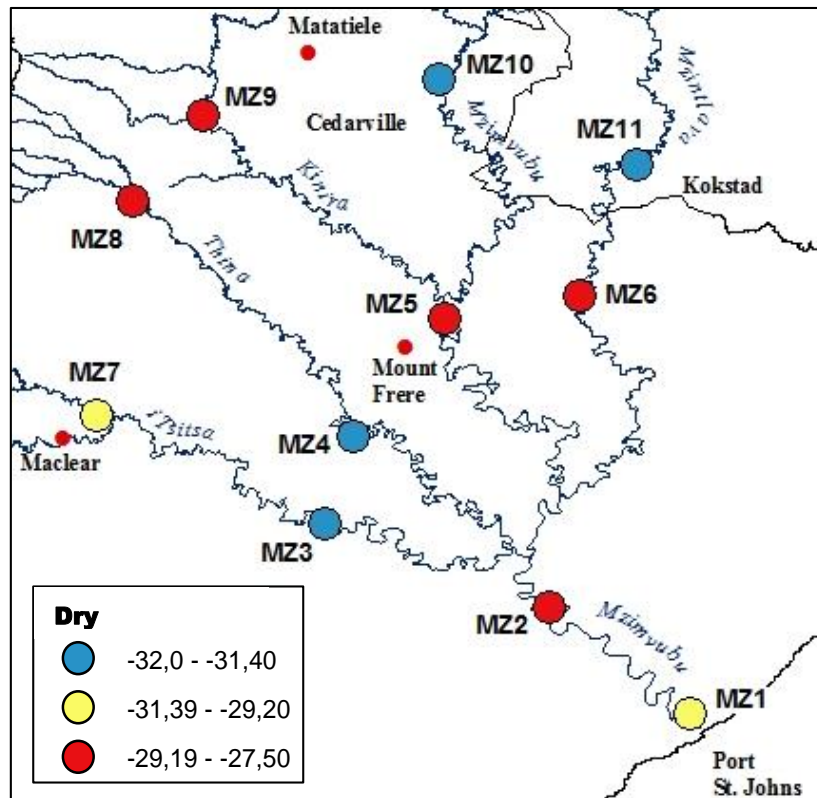


iii.

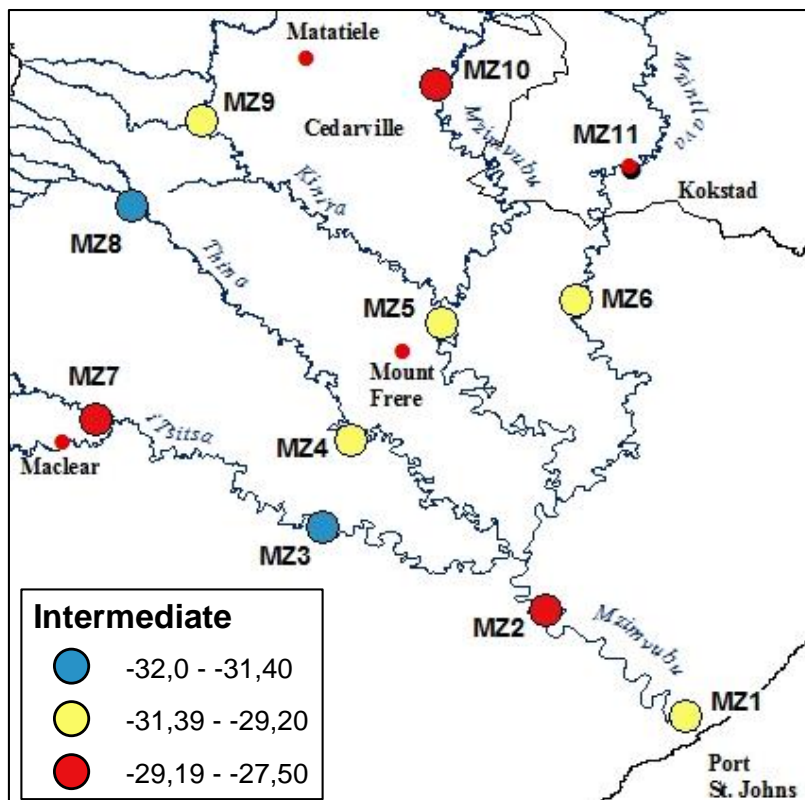


E. $\delta^{13}\text{C}$ (Carbon Isotope) for the dry, intermediate and wet season.

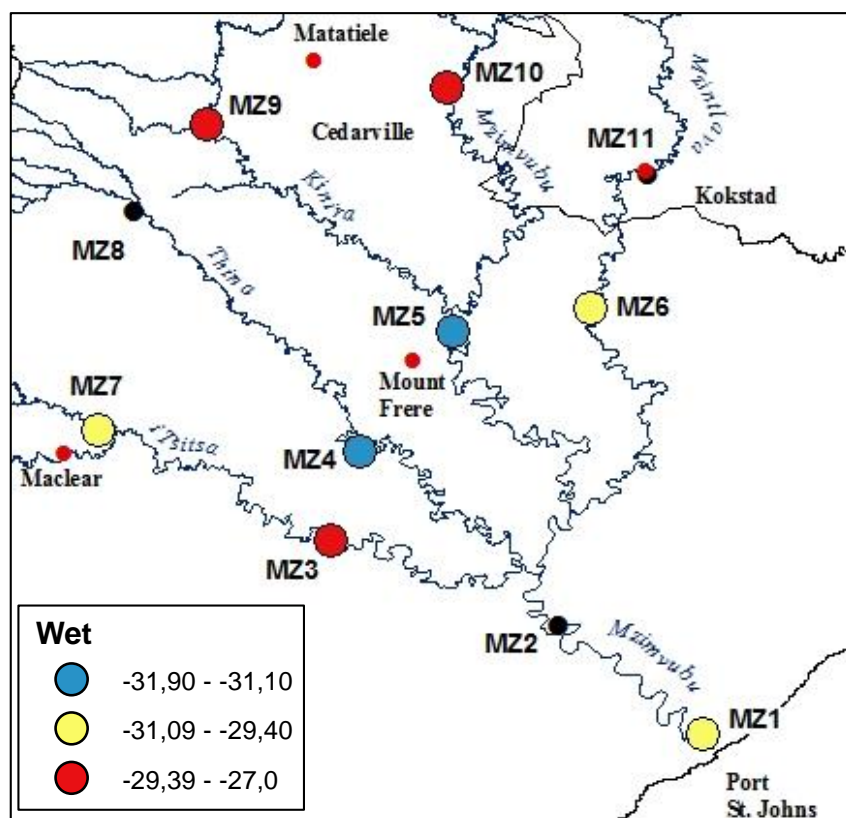
i.



ii.

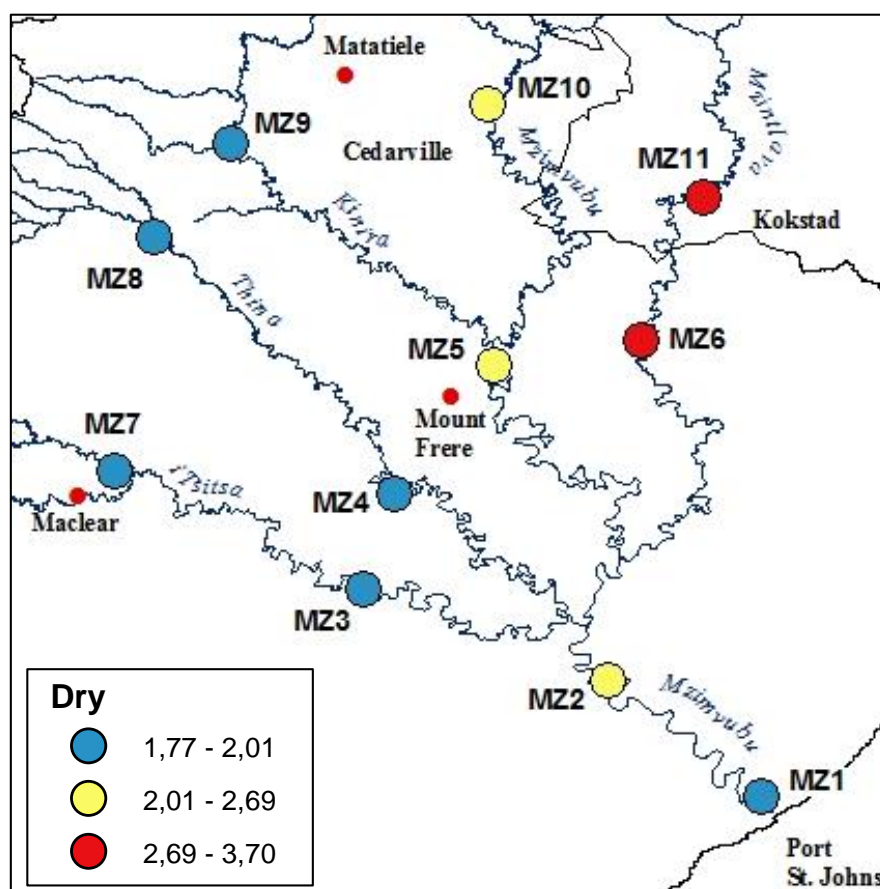


iii.

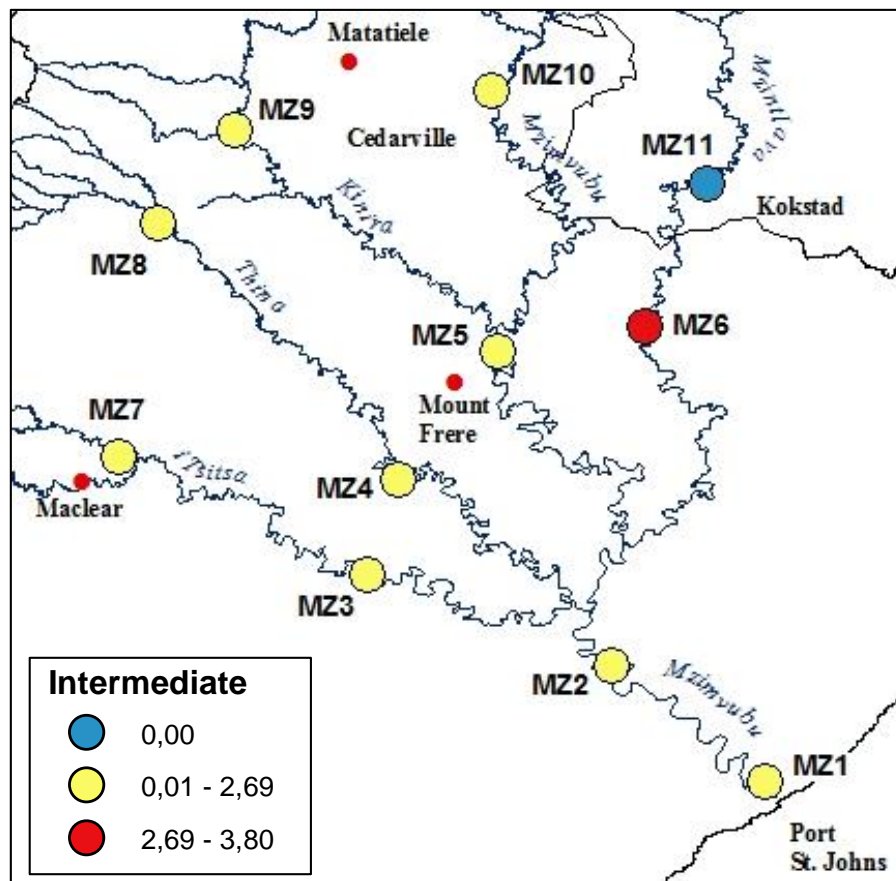


F. *FeK (Iron/Potassium) for the dry, intermediate and wet season.*

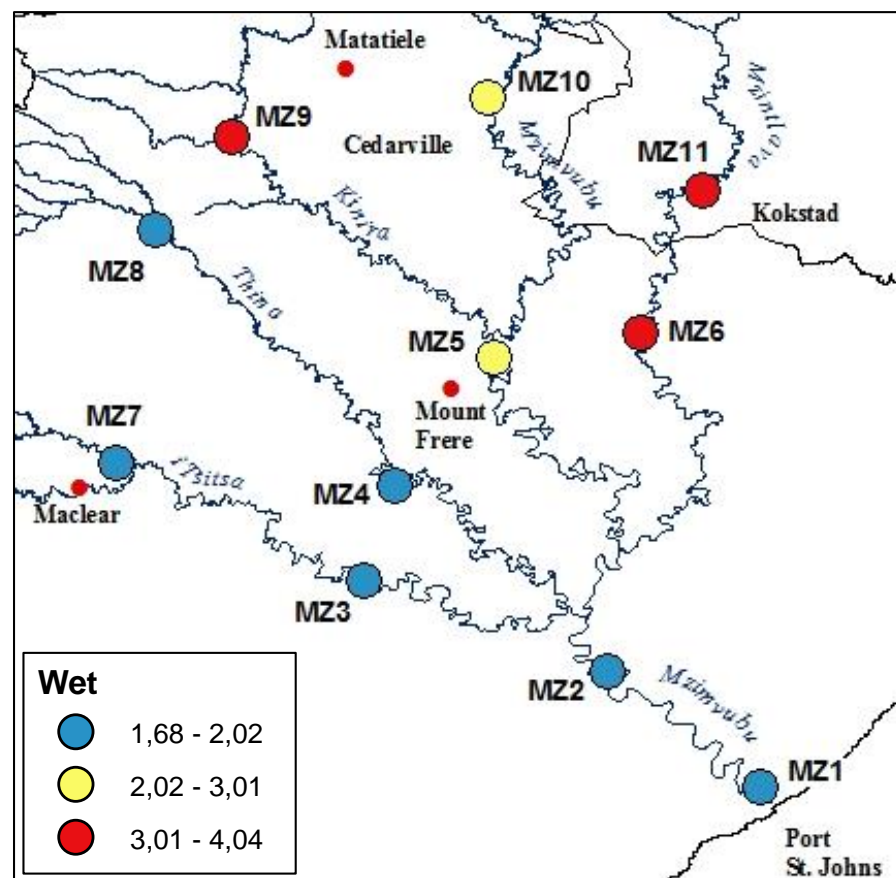
i.



ii.

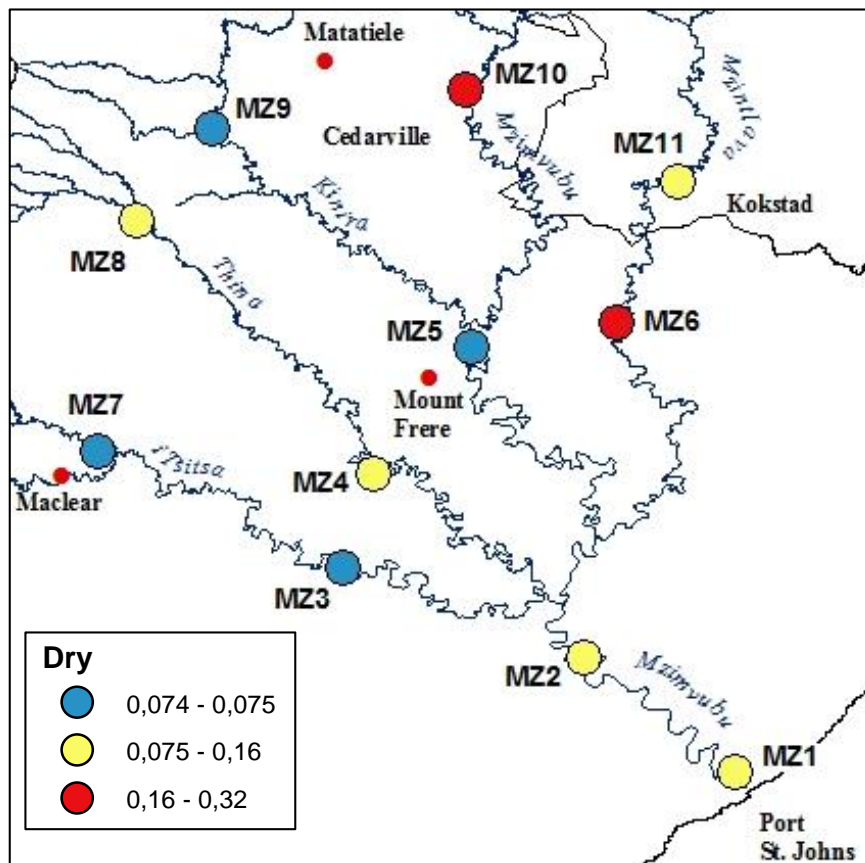


iii.

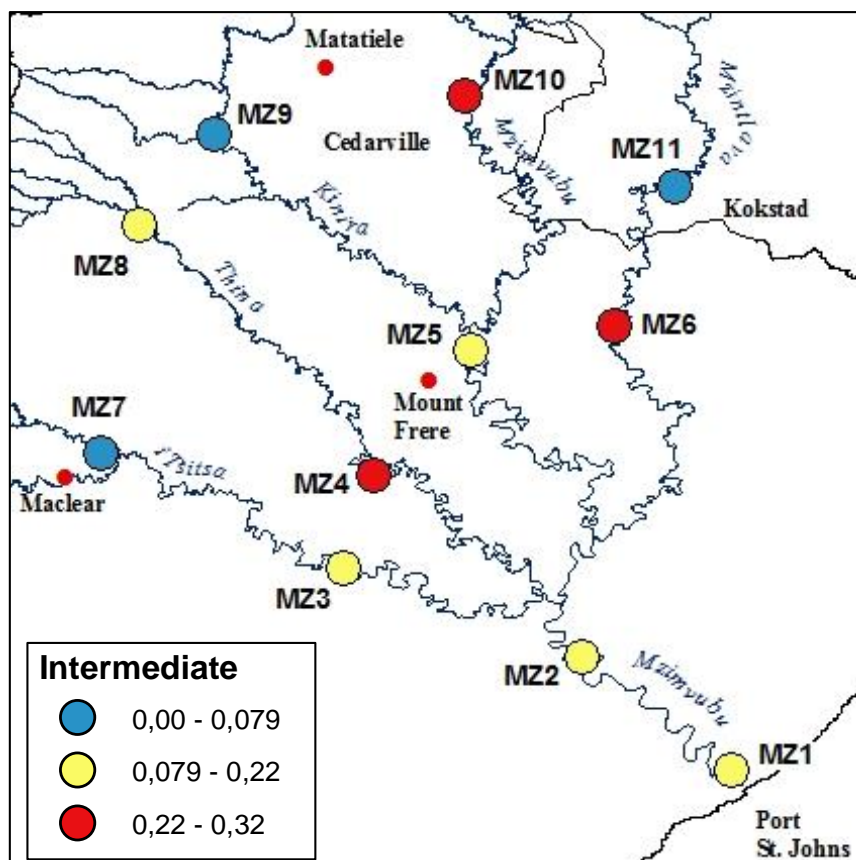


G. AlSi (Aluminium/Silicon) for the dry, intermediate and wet season.

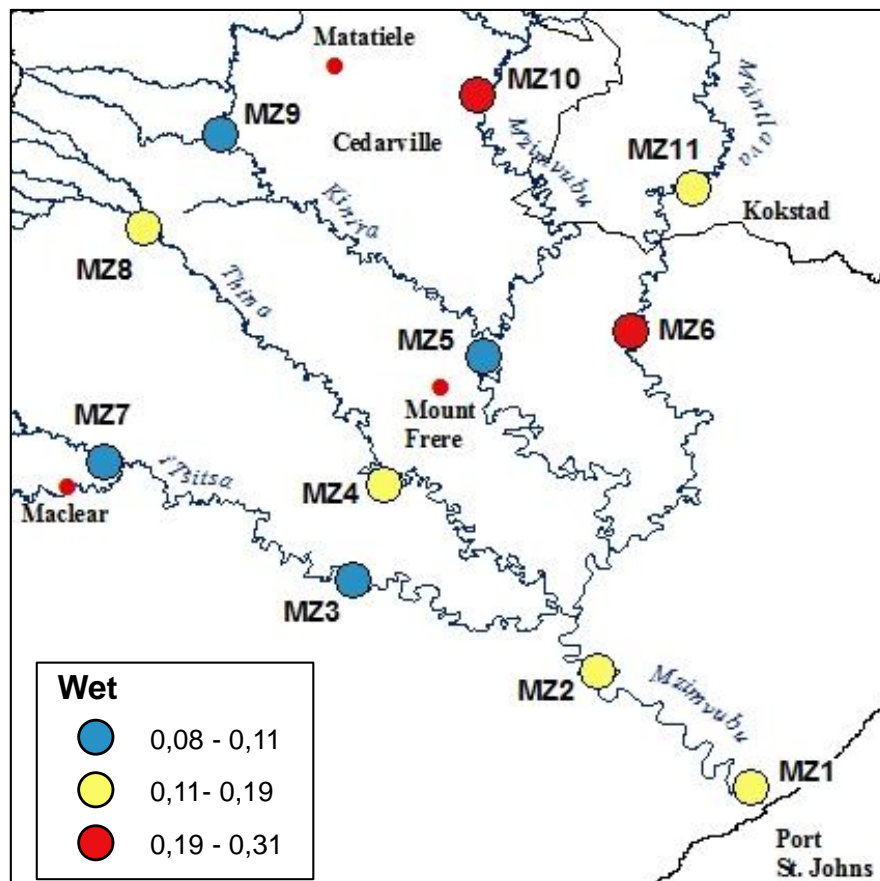
i.



ii.

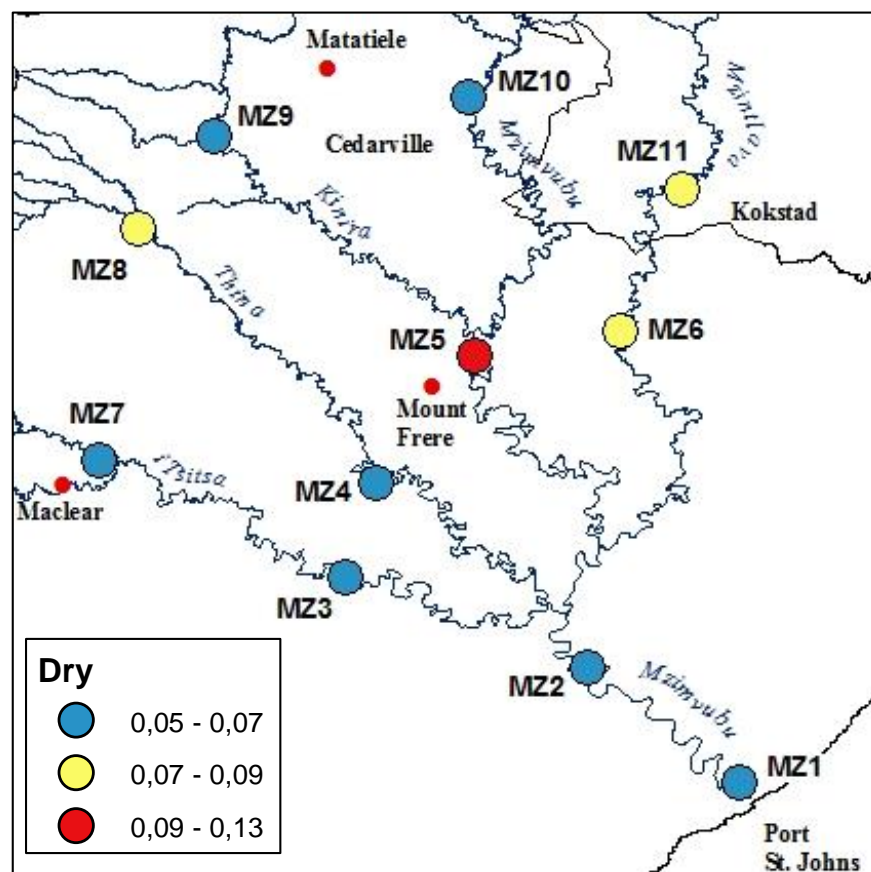


iii.

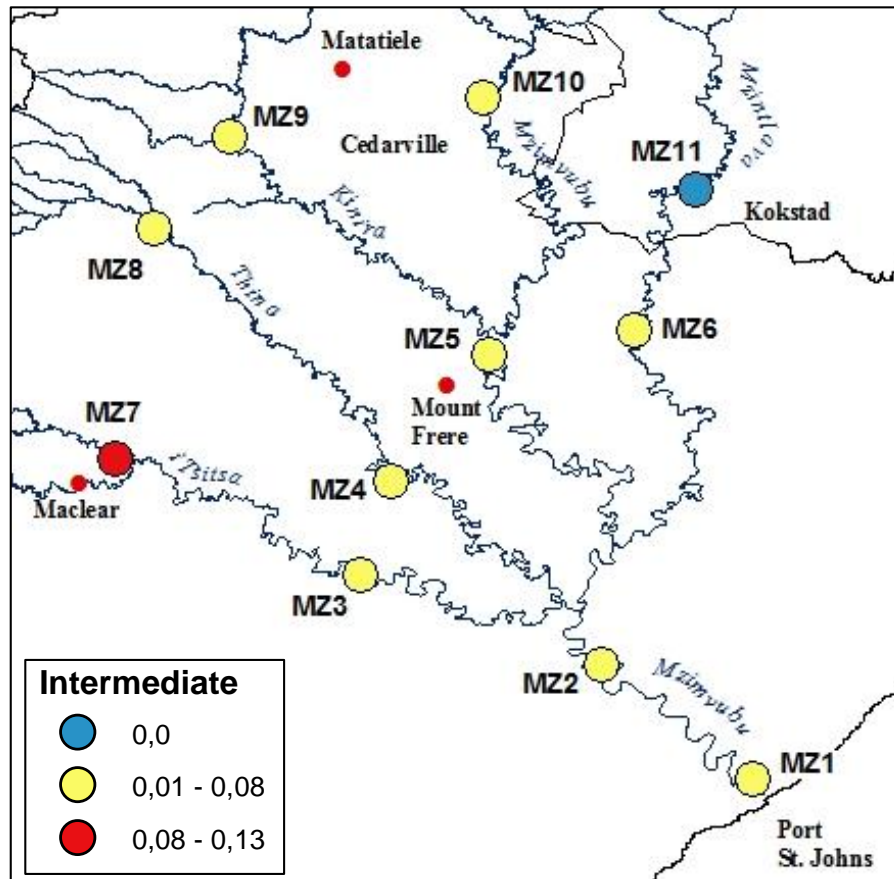


H. *TiAl* (Titanium/Aluminium) for the dry, intermediate and wet season.

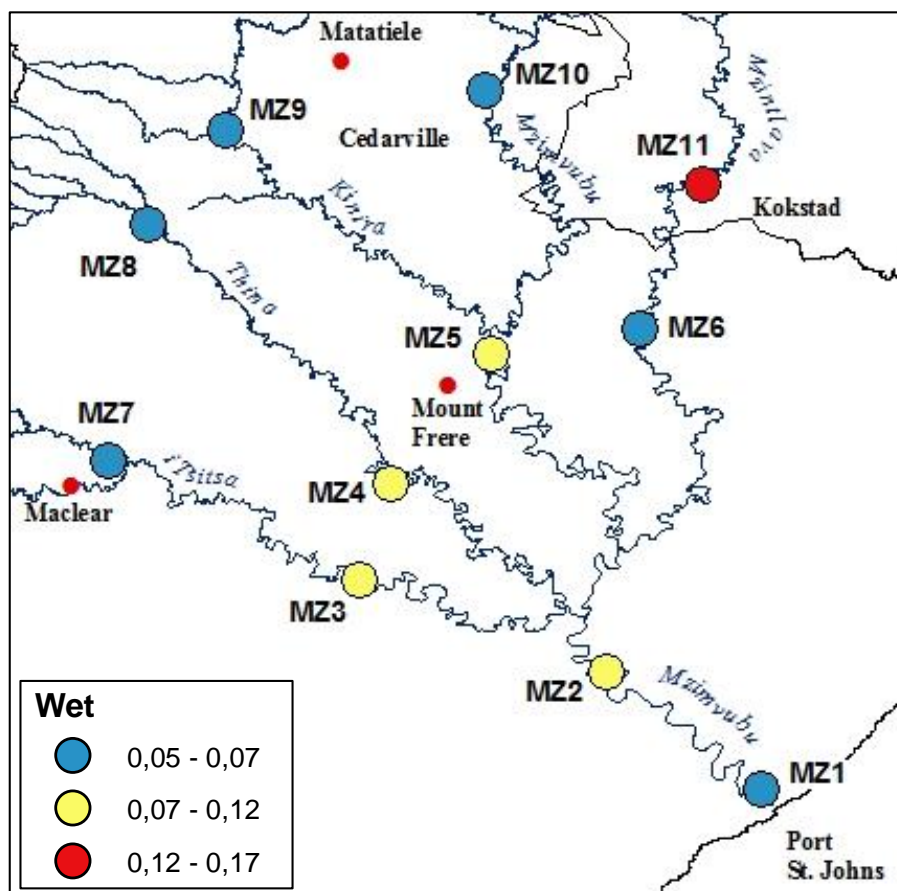
i.



ii.



iii.



APPENDIX H

1. All proxy correlation

	RBS Fe/K	RBS Al/Si	RBS Ti/Al	SPM Fe/K	SPM Al/Si	SPM Ti/Al	RBS Norm31	SPM Norm31	RBS δD_{29}	RBS δD_{31}	RBS δD_{29-31}	RBS $\delta^{13}C_{29}$	RBS $\delta^{13}C_{31}$	RBS $\delta^{13}C_{29-31}$	SPM $\delta^{13}C_{29}$	SPM $\delta^{13}C_{31}$	SPM $\delta^{13}C_{29-31}$	CPI RBS	CPI SPM
RBS Fe/K	1																		
RBS Al/Si	0.389	1																	
RBS Ti/Al	0.419	-0.041	1																
SPM Fe/K	1	0.389	0.419	1															
SPM Al/Si	0.389	1	-0.041	0.389	1														
SPM Ti/Al	0.419	-0.041	1	0.419	-0.041	1													
RBS Norm31	0.132	0.140	0.208	0.132	0.140	0.208	1												
SPM Norm31	0.303	0.186	0.119	0.303	0.186	0.119	0.340	1											
RBS δD_{29}	0.055	-0.436	-0.056	0.055	-0.436	0.056	-0.029	-0.204	1										
RBS δD_{31}	0.024	-0.434	-0.028	0.024	-0.434	0.028	-0.090	-0.202	0.986	1									
RBS δD_{29-31}	0.039	-0.436	-0.042	0.039	-0.436	0.042	-0.060	-0.203	0.996	0.997	1								
RBS $\delta^{13}C_{29}$	0.039	-0.247	0.257	0.039	-0.247	0.257	-0.211	-0.052	0.620	0.669	0.648	1							
RBS $\delta^{13}C_{31}$	0.032	-0.287	0.260	0.032	-0.287	0.260	-0.245	-0.061	0.617	0.669	0.646	0.994	1						
RBS $\delta^{13}C_{29-31}$	0.036	-0.267	0.259	0.036	-0.267	0.259	-0.228	-0.057	0.620	0.670	0.648	0.999	0.998	1					
SPM $\delta^{13}C_{29}$	0.307	-0.103	-0.088	0.307	-0.103	0.088	-0.275	-0.299	0.017	0.005	-0.006	0.048	0.070	0.059	1				
SPM $\delta^{13}C_{31}$	0.296	-0.091	-0.125	0.296	-0.091	0.125	-0.338	-0.498	0.056	0.081	0.069	0.134	0.167	0.150	0.842	1			
SPM $\delta^{13}C_{29-31}$	0.309	-0.091	-0.124	0.309	-0.091	0.124	-0.322	-0.404	0.020	0.047	0.034	0.098	0.126	0.112	0.965	0.955	1		
CPI RBS	0.160	0.117	-0.003	0.160	0.117	0.003	-0.078	0.103	0.369	0.388	-0.380	0.563	-0.543	-0.554	-0.104	-0.171	-0.148	1	
CPI SPM	0.091	0.011	-0.048	0.091	0.011	0.048	0.204	-0.081	0.156	0.125	0.141	0.001	0.020	0.010	-0.496	-0.361	-0.445	0.064	1

2. Dry Season

XXX

	<i>RBS</i> <i>Fe/K</i>	<i>RBS</i> <i>Al/Si</i>	<i>RBS</i> <i>Ti/Al</i>	<i>SPM</i> <i>Fe/K</i>	<i>SPM</i> <i>Al/Si</i>	<i>SPM</i> <i>Ti/Al</i>	<i>RBS</i> <i>Norm31</i>	<i>SPM</i> <i>Norm31</i>	<i>RBS</i> δD_{29}	<i>RBS</i> δD_{31}	<i>RBS</i> δD_{29-31}	<i>RBS</i> $\delta^{13}C_{29}$	<i>RBS</i> $\delta^{13}C_{31}$	<i>RBS</i> $\delta^{13}C_{29-31}$	<i>SPM</i> $\delta^{13}C_{29}$	<i>SPM</i> $\delta^{13}C_{31}$	<i>SPM</i> $\delta^{13}C_{29-31}$	<i>CPI</i> <i>RBS</i>	<i>CPI</i> <i>SPM</i>
RBS Fe/K	1																		
RBS Al/Si	0.565	1																	
RBS Ti/Al	0.472	-0.175	1																
SPM Fe/K	1	0.565	0.472	1															
SPM Al/Si	0.565	1	-0.175	0.565	1														
SPM Ti/Al	0.472	-0.175	1	0.472	-0.175	1													
RBS Norm31	0.046	0.078	0.187	0.046	0.078	0.187	1												
SPM Norm31	0.066	-0.087	0.172	0.066	-0.087	0.172	0.426	1											
RBS δD_{29}	-0.166	-0.619	0.409	-0.166	-0.619	0.409	0.265	-0.289	1										
RBS δD_{31}	-0.074	-0.586	0.458	-0.074	-0.586	0.458	0.145	-0.358	0.986	1									
RBS δD_{29-31}	-0.119	-0.604	0.436	-0.119	-0.604	0.436	0.205	-0.326	0.996	0.997	1								
RBS $\delta^{13}C_{29}$	0.332	-0.314	0.608	0.332	-0.314	0.608	-0.238	-0.386	0.661	0.748	0.708	1							
RBS $\delta^{13}C_{31}$	0.297	-0.369	0.616	0.297	-0.369	0.616	-0.281	-0.379	0.658	0.746	0.705	0.995	1						
RBS $\delta^{13}C_{29-31}$	0.315	-0.341	0.612	0.315	-0.341	0.612	-0.259	-0.383	0.660	0.748	0.707	0.999	0.999	1					
SPM $\delta^{13}C_{29}$	0.183	-0.033	0.096	0.183	-0.033	0.096	-0.382	0.396	-0.339	-0.273	-0.306	0.130	0.125	0.128	1				
SPM $\delta^{13}C_{31}$	0.479	0.166	0.275	0.479	0.166	0.275	-0.590	-0.090	-0.264	-0.161	-0.212	0.517	0.524	0.521	0.503	1			
SPM $\delta^{13}C_{29-31}$	0.338	0.049	0.188	0.338	0.049	0.188	-0.527	0.242	-0.354	-0.263	-0.309	0.317	0.316	0.317	0.927	0.791	1		
CPI RBS	-0.602	0.161	-0.502	-0.602	0.161	-0.502	-0.123	0.107	-0.600	-0.660	-0.633	-0.766	-0.740	-0.754	-0.026	-0.252	-0.128	1	
CPI SPM	-0.204	-0.070	-0.074	-0.204	-0.070	-0.074	0.045	-0.528	0.245	0.217	0.232	0.077	0.111	0.094	-0.636	-0.168	-0.524	0.071	1

3. Intermediate Season

	RBS Fe/K	RBS Al/Si	RBS Ti/Al	SPM Fe/K	SPM Al/Si	SPM Ti/Al	RBS Norm31	SPM Norm31	RBS δD_{29}	RBS $d\delta D_{31}$	RBS δD_{29-31}	RBS $\delta^{13}C_{29}$	RBS $\delta^{13}C_{31}$	RBS $\delta^{13}C_{29-31}$	SPM $\delta^{13}C_{29}$	SPM $\delta^{13}C_{31}$	SPM $\delta^{13}C_{29-31}$	CPI RBS	CPI SPM
RBS Fe/K	1																		
RBS Al/Si	0.483	1																	
RBS Ti/Al	0.680	0.150	1																
SPM Fe/K	1	0.483	0.680	1															
SPM Al/Si	0.483	1	0.150	0.483	1														
SPM Ti/Al	0.680	0.150	1	0.680	0.150	1													
RBS Norm31	0.613	0.597	0.519	0.613	0.597	0.519	1												
SPM Norm31	0.644	0.380	0.510	0.644	0.380	0.510	0.670	1											
RBS δD_{29}	-0.730	-0.567	-0.658	-0.730	-0.567	-0.658	-0.630	-0.697	1										
RBS δD_{31}	-0.746	-0.609	-0.647	-0.746	-0.609	-0.647	-0.780	-0.725	0.971	1									
RBS δD_{29-31}	-0.743	-0.593	-0.657	-0.743	-0.593	-0.657	-0.713	-0.717	0.992	0.993	1								
RBS $\delta^{13}C_{29}$	-0.495	-0.494	-0.512	-0.495	-0.494	-0.512	-0.381	-0.187	0.695	0.676	0.690	1							
RBS $\delta^{13}C_{31}$	-0.480	-0.538	-0.525	-0.480	-0.538	-0.525	-0.451	-0.196	0.672	0.669	0.676	0.987	1						
RBS $\delta^{13}C_{29-31}$	-0.489	-0.517	-0.520	-0.489	-0.517	-0.520	-0.417	-0.192	0.686	0.675	0.685	0.997	0.997	1					
SPM $\delta^{13}C_{29}$	-0.452	-0.130	-0.509	-0.452	-0.130	-0.509	-0.652	-0.461	0.441	0.531	0.491	0.154	0.204	0.179	1				
SPM $\delta^{13}C_{31}$	-0.444	-0.176	-0.517	-0.444	-0.176	-0.517	-0.674	-0.468	0.439	0.526	0.487	0.155	0.217	0.186	0.993	1			
SPM $\delta^{13}C_{29-31}$	-0.448	-0.153	-0.514	-0.448	-0.153	-0.514	-0.664	-0.465	0.441	0.529	0.490	0.155	0.211	0.183	0.998	0.998	1		
CPI RBS	0.455	0.319	0.382	0.455	0.319	0.382	0.224	0.303	-0.755	-0.633	-0.697	-0.602	-0.576	-0.591	-0.140	-0.160	-0.150	1	
CPI SPM	0.142	0.101	0.007	0.142	0.101	0.007	0.278	-0.301	-0.174	-0.277	-0.229	-0.326	-0.304	-0.316	-0.395	-0.345	-0.371	0.123	1

4. Wet season

	<i>RBS</i> <i>Fe/K</i>	<i>RBS</i> <i>Al/Si</i>	<i>RBS</i> <i>Ti/Al</i>	<i>SPM</i> <i>Fe/K</i>	<i>SPM</i> <i>Al/Si</i>	<i>SPM</i> <i>Ti/Al</i>	<i>RBS</i> <i>Norm31</i>	<i>SPM</i> <i>Norm31</i>	<i>RBS</i> δD_{29}	<i>RBS</i> δD_{31}	<i>RBS</i> δD_{29-31}	<i>RBS</i> $\delta^{13}C_{29}$	<i>RBS</i> $\delta^{13}C_{31}$	<i>RBS</i> $\delta^{13}C_{29-31}$	<i>SPM</i> $\delta^{13}C_{29}$	<i>SPM</i> $\delta^{13}C_{31}$	<i>SPM</i> $\delta^{13}C_{29-31}$	<i>CPI</i> <i>RBS</i>	<i>CPI</i> <i>SPM</i>
RBS Fe/K	1																		
RBS Al/Si	0.231	1																	
RBS Ti/Al	0.041	-0.088	1																
SPM Fe/K	1	0.231	0.041	1															
SPM Al/Si	0.231	1	-0.088	0.231	1														
SPM Ti/Al	0.041	-0.088	1	0.041	-0.088	1													
RBS Norm31	-0.670	-0.681	-0.238	-0.670	-0.681	-0.238	1												
SPM Norm31	0.331	-0.094	0.062	0.331	-0.094	0.062	-0.014	1											
RBS δD_{29}	0.282	-0.201	-0.179	0.282	-0.201	-0.179	0.214	0.338	1										
RBS δD_{31}	0.302	-0.210	-0.148	0.302	-0.210	-0.148	0.218	0.389	0.991	1									
RBS δD_{29-31}	0.293	-0.206	-0.163	0.293	-0.206	-0.163	0.217	0.365	0.997	0.998	1								
RBS $\delta^{13}C_{29}$	0.194	0.114	0.499	0.194	0.114	0.499	-0.147	0.443	0.538	0.600	0.572	1							
RBS $\delta^{13}C_{31}$	0.186	0.086	0.509	0.186	0.086	0.509	-0.144	0.418	0.545	0.605	0.578	0.997	1						
RBS $\delta^{13}C_{29-31}$	0.190	0.100	0.504	0.190	0.100	0.504	-0.146	0.431	0.542	0.603	0.575	0.999	0.999	1					
SPM $\delta^{13}C_{29}$	-0.597	-0.145	0.134	-0.597	-0.145	0.134	0.263	-0.728	-0.054	-0.108	-0.082	-0.130	-0.101	-0.116	1				
SPM $\delta^{13}C_{31}$	-0.529	-0.077	0.028	-0.529	-0.077	0.028	0.221	-0.739	-0.016	-0.053	-0.035	-0.091	-0.063	-0.077	0.999	1			
SPM $\delta^{13}C_{29-31}$	-0.532	-0.083	0.047	-0.532	-0.083	0.047	0.221	-0.735	-0.021	-0.058	-0.041	-0.086	-0.058	-0.073	1	1	1		
CPI RBS	0.511	-0.068	-0.009	0.511	-0.068	-0.009	-0.419	0.102	-0.082	-0.144	-0.114	-0.400	-0.386	-0.393	-0.171	-0.209	-0.204	1	
CPI SPM	0.312	-0.205	-0.085	0.312	-0.205	-0.085	0.165	0.682	0.614	0.646	0.632	0.479	0.479	0.479	-0.641	-0.597	-0.599	0.018	1